Development of a novel process for the removal of selected organic compounds from waste streams

Development of a Novel Process for the Removal of Selected Organic Compounds from Waste Streams

Deirdre Enright

A thesis submitted for the degree of Doctor of Philosophy at the College of Science, University of Limerick, Ireland

Research Supervisors: Dr. Teresa Curtin and Dr. Tom O'Dwyer

Submitted to the University of Limerick June 2015

Development of a Novel Process for the Removal of Selected Organic Compounds from Waste Streams

Deirdre Enright

Abstract

The aim of this research work was to develop a solid regenerable catalytic adsorbent for the removal of organics from industrial wastewater. This was to be achieved by a two-step process. The first step involved the removal of the aqueous contaminant of concern by adsorption onto a selective adsorbent/catalyst. The second step involved the oxidation of this adsorbed pollutant into carbon dioxide, water and nitrogen whilst minimising the formation of nitrogen oxides. 2-nitrophenol was selected as the model pollutant for this study because it is a simple nitrogen containing organic compound. The adsorbent chosen in this study was Beta zeolite with varying silica to alumina ratios of 25:1; 75:1; 150:1 and 300:1. Beta zeolite was chosen due to its high surface area, it catalytic properties and its ion exchange capacity.

Experimental results reported 2-nitrophenol adsorption levels of 40-50 mg g^{-1},80-90 mg g^{-1}, 80-90 mg g^{-1} and 80-90 mg g^{-1} on the unmodified Beta zeolite with varying silica-to-alumina ratios, 25:1, 75:1, 150:1 and 300:1 respectively. The adsorption process was found to follow the Langmuir model for β(25), β(75) and β(150), while the Freundlich model was found to fit the adsorption data of β(300). The adsorption process was found to follow the pseudo-second-order model which suggested that the adsorption on 2-nitrophenol was dependent on the availability of outer surface sites on the Beta zeolite. The thermodynamic parameters show that the adsorption process is mildly exothermic in nature. The magnitude of the enthalpy change indicate that the adsorption is physical in nature involving weak forces of attraction on the outer surface of the Beta zeolite. The adsorption process for 2-nitrophenol on β(25), β(75), β(150) and β(300) is largely independent on the pH of the adsorbate solution below pH 7.

The Beta zeolite was modified by a catalytic component in order to enhance its potential adsorption and catalytic capabilities. The Beta zeolite was modified with copper in a one-step ion exchange procedure. The introduction of extra-framework copper cations into all the Beta zeolite samples was found to enhanced the adsorption capacity of 2-nitrophenol. The adsorption of 2-nitrophenol was also found to increase with increasing copper loadings on all the Beta zeolite samples. The introduction of copper cations was found to alter the adsorption model from Langmuir to Freundlich model which suggests a change in the nature of adsorption process from monolayer to multilayer. The thermodynamic study showed that the adsorption of 2-nitrophenol onto the copper modified Beta zeolite samples was influenced by the presence of extra-framework copper cations as it increased the spontaneous nature of the overall adsorption process.

During the catalytic oxidation step the presence of copper on the Beta zeolite was found to enhance the oxidation process by increasing the total oxidation of the adsorbed 2-nitrophenol into CO_2. While carbon dioxide was the main species detected in the exit steam during the temperature programmed oxidation of the prepared samples, other minor products were also detected such as phenol, benzene, nitrogen oxide, nitrogen dioxide and carbon monoxide/nitrogen. However, the presence of copper greatly reduced the formation of these minor products.

In summary, this study demonstrated the potential of copper modified Beta zeolites to treat industrial wastewater containing 2-nitrophenol by adsorption and catalytic oxidation of the adsorbed 2-nitrophenol into carbon dioxide, water and nitrogen.

Declaration

I, the undersigned, hereby declare that the material contained within this Ph.D thesis is entirely my own work, and has not been submitted for any other awards at this or any other academic institution. Where use has been made of the work of others, it has been fully acknowledged and referenced.

Deirdre Enright

Acknowledgements

I would sincerely like to thank my project supervisors, Dr. Teresa Curtin and Dr. Tom O'Dwyer for their support and guidance throughout my Ph.D.

I would also like to thank all the members of the Material Science and Surface Institute and the Chemical and Environmental Science Department.

I would also like to thank the Head of School of Science Technology Engineering and Mathematics (STEM) at the Institute of Technology Tralee, Dr. Joseph Walsh and the Head of the Department of STEM Dr. Brendan O' Donnell for all their support.

Dedication

To my parents and family,

for their love and support throughout this journey.

Table of Contents

Chapter 1

Introduction

1.1 Review of the European Pollutant Emissions Register Database

EPER is the European Pollutant Emission Register; it is the first European – wide register of industrial emissions into air and water, which was established by a Commission Decision of 17th July 2000. The EPER Decision is based on Article 15(3) of Council Directive 96/61/EC concerning integrated pollution prevention and control. The EPER provides a database of 50 chemicals or classes of chemicals that are reported as hazardous to human health or to the environment such as benzene, toluene, xylenes (BTXs), carbon dioxide (CO_2), copper and its compounds. Of the organic chemicals listed by the EPER, phenols form one of the largest releases to water beyond the prescribed thresholds (500 tonnes direct to water and some 2,177 tonnes indirect to water after transfer to offsite wastewater treatment facilities).

According to the EPER Decision, Member States have to produce a triennial report, which covers these 50 pollutants if the threshold values indicated in Annex A1 of the EPER Decision are exceeded. The first report year was produced in 2001 (although Member States also had the option of providing data for 2000 and 2002); this information was reported in June 2003 and published on the internet in February 2004. The website, which is hosted by the European Environment Agency (EEA), gives access to information on the annual emissions of approximately 9,200 industrial facilities in the 15 old member states of the EU as well as Hungary and Norway. The information on the website is easily accessible and can be obtained by pollutant, activity (sector), air and water (direct or via a sewage system) or by EU/country. It is also possible to see data on individual facilities and rank them by the size of their pollutant emissions. The site also allows data from reporting years 2001 and 2004 to be compared. The EPER was succeeded by the European Pollutant and Transfer Register (E-PRTR). It is based on Regulation (EC) No. 166/2006 and fully implements the obligations of the UN-ECE PRTR Protocol, which was signed by the European Community and 23 Member States in May 2003 in Kiev and which is Protocol to the Aarhus Convention. The Regulation establishes the integrated pollutant release and transfer register at community level in the form of a publicly accessible electronic database and lays down rules for its functioning, in order to implement the UN-ECE Protocol on Pollutant Release and Transfer Registers and facilitate public participation in environmental decision making, as well as contributing to the prevention and reduction of pollution of the environment. The obligations under the E-PRTR Regulation extend beyond the scope of EPER. The E-PRTR covers the 27 EU Member States as well as Iceland, Liechtenstein, Norway, Serbia and Switzerland. The register contains annual data reported by some 28,000 industrial facilities. It provides data on 65 economic activities within 9 industrial sectors and it covers 91 pollutants. It details information on releases to land, off-site transfers of waste and releases from diffuse sources. Under the E-PRTR Regulations annual reporting is required. The first reporting year under the E-PRTR was in 2007 and respective information was reported by Member States in 2008, 2009 and 2010.

Table 1.1 shows how Ireland's emission levels of phenols compares to other EU member states, Ireland contributes 0.29% to the European total phenol emissions with the United Kingdom reporting the highest level accounting for 72% of the European total in the reporting year of 2010.

Table 1.1: Phenol emissions direct to water per member state in the 2010 reporting year. (European Pollutant Emission Register, 2006, European Environment Agency)

Country	European Total (tonnes)	%
Portugal	9.92	0.96
Finland	0.38	0.036
Austria	0.25	0.024
Bulgaria	127	12.30
Belgium	2.84	0.275
Latvia	0.14	0.013
Ireland	**3.01**	**0.291**
Czech Republic	3.31	0.320
Norway	1.50	0.145
Hungry	4.41	0.427
Romania	5.05	0.489
Greece	1.47	0.142
Serbia	0.45	0.043
Switzerland	0.97	0.093
Netherlands	1.15	0.111
Slovakia	1.74	0.168
Sweden	1.03	0.099
Germany	5.48	0.531
Poland	14.4	1.395
Italy	60.4	5.852
France	20.9	2.025
United Kingdom	747	25.68

1.2 Phenols

Phenols, sometimes called phenolics, are a class of chemical compounds consisting of a hydroxyl group (-OH) attached to an aromatic hydrocarbon ring. Phenol, (C_6H_5OH) is the name of the simplest member of the class of chemicals of that generic name. Pure phenol is a colourless or white crystalline solid with a powerful sickly sweet antiseptic odour. Although similar to alcohols, phenols have unique properties and are not classified as alcohols (since the hydroxyl group is not bonded to a saturated carbon atom). They have relatively higher acidities due to the aromatic ring's tight coupling with the oxygen and a relatively loose bond between the oxygen and the hydrogen. The acidity of the hydroxyl group in phenols is between that of aliphatic alcohols and carboxylic acids (their pKa is usually between 10 and 12). Loss of a positive hydrogen ion (H^+) from the hydroxyl group of a phenol forms a negative phenolate ion (equation 1.1).

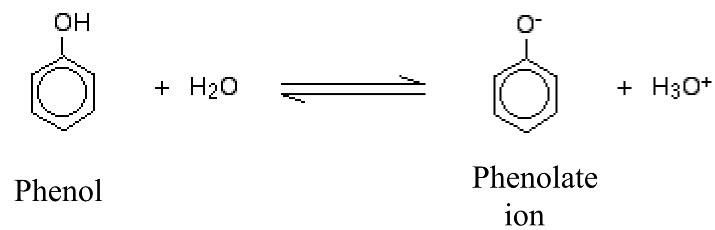

Equation 1.1: Equilibrium equation for the ionisation of phenol.

Nitrophenols are a family of nitrated phenols with the formula $HOC_6H_4NO_2$. They are produced either by the catalytic hydrolysis of 2-nitrochlorobenzene with NaOH or by electrophilic nitration of phenol using dilute HNO_3 (equation1.2), forming 2-nitrophenol.

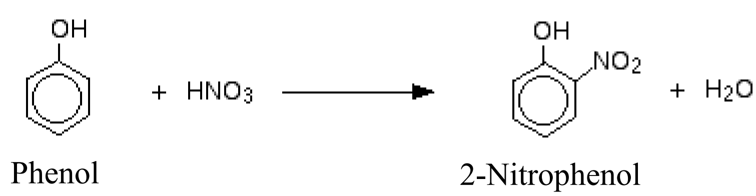

Equation 1.2: Electrophilic nitration of phenol forming 2-nitrophenol.

Three isomeric nitrophenols exist:

- *o*-Nitrophenol (1-hydroxy-2-nitrobenzene, 2-nitrophenol; OH and NO_2 groups are neighbouring), a yellow crystalline solid (m.p. 46 °C)
- *m*-Nitrophenol (1-hydroxy-3-nitrobenzene, 3-nitrophenol), a yellow crystalline solid (m.p. 97°C)
- *p*-Nitrophenol (1-hydroxy-4-nitrobenzene, 4-nitrophenol), yellow crystals (m.p. 114°C). It is a precursor to the rice herbicide fluorodifen and pesticide parathion.

2-nitrophenol is the model organic pollutant chosen for study in this work and some of its physical properties are outlined in Table 1.2. It is a light yellow solid with a melting point of 45 - 46ºC, and a density of 1.49 g/cm^3. Nitrophenols are weak acids but the nitro substitution makes them stronger acids than phenol. Nitrophenols can be converted to their water soluble salts by alkaline hydroxides. The pKa of 2-nitrophenol is 7.21 - 7.23. Under acid conditions, 2-nitrophenol is in the uncharged, protonated form and in the charged (anionic) form under basic conditions.

Other members of the class include chlorophenols. Chlorophenol is any organochloride of phenol that contains one or more covalently bonded chlorine atoms. Chlorophenols are produced by electrophilic halogenation of phenol with chlorine. Chlorophenols are typically crystalline with a characteristic phenolic odour. The structure and physical properties of three chlorophenols, namely 2-chlorophenol, 4-chlorophenol and 2, 4, 6-trichlorophenol, are presented in Table 1.2, as representatives of this class of phenolic compounds.

Table 1.2 Chemical properties of representative phenolic compounds.

Phenolic Compounds	Chemical Structure	Boiling point (°C)	pKa at 25°C	Aqueous solubility at 25 °C (g l^{-1})
Phenol	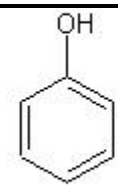	182	9.89	93
2-chlorophenol	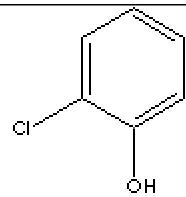	204	8.52	28
4-chlorophenol	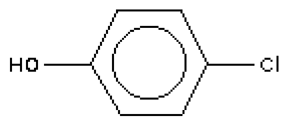	220	9.37	27
2,4,6-trichlorophenol	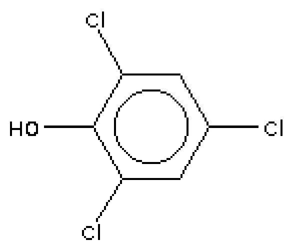	246	5.99	28.6
2-nitrophenol	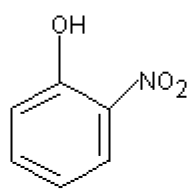	215	7.21	2.0
3-nitrophenol	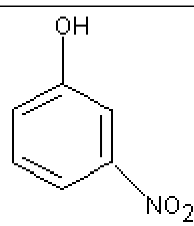	194	8.28	1.35
4-nitrophenol	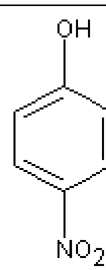	279	7.15	1.69

1.3. Uses of phenols and Emission Sources

Phenolic compounds have been used as model compounds in many instances (Smisek and Cerny 1970; Damjanović et al., 2010; Hussain et al., 2013; Kim and Ihm 2011), because they are common environmental contaminants and typical of many industrial wastes. Phenol is also considered to be an intermediate in the oxidation pathway of higher molecular weight aromatic compounds. Phenols are a major chemical intermediate, used for the manufacture of phenolic resins and synthetic fibres. In 2008 the worldwide capacity for phenol production was around 9.9 million tons with 98.5% based on the cumene to phenol process. Total production in 2008 was around 8.7 million tons (Pilato, 2010).

Table 1.3 shows the major phenol producers in the world. The main chemical intermediates and derivatives of phenol are bisphenol A (BPA), which is used to make polycarbonate (PC) and epoxy resins, caprolactam, alkylphenols, aniline and adipic acid. In 2008 the largest use with about 44% was for the production of bisphenol A, followed by phenolic resins 26% cyclohexanone / caprolactam and other alkylphenols 4% (Pilato, 2010).

The BPA market has been driven by the strong growth in polycarbonate resins, accounting for two thirds of BPA demand. The driving force in polycarbonate demand has been growth in optical media such as compact discs (CDs), CD-ROMs, recordable CDs. The second largest outlet for phenol, accounting for 28% of demand, is phenolic resins which are largely used as durable binders and adhesives in structural wood panels and as binders in mineral wool insulation (Pilato, 2010). They have a wide spectrum of uses in the automotive and construction industry including brake linings and foundry binders, insulation foams and composites.

Table 1.3: Major phenol producers in the world in 2008 (Pilato, 2010).

Company	Phenol capacity in thousands of tonnes per year
Ineos Phenol	1870
Sunoco	800
Mitsui Chemicals	750
Shell	600
CEPSA Quimical	600
Polimeri Europa	480
FCFC	400
Mt. Vernon Phenol (sabic)	340
Kumho	330
DOW	300
Taiwan Prosperity	200
Mitsubishi Chemicals	250
Chiba Phenol	230
Georgia Gulf	230
LG Chem	200
Chang Chun PC	200
Rhodia	195
NOVAPEX	180

Nitro-phenolic compounds can be formed by photochemical atmospheric reactions owing to the presence of nitrogen oxides (NO_x) in industrial and automotive emission gases. These compounds have been detected not only in industrial wastewaters but also in freshwater and marine environments. Some of the most toxic members of phenol compounds are the chlorinated and nitro-substituted phenols that are used as pesticides and anti-bacterials.

The content of phenolic compounds in industrial wastewater, such as refineries, coking operations, coal processing, and manufacture of petrochemicals, (about 200-2000 mg l^{-1}), is higher than the standard limits (mostly less than 0.5 mg l^{-1}) established for their release into aquatic environment (Sihem et al., 2012). Phenols are also the main organic constituents present in condensate streams in coal gasification and liquefaction processes. Other sources of waste streamwater containing phenols are pharmaceutical, plastics, wood products, paint pulp and paper industries (0.1-1600 mg l^{-1}) (Cordero et al., 2008). The EPER database provides information on the emission of phenol per industrial activity within the 25 member states of the EU. Table 1.4., shows the aggregated emissions of phenol from industrial activities.

Table 1.4 Emissions of phenol from industrial sources as reported by the EPRTR 2012. (European Pollutant and Transfer Register, 2012, European Environment Agency)

Industrial Activity	Facilities	Emissions to air (Tonne per year)	Emission to water (Tonne per year)
Energy sector	152	-	728
Production processes of metals	32	0.008	39.3
Mineral Industry	7	28.1	0.765
Chemical Industry	57	0.011	34.4
Waste and waste water management	137	-	213
Paper and wood production processing	23	-	15.2
Intensive livestock production and aquaculture	2	-	0.259
Animal and vegetable products from the food and beverage sector	2	-	0.447
Other additives	2	-	0.311
Total	**414**	**28.12**	**1,032**

The energy sector report the highest emission levels of phenol accounting for (728 tonnes) of the total emissions from 152 listed activities. Phenol and many substituted phenols are also natural components of many substances (e.g., tea, wine and smoked food), and phenol is also emitted from the combustion of fossil fuels and tobacco. It is also present in animal wastes and decomposing organic material and may be formed in air as a product of benzene photooxidation.

1.4. Toxicity of Phenols

Phenol is one of the most common organic water pollutants. It is toxic even at low concentrations, and also its presence in natural waters can lead further to the formation of substituted compounds during oxidation processes (Qiuli and Sorial 2007). It is acknowledged that phenolic compounds are extremely toxic for aquatic organisms at parts per million concentrations (Buttino et al., 1991). For example, a significant decrease in erythrocytes, total proteins and cholesterol in blood plasma of *Mugilus auratus* was observed following an 8-day exposure to 7.5 mg l^{-1} of phenol (Karnovic-Ozretic and Orzetic 1988). Decreasing reproduction and growth rate of marine organisms have been observed after exposure to phenolic compounds. Buttino reported a negative influence on egg production and assimilation rates of copepods after eight exposure days to 500 μg l^{-1} phenol concentration (Buttino 1994). Both the decline in egg deposition rates and fecal pellet production suggest that the prime action of phenol is to inhibit feeding rates.

The manufacture and transportation of phenol as well as its many uses may lead to worker exposures to this substance, through inhalation, ingestion, eye or skin contact, and absorption through the skin. Phenol is rapidly absorbed through the skin and can cause skin and eye burns upon contact. Comas, convulsions, cyanosis, and death can result from over exposure to it. The ingestion of such contaminated water in the human body causes protein degeneration, tissue erosion and paralysis of the central nervous system and also damages the kidney, liver and pancreas. Internally phenol affects the liver, kidneys, lungs, and vascular system, while the ingestion of 1 g of phenol is fatal for man (Karnovic-Ozretic and Orzetic 1988). Therefore, it is considered necessary to remove phenol from industrial effluents before discharging into water streams (Guerra 2001).

Thirteen phenol compounds: catechol, phenol, 4-nitrophenol, 4-methylphenol, 2,4-dinitrophenol, 2-nitrophenol, 2-chlorophenol, 4-chorophenol, 3-chlorophenol, 4-chloro-3-methylphenol, 2,4-dichlorophenol, 2,4,6-trichlorophenol and pentachlorophenol, are included in the priority pollutants list of the US Environmental Protection Agency and in the European Union list 76/464. Phenols are considered as priority pollutants since they are harmful to organisms at low concentration (Calace et al., 2002) due to their toxicity and carcinogenicity properties. Thus it is fully recommended to remove the phenol compounds from industrial effluents before entering the water stream (Ozkaya 2006). The US Environmental Protection Agency has set a water purification standard of less than 1 part per billion (ppb) of phenol in surface waters (Suarez-Ojeba et al., 2008). 2-nitrophenol is one of the most persistent, highly hazardous and toxic nitrophenols which can cause significant damage to human health and the environment. The USEPA recommended the restriction of its concentration in natural waters to less than 4.8 $\mu g\ l^{-1}$ (Oturan et al., 2011) and the 80/778/EC directive lays down a maximum concentration of 0.5 $\mu g\ l^{-1}$ for total phenols in drinking water (Rodriguez et al., 2000).

1.5 Current Waste Stream Treatment Technologies

Less than 3% of the water on our planet exists in readily usable form for human activities (United Nations Educational, Scientific and Cultural Organisation Water Portal, 2011 and US Geological Survey's, Water Science for Schools, 2011). It is not surprising that the world is facing a water crisis due to the fast industrial development and consequent huge quantity of pollutants discharged into soils and water systems.

For many industrial sectors, pollution prevention, waste minimisation and reuse are being increasingly integrated into their environmental policies. Thus, the challenge faced by chemical and related industries is to design efficient and cheap remediation processes and minimisation strategies for water pollution. A large portion of the waste generated by chemical and related industries is in the form of aqueous streams. In many cases, theses aqueous streams contain organic compounds in too small concentration so that economic recovery is not feasible. Recovery of phenol in industrial wastewater is not profitable in the concentration range 50-2000 mg l^{-1} (Santos et al., 2006), yet these concentrations are high enough to pollute the environment, if they are released without treatment.

Numerous approaches have been used to remove organic pollutants from industrial aqueous streams. The suitability of a process or method for treating a particular waste stream is highly dependent on factors such as type(s) and concentration of pollutants, pH, temperature, level of toxicity and volume of waste stream requiring treatment. Because of the high toxicity of the nitrophenols, biological methods for the treatment of industrial waste are often unsuitable (Milner and Goulder 1984).

Of the variety of physical and chemical processes and their combination outlined in Figure 1.1., each technique has its inherent limitations in effectiveness and cost and will be discussed in further detail.

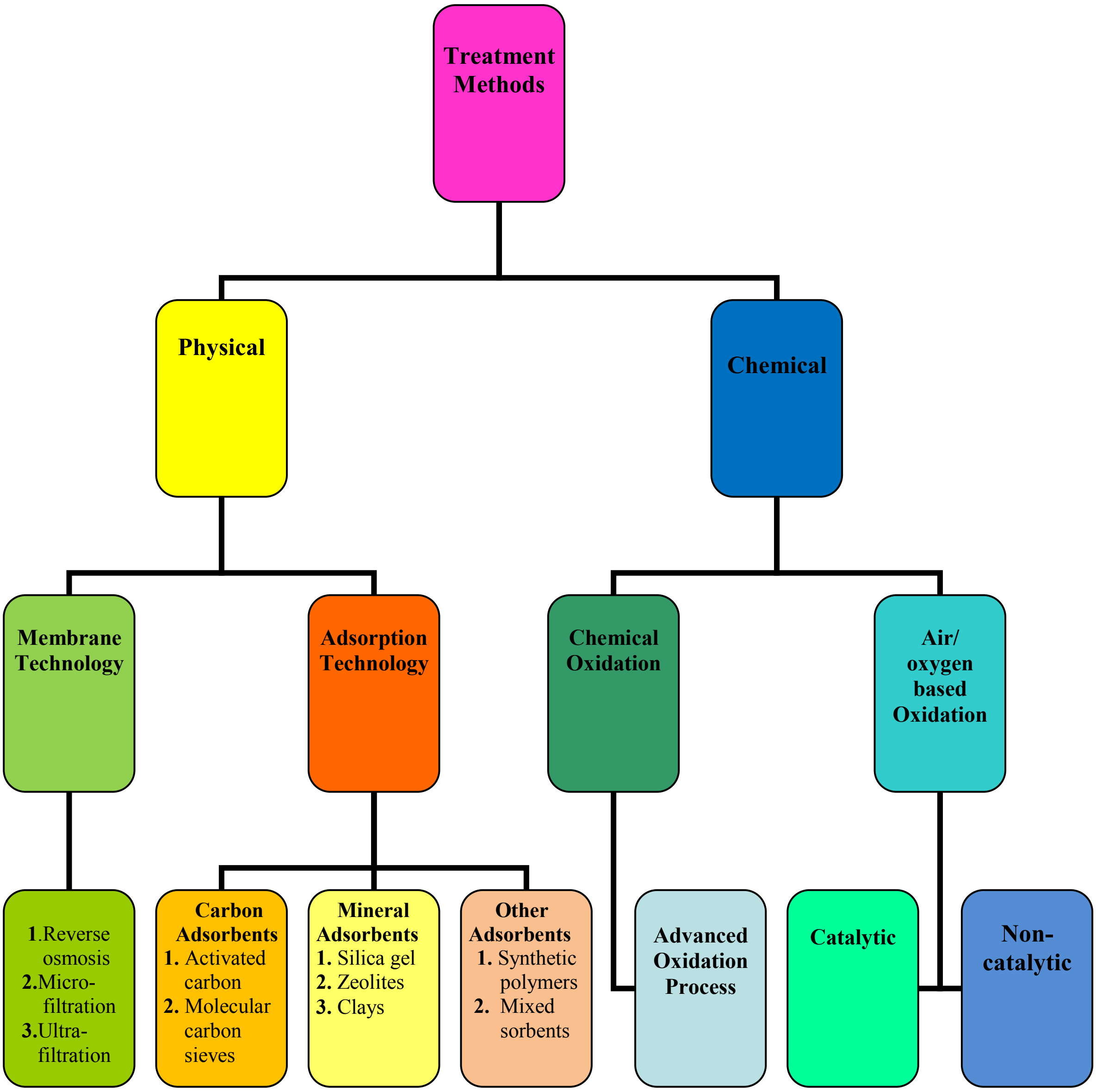

Figure 1.1 Current treatment methods for organic pollutants.

1.5.1 Membrane Technology

Membrane technology is a physical treatment and it encompasses reverse osmosis (RO), microfiltration (MF) and ultrafiltration (UF) (Yoon and Lueptow 2005; Ozaki and Li 2002; Bennett 2000; Hancock 1999). Reverse osmosis in particular has been used for the treatment of wastewater. During reverse osmosis (RO), water is drawn through a filter unit. Pressure, applied to the solution on one side of a semipermeable membrane, forces the liquid to diffuse through the membrane to a solution of weaker concentration. The process has the ability to remove a broad range of substances including ionic impurities, colloids, organics and pyrogenic materials from water. Reverse osmosis therefore allows production of pure water for electronic and pharmaceutical processes (Jawad et al., 2011; DeSilva 1996; Parekh 1991), however it is not frequently used because of the high costs resulting from membrane replacement.

1.5.2 Adsorption and Adsorbents

Adsorption is another example of a physical treatment used for treating wastewater. Adsorption is considered as the best wastewater treatment method due to its universal nature and ease of operation. Adsorption is the accumulation of a substance at surface or interface. In the case of water treatment, the process occurs at an interface between a solid adsorbent and contaminated water. The pollutant being adsorbed is called the adsorbate and the adsorbing phase is referred to as the adsorbent (Ali et al., 2012). Desorption in contrast is the reverse process to adsorption, during desorption the attachment to the surface is broken (Campbell 1988).

The adsorption process can be a conventional fixed bed process involving a saturation, adsorption or loading step, followed by desorption, elution or regeneration step. However, regeneration may not be possible or convenient. In this case the saturated adsorbent bed is removed and disposed of, or destroyed by burning in appropriate furnaces (Jung et al., 2001).

The most important criteria for selecting a suitable adsorbent material are:

1) High affinity, capacity and selectivity for target compounds,
2) Regeneration must be possible,

3) There must be a safe and economically viable treatment/disposal method for spent adsorbent,
4) It must have a tolerance for a wide range of wastewaters (Karcher et al., 2001).

Commercially available activated carbon is the most widely used adsorbent for the removal of a variety of organics from waters, but the disadvantages associated with its high cost and regeneration has stimulated research into low cost adsorbents for the removal of organic pollutants from wastewaters (Ali et al., 2012). Numerous reports are cited in literature on the research and development of low cost adsorbent materials such as seaweed waste based activated carbon (Rathinam et al., 2011), clay minerals (Cheknane et al., 2010 and Malusis et al., 2010), agriculture wastes (Han et al., 2011) biomass (Loukidou et al., 2003), bamboo (Fu et al., 2012), zeolites (Lin and Juang et al., 2009 and Dong et al., 2010), metal oxides (Benselka-Hadj et al., 2011), polymeric material (Zhang et al., 2007).

Adsorption can remove both soluble and insoluble organic pollutants. The removal capacity by this method may be up to 99.9% (Ali et al., 2012). Due to these facts, adsorption has been used for the removal of a variety of organic pollutants from various contaminated water sources such as phenolic compounds (Liu et al., 2010). The adsorption process offers flexibility in design and operation and in many cases produces treated effluent suitable for reuse, free of colour and odour. In addition, because adsorption is sometime reversible, the regeneration of the adsorbent, with resultant economy of operation, may be possible.

From the recent literature reviewed, adsorbents that stand out for high adsorption capacities for the removal of phenol from wastewater are commercial activated carbons (500 mg g^{-1}), dried activated sludge (287 mg g^{-1}), modified bentonite

(176 mg g^{-1}) and fly ash (118 mg g^{-1}). Table 1.5 presents a summary of adsorption capacities for nitro-substituted phenols. The adsorbents with max *p*-nitrophenol adsorption capacities are found to be commercial activated carbon (526 mg g^{-1}), microporous dextrin (167 mg g^{-1}), charred sawdust (147 mg g^{-1}), modified bentonite (139 mg g^{-1}), modified starch (131 mg g^{-1}), and silica beads (116 mg g^{-1}). These adsorbents are efficient and can be used effectively for the removal of phenolic compounds from aqueous solutions. The comparison of adsorption capacities for various chloro-phenolic compounds on low cost adsorbents and commercial activated carbon is shown in table 1.6. From this data it is evident that some low-cost adsorbents such as fungal biomass, dried sludge, starch and bentonite can be used in place of commercial activated carbon.

Table 1.5: **Comparison of nitro-substituted phenols adsorption on various low-cost adsorbents.**

Phenolic compound	Adsorbents	Capacity (mg g^{-1})	References
2-Nitrophenol	Wood fly ash Fly ash	144.0 5.8 - 6.4	Daifullah and Gad 1998; Singh and Nayak 2004
3-Nitrophenol	Fly ash	6.5 - 8.1	Singh and Nayak 2004
4-Nitrophenol	Sugar fly ash	0.8 - 1.2	Gupta et al., 1998
	Wood fly ash	0.8 - 1.2	Gupta et al., 1998
	Fly ash	7.8 - 9.7	Singh and Nayak 2004
	Samla coal	51.5	Ahmaruzzaman and Sharma 2005
	Commercial AC	526.3	Ahmaruzzaman and Sharma 2005
	Microporous cyclodextrin	167.0	Grini 2005
	Charred saw dust	147.0	Akcay and Akay 2004
	Modified bentonite	139.4	Dutta et al., 2001
	Modified starch	131.5	Delval et al., 2006
	Silica bead	116.0	Phan et al., 2002
	Bagassse fly ash	8.3	Gupta et al., 1998
	Zeolite	1.0	Sismanoglu and Pura 2001
	Pyrolysed reidue from animal bones	111.0	Xiaoli and Youcai 2006

Table 1.6. Comparison of chloro substituted phenol adsorption on various low- cost adsorbents.

Adsorbents	Capacity (mg g^{-1})	References
Fungal biomass	391	Denizli et al., 2005
Samla coal	50	Ahmaruzzaman and Sharma 2005
Petroleum coke	9	Ahmaruzzaman and Sharma 2005
Commercial activated carbon	500	Ahmaruzzaman and Sharma 2005
Modified bentonite	176	Akcay and Akcay 2004
Modified starch	68	Delval et al., 2006
Activated sludge	116	Aksu and Yerner et al., 1998
Dried activated sludge	287	Aksu and Yerner et al., 2001
Fly ash	118	Aksu and Yerner et al., 2001
Bentonite	10	Mortland et al., 1986
Sargassum muticum	251	Rubin et al., 2006
AC prepared from coconut shell	72	Radhika and Palsnivelu 2006

1.5.2.1 Activated Carbon

Since the 1940s activated carbons have been used as adsorbents for wastewater treatment and today adsorption of phenolic compounds from aqueous solutions presents the most widespread use of activated carbons in water treatment (Dabrowski et al., 2005, Ali et al., 2012). Adsorption onto activated carbon is often considered as the most economical and efficient process for the removal of organic compounds from aqueous solutions. It has also been cited by the USEPA as one of the best available environmental control technologies (Hamdaoui and Naffrechoux 2007).

Activated carbons (ACs) are made up of small hydrophobic graphite layers with disordered, irregular and heterogeneous surfaces bearing hydrophilic functional groups (Soto et al., 2011). They include a broad range of carbonaceous materials, which exhibit a high degree of porosity and extended inter particulate surface area (Ali et al., 2012). Typically activated carbons possess high surface area (60 – 2000 m^2 g^{-1}) and well defined microporous structure (average pore opening is about 1.5 nm) (Streat et al., 1995, Ali et al., 2012). The adsorbent properties of ACs depend on their physiochemical properties and mechanical strength derived from their composition. (Soto et al., 2011). A huge variety of carbon containing feedstocks are utilized to prepare activated carbon of different grades preferably by the catalytic activation of an initially pyrolysed char. Principally, commercially available carbons are prepared from pine wood and coal but there is continuous research for low cost alternatives. Ali et al., reported the most common feedstocks for the production of activated carbons on a commercial level to be wood, anthracite, bituminous coal, lignite, peat and coconut shell (Ali et al., 2012).

There are two main processes used to prepare activated carbons involving carbonization of the raw material below 800°C in the absence of oxygen, followed by activation at elevated temperatures using an oxidant (steam, carbon dioxide or air) and sometimes catalysts (Jung and Ahn 2001, Ali et al., 2012). The heating rate, the timing of carbonization and activation have been reported as the important parameters which will ultimately affect the final pore structure, surface area and chemistry of the prepared carbon (Rodriguez-Reinoso et al., 1982, Ali et al., 2012).

Activation maybe accomplished by chemical or physical treatment. During chemical activation a catalyst is impregnated into the feedstock. Chemical activation can be accomplished in a single step by carrying out thermal decomposition of raw materials with chemical reagents. The most widely used chemicals include $ZnCl_2$, H_3PO_4, H_2SO_4, KOH and K_2CO_3 (Ucar et., al 2009, Girgis et al., 2009, Gercel et al., 2007, Basta et al., 2011). $ZnCl_2$ and H_3PO_4 are usually used for activating biomass which is rich in cellulose, hemicellulose and lignin such as wood and nut shell (Puziy et al., 2002, Hussein et al., 1996). KOH, K_2CO_3 and Na_2CO_3 are usually used for activating residue that is rich in ash (Guo et al., 2000). K_2CO_3 has been reported to be the optimum chemical activator (Guo et al., 2000, Liu et al., 2012). During this process, a near saturated solution of catalyst impregnated feedstock is dried to influence pyrolysis in order to reduce tar formation and to keep volatilization to a minimum. (Bagreev et al., 2001, Ali et al., 2012). The resultant product is then carbonized and activated in a single step (Smisek and Cerny 1970).

The physical activation involves the direct reaction between the carbonized char and the activator. As in chemical activation, the principle objective is the removal of tarry amorphous carbon from the interstitial layers of the structure in order to develop the porosity and make accessible the internal surface area. Steam, CO_2 and air are the most common activators.

There are many reports cited in literature of the effect of feedstock and the chosen activation method on the surface area of the produced activated carbon and on their adsorption capacity for organic compounds. Wu et al.,. report on the adsorption properties of activated carbon prepared by treating a densified refuse derived fuel by KOH (Wu et al., 2013). They reported a BET surface area of up to 1655 m^2 g^{-1}, which exhibited excellent adsorption capability with maximum uptake for 4-chlorophenol, methylene blue and dye acid blue 74 of 494, 571 and 413 g kg^{-1} respectively (Wu et al., 2013). Miao et al.,. reported on the adsorption of phenol by activated carbon prepared from soybean straw activated by $ZnCl_2$. They reported the BET surface area as high as 2271 m^2 g^{-1}. They reported the maximum monolayer adsorption capacity of phenol at 278 mg g^{-1} (Miao et al., 2013). Tseng et al.,. investigated the adsorption of phenol, 4-chlorophenol and 2, 4-dichlorophenol from water using activated carbon prepared from pistachio shells at different NaOH/char ratios (Tseng et al., 2010). They classified the activated carbons as microporous materials with a surface area ranging from 939 to 1936 m^2 g^{-1} (Tseng et al., 2010). They reported that adsorption of the phenolic compounds at equilibrium increased with increasing NaOH/char ratio, with maximum reported uptake levels of 286.09, 430.66 and 624.29 mg g^{-1} for phenol, 4-chlorophenol and 2, 4 - dichlorophenol respectively (Tseng et al., 2010).

Lui et al.,. investigated the simultaneous preparation of silica and activated carbon from rice husk ash (Lui et al., 2012). They prepared a series of activated carbons and silica using different impregnation ratios of K_2CO_3. Again the impregnation was reported to be one of the most important parameters in the preparation of activated carbon using chemical activators (Lui et al., 2012). They observed an increasing pore volume of the prepared activated carbon with increasing impregnation ratio (Lui et al., 2012). They reported values of 1713 m^2 g^{-1} and 4 nm for the surface area and average pore size of the prepared activated carbon respectively. The activated carbon prepared by Lui et al.,. was reported to be rich in micropores and mesopores with a maximum adsorption capacity of 210 mg g^{-1} for methylene blue (Lui et al., 2012). They further investigated the possibility of recycling the chemical activator potassium carbonate and revealed that it could be effectively recycled. They concluded that their synthetic procedure was simple, environmentally friendly and economically effective (Lui et al., 2012).

Although activated carbon has a great capacity for adsorbing various organic compounds and can be easily modified by chemical treatment to increase its adsorption capacity, it has several disadvantages. It is expensive and in the powdered form it is difficult to separate from aquatic systems when it becomes exhausted or the effluent reaches maximum allowable discharge level. Furthermore, the adsorption process just transfers the pollutant from one phase to another rather than eliminating them from the environment. The reuse of the activated carbon is necessary for an economically feasible operation (Carratala-Abril et al., 2010). Regeneration of the activated carbon can be performed using different methods such as thermal (Guo and Du 2012, Sabio et al., 2004), chemical (He et al., 2012, Lu et al., 2011) electrochemical (Weng and Hsu 2008, You et al., 2013, Zhang 2002) and biologically (He et al., 2012), as well as others less common such as photochemical regeneration (Yap and Lim 2012).

Thermal regeneration of activated carbon is considered one of the most effective methods (Pelech et al., 2005). It consists of heating the activated carbon under a purge gas flow which removes the adsorbate as it is being desorbed (Carratala – Abril et al., 2010). The selection of temperature and type of purge gas is crucial for regeneration, especially from an economic point of view, but also considering the efficiency (Carratala – Abril et al., 2010). There have been reports cited in literature regarding the regeneration with inert gas (Nahm et al., 2012), steam or liquid water at high pressure (Bonjour et al., 2005). The successive adsorption-regeneration cycles are usually termed thermal swing adsorption (Hwang et al., 1997). the most common process but it requires high temperatures (800 - 850ºC) and consequently is usually not conducted in situ, requiring shipment of the spent AC to special regeneration units and thus contributing significantly to its cost.

The main disadvantage of the thermal regeneration of the activated carbon is the loss of carbon (5 - 10% per cycle) due to oxidation and attrition, and the energy cost of heating. Moreover, high temperatures are economically feasible only for large systems that use more than 200,000 t granular AC per year (Sonyheimer et al., 1988). The catalytic regeneration of the spent adsorbents (AC) has been considered as an alternative to thermal regeneration. Catalytic regeneration for ACs impregnated with a catalyst was first applied by Nwankwo and Turk, with metal oxides like Cr_2O_3, CuO, Co_3O_4 (Nwankwo and Turk 1974). Table 1.7 presents some examples of AC modified with a catalytic component used to remove organics from waste streams.

Table 1.7 Catalytic Regeneration of ACs impregnated with catalysts.

Catalyst Impregnated	Compound Adsorbed	Regeneration Temperature (°C)	Reference
Pt, Pd, CuO Cr_2O_3, Co_3O_4, V_2O_5	Toluene, benzene, styrene	20-350	Nwankwo and Turk 1974
MnO	Dyes, surface active agents	280-350	Koganovskii and Kanniskaya 1981
Fe_2O_3	Phenol	350	Prodan et al., 1988
Fe_2O_3, CuO	Dyeing waste water	280-350	Koganovskii and Kanniskaya 1981
Fe_2O_3, CuO, Cr_2O_3	Phenol halogenated phenol	250-280	Matatov-Meytal and Sheintuch 1999
TiO_2	Phenol	25	Tang et al., 2013

Solvent regeneration processes are applicable to methods with reversible adsorption, such as high organic concentration wastewater treatment and recycled wastewater containing precious metals (Guo et al., 2011). The advantage of solvent regeneration have been cited in literature as allowing the process to recover useful substances from the regeneration liquid, adsorbent reactivation can be operated in an absorption tower, the technical process is easy to implement in practical processes and activated carbon loss is less in solvent regeneration process. Numerous drawbacks to solvent regeneration such as the necessity to find a method for recovering organic solvents free of pollutants, the solvent used can make several pollutants become desorbed and regeneration may not be complete due to the fact that the pores in the activated carbon can become air logged which ultimately effects the recovery rate.

Despite its frequent use in the water and waste industries, AC remains an expensive material. Regeneration efficiency has been a major environmental concern in activated carbon usage. In view of the high cost and tedious procedures for the preparation and regeneration of activated carbons, there is a continuing search for low cost potential adsorbents. In recent years, many researchers have tried to produce activated carbons for removal of various pollutants using renewable and cheaper precursors which were mainly industrial and agricultural by products. These include coconut shell which is a well-known precursor for the production of high quality granular activated carbon and has been cited in literature by Vieira et al.,. for the removal of textile dyes (Vieira et al., 2011), Gupta et al., Li et al., Troca-Torrado et al.,. have reported on the adsorption of various dyes and phenols by activated carbon derived from scrap tyre rubbers (Gupta et al., 2011, Li et al., 2010, Troca-Torrado et al.,. 2011) and Rathinam et al.,. reported on the potential use of brown seaweed biomass as a precursor of activated carbon for the removal of phenol from aqueous solutions (Rathinam et al., 2011).

1.5.2.2 Polymeric Adsorbents

In the past decades polymeric adsorbents have been emerging as highly effective alternatives to activated carbons for pollutant removal and subsequent recovery from industrial effluents (Pan et al., 2009). Synthetic polymeric adsorbents include materials with hydrophilic or hydrophobic nature, such as polystyrene – divinylbenzene copolymers, polymethacrylate, dibenzene–ethyvinylbenzene copolymers and vinylpyridine (Soto et al., 2011). Even though the effective surface areas are smaller than in the case of activated carbon, polymeric adsorbents have been increasingly viewed as an alternative to activated carbon or zeolites for the selective removal of specific organic substances from contaminated water due to their durable and stable nature, their chemically inertness, high adsorption capacity, efficiency, selectivity and ease of regeneration, with relative low cost and limited toxicity (Soto et al., 2011). As compared to activated carbon, the exhausted polymeric adsorbents can be regenerated under milder conditions like acid or alkaline rinsing (Pan et al., 2009).

In order to synthesize polymeric adsorbents with high specific surface areas, hypercrosslinked polystyrene was first introduced in the 1970s by Davankou (Davankou et al., 1990). The hypercrosslinked resins were obtained crosslinked by an extensive post cross linking of a preformed linear polystyrene or low – crosslinked poly(styrene-co-divinylbenzene) using a bifunctional crosslinking agent and a Freidel –Crafts catalyst (Zeng et al., 2009). The hypercrosslinked polymer shows an extremely high specific surface area and excellent sorption properties. At present, hypercrosslinked adsorbents are produced by several companies such as Purolite International in the UK and USA (Purolite International Ltd., in collaboration with the Russian inventors, have developed an optimal series of Hypersol–Macronet adsorption resins for industrial applications (Lin and Juang 2009)), Dow Chemical in the USA, and Chemical Plant of Nankai University in China (Zeng et al., 2009). However it has been reported that the preparation of hypercrosslinked adsorbents has serious environmental implications due to the utilization of the reported carcinogenic chloromethyl methyl ether as bifunctional crosslinking agent in the post-crosslinking reaction (Zeng et al., 2009).

A wide variety of polymeric resins are reported such as macroporous resins without functional groups by Zabkova et al., chemically modified resins by Li et al., and cross linked resins by Zeng et al.,. (Zabkova et al., 2006, Li et al., 2002 and Zeng et al., 2009).

Amberlite XAD-4 has been reported to be one of the best commercially available macroporous polystyrene-co-divinylbenzene adsorbents for the removal of phenol and phenolic compounds from waste water (Yuan et al., 2008). It possesses a relatively high Brunauer-Emmet-Teller (BET) surface area (750.2 m^2 g^{-1}), pore volume (1.045 cm^3 g^{-1}) and medium pore diameter of 5.58nm and hence it has excellent adsorption towards hydrophobic small organic molecules dispersed in aqueous media (Li et al., 2013). Ku and Lee reported the adsorption of phenols (2-chlorophenol, 2,4-dichlorophenol, 2,4,6-trichlorophenol, 2-nitrophenol, 2,4-dinitrophenol, 2-methylphenol and 2,4-dimethylphenol) from aqueous solution under different experimental conditions (Ku and Lee 2000). They reported the removal of phenols by XAD-4 resin to be feasible under acidic conditions but decreased significantly with increasing solution pH. The observed adsorption behaviour was reported to be highly dependent on the solution pH and the species distribution of phenolic compounds varies at different pH values (Ku and Lee 2000).

The polystyrene matrix of XAD-4 creates an extremely hydrophobic surface which induces a relatively smaller adsorption capacity towards hydrophilic organic compounds from aqueous solutions. In order to improve the adsorption capacity of macroporous polymeric adsorbents for hydrophilic organic compounds, chemical modification is a typical method and it is often adopted by introducing some special functional groups on the matrix of the adsorbent (Ghaedi et al., 2009). These added functional groups modify the chemical composition of the adsorbent surface and hence improve the adsorption behaviours (Seyhan et al., 2008, Depecker et al., 2009). Carbonyl groups have been reported to be the most efficient functional groups for improving the adsorption behaviours of the polymeric adsorbents (Huang et al., 2012).

Adsorption capacity for phenolic compounds has been reported by Li et al.,. to be increased by chemical modification of Amberlite XAD-4 with carbon tetrachloride and benzoyl chloride (XAD-4-I and XAD-4-II) according to the Friedel–Crafts reaction (Li et al., 2013). Li et al.,. reported that after chemical modification, the Brunauer–Emmet–Teller (BET) surface area and pore volume of the resins increased about 50% while their median pore size remained constant. More importantly, they reported that the modified resin adsorbed about 20% more phenol from aqueous solution than the original XAD-4 over all experimental temperatures. With reported initial phenol concentration of 574.0 mg l^{-1}, the dynamic adsorption capacities of XAD-4, XAD-4-I and XAD-4-II were measured to be 80.6, 94.8 and 93.6 mg g^{-1}, respectively (Li et al., 2013).

As discussed, polymeric adsorbents and their derivatives are potential alternatives to activated carbons for the adsorption of pollutants from contaminated waters. However, there are still many challenging issues reported on the synthesis and application of polymeric adsorbents for environmental concerns (Pan et al., 2009). The adsorption capacities of polymeric adsorbents towards water – soluble pollutants, i.e. hydrophobic ionisable organic compounds, is relatively low and frequent regeneration is required for repeated use, resulting in high operation costs in industrial applications.

1.5.2.3 Zeolites

Zeolites have been investigated as potential sorbents because of their (i) high selectivity; (ii) high specific capacity; (iii) reliable release performances (to be exploited within regenerative methodologies) and (iv) excellent resistance to chemical, biological, mechanical and thermal stress (Perego et al.,. 2013).

Zeolites are an important class of hydrated aluminosilicates, they possess cage-like structures with internal and external surface areas up to several hundred square meters per gram (Damjanovic et al., 2010). They were first described as a mineral group by the Swedish mineralogist Baron Axel Cronstedt in 1956. Zeolites do not comprise an easily definable family of crystalline solids and since there are over 200 synthetic and 50 natural zeolites, a particular zeolite may best be described in terms of its framework topology. Each unique framework topology is designated a structure code by the Structure Commission of the International Zeolite Association (IZA-SC) consisting of three capital letters. There are 152 framework codes, 133 of these appear in the fifth edition of the Atlas of Zeolite Framework Types. Since its publication, 34 additional codes have been approved (Baerlocher et al.,. 2001). They are a class of crystalline aluminosilicates based on rigid anionic frameworks with well defined channels and cavities. The general formula for the composition of a zeolite is:

$$M_{x/n}\left[(AlO_2)_x(SiO_2)_y\right]\cdot mH_2O \qquad \textbf{Equation 1.3}$$

where cations M of valence n neutralize the negative charges on the aluminosilicate framework. The framework is constructed from SiO_4 and AlO_4 tetrahedra (figure 1.2), which are interlinked by oxygen atoms (these tetrahedra are the primary building units of zeolites) (Dann 2000; Hagen 1999). The net formula of the tetrehedra is SiO_2 and AlO_2^- i.e. one negative charge resides at each tetrahedron in the framework which has aluminium at its centre (Weitkamp 2000). This is attributed to the fourth oxygen, which imparts a negative or anionic charge to the Al atom; aluminium atoms require three bound atoms before they join the framework. The electrical imbalance is neutralized by a cation or positively charged ion held electrostatically within the zeolite (figure 1.2). The zeolite Si/Al-O framework is rigid, but the cations are not an integral part of this framework and are often called exchangeable cations: they are fairly mobile and readily replaced by other cations.

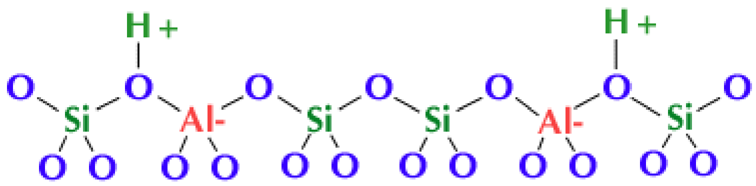

Figure 1.2: Basic structure of zeolites including Bronsted acid sites.

The Si/Al ratio plays a very important role in determining the adsorptive properties of zeolites. The Si/Al ratio in a zeolite is never less than 1 but there is no upper limit and pure silica analogs of some of the zeolite structures have been prepared. Clearly, changing the Si/Al ratio of the zeolite also changes its cation content; the fewer the aluminium atoms there are, the fewer exchangeable cations will be present. The presence and position of these cations in the zeolite framework is important for several reasons. The cross section of the rings and channels in the structures can be altered by changing the size or charge of the cations and this significantly affects the size of the molecule that can be adsorbed. A change in cationic occupation also changes the charge distribution within the cavities, and thus the adsorptive behaviour. These cations cause the surface of the zeolite to be more heterogeneous, attracting more polar molecules.

The stability of the zeolite framework increases with increasing Si/Al ratio. Zeolites with high Si/Al ratios are stable in the presence of concentrated acids but those with low Si/Al ratios are not.

Properties affected by framework Al content include:

- their microporous character with uniform pore dimensions, allowing certain hydrocarbon molecules to enter the crystals while rejecting others based on too large a molecular size,
- the ion exchange properties which allow to perform all sorts of ion exchange reactions,
- the ability to develop internal acidity which makes zeolites interesting materials for catalyzing organic reactions,
- their high thermal stability allowing them to be regenerated while keeping their initial properties,
- All metal oxygen tetrahedral exposed to the surface,
- Hydrophilic or hydrophobic surface properties.

Zeolites have been given the name of molecular sieves because of this ability to discriminate i.e. selectively adsorb or reject molecules based upon molecular size, shape and other properties including polarity (Kirk-Othmer 1995). The adsorptive properties of zeolites show a systematic transition from the aluminium-rich types, which have very high affinities for water and other polar molecules (Damjanovic et al.,. 2010), to the highly siliceous types which are essentially hydrophobic and adsorb hydrocarbons in preference to water (Shu et al.,. 1997). The important structural feature of zeolites, which can be exploited for various uses, is the network of linked cavities or pores forming a system of channels throughout the structure. These cavities are of molecular dimensions and can adsorb species small enough to gain access to them. A controlling factor in whether molecules can be adsorbed within the cavities is the size of the window or pore openings in the channel (Damjanovic et al., 2010). Hence, the importance of the number of tetrahedrals forming the window, i.e. the ring size.

These properties make zeolites unique in comparison to crystalline inorganic oxide materials. Synthetic and natural zeolites have been widely used as adsorbents, catalysts, ion exchangers, membrane sieves (Damjanovic et al., 2010, Yousef et al., 2011, Ali et al., 2012, Liotta, L., F. 2010 and Adam et al., 2013). Zeolites will therefore fulfil the initial prerequisite for this work by functioning as an adsorbent which removes nitrogen containing organic species from solution.

1.5.3. Oxidation Processes

Organic pollutants are in general harmful to health and the environment and adsorption merely transfers the pollutant from the liquid or air to the solid leaving a contaminated adsorbent for further disposal (Gitchel et al., 1975; Charest et al., 1976; Perrich 1981), therefore, other treatment methods are required such as Wet Air Oxidation and catalytic treatment methods, to eliminate the offending pollutant. Oxidation processes are one of the major techniques used during water treatment for the destruction of organic pollutants. They can be divided into the following categories: chemical oxidation and air/oxygen based oxidation. The first category includes advanced oxidation processes (AOPs). The second category includes wet air oxidation, catalytic wet air oxidation and dry oxidation.

1.5.3.1 Advanced Oxidation Processes

The degradation and mineralization of organic pollutants in wastewater by AOPs is based on the generation of a very reactive free hydroxyl radical ($OH^{\bullet}$). This radical is highly reactive, non-selective and may be used to degrade a wide range of organic pollutants. It reacts with most organic compounds by forming a double bond or by abstracting hydrogen atoms from organic molecules (Safarzadeh-Amir et al., 1997; Buxton et al., 1988). The resulting organic radicals then react with oxygen, which leads to complete mineralization to CO_2, H_2O and mineral acids (Oliveros et al., 1997). However, these processes tend to be limited by their intensive costs. Fenton systems (Fe^{2+} / Fe^{3+}/ H_2O_2) are often used for industrial water treatment based on AOPs (Fenton 1894, Neynes and Baeyens 2003, Babuponnusamia and Muthukumarb 2013). The degradation rate of organic pollutants with Fenton regents strongly depends on irradiation with ultraviolet light (UV), and increases with increased UV irradiation intensity (Safarzadeh-Amiri et al., 1996). The use of UV light results in a significant increase in the cost of industrial water treatment. Post treatment requires the elimination of Fenton reagents as colloidal precipitates. The separation of colloidal precipitates requires the use of additional processes such as coagulation, sedimentation and filtration.

1.5.3.2 Wet Air Oxidation

Wet air oxidation (WAO) is an attractive method for the treatment of waste streams which are too dilute to incinerate and yet too toxic to treat biologically (Dietrich et al., 1985). It involves the aqueous phase oxidation of organics or oxidizable inorganic components at elevated temperatures and pressures using a gaseous source of oxygen (usually air) (Mishra et al., 1995). Although the reactants necessary for oxidation are inexpensive, the process itself can become very expensive if it is used for complete oxidation of all contaminants present in the wastewater (Suarez-Ojeba et al., 2008).

The efficiency of aqueous phase oxidation can be largely improved by the use of catalysts, either in the form of solids or as homogeneous catalysts.

1.5.3.3 Catalytic Wet Air Oxidation

The use of a catalyst strongly improves the degradation of organic pollutants by using milder conditions of temperature and pressure (Liotta et al., 2010). Depending on the type and amount of organic compounds dissolved in wastewater, the process can be designed either to reduce their concentration or ultimately destroy them. In the former case the intermediate products formed during the oxidation process must be biodegradable (Hamoudi and Sayari 2000).

The catalysts used in CWAO can be generally divided into three categories: (1) oxides of the transition metals, (2) supported noble metals and (3) metal salts and their complexes.

Homogenous catalysts such as copper cations are in general very effective WAO catalysts (Chowdhury and Ross 1975; Imamura et al., 1982; Kulkarni and Dixit 1991; Shende and Mahsjani 1994; Lin et al., 1996, Arena et al., 2010) but their recovery from the treated effluent requires additional separation costs (Gallezot et al., 1997). Consequently, heterogeneously catalyzed WAO has attracted a lot of attention because of its potential as a method for purifying wastewaters. Heterogeneously catalyzed applications based on noble metals (Pt, Ru, Pd, Rh, Ir, Ag) and metal oxides (Mn, Co, Cu, Zn,V, Ni, Fe, Bi, and Ti) using different supports (Al_2O_3, CeO_2, TiO_2, ZrO_2, NaY zeolite) have been studied (Luck 1999; Mishra et al., 1995; Matatov-Meytal and Sheintuch 1999 and Imamura 1999). Regarding heterogeneous catalysts, both categories present advantages and drawbacks. Noble metals are expensive components increasing considerably the process cost. On the other hand, oxides of transition metals have been found in some cases to be unstable due to deactivation by leaching of the metals to the liquid phase, fouling of surface and adsorption of carbonyl compounds by the catalysts (Matatov-Meytal and Sheintuch 1999). In this context, it is quite important to develop economical, active and stable catalysts that can be effective for degradation of organic compounds by CWAO.

Most of the active catalysts proposed for CWAO of phenolic compounds are solids containing either noble metals (Pt, Ru) or transition metal cations (Cu, Co, Mn, Fe). Frequently, such active phases are supported on alumina or carbon carriers (Suarez-Ojeba et al., 2008). In table 1.8, some results on the catalytic oxidation of phenol using transition metal oxides in CWAO systems are listed. One of the most active catalysts that have been developed for CWAO of phenol, in terms of total organic carbon (TOC) removal, is PtAg-MnO_2/CeO_2. This achieved 80% TOC removal in 1 hour at 80ºC using an oxygen partial pressure of 0.5 MPa (Levec and Pintar 2007). Pintar and Levec studied the CWAO of phenol over mixed copper and zinc oxides supported on alumina and found this catalyst to be very effective for complete removal of phenol within 100 min at 130°C (Pintar and Levec 1997). Treatment of nitrogen–containing compounds is one of the main fields where CWAO has worked well. The wet oxidation of nitrophenol has been studied at 150°C and 200°C in a stirred autoclave. It decomposed to give lower molecular weight compounds including formic and acetic acids (Kunishige et al., 1992).

Table 1.8: Catalytic wet oxidation of phenol substrates over transition metal oxides.

Catalysts	%Phenol conversion or (% TOC removal)	Conditions	Reference
Cu/Ni/Al-Hydrotalcite	100, (99.1)	T=140°C P_{O2}=900 kPa, 2.5 h	Alejandre et al., 2007
Cu-Zn-Al_2O_3	100	T=130°C P_{O2}=300; 560 kPa, 2.5 h	Levec 1990
ZnO-CuO-C Al_2O_3	100	T=130°C P_{O2}=500 kPa, 40 min	Akyurtlu et al., 1998
Bimetallic catalysts: CuO-CoO; $CuOFe_2O_3$;	>80; 50; 20-30%	T=140°C P_{O2}=900 kPa, 0-6 h; 24 h;>96 h	Fortuny et al., 1995
CeO_2	(90)	T=160°C P_{O2}= 1000 kPa, 3 h	Lin et al., 2003
CeO_2/y-Al_2O_3	100	T=180°C P_{O2}=1500 kPa, 2 h	Chen et al., 2004; Chang et al., 2005
Al-Fe pillared clay	100	T=130°C P_{air}=1500 kPa, 100 min	Quintanilla et al., 2006
Fe/AC	100, (80)	T=127°C P_{O2}=808 kPa,	Quintanilla et al., 2006
Activated carbons	100	T=160°C P_{O2}=1600 kPa	Santos et al., 2006

The activity of different noble metals (Pt, Pd, Ru, Rh, Ag) supported on alumina or titania in the oxidation of p-chlorophenol has also been reported, Pt gave the best results by reaching 100% conversion after 30 minutes.

CWAO may not be economically attractive for low concentration of organics because of the energy requirements to heat up wastewater streams. High organic concentrations in wastewater provide however, enough heat so that the process is thermally self sufficient, in these cases the process becomes economically feasible.

The disadvantages associated with CWAO include (1) the extremely large volume of raw water that needs to be treated in the oxidation system and (2) incomplete mineralization can lead to the production of secondary more toxic substances.

Compared to other organic removal processes such as filtration and adsorption, CWAO produces no liquid or solid waste, providing 100% organic oxidation is achieved and the catalysts are stable and/or are easily removed.

1.5.3.4 Catalytic Oxidation

Catalytic oxidation is a technique in which volatile organic compounds (VOCs) that are usually contained in a gaseous stream are oxidized in the presence of catalysts. The desired reaction is the total oxidation of these pollutants to H_2O and CO_2 without the formation of by-products. The presence of the catalysts allows the gas phase reaction to proceed a lower temperatures compared to the reaction in the absence of a catalytic component. The commercial catalysts used in the gas phase total catalytic oxidation of VOCs can be divided into three categories:

1.0 Supported noble metals, e.g. Pt/Al_2O_3, Pd/SiO_2

1.2 Metal oxides or supported transition metal oxides, e.g. Fe_2O_3, V_2O_5, CuO/Al_2O_3

1.3 Mixtures of noble metals and metal oxides.

Although in principle any of these metals may be used as oxidation catalysts, in most practical systems, only Pt, Pd and a few alloys are used because the generally higher temperatures employed for most oxidation catalysts applications can cause sintering, volatility loss, and irreversible oxidation of the other metals (Spivey 1987). It has been reported in literature that palladium catalysts are slightly more active, while platinum catalysts are more selective to CO_2 (Lopez-Fonseca et al., 2005; Cordi et al.,. 1997; Parida and Amarendra 1999; Gangwal et al.,. 1988 and Centi et al.,. 1995). Noble metals such as Pd, Pt, Ag, and Au are usually supported on an oxide support such as γ-Al_2O_3 or SiO_2 (Lopez-Fonseca et al., 2005). It is well known that the characteristics of the support can play a significant role in determining catalytic performance (Lopez-Fonseca et al., 2005).

Metal oxides generally have somewhat lower activity than noble metal catalysts for VOC total oxidation, but they have greater resistance to certain poisons (especially halogens, As, Pb, and P). This poison resistance is largely attributed to their high active surface area compared to that of supported noble metals. These oxides are characterized by high electron mobility and positive oxidation states. The most active single metal oxide catalysts for the complete oxidation for a variety of oxidation reactions are usually found to be oxides of V, Cr, Mn, Fe, Co, Ni, and Cu (Spivey 1987). The catalytic activity of oxides of Cu Mn, Fe, Co, V, Mo, Cr, Ni, and Zn supported on γ–Al_2O_3 were investigated for the oxidation of VOCs and Cu/γ-Al_2O_3 proved to be the most promising catalyst, followed by Mn and Fe; the least active samples were Ni and Zn (Kim 2002). The gas phase oxidation of toluene was carried out over Cu, Mn, Fe, Co, V, Mo, Cr, Ni and Zn supported on – γ-Al_2O_3. The complete oxidation of toluene was preformed with 1000 ppm concentrations in air within a temperature range of 200 – 300°C and similarly the most active catalyst was Cu/γ-Al_2O_3. (Kim and Parker 2002).

Since Blocki (1993) proposed hydrophobic zeolites as promising adsorbents, due to their thermal stability, their pore structure and their ion exchange capacity the use of hydrophobic molecular sieves such as high silica zeolites as potential active catalysts for the oxidation of VOCs has grown (Blocki 1993 and Sipvey 1987). They are generally useful as supports for transition metals or noble metals which are exchanged onto the zeolites. Some examples of zeolite use or potential use as environmental catalysts are listed in table 1.9.

Table 1.9: Examples of zeolites in environmental applications.

Zeolite Catalyst	Application
High silica, hydrophobic ZSM-5, and zeolite Y	VOC removal
Fe/ZSM-5	Nitrogen oxide selective catalytic reduction with ammonia
Cu/ZSM-5, Co/ZSM-5, Fe/ZSM-5, Cu/mordenite, Co/mordenite and Fe/ mordenite	N_2O decomposition
Co/ZMS-5, Cu-ZMS-5, Cu/β, and Co/β	Nitrogen oxide selective catalytic reduction with hydrocarbons

For these applications, transition metal exchange zeolites often exhibit greater activities than traditional metal oxide catalysts. The catalytic activity of the transition metal–exchanged zeolite depends on the identity of the zeolite host and of the exchanged transition metal. For example, copper exchanged ZSM-5 is active for the direct decomposition of NO_x, but copper exchanged Y zeolite is not active. Similarly, cobalt–exchanged ZSM-5 is active for the selective catalytic reduction of NO_x with CH_4 but copper–exchanged ZSM-5 is not active.

The advantage of zeolite catalysts over conventional catalysts include:

1. their ease of synthesis,
2. their high surface area (typically 600 m^2g^{-1}), the majority of which (95%) is internal and accessible through apertures of defined dimension (Thomas and Thomas 1997).
3. the thermal stability of zeolites (e.g. they are capable of surviving heat treatments in air up to 1000°C, depending upon the composition of the zeolite

framework) hence it is possible to regenerate them by combustion of carbon deposits.

1.6. Proposed System for the Removal of Organic Compounds from Waste Streams.

The aim of this research project is to develop a solid regenerable catalytic adsorbent capable of removing selected organic compounds from aqueous waste streams.

This is to be achieved by the development of a two step process involving:

1. The removal of the aqueous contaminant of concern by adsorption onto a selective adsorbent/catalyst.
2. The oxidation of this adsorbed pollutant into carbon dioxide, water and nitrogen whilst regenerating the adsorbent/catalyst material.

A simple schematic of this proposed is presented in Figure 1.3. The process is a closed loop, whereby the process wastewater is recycled.

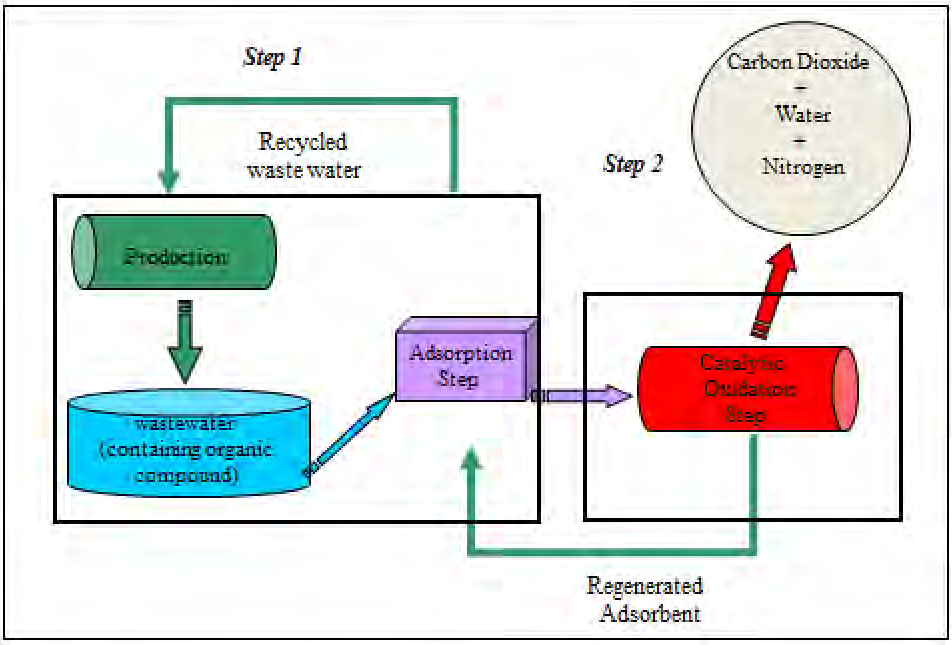

Figure 1.3: Schematic representation of the adsorption/catalytic process.

The production of a wastewater containing 2-nitrophenol is to be subsequently treated by an adsorption process (step1). During the adsorption process a known quantity of adsorbent (Beta zeolite) is to be contacted with the rinse water containing 2-nitrophenol. Once the adsorbent has become saturated with the adsorbate (2-nitrophenol) it must be regenerated to allow successive adsorption steps to be carried out. The second step of this work examines this issue and proposes the total oxidation of the adsorbed 2-nitorphenol in the presence of a catalytic element which would promote the oxidation of the adsorbed 2-nitorphenol and enable the adsorbent / catalyst to be simultaneously regenerated.

Nitrophenols are among the most important and versatile industrial organic compounds and are common pollutants found in effluents from pesticides, pharmaceutical, petrochemical and other industries (Qiuli and Sorial 2004). 2-nitrophenol was chosen as the model pollutant in this work because it is a simple nitrogen containing hydrocarbon representative of nitrophenol compounds typically occurring in waste streams. Zeolites were the adsorbents of choice in this study as they have high surface area, are highly porous and thermally stable. They have the ability to discriminate, i.e. selectively adsorb or reject molecules, based upon molecular size, shape and other properties including polarity and they can therefore function as adsorbents. Zeolites also have the ability to function as catalysts. Copper exchanged zeolites have been shown to be extremely active for the catalytic oxidation of ammonia to nitrogen and water with low levels of NO and N_2O being formed (Lenihan and Curtin 2003). It is envisaged that these findings may be extended to the oxidation of 2-nitrophenol (adsorbed on the exchanged zeolite surface). In this case the objective would be to totally oxidize the adsorbed 2-nitrophenol to carbon dioxide, water and nitrogen with minimum formation of undesirable products such as NO and NO_2. In this research work, unmodified and copper modified beta zeolite were investigated with a view to examining their potential as adsorbents for the removal of 2-nitrophenol from aqueous solutions with subsequent catalytic dry oxidation of the adsorbed 2-nitrophenol at atmospheric pressure to carbon dioxide, nitrogen and water.

1.7 References

Adam. F., Wong, J-T. and E-P Ng, (2013) 'Fast Catalytic Oxidation of Phenol over Iron Modified Zeolite L Nanocrystals', *Chemical Engineering Journal*, **214**, 63-67.

Ahmaruzzaman, M. and D. K. Sharma. (2005) 'Adsorption of Phenols from Waste Water', *Journal of Colloid and Interface Science*, **287,** 14-24.

Akcay M. and G. Akay. (2004), 'The Removal of Phenolic Compounds from Aqueous Solutions by Organophilic Bentonite', *Journal of Hazardous Materials*, **113,** 189- 193.

Aksu, Z. and J. Yener (1998) 'Investigation of the Bioadsorption of Phenol and Mono chlorinated Phenols on the Dried Activated Sludge', *Process Biochemistry*, **33,** 49-655.

Aksu, Z. and J. Yener (2001) 'A Comparative Adsorption/Biosortion Study of Mono-Chlorinated Phenols onto various Sorbents', *Waste Management*, **21,** 695-702.

Akyurtlu, J., Akyurtlu, A. and S. Kovenklioglu (1998) 'Catalytic Oxidation of Phenol in Aqueous Solutions', *Catalysis Today*, **40**, 343-352.

Alejandre A., Medina, F., Salagre, P., Fabregat, A. and J. Sueiras (1998) 'Characterization and Activity of Copper and Nickel Catalysts for the Oxidation of Phenol Aqueous Solutions', *Applied Catalysis B*: *Environmental*, **18**, 307-315.

Ali, I., Asim, M. and T. A. Khan (2012) 'Low cost adsorbents for the removal of organic pollutants from wastewater', *Journal of Environmental Management*, **113**, 170-183.

Arena, F., Italiano, C., Raneri, A. and C. Saja (2010) 'Mechanistic and kinetic insights into the wet air oxidation of phenol with oxygen (CWAO) by homogeneous and heterogeneous transition – metal catalysts', *Applied Catalysts B: Environmental*, **99**, 321-328.

Babuponnusamia, A. and K. Muthukumarb (2012) 'Advanced oxidation of phenol: A comparison between Fenton, electro-Fenton and photo-electro-Fenton processes', *Chemical Engineering Journal*, **183**, 1-9.

Baerlocher, C., Meier, W.M. and D.H. Olson (Eds.) (2001) Atlas of Zeolite Framework Types Elsevier, Amsterdam.

Bagreev, A., Rahman, H. and T. J. Bandosz, (2001) 'Thermal Regeneration of Spent Coconut-based Activated Carbon Previously used as Hydrogen Sulfide', *Adsorbent Carbon* **39**, 1319-1326.

Basta, A. H., Fierro, V., Sailed, H. and A. Celzard (2011) ' Effects of deashing rice straws on their derived activated carbons produced by phosphoric acid activation', *Biomass and Bioenergy,* **35**, 1954 – 1959.

Bennett, A. (2000) 'Developments in Industrial Water Re-use', *Filtration and Separation*, **39,** 26-28.

Benselka – Hadj Abdelkader, N., Bentouami, A., Derriche, Z., Bettahar, N. and L. C. de Menorval (2011) 'Synthesis and characterisation of Mg-Fe layer double hydroxides and its application on adsorption of orange G from aqueous solution, *Chemical Engineering Journal*, **169**, 231-238.

Blocki, S. W. (1993) 'Hydrophobic zeolite adsorbent: A proven advancement in solvent separation technology', *Environmental Progress,* **12**, 226-230.

Bonjour, J., Clausse, M. and F. Meunier (2005) 'A TSA process with indirect heating and cooling: parametric analysis and scaling-up to practical sizes' *Chemical Engineering Process*, 44, 969-977.

Buttino, I. (1994) 'The Effect of Low Concentrations of Phenol and Ammonia on Egg Production Rates, Fecal Pellet Production and Egg Viability of the Calanoid Copepod Acartia clausi', *Marine Biology*, **119,** 629-634.

Buttino, I., Filippi, M. and N. Cardellicchio (1991) 'Tossicita dei composti fenolici nell' ambiente marino', *Acqua Aria*, **9,** 853-861.

Buxton, G. V., Greenstock, G. L., Helman, W. P. and Ross, A. B (1988) 'Critical Review of Rate Constants for Reactions of Hydrated Electrons', *Journal of Physical Chemistry Reference Data*, **17**, 513-886.

Calace, N., Nardi, E., Petronio, M. B. and M. Pietroletti (2002) '*Adsorption of phenols by papermill sludge*', **118**, 315-319.

Campbell, I. M. (1988) Catalysis at Surfaces, Chapman and Hall, London; New York.

Carratala-Abril, J., Lillo-Rodenas, M. A., Linares-Solano, A. and D. Cazorla-Amoros (2010) ' Regeneration of activated carbons saturated with benzene ot toluene using an oxygen-containing atmosphere', *Chemical Engineering Science*, **65**, 2190-2198.

Centi, G., Perathoner S., Biglino D. and E. Giamello (1995) 'Adsorption and Reactivity of NO on Copper-on-Alumina Catalyst: Formation of Nitrate Species and Their Influence on Reactivity in NO and NH_3 Conversion', *Journal of Catalysis* , **152**, 75-92.

Chang, L., Chen, I. P. and S. S. Lin (2005) 'An Assessment of the Suitable Operation Conditions for the $CeO_2/\gamma\text{-}Al_2O_3$ Catalyzed Wet Air Oxidation of Phenol', *Chemosphere*, **58**, 485-492.

Charest, F., Chornet, E. and J. Can (1976) 'Wet Oxidation of Active Carbon', *Chemical Engineering*, **54**, 190.

Cheknane, B., Bauda, M., Basly, J. P. and O. Bouras (2010) 'Adsorption of basic dyes in single and mixture systems on granular inorganic-organic pillared clays', *Environmental Technology*, **7**, 815-822.

Chen, I. P., Lin, S. S., Wang, C. H., Chang, L. and J. S. Chang (2004) 'Preparing and Characterizing an Optimal Support Ceria Catalyst for Catalytic Wet Air Oxidation of Phenol', *Applied Catalysis B: Environmental*, **50**, 49-58.

Chowdhury, A. K. and L. W. Ross (1975) 'The Catalytic Wet Oxidation of Strong Waste Waters', *American Institute of Chemical Engineering Symposium Series*, **71**, 46-48.

Cordero. T., Rodriguez, M., Bedia J., Gomis, S., Yustos, P., García-Ochoa, F. and A. Santos (2008) 'Activated Carbon as Catalysts in Wet Oxidation of Phenol: Effect of the Oxidation Reaction on the Catalysts Properties and Stability', *Applied Catalysts B*: *Environment*, **81,** 122-131.

Cordi. M. O' Nell, P. J. and L. Falconer. (1997) 'Transient Oxidation of Volatile Organic Compounds on a CuO/Al_2O_3' *Applied Catalysis B: Environmental*, **14**, 23-36.

Dabrowski, A., Podkoscielny, P., Hubicki, Z. and M. Barczak. (2005) 'Adsorption of phenolic compounds by activated carbon - a critical review', *Chemosphere*, **58**, 1049-1070.

Damjanovic, L., Rakic, V., Rac, V., Stosic, D. and A. Auroux. (2010) 'The Investigsation of Phenol Removal from Aqueous Solutions by Zeolites as Solid Adsorbents', *Journal of Hazardous Materials*, **184**, 277-484.

Dann, S. E (2000) Reactions and Characterization of Solids, Royal Society of Chemistry Cambridge.

Daifullah, A. E. H. and H. Gad. (1998) 'Sorption of Semi-Volatile Organic Compounds by Bottom and Fly Ashes using HPLC', *Adsorption Science and Technology*, **16,** 273-283.

Davankov, V. A., Rogozhin, S.V. and M. P. Tsyurupa (1971) US Patent Application 3, 729, 457.

Davankov, V. A. and M. P. Tsyurupa (1990) 'Structure and properties of hypercrosslinked polystyrene – the first representative of a new class of polymer networks', *Reactive Polymer*,**13**, 27-42.

Delval, F., Crini, G. and J. Vebrel. (2006) 'Removal of Organic Pollutants from Aqueous Solutions by Adsorbents prepared from an Agroalimentary by-product', *Bioresource Technology*, **97,** 2173-2181.

Denizli, A., Cihangir, N., Tuzmen, N. and G. Alsancak (2005) 'Removal of Chlorophenols from Aquatic Systems using the Dried and Dead Fungus Pleurotus sajorcaju', *Bioresource Technology*, **96,** 59-62.

Depecker, G.., Branger, C., Margaillan, A., Pigot, T., Blanc, S., Robert-Peillard, F., Coulomb, B. and J. L. Boudenne (2009) 'Synthesis and application of XAD-4 – DAN chelate resin for the separation and determination of Se(IV), *Reactive and Functional Polymers*, **69**, 877-833.

DeSilva, F. (1996) 'Tips for Process Water Purification', *Chemical Engineering. Journal*, **103**, 72-82.

Dietrich, M. J., Randall, T. L. and P. J. Canney (1985) 'Wet Air Oxidation of Hazardous Organics in Wastewater', *Environmental Progress*, **4**, 171-177.

Dong, Y., Wu, D., Chen, X. and Y. Lin (2010)'Adsorption of bisphenol A from water by surfactant modified zeolite', *Journal of Colloid Interface Science*, **348**, 585-590.

Dutta., S., Basu, J. K. and R. N. Ghar (2001) 'Studies on Adsorption of p-nitrophenol on Charred Saw Dust', *Separation and Purification Technology*, **21,** 227-235.

European Pollutant Emission Register, 2006, European Environment Agency. http://www.eper.cec.eu.int/eper/

Fenton, H. J. H. (1894) 'Oxidation of tartaric acid in presence of iron' *Journal of the Chemical Society*, **65**, 899-910.

Fortuny, A., Ferrer, A., Bengoa, C., Font, J. and A. Fabregat. (1995) 'Catalytic Removal of Phenol from Aqueous Phase using Oxygen or Air as Oxidant', *Catalysis Today*, **24,** 79.

Fu, D., Zhang, Y., Lv. F, Chu, P. K. and J. Shang (2012) 'Removal of organic materials from TNT red water by Bamboo Charcoal adsorption', *Chemical Engineering Journal*, **193–194**, 39-49

Gallezot, P., Chaumet, S., Perrard, A. and P. Isnard (1997) 'Catalytic Wet Air Oxidation of Acetic Acid on Carbon-Supported Ruthenium', *Journal of Catalysis*, **168**, 104-109.

Gangwal, S. K., Mullins, M. E. Spivey, J. J. and P. R. Caffrey. (1988) 'Kinetics and Selectivity of Deep Catalytic Oxidation of n-Hexane and Benzene', *Applied Catalysis*, **36**, 231-247.

Gercel,O., Ozcan, A., Ozcan, A. S. and H. F. Gercel (2009) ' Preparation of activated carbon from a renewable bio – plant of Euphorbia rigida by H_2SO_4 activation and its adsorption behaviour in aqueous solution', *Applied Surface Science*, **253**, 4843-4852.

Ghaedi, M., Karami, B., Ehsani, S., Marahel, F. and M. Soylak (2009) ' Preconcentration – separation of Co^{2+}, Ni^{2+}, Cu^{2+} and Cd^{2+} in real samples by solid phase extraction of a calix[4] resorcinarene and modified Amberlite XAD-16 resin', *Journal of Hazardous Material*,**172**, 802-808.

Girgis, B. S., Smith, E. Louis, M. M. and A. N. A. El–Hendawy (2009) 'Pilot production of activated carbon from cotton stalks using H_3PO_4, *Journal of Analytical and Applied Pyrolysis*, **86**, 180-184.

Gitchel, W, B., Meidl, J. A. and W. Burant (1975) ‘Carbon Regeneration by Wet Air Oxidation’, *Chemical Engineering*, Journal, **151,** 90-91.

Grini, G. (2005) ‘Recent Developments in Polysaccharide – Based Materials used as Adsorbents in Wastewater Treatment’, *Progress in Polymer Science, Sci.* **30**, 38-70.

Guerra, G. (2001) ‘Ecotoxicological and Chemical Evaluation of Phenolic Compounds in Industrial Effluents’, *Chemosphere,* **44**, 1737-1747.

Guo, Y. and E. Du (2012) ‘The effects of thermal regeneration conditions and inorganic compounds on the characteristics of activated carbon used in power plant’, *Energy Procedia*, **17**, 444-449.

Guo, D., Shi, Q., He, B. and X. Yuan (2011) ‘Different solvents for the regeneration of the exhausted activated carbon used in the treatment of coking wastewater’, *Journal of Hazardous Materials*, **186**, 1788-1793.

Guo, Y. P., Yu, K. F., Wang, Z. C. and Xu, H. D. (2000) ‘Effects of activation conditions on preparation of porous carbon from rice husk’, *Carbon*, **41**, 1645-1687.

Gupta, V.K., Gupta, B., Rastogi, A., Agarwal, S. and A. Nayak (2011) ‘Pesticides removal from waste water by activated carbon prepared from waste rubber tire’, *Water Research*, **45**, 4047-4055.

Gupta, V. K., Sharma, S., Ysdav. I .S. and D. Mohan (1998) ‘Utilization of Bagasse Fly Ash in the Sugar Industry for the Removal and Recovery of Phenol and p-nitrophenol from Wastewater’, *Journal of Chemical Technology and Biotechnology*, **71**, 180-186.

Hagen, J. (1999) Industrial Catalysis – A Practical Approach, Wiley-VCH.

Hamdaoui, O. and E. Naffrechoux (2007) ‘Modeling of adsorption isotherms of phenol and chlorophenols onto granular activated carbon Part I. Two parameter models and equations allowing determination of thermodynamic parameters’, *Journal of Hazardous Materials*, **147**, 381-394.

Hamoudi, S. and Sayari, A. (2000) ‘Catalytic Wet Oxidation of Phenol over PtAg 1-$MnO_2/Ce/O_2$ Catalysts’, *Catalysis Today*, **62**, 379-388.

Han, X., Wang, W. and X. Ma (2011) ‘Adsorption characteristics of methylene blue onto low cost biomass material lotus leaf’, *Journal of Chemical Engineering*, **171**, 1-8.

Hancock, F. E. (1999) ‘Catalytic Strategies for Industrial Water Re-use’, *Catalysis Today*, **53**, 3-9.

He, W., Lu, G., Cui, J., Wu, L. and L. Liao (2012) ‘ Regeneration of spent activated carbon by yeast and chemcial methods’, *Chinese Journal of Chemcial Engineering*, **20**, 659-664.

Huang, J. H., Jin, X. Y. and S. G. Deng (2012) 'Phenol adsorption on an N-methylacetamide –modified hypercrosslinked resin from aqueous solutions', *Chemical Engineering Journal*,192, 192-200.

Hussain, S. N., Roberts, E.P.L. Asghar, H.M.A., Campen, A.K. and N.W. Brown (2013) 'Oxidation of phenol and the adsorption of breakdown products using a graphite adsorbent with electrochemical regeneration', *Electrochimica Acta*, **92**, 20-30.

Hwang, K. S., Choi, D. K., Gong, S. Y. and Y. Cho (1997) 'Adsorption and thermal regeneration of methylene chloride vapour on an activated carbon bed', *Chemical Engineering Science*, **52**, 1111-1123.

Imamura, S. (1999) 'Catalytic and Noncatalytic Wet Oxidation', *Industrial Engineering Chemistry Research*, **38,** 1743-1753.

Imamura, S., Hirano, A. and N. Kawabata (1982) 'Wet Oxidation of Acetic Acid Catalyzed by Co-Bi Complex Oxides', *Industrial and Engineering Chemistry Product Research Development*, **21,** 570-575.

Jawad, H. A. R., H. Khabbaz and A. I. Schafer (2011) 'Removal of pharmaceuticals and endocrine disrupting compounds in a water recycling process using reverse osmosis system', *Separation and Purification Technology*, **77**, 60-67.

Jung, W. and K. Ahn (2001), 'Adsorption Characteristics of Phenol and Chlorophenol on Granular Activated Carbon', *Microchemical Journal*, **70**, 123-131.

Karcher, S., Kornmuller, A. and M. Jekel (2001) 'Screening of Commercial Sorbents for the Removal of Reactive Dyes and Pigments', *Dyes and Pigments,* **51**, 111-125.

Karnovic-Ozretic, M. and B. Orzetic (1988) 'Toxic Effects of Phenol on Grey Mullet. Mugilus auratus Slva Risso', *Bulletin of Environmental Contamination and Toxico*logy, **40**, 23-29.

Kim, H. S. (2002) 'The Catalytic Oxidation of Aromatic Hydrocarbons over Supported Metal Oxide', *Journal of Hazardous Materials* B, **91**, 285-299.

Kim K.-H. and S.- K. Ihm (2011), 'Heterogeneous catalytic wet air oxidation of refractory organic pollutants in industrial wastewaters: A review', *Journal of Hazardous Material*, **186**, 16-34.

Kim, S.C. and C.Y. Park (2002) 'The Complete Oxidation of a Volatile Organic Compound (Toluene) Over Supported Metal Oxide Catalysts', *Research on Chemical Intermediates*, **28 (5),** 441-449.

Kirk- Othmer (Ed.) (1995) Encyclopedia of Chemical Technology, John Wiley and Sons, London New York.

Koganovskii, A. M. and R. L. Kanniskaya (1981), *Technology Today*, **3**, 437.

Ku, Y., and K.C. Lee (2000) ‘Removal of phenols from aqueous solution by XAD-4 resin’, *Journal of Hazardous Materials*,**80**, 59-68.

Kunishige, H., Kawahara, Murakami, Y., Wakida, S., Yamane, M. and S. Takeda (1992) ‘Decomposition of Nitrophenol by Wet Air Oxidation in the Presence of Nobel Metal Catalysts’, *Kankyo Gijutsu*, **21**, 689-694.

Kulkarni, U. S. and S. G. Dixit (1991) ‘Destruction of Phenol from Wastewater by Oxidation with Sulfite-oxygen’, *Industrial Engineering Chemistry Research*, **30**, 1916 -1920.

Levec, J. and A. Pintar. (2007) ‘Catalytic Wet –Air Oxidation Processes: A Review’, *Catalysis Today*, **124**, 172-184.

Li, A., Zhang, Q., Zhang, G., Chen, J., Fei, Z. and F. Liu (2002) ‘Adsorption of Phenolic Compounds from Aqueous Solutions by a Water Compatible Hypercrosslinked Polymeric Adsorbent’, *Chemosphere***, 47,** 981-989.

Li, C., Xu, M., Sun, X., Han, S., Wu, X., Liu, Y. N., Huang, J. and S. Deng (2013) ‘Chemical modification of Amberlite XAD-4 by carbonyl groups for phenol adsorption from wastewater’, *Chemical Engineering Journal*, **229**, 20-26.

Lin, S.S.S., Chen, C. L., Chang, D. J. and C. C. Chen (2003) ‘Catalytic Wet Air Oxidation of Phenol by Various CeO_2 Catalysts’, *Water Research*, **36**, 3009-3014.

Lin, S. H. and S. J. Ho (1996) ‘Catalytic wet-air oxidation of high strength industrial wastewater’, *Applied Catalysis B: Environmental*, **9**, 133-147.

Lin, S.H. and R.S. Juang (2009) ‘ Adsorption of phenol and its derivatives from water using synthetic resins and low cost natural adsorbents: A review’, *Journal of Environmental Management*, **90**, 1336-1349.

Li, L., Liu, S. and T. Zhu (2010) ‘ Application of activated carbon derived from scrap tires for adsorption of Rhodamine B’, *Journal of Environmental Science,* **22**, 1273-1280.

Liotta, L., F. (2010) ‘Catalytic Oxidation of Volatile Organic Compounds’, *Applied Catalysis B: Environmental*, **100**, 403-312.

Lui, Y., Guo, Y., Gao, W., Wang, Z., Ma, Y. and Z. Wang (2012) ‘Simultaneous preparation of silica and activated carbon from rice husk ash’, *Journal of Cleaner Production*, **32**, 204-209.

Liu,F., Guo, Z., Zheng, S and Z. Xu (2012) ‘ Adsorption of tannic acid and phenol on mesoporous carbon activated by CO_2’, *Chemical Engineering Journal*,**183**, 244-252.

Liu, Q. S., Zheng, T., Wang, P., Jiang, J. P. and N. Li (2010) ‘Adsorption isotherm, kinetic and mechanism studies of some substituted phenols on activated carbon fibres’, *Chemical Engineering Journal*, **157**, 348-356.

Lopez –Fonseca, R., Gutierrez-Ortiz, J. I., Gutierrez-Ortiz, M. A. and J. R. Gonzalez-Velasco (2005) 'Catalytic oxidation of aliphatic chlorinated volatile organic compounds over Pt/H-BETA zeolite catalyst under dry and humid conditions', *Catalysts Today*, **107-108**, 200-207.

Loukidou, M. X., Matis, K. A., Zouboulis, A. I. and M. Liakopoulou – Kyriakidou (2003) 'Removal of As (V) from wastewaters by chemically modified fungal biomass', *Water Research*, **37**, 4544-4552.

Luck, F. (1999) 'Wet Air Oxidation: Past, Present and Future', *Catalysis Today*, **53,** 81-91.

Lu, P. J., Lin, H. C., Yu, W. T. and J. M. Chern (2011) 'Chemical regeneration of activated carbon used for dye adsorption', *Journal of the Taiwan Institute of Chemical Engineers*, **42**, 305-3011.

Malusis, M. A., Maneval, J. E., Barben, E. J., Shackelford, C. D. and E. R. Daniels (2010) 'Influence of adsorption on phenol transport through soil – bentonite vertical barriers amended wit activated carbon', *Journal of Contaminated Hydrology*, **116**, 58-72.

Matatov-Meytal, Y. I. and M. Sheintuch (1999) 'Comparison of Catalytic Processes with other Regeneration methods of Activated Carbon', *Industrial Engineering Chemistry Research*, **53**, 73-80.

Miao, Q., Tang, Y., Xu, J., Liu, X., Xiao, L. and Q. Chen (2013) 'Activated carbon prepared from soybean straw for phenol adsorption', *Journal of the Taiwan Institute of Chemical Engineers*, **44**, 458-460.

Milner, R. C. and Goulder, R. (1984) 'Bacterioplankton in an urban river: The effects of a metal bearing tributary', *Water Research*, **18**, 1395-1399.

Mishra, V. S., Mahajani, W. and J. B. Joshi (1995) 'Wet Air Oxidation Industrial', *Industrial Engineering Chemistry Research*, **34,** 2-48.

Mortland, M. M., Shaobai, S. and A. Stephen Boyd (1986) 'Clay –Organic Complexes as Adsorbents for Phenol and Chlorophenols', *Clays and Clay Minerals*, **34,** 581-585.

Nahm, W. S., Shim, W. G., Park, Y. K. and S. C. Kim (2012) 'Thermal and chemical regeneration of spent activated carbon and its adsorption property for toluene', *Chemical Engineering Journal*, **210**, 500-509.

Neyens, E. and J. Baeyens (2003) 'A Review of Classic Fentons Preoxidation as an Advanced Oxidation Technique', *Journal of Hazardous Materials*, **98**, 33-50.

Nwankwo, J. and A. Turk. (1974) Catalytic Oxidation of Adsorbed Hydrocarbons. Annals of the New York Academy of Sciences-Blackwell Synergy.

Oliveros, E., Legrini, O., Holb, M., Muller, T. and A. Braun (1997) 'Industrial Wastewater Treatment: Large Scale Development of a Light-Enhanced Fenton Reaction.', *Chemical Engineering and Processing*, **36,** 397-405.

Oturan, N., Hamza, M., Ammar, S., Abdelhedi, R., and A. M. Oturan (2011)'Oxidation / mineralization of 2-nitrophenol in aqueous medium by electrochemical advanced oxidation processes using Pt / carbon-felt and BDD / carbon-felt cells'. *Journal of Electroanalytical Chemistry*, **661**, 66-71.

Ozaki, H. and H., Li (2002) 'Rejection of organic compounds by ultra-low pressure reverse osmosis membrane' *Water Research,* **36**, 123-130.

Ozkaya, B. (2006) 'Adsorption and desorption of phenol on activated carbon and a comparison of isotherm models', *Journal of Hazardous Material*, **129**, 158-163.

Pan, B., Pan, B., Zhang, W., Lv, L., Zhang, Q. And S. Zheng (2009) 'Development of polymeric and polymer –based hybrid adsorbents for pollutants removal from waters', *Chemical Engineering Journal*, **151**, 19-29.

Parida, K. M. and S. Amarendra. (1999) 'Catalytic combustion of volatile organic compounds on Indian Ocean manganese nodules', *Applied Catalysis A: General,* **182**, 249-256

Parekh, B. S. (1991) 'Get Your Process Water to Come Clean', *Chemical Eingineering*, **98**, 70-95.

Pelech, R., Milchert, E. and A. Wroblewska (2005) 'Desorption of chloroorganic compounds from a bed of activated carbon', *Journal of Interface Science*, **285**, 518-524.

Perego, C., Bagatin, R., Tagliabue, M. and Rodolfo Vignola (2013) ' Zeolites and related mesoporous materials for multi- talented environmental solutions' *Microporous and Mesoporous Materials*, **166**, 37-49.

Perrich, J. R. (Ed), 1981 Handbook of Activated Carbon as an Option for Wastewater Treatment. CRC Press, Boca Raton.

Phan, T. N. T., Bacquet, M. and M. Morcellet (2002) 'The Removal of Organic Pollutants from Water Using New Silica-supported β-cyclodextrin Derivatives', *Reactive and Functional Polymers*, **52**, 117-125.

Pilato, L. (Ed), 2010 Phenolic Resins: A Century of Progress. Springer – Verlag Berlin Heidelberg.

Pordan, L. N. Koganovskii, A. M., and V. I. Kofan (1988) 'Catalytic Regeneration of Activated Carbon Saturated with Surface Active Agents, Dyes and Phenol', *Catalysis Today* **10**, 278-283.

Puziy, A. M., Poddubnaya, O.I., Mart nez-Alonso, A., Su rez-Garc a, F. and J.M.D. Tascón (2002) 'Characterization of synthetic carbons activated with phosphoric acid', *Applied Surface Science*, **200**, 196-202.

Qiuli, L. and G. Sorial (2004) 'Adsorption of Phenolics on Activated Carbon – Impact of Pore Size and Molecular Oxygen', *Chemosphere*, **55,** 672-679.

Quili, L. and G. Sorial (2007) 'The Effect of Functional Groups on Oligomerization of Phenolics on Activated Carbon', *Journal of Hazardous Materials*, **148**, 436-445.

Quintanilla, A., Casas, J. A., Zazo, J. A., Mohedano, A. F. and J. J. Rodriguez (2006) 'Wet Air Oxidation of Phenol at Mild Conditions with a Fe/activated Carbon Catalysts', *Applied Catalysis B: Environmental*, **62,** 115-120.

Radhika, M. and K. Palanivelu (2006) 'Adsorption Removal of Chlorophenols from Aqueous Solution Low Cost Adsorbent – Kinetics and Isotherm Analysis', *Journal of Hazardous Materials*, **138**, 116-124.

Rathinam, A., Rao, J. R. and B.U. Nair (2011) 'Adsorption of phenol onto activated carbon from seaweed: Determination of the optimal experimental parameters using factorial design', *Journal of Taiwan Institute if Chemical Engineers*, **42**, 952-956.

Rodriguez – Reinso, F., Lopez – Gonzalez, J. de D. and C. Berenguer (1982) 'Activation carbons from almond shells – I. Preparation and characterisation by nitrogen adsorption', *Carbon*, **20**, 513-518.

Rodrizgue, I., Llompart, M. P. and R. Cela (2000) 'Solid –Phase Extraction of Phenols', *Journal of Chromatography*, **885**, 291-304.

Rubin, E., Rodriguez, P., Herrero, R. and M. E. S. Sastre de Vicente (2006) 'Biosorption of Phenolic Compounds by the Brown Alga Sargassum Muticum', *Journal of Chemical Technology and Biotechnology*, **81**, 1093-1099.

Sabio, E., Gonzalez, E., Gonzalez, J. F., Gonalez – Garcia, C. M., Ramiro, A. and J. Ganan (2004) 'Thermal regeneration of activated carbon saturated with p-nitorphenol', *Carbon***, 42**, 2285-2293.

Safarzadeh-Amiri, A., Bolton, J. R. and S. R. Carter (1996) 'The Use of Iron in Advanced Oxidation Processes', *Journal of Advanced Oxidation Technology*, **1,** 18-26.

Safarzadeh-Amiri, A., Bolton, J. R and S. R. Carter (1997) 'Ferrioxalate-Mediated Photo Degradation of Organic Pollutants in Contaminated Water', *Journal of Water Research*, **31,** 787-798.

Santos, A., Yustos, P., Gomis, S., Ruiz, G. and F. Garcia - Ochoa. (2006) 'Reaction Network and Kinetic Modelling of Wet Oxidation of Phenol Catalyzed by Activated Carbon', *Journal of Chemical Engineering and Science*, **61,** 2457-2467.

Seyhan, S., Merdivan, M. and N. Demirel (2008) 'Use of o-phenylene dioxydiacetic acid impregnated in Amberlite XAD resin for separation and preconcentration of uranium (VI) and thorium (IV)', *Journal of Hazardous Materials*, *152*, 79-84.

Shende, R. V. and V. V. Mahajani, (1994) 'Wet Air Oxidation of Glyoxalic Acid and Oxalic Acid', *Journal of Industrial Engineering and Chemical Research*, **33**, 3125-3130.

Shu, H. T, Li, D., Scala, A., A. and Y. H. Ma (1997) 'Adsorption of Small Organic Pollutants from Aqueous Streams by Aluminosilicate-Based Microporous Materials' Separation and Purification Technology, 11, 27-36.

Sihem, A., Bencheikh Lehocine, M. and H. A. Miniai (2012) 'Batch adsorption of phenol from industrial waste water using cereal by – products as a new adsorbent', *Energy Procedia*, **18**, 1135-1144.

Singh, B. K. and P. S. Nayak. (2004) 'Sorption Equilibrium Studies of Toxic Nitro-substituted Phenols on Fly Ash', *Adsorption Science and Technology*, **22,** 295-309.

Sismanoglu, T. and S. Pura (2001) 'Adsorption of Aqueous Nitrophenols on Clinoptilolite', *Colloids and Surfaces A: Physicochemical and Engineering Aspects*, **180,** 1-6.

Smisek, M. and S. Cerny, (1970) Active Carbon, Elsevier, Amsterdam, Netherlands.

Sonyheimer, J., Crittenden., J. C and R. S. Summers. 1988 (2nd ed.) Activated Carbon for Water Treatment, DVGW - Forschungsstelle, Karslruhe, Germany (1988).

Soto, M. L., Moure, A., Dominguez, H. and J. C. Parajo (2011) 'Recovery, concentration and purification of phenolic compounds by adsorption', *Journal of Food Engineering*, **105**, 1-27.

Spivey, J. J. (1987) 'Complete Oxidation of Volatile Organics', *Industrial Engineering and Chemical Research*, **26**, 2165-2180.

Streat, M., Patrick, J. W. and Camporro – Perez, M. J. (1995) 'Sorption of phenol and p-chlorophenol from water using conventional and novel activated carbons', *Water Resource*, **29**, 467-472.

Suarez-Ojeba, E., Carrera, J., Metcalfe, I. S. and J. Font (2008) 'Wet Air Oxidation as a Precursor to Biological Treatment of Substituted Phenols: Refectory Nature of the WAO Intermediates', *Journal of Chemical Engineering*, **144,** 205-212.

Tang, S., Lu, N., Li, J., Shang, K. and Y. Wu (2013) 'Improved phenol decomposition and simultaneous regeneration of granular activated carbon by the addition of a titanium dioxide catalyst under a dielectric barrier discharge plasma', *Carbon*, **53**, 380-390.

Thomas, J. M. and W. J. Thomas (1997) 'Principles and Practice of Heterogeneous Catalysis' VCH, Weinheim.

Troca – Torrado, C., Alexandre – Franco, M., Fernandez – Gonzalez, C., Alfaro – Dominguez, M. and V. Gomez – Serrano (2011) 'Development of adsorbents from used tire rubber: Their use in the adsorption of organic and inorganic solutes in aqueous solution', *Fuel Processing Technology*, **92**, 206-212.

Tseng, R. L., Wu, K. T., Wu, F. C. and R. S. Juang (2010) 'Kinetic studies on the adsorption of phenol from water using activated carbons', *Journal of Environmental Engineering*, **91**, 2208-2214.

Ucar, S., Erdem, M., Tay, T. and S. Karagoz (2009) 'Preparation and characterisation of activated carbon produces from pomegranate seeds by $ZnCl_2$ activation', *Applied Surface Science*, **255**, 8890-8896.

United Nations Educational, Scientific and Cultural Organisation (UNESCO), Water Portal, (2011), Paris (France). http://www.unesco.org/water/

US Geological Survey's (USGS), Water Science for Schools, (2011), US Geological Survey (USGS), Reston, VA. http://ga.water.usgs.gov/edu/index.html

Vieira, A. P., Santana, S. A. A., Bezerra, C. W. B., Silva, H. A. S., Chaves, J. A. P., Melo, J. C. P., Filho, E. C. S. and C. Airoldi (2011) 'Removal of textile dyes from aqueous solution by babassu coconut epicarp (Orbignya speciosa)' *Chemical Engineering Journal*, **173**, 334-340.

Weitkamp, J. (2000) 'Zeolites and Catalysis', *Solid State Ionics*, **131**, 175-188.

Weng, C. H. and M. C. Hsu (2008) 'Regeneration of granular activated carbon by an electrochemical process', *Separation and Purification Technology*, 64, 227-236.

Wu, K. T., Wu, P. H., Wu, F. C., Jreng, R. L. and R. S. Juang (2013) 'A novel approach to characterizing liquid-phase adsorption on highly porous activated carbons using the Toth equation', *Chemical Engineering Journal*, **221**, 373-381.

Xiaoli, C. and Youcai, Z. (2006) 'Adsorption of Phenolic Compounds by Aged Refuse', *Journal of Hazardous Materials* **137**, 410-417.

Yap, P. S. and T. T. Lim (2012) 'Solar regeneration of powdered activated carbon impregnated with visible – light responsive photocatalysts: Factors affecting performances and predictive model', *Water Research*, **46**, 3054-3064.

You, X. Y., Chai, L. Y., Wang, Y. Y., Su, Y. R., Zhao, N. and Y. D. Shu (2013) ' Regeneration of activated carbon adsorbed EDTA by electrochemical method', *Transactions of Nonferrous Metals Society of China*, **23**, 855-860.

Yoon, Y. and R. M. Lueptow (2005) 'Removal of organic contaminants by RO and NF membranes', *Journal of Membrane Science*, **261**, 76-86.

Yousef, R., I., El-Eswed, B. and A., H., Al- Muhtaseb, (2011) 'Adsorption Characteristics of Natural Zeolites as Solid Adsorbents for Phenol Removal from

Aqueous Solutions: Kinetics, Mechanism and Thermodynamics Studies', *Chemical Engineering Journal*, **171**, 1143-1149.

Yuan, X., Li, X., Zhu, E., Hu, J., Sheng, W. and S. Cao (2008) 'A novel hypercrosslinked polymeric adsorbent modified by phenolic hydroxyl group of 2-naphthol with bromoethane as crosslinking reagent', *Carbohydrate Polymers*, **74**, 468-473.

Zabkova, M., Otero, M., Minceva, M., Zabka, M. and A. E. Rodrigues (2006) 'Separation of synthetic vanillin at different pH onto polymeric adsorbents Sephabeads SP206', *Chemical Engineering and Processing: Process Intensification*, **45**, 598-607.

Zeng, X., Fan, Y., Wu, G., Wang, C. and R. Shi (2009) 'Enhanced adsorption of phenol from water by a novel polar post-crosslinked polymeric adsorbent', *Journal of Hazardous Materials*, **169**, 1022-1028.

Zhang, H. (2002) 'Regeneration of exhausted activated carbon by electrochemical method', *Chemical Engineering Journal*, **85**, 81-85.

Zhang, G. S., Qu, J. H., Liu, H. J., Copper, A. T. and R. C. Wu (2007) '$CuFe_2O_4$/ Activated Carbon Composite: A Novel Magnetic Adsorbent for the Removal of Acid Orange II and Catalytic Regeneration', *Chemosphere*, **68**, 1058-1066.

Chapter 2

Adsorption of 2-Nitrophenol from Aqueous Solution by Unmodified Beta Zeolite

2.1.1 Introduction

Adsorption is one of the most effective processes of advanced wastewater treatment which industries employ to prevent the release of hazardous wastes into the aquatic environment by industries such as coke ovens in steel plants, petroleum refineries, phenolic resin, fertilizers, pharmaceutical, chemical and dye industries. Adsorption occurs when a solid surface (adsorbent) is exposed to a specific adsorbate species. The extent of adsorption is a function of the absolute temperature (T), the concentration of the adsorbing species (C), the number of suitable adsorption sites on the adsorbent (S) and the interaction potential energy (E) between the adsorbate and the surface. Hence, the quantity adsorbed (W), is a function of the adsorbate concentration and interaction potential when measured at constant temperature and when availability of adsorption sites is not limited (Gregg and Sing 1982).

$$W = f(C, E, S) \qquad \textbf{Equation 2.1}$$

The interaction potential energy (E) varies with the properties of the adsorbate and adsorbent and ultimately determines the extent of adsorption. Figure 2.1 outlines the variation of the interaction potential energy as a function of the distance of the adsorbate atom or molecule from the adsorbent surface (Atkins 1994). As the adsorbing species approaches the adsorbent surface, the potential energy drops as it is physisorbed. The energy of the system then rises as the adsorbate /surface bonds are formed and are at full stretch. This energy decreases sharply when the adsorbate / surface bond length contracts to its normal size leading to the chemisorbed state. The enthalpy changes (ΔH_{ads}) resulting from both forms of adsorption are also shown in Figure. 2.1

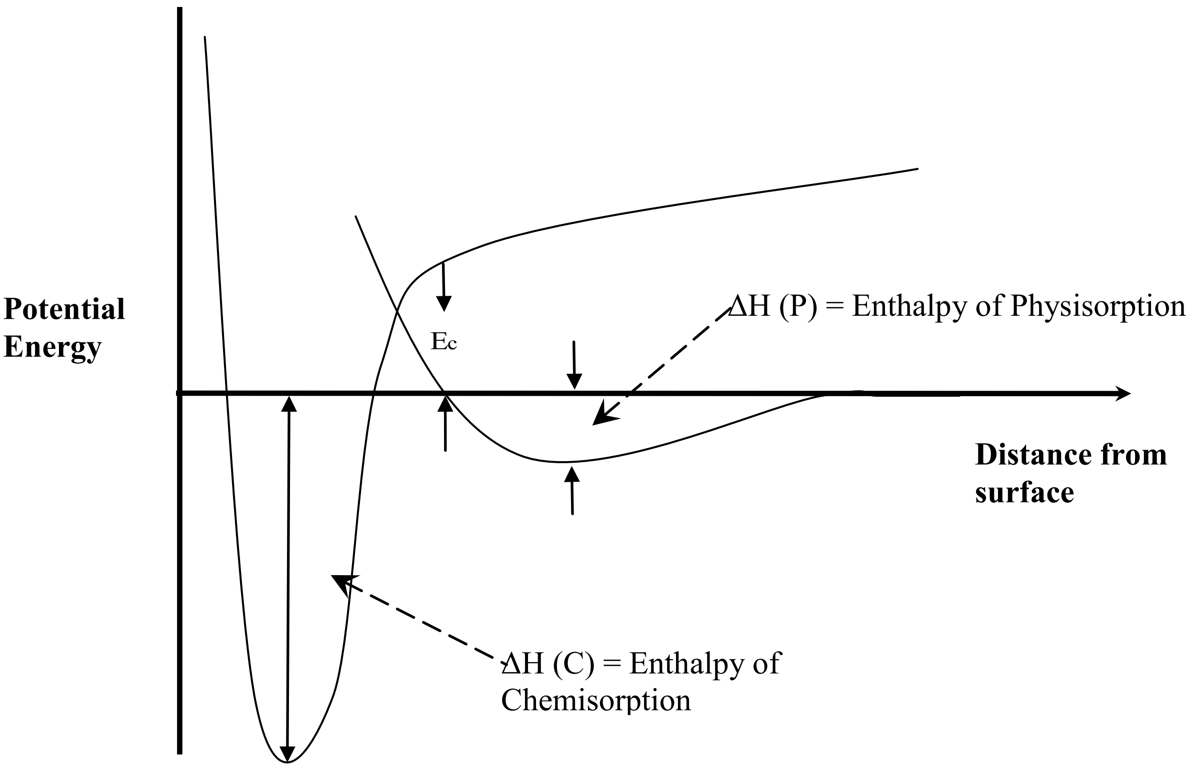

Figure 2.1: Potential energy profiles for the adsorption process.

Chemisorption is characterized by large interaction potentials leading to high enthalpies of adsorption (~ 200 kJ mol $^{-1}$), often approaching the value of chemical bonds. Spectroscopic evidence confirms this to be true chemical bonding between adsorbate and adsorbent, a fact which necessarily limits chemisorption to single layer coverage of the adsorbent surface. Desorption of the adsorbed species in its original form is often not possible. In contrast, physisorption is accompanied by low enthalpies of adsorption (~ 20 kJ mol^{-1}), no bond breaking or formation occurs and more than one layer of coverage is possible. Physical adsorption equilibrium is achieved rapidly since no activation energy is required as in chemisorption. Physisorption is fully reversible allowing the desorption process to be studied.

A plot of the quantity adsorbed (W) versus the corresponding equilibrium solution concentration of adsorbate (C) at fixed temperature, for a range of adsorbate concentrations constitutes an adsorption isotherm. Brunauer et al., (Brunauer et al., 1940) have outlined the characteristic shapes of the most common isotherms and these are presented in Figure 2.2.

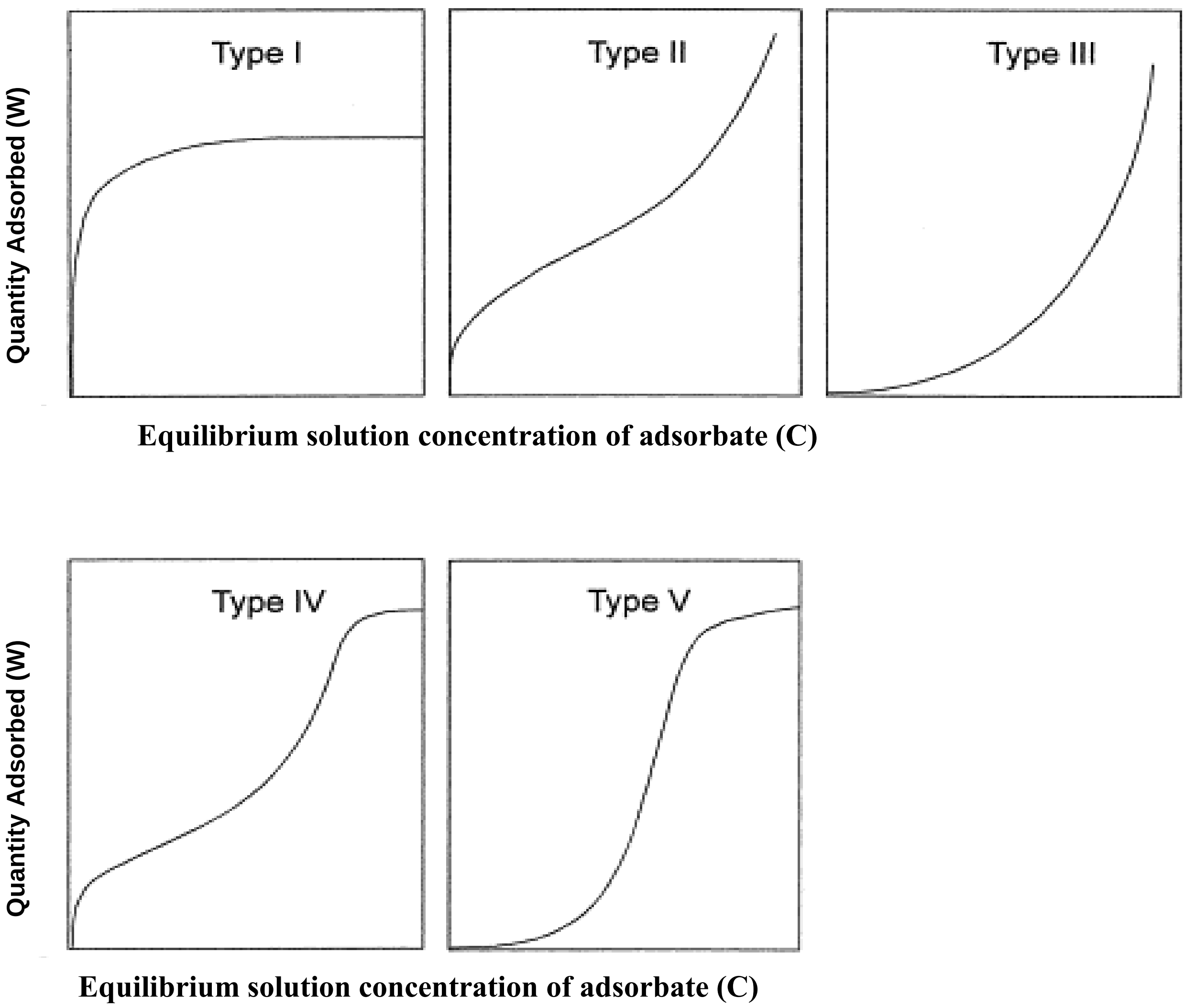

Figure 2.2 The Brunauer classifications of isotherms.

Type I profiles may result from either physisorption or chemisorption processes. In the physical adsorption of species by microporous solids where the pore diameter of the adsorbent does not exceed that of the adsorbing species by a significant amount, a plateau is reached when the micropores are completely saturated with the adsorbate.

For chemisorption systems the adsorbate species has completely adsorbed on all suitable surface sites and no further sites are available.

Type II and III isotherms are observed when the adsorbent possesses a range of pore sizes but are usually described as macroporous adsorbents. The continuous progression from monolayer to multilayer adsorption is seen as the adsorbate concentration increases. The inflection point (knee) in the type II isotherm usually occurs near the completion of the first fully adsorbed monolayer, with increasing concentration second and higher layers are completed, until at saturation when the number of adsorbed layers becomes infinite. Type III is a convex isotherm. The weakness of the adsorbent-adsorbate forces causes uptake at low relative concentrations to be small but once the molecules have become adsorbed, additional adsorption is facilitated because the adsorbate interaction with the adsorbed layer is greater than the interaction with the adsorbent.

Two surface layers are formed in type IV isotherms leading to a double inflection in the profile. The slope increase at higher concentrations indicates an increased uptake of adsorbate as the pores are being filled. As the case for the type II isotherms, the knee of the type IV isotherm generally occurs near the completion of the first monolayer. Type IV isotherms occur on porous adsorbents possessing pores in the radius range of approximately 15-1000Å.

Type V profiles result from small adsorbate–adsorbent interaction potentials similar to the Type III isotherms. However, Type V isotherms are also associated with pores in the small range similar to the Type IV isotherms. There is a point of inflection at fairly high relative concentrations so that the isotherm bends over and reaches a plateau in the multilayer region of the isotherm attributable to adsorption in coarse mesopores and macropores (Barrer 1978; Lowell and Shields 1991).

Typical adsorbate/adsorbent interactions contributing to adsorption processes include:

- Ion / Dipole – an ionic solid and an electrically neutral but polar adsorbate,
- Dipole / Dipole – a polar solid and polar adsorbate,
- Ion / Induced Dipole – a polar solid and polarized adsorbate,
- Ion / Ion – a charged surface and charged adsorbate producing an electrostatic attraction.

Adsorption technology is recognised as both an effective and economic measure for the removal of soluble and stable non-biologically degradable organics from wastewaters (Al-Duri et al., 1992). There are a number of important attributes necessary for consideration prior to the selection of a particular adsorbent for use. These include capacity, selectivity, regenerability, kinetics, compatibility and cost (Knaebel 1995).

2.1.2 Thermodynamics of Adsorption

The Gibbs function (free energy) of an adsorbate (A) in solution at any concentration (C) can be expressed as:

$$G_L = G_L^{o} + nRT \ln C_A \qquad \textbf{Equation 2.2}$$

Or alternatively the Gibbs function can be given in molar terms as:

$$\mu_L = \mu_L^{o} + RT \, ln \frac{C_A}{C_A^{o}} \qquad \textbf{Equation 2.3}$$

Where:

μ_L = the chemical potential of the liquid phase (kJ mol^{-1})

μ_L^c = the standard chemical potential of the liquid phase (kJ mol^{-1})

T = the standard temperature in Kelvin (K)

R = the gas constant (8.3144621 J K^{-1} mol^{-1})

During adsorption, it is necessary to consider the surface layer which consists of the adsorbent and adsorbate as being in a single phase and having the general properties of a solution. The condition for equilibrium between the adsorbed layer and the bulk solution phase can be described as follows in **Equation 2.4**.

$$\mu_A = \mu_L \qquad \textbf{Equation 2.4}$$

Where:

μ_A = the chemical potential of the adsorbed layer

If **Equation 2.3** is incorporated into **Equation 2.4** then a relationship between the Gibbs free energy of the adsorbed layer and the adsorbate in solution is generated.

$$\mu_A = \mu_L^o + RT \ln \frac{C_A}{C_A^o} \qquad \textbf{Equation 2.5}$$

Where:

C_A^c = the concentration of adsorbate in solution under standard conditions

In order to establish the enthalpy change resulting from the adsorption process, it is necessary to cite the Gibbs-Helmholtz relationship, which outlines the temperature dependence of the chemical potential of the adsorbed layer.

$$\left(\frac{\partial(\mu_A/T)}{\partial T}\right) = \frac{-H_A}{T^2}$$ **Equation 2.6**

Where

H_A = the enthalpy of the adsorbed layer (kJ mol^{-1})

Substitution of **Equation 2.6** into **Equation 2.5** results in:

$$\frac{-H_A}{T^2} = \frac{-H_L^o}{T^2} + R\left(\frac{\partial \ln C_A}{\partial T}\right)_w$$ **Equation 2.7**

Where:

H_L^o = the standard enthalpy of the solution phase at a constant adsorbed weight (W)

Equation 2.7 can be rearranged to give an expression that relates the variation in adsorbed adsorbate concentration with temperature to the enthalpy change resulting from the adsorption process.

$$\left(\frac{\partial \ln C_A}{\partial T}\right)_w = \frac{H_L^o - H_A}{RT^2}$$ **Equation 2.8**

Assuming that the standard enthalpy of the bulk solution is independent of composition then H_L^o is equal to H_L and therefore **Equation 2.8** can be rewritten as:

$$\left(\frac{\partial \ln C_A}{\partial T}\right)_w = \frac{\Delta H_{ads}}{RT^2}$$ **Equation 2.9**

Where:

ΔH_{ads} = the enthalpy change resulting from adsorption (kJ mol^{-1})

If the difference in heat capacity of the bulk of the solution phase and the adsorbate in the adsorbed phase is negligible, then the enthalpy change on adsorption ΔH_{ads} is independent of temperature and **Equation 2.9** can be integrated directly to generate:

$$ln\,C_A = constant - \left(\frac{\Delta H_{ads}}{RT}\right) \quad \textbf{Equation 2.10}$$

Where:

ΔH_{ads} = the enthalpy change resulting from adsorption (kJ mol^{-1})

A plot of $ln\,C_A$ versus $1/T$ results in a straight-line relationship where the enthalpy of adsorption can be determined from the slope.

The heat change resulting from adsorption can be experimentally determined in conjunction with the Van't Hoff equation by carrying out adsorption experiments at two different temperatures (Singh et al., 1988).

$$\Delta H_{ads} = R\left(\frac{T_1 T_2}{T_2 - T_1}\right) ln\left(\frac{K_{c2}}{K_{c1}}\right) \quad \textbf{Equation 2.11}$$

Where:

K_c = the equilibrium constant for the adsorption process at a specified temperature.

The change in surface free energy resulting from adsorption (ΔG°_{ads}) can be calculated using:

$$\Delta G^{o}_{ads} = -RT\,ln\,K_c \quad \textbf{Equation 2.12}$$

Using a form of the equation for the Gibbs free energy change and its rearrangement leads to an estimation of the entropy change ($\Delta S°_{ads}$) for the resulting adsorption process.

$$\Delta G^{o}{}_{ads} = \Delta H^{o}{}_{ads} - T\,\Delta S^{o}{}_{ads} \qquad \textbf{Equation 2.13}$$

$$\Delta S^{o}{}_{ads} = \frac{\Delta H^{o}{}_{ads} - \Delta G^{o}{}_{ads}}{T} \qquad \textbf{Equation 2.14}$$

In the bulk of a solid adsorbent, atoms are symmetrically distributed about each other on a stoichiometric basis leading to a net charge balancing effect. However, on moving from the bulk of the solid to its surface, broken bonds must exist and atoms in this region are subject to an asymmetrical distribution of forces leading to significant entropy. This state can be partially relieved by an adsorption process, which reduces the surface disorder or entropy implying a negative change in entropy for the process (($\Delta S°_{ads}$) is negative) and typically the following thermodynamic situation might arise resulting from the adsorption process. The ($T(\Delta S°_{ads})$) term in **Equation 2.13** is negative. Given that this value is negative and that in order for the adsorption process to be spontaneous $\Delta G°_{ads}$ must be negative, then the enthalpy change accompanying adsorption must be negative leading to an exothermic reaction. **Table 2.1** lists the potential thermodynamic situations (1 - 4) that may arise during the adsorption process, the most undesirable being situation (4) which is indicative of an unfavourable process.

Table 2.1: Potential thermodynamic situations during adsorption

	ΔG°	ΔH°	ΔS°	Spontaneous
(1)	(-)	(-)	(+)	At all temperatures
(2)	(-)	(-)	(-)	At low temperatures
(3)	(-)	(+)	(+)	At high temperatures
(4)	(+)	(+)	(-)	Non spontaneous at all temperatures

2.1.3 Adsorption Isotherm Models

An adsorption isotherm is an expression relating parameters involved in dynamic equilibrium at a defined temperature (Campbell, 1988). Adsorption isotherms describe how adsorbates interact with adsorbents and so are critical in optimizing the use of adsorbents (Ng et al., 2003). The most common mathematical models for predicting adsorption are the distribution coefficient, the Langmuir isotherm (Langmuir, 1918) and Freundlich isotherm (Freundlich 1906).

2.1.3.1 The Distribution Coefficient

The distribution coefficient (K_d) is a simple ratio, at equilibrium, of the quantity of adsorbate adsorbed per gram of adsorbent to the quantity of adsorbate remaining in solution. This is illustrated in Equation 2.16 for the reaction between the adsorbent (S) and the adsorbate (A).

$$S \quad + \quad A \quad \longleftrightarrow \quad S-A$$ **Equation 2.15**

then $$K_d = \frac{C_{Ao} - C_{Aeqb}}{C_{Aeqb}}$$ **Equation 2.16**

C_{Ao} = the initial adsorbate concentration in the solution

C_{Aeqb} = the adsorbate concentration in the solution at equilibrium

Where

K_d is not an isotherm but a single constant and it is specific to the conditions of the particular adsorption experiment, i.e. adsorbent, chemical environment and temperature.

2.1.3.2 Langmuir Adsorption Isotherm

The Langmuir isotherm is the most common isotherm expression and can generally provides a good correlation for data corresponding to Type I plots (Section 2.1.1).

In respect of Equation 2.17, if θ_A is assumed to be the fraction of adsorption sites covered by the adsorbate species (A), then $(1-\theta_A)$ is the fraction of free adsorbent sites. The rate of adsorption should be related to the fraction of the concentration of adsorbate species C_A and the fraction of available sites on the adsorbent $(1-\theta_A)$.

$$(rate)_{ads} = k_{ads} C_A (1 - \theta_A) \qquad \textbf{Equation 2.17}$$

Where:

k_{ads} = adsorption rate constant

Similarly the rate of desorption is given by the desorption rate constant times the fraction of occupied sites.

$$(rate)_{des} = k_{des} \theta_A \qquad \textbf{Equation 2.18}$$

At equilibrium the rate of adsorption and desorption are equal and therefore:

$$k_{ads} C_A (1 - \theta_A) = k_{des} \theta_A \qquad \textbf{Equation 2.19}$$

$$\frac{\theta_A}{(1-\theta_A)} = \frac{k_{ads} C_A}{k_{des}}$$ **Equation 2.20**

$$\frac{\theta_A}{(1-\theta_A)} = \frac{k_{ads} C_A}{k_{des}}$$ **Equation 2.21**

$$\frac{\theta_A}{(1-\theta_A)} = K_L C_A$$ **Equation 2.22**

Where:

$$K_L = k_{ads} / k_{des}$$ **Equation 2.23**

Solving for θ_A, the extent of adsorption is given by:

$$\theta_A = \frac{K_L C_A}{1 + K_L C_A}$$ **Equation 2.24**

Rearranging **Equation 2.24** to the linear form gives:

$$\frac{C_A}{\theta_A} = C_A + \frac{1}{K_L}$$ **Equation 2.25**

Assuming :

$$\theta_A = \frac{Fraction\ of\ adsorption\ sites\ occupied\ by\ A}{Total\ number\ of\ adsorption\ sites\ available}$$ **Equation 2.26**

then $$\theta_A = \frac{W_A}{W_{max}}$$ **Equation 2** where (W_A) is the mass of the adsorbate on the adsorbent at any time and (W_{max}) is the maximum mass of adsorbate which can be accommodated on the adsorbent. Combination of equations 2.25 and 2.27 results in equation 2.28.

$$\frac{C_A}{W_A} = \frac{C_A}{W_{max}} + \frac{1}{K_L W_{max}}$$ **Equation 2.28**

Where:

C_A = the equilibrium concentration of adsorbate in solution

W_A = the mass of adsorbate on adsorbent at equilibrium

W_{max} = the mass of adsorbate on adsorbent at saturation coverage

K_L = the Langmuir adsorption constant

A plot of (C_A/W_A) versus (C_A) results in a linear representation of the adsorption data with slope ($1/W_{max}$) and intercept ($1/K_LW_{max}$).

The adsorption process results in a dynamic equilibrium between adsorbate in the solution and in the adsorbed state. This equilibrium (as defined in Equation 2.19) is achieved when the rate of adsorption of solute A equals the rate of desorption.

The Langmuir isotherm makes use of a number of assumptions listed as follows.

- ❖ A finite number of adsorption sites are available on which adsorption occurs with no electrostatic or chemical interactions between adsorbate ions even on adjacent sites.
- ❖ All adsorption sites are identically equivalent giving the same binding energy for a specific adsorbate.
- ❖ The ability of the adsorbate ion to bind to a surface site is independent of whether or not neighbouring sites are occupied and maximum adsorption is limited to monolayer coverage.

The Langmuir isotherm can be applied to another case, where the adsorbate /adsorbent interaction for a single adsorbate occurs on a multiple site surface. In this case the Langmuir isotherm can be further generalised to Equation 2.29.

$$W_A = \Sigma\left(\frac{(K_{L,i})(W_{max,i}C_A)}{1+(K_{L,i}C_A)}\right) \qquad \textbf{Equation 2.29}$$

This summation is over all possible sites (i), where ($W_{max,i}$) is the maximum weight of the adsorbate which can be accommodated on sites of type (i) and ($K_{L,i}$) is the Langmuir constant binding to that site (i). In a two site case the total adsorption can be treated as the sum of the binding of the single adsorbate to both sites. A plot of (C_A/W_A) versus (C_A) would consist of two straight line segments of differing slopes each yielding a separate Langmuir constant ($K_{L,i}$) corresponding to different site binding energies.

2.1.3.3 Freundlich Adsorption Isotherm

Many of the assumptions on which the Langmuir model is based are not observed for all adsorption processes. In some cases, it appears that non-uniformity exists among the adsorption sites and the change in the free energy of adsorption ($\Delta G°_{ads}$) becomes less negative as the weight of adsorbed species (q_e) increases. This suggests that the adsorbent sites occupied first are energetically more favourable. The Freundlich isotherm is given by the Equation 2.30.

$$q_e = K_F C_e^{1/n} \qquad \textbf{Equation 2.30}$$

where K_F is the Freundlich adsorption constant and 'n' is greater than or equal to 1 and is a function of the adsorption density. As the quantity adsorbed increases, 'n' exceeds 1. In contrast to the Langmuir type adsorption, the change in energy arising from adsorption varies logarithmically with the quantity adsorbed (q_e). For practical applications of the Freundlich model, the natural log of Equation 2.30 yields the linear expression;

$$\ell n q_e = \frac{1}{n} \ell n C + \ell n K_F$$ **Equation 2.31**

A plot of $\ell n q_e$ versus $\ell n C_e$ gives a straight line of intercept ($\ell n K_F$) and slope (1/n). The free energy of adsorption can be determined from the intercept.

2.1.4 Kinetics of Adsorption

The adsorption of an organic solute (O) from aqueous solution onto an adsorbent (S) is given by the equation 2.32:

$$S \quad + \quad O \quad \underset{k_{des}}{\overset{k_{ads}}{\rightleftharpoons}} \quad S-O$$ **Equation 2.32**

Where:

k_{ads} = adsorption rate constant

k_{des} = desorption rate constant

The overall rate (k') for the system is given by:

$$k' = k_{ads} + k_{des}$$ **Equation 2.33**

Evaluation of the overall rate constant (k') can be carried out using the integrated form of a first order rate equation as in Equation 2.34 (Poots and McKay, 1997).

$$ln\left(1-F\right) \quad = \quad k'\,t \qquad \textbf{Equation 2.34}$$

Where F is the fractional attainment of maximum adsorption at time t. From a practical perspective where the adsorbate is an organic compound 'O', the fractional attainment can be calculated as:

$$F \quad = \quad \frac{O_o - O_t}{O_o - O_{eqb}} \qquad \textbf{Equation 2.35}$$

Where;

O_o = initial concentration of adsorbate in solution

O_t = adsorbate solution concentration at time t

O_{eqb} = adsorbate solution concentration at equilibrium (maximum adsorption)

A plot of $\ell n(1-F)$ versus (t) results in a straight line with a slope equal to the overall rate constant (k'). The value of (k') can be further related to the equilibrium constant (K_c) and the rate constant for the adsorption reaction (Bhattacharya and Venkobachar, 1984) by Equation 2.36.

$$k' \quad = \quad k_{ads}\left(1+1/K_c\right) \qquad \textbf{Equation 2.36}$$

At equilibrium the rate constant of adsorption equals the rate constant of desorption and

$$K_c \quad = \quad \frac{k_{ads}}{k_{des}} \qquad \textbf{Equation 2.37}$$

In a practical application (K_c) can be calculated from:

$$K_c \quad = \quad \frac{O_o - O_{eqb}}{O_{eqb}} \qquad \textbf{Equation 2.38}$$

where:

O_o = initial concentration of adsorbate in solution

O_{eqb} = concentration of adsorbate remaining in the solution at equilibrium

Calculations of K_c from Equation 2.38 and k' from Equation 2.36 can be substituted into Equations 2.33 and 2.34 to estimate the rates of adsorption and desorption (k_{ads}) and (k_{des}).

2.1.5 Kinetics Models

In order to investigate the mechanism of sorption and potential rate controlling step such as mass transport and chemical reaction processes, kinetic models have been used to test experimental data. The pseudo first order (Lagergren, 1898) rate equation was the first rate equation for the sorption of a liquid / solid system based on solid capacity and is one of the most widely used sorption rate equations for the sorption of a solute from a liquid solution. It may be represented in the linear form as:

$$\frac{dq_t}{dt} = k_1(q_e - q_t) \qquad \textbf{Equation 2.39}$$

$$ln(q_e - q_t) = ln\, q_e - k_1 t \qquad \textbf{Equation 2.40}$$

where q_e and q_t are the sorption capacity at equilibrium and at time t respectively and k_1 is the pseudo first order rate constant for the sorption process. This equation differs from a true first order equation in two ways as outlined by Aharoni et al., (Aharoni et al., 1991). Firstly the term $k_1 (q_e - q_t)$ does not represent the number of available sites. And secondly the parameter ($\ell n q_e$) is an adjustable parameter and is often found not to be equal to the intercept of the plot of $\ell n(q_e - q_t)$ versus t, whereas in a true first order equation, $\ell n q_e$ should be equal to the intercept of the plot. In most cases in literature (Ho and McKay,1999) the pseudo first order equation does not fit well for the whole range of contact time thus making it necessary to either (a) find some other means of extrapolating the experimental data to t =∞, or (b) alternatively treat q_e as an adjustable parameter to be determined by trial or error. If the rate of sorption is a second order mechanism, the pseudo-second-order chemisorption kinetic rate equation is expressed as:

$$\frac{dq_t}{dt} = k_2 (q_e - q_t)^2 \qquad \textbf{Equation 2.41}$$

Where k_2 is the overall rate constant for the adsorption process, q_e is the amount of adsorbate adsorbed at equilibrium and q_t is the amount of adsorbate adsorbed at time, t.

This equation demonstrates how the rate depends on the sorption equilibrium capacity and not concentration of the sorbate:

Integration of Equation 2.41 leads to:

$$\frac{t}{q_t} = \frac{1}{h} + \frac{1}{q_e} t \qquad \textbf{Equation 2.42}$$

Where h is the initial sorption rate and is given by:

$$h = k_2 q_e^2 \qquad \textbf{Equation 2.43}$$

The application of the pseudo second order rate equation on solid–liquid sorption data has a number of advantages associated with it, it does not have the problem of assigning an effective sorption capacity; the sorption capacity, rate constant of the pseudo-second-order and the initial sorption rate all can be determined from the equation without knowing any parameter beforehand.

Predicting the rate-limiting step is an important factor to be considered in the adsorption process. The mechanism of adsorption is generally considered to involve three steps, one or any combination of which can be the rate-controlling mechanism:

(i) mass transfer across the external boundary layer film of liquid surrounding the outside of the particle; (ii) diffusion of the adsorbate molecules to an adsorption site either by a pore diffusion process through the liquid filled pores or by a solid surface diffusion mechanism, (iii) adsorption at a site on the surface (internal or external) and the energy will depend on the binding process (physical or chemical); this step is often assumed to be extremely rapid (Cheung et al., 2007).

The intraparticle diffusion model proposed by Weber and Morris (Weber and Morris, 1963) provided the rate for intraparticle diffusion by a relationship between q_t and the square root of time, $t^{1/2}$, expressed as:

$$q_t = k_{id} t^{1/2} + C_I \qquad \textbf{Equation 2.44}$$

where k_{id} (mg/g $h^{0.5}$) is the intraparticle diffusion constant and C_i is associated to the boundary layer thickness. If the intraparticle diffusion occurs, then q_t versus $t^{1/2}$ will be linear and if the plot passes through the origin, then the rate limiting process is only due to the intraparticle diffusion. Otherwise, some other mechanism along with intraparticle diffusion is also involved.

In order to investigate the contribution of film resistance to the kinetics of 2-nitrophenol adsorption from aqueous solution, the Boyds film-diffusion model was employed Boyd et al., 1974. This model has the assumption that the boundary layer surrounding the adsorbent particle is the main resistance to diffusion. The film diffusion model is expressed by the equation 2.45 as follows:

$$F(t) = 1 - \left(\frac{6}{3.14^2}\right)\sum_{n-1}^{\infty}\left(\frac{1}{n^2}\right)\exp\left(-n^2 Bt\right) \qquad \textbf{Equation 2.45}$$

where F(t) is the fractional attainment of equilibrium, a different times, t(min) and Bt is a function of F(t) as expressed in equation 2.46:

$$F(t) \quad = \left(\frac{q_t}{q_e} \right) \qquad \textbf{Equation 2.46}$$

Where q_t and q_e are adsorbate uptake levels in mg g^{-1} at times, t (min) and at equilibrium respectively. By applying the Fourier transform and the integration to equation 2.45, the following approximations are obtained by Reichenberg 1953, if the value of F(t) is higher than 0.85:

$$Bt \quad = \ 0.4977 - In(1 - F(t)) \qquad \textbf{Equation 2.47}$$

If the value of F(t) is lower than 0.85:

$$Bt = \left(\sqrt{3.14} - \sqrt{3.14 - \left(\frac{3.14^2 F(Ft)}{3} \right)} \right)^2 \qquad \textbf{Equation 2.48}$$

According to this model, the plot of Bt against time should be linear and pass through the origin if the intra-particle diffusion controls the rate of mass transfer. If the plot is nonlinear or linear but does not pass through the origin, then it is concluded that the adsorption rate is controlled by film-diffusion or chemical reaction.

In this study the non-linear Chi-square error analysis method was used to test the best-fit of the kinetic model to the experimental data. The Chi-square test statistic is basically the sum of the squares of the difference between the experimental data and data obtained by calculating from models, with each squared difference divided by the corresponding data obtained by calculating from models. The equivalent mathematical statement is:

$$\chi^2 = \sum \left(q_e - q_{e,m}\right) \frac{\left(q_e - q_{e,cal}\right)^2}{q_{e,cal}}$$ **Equation 2.49**

$q_{e,m}$ equilibrium capacity obtained by calculating from model (mg g^{-1}), q_e experimental data of equilibrium capacity mg g^{-1}. If the data from the model are similar to the experimental data, χ^2 will be a small number and if they are different, χ^2 will be a bigger number.

2.1.6 Beta Zeolites

In this research work unmodified beta zeolite and copper modified beta zeolite were investigated with a view to examining their potential as adsorbents for the removal of 2-nitrophenol from aqueous solutions. Zeolites are microporous crystalline alumino-silicates with frameworks based on a three dimensional network of corner sharing [TO_4] tetrahedrals. Commonly, T corresponds to Si and Al but structures based on other cations (e.g. Be, Ge, Fe, P, Zn) have been described as well (Breck, 1974 and Weitkamp, 2000). They are characterised by the presence of regular voids with free dimensions ranging from about 0.3 to 1 nm (Perego et al., 2013). Their three dimensional framework creates nanometre sized channels and cages, which imparts high porosity and a large surface area onto these materials. One of their defining features is that the shape of their internal pore structure can strongly affect their adsorption selectivity towards host molecules (Cejka et al., 2007).

Presence of aluminium in the framework induces negative charges which are compensated by loosely bound extra framework cations (alkali- or alkaline earth metals) which can be readily exchanged with other cations. When the extra framework cations are exchanged for protons, zeolites assume strong acidic properties which can be exploited for several important acid catalysed reactions (Perego et al., 2013).

The adsorption properties of zeolites are strongly dependent on the pore properties, but also the chemical properties (Martucci et al., 2012). With respect to the chemical properties, the ratio of silicon (silica) to aluminium (alumina) of the zeolite determines its surface chemistry (Tsai et al., 2009). Zeolites found in nature and those that are synthesised are usually obtained by hydrothermal treatment and have been divided into two categories based on their Si/Al ratio, those having a low Si/Al molar ratio (from 1 to 5 mol/mol) and those having high Si/Al ratios (from 5 to ∞ mol/mol) which are more hydrophobic in nature (Perego et al., 2013).

The adsorption work in this study focuses on the use of Beta zeolite which is a large pore highly crystalline aluminosilicate. It was first synthesized in 1967 by Mobil (Wadlinger et al., 1967) however, its structure was not determined until 1988 by Treacy and Newsam (Treacy and Newsam 1988). Its designated framework structure code is *BEA (Baerlocher et al., 2001). Beta zeolite is a disordered intergrowth of two distinct but closely related structures, polymorph A (tetragonal) and polymorph B (monoclinic). The Beta zeolite is therefore a combination of the polymorph A structure, which has straight channels of 0.73 nm x 0.60 nm and tortuous channels of 0.56 nm x 0.56 nm and polymorph B, which has straight channels of 0.73 nm x 0.60 nm and tortuous channels of 0.55 x 0.55 nm (Smirniotis and Ruckenstein 1993). As evident in Figure 2.3, the pore system in *BEA frameworks can be easily visualised as two perpendicular channels which partially intersect, the intersection aperture defines a third pore system roughly perpendicular to the other two.

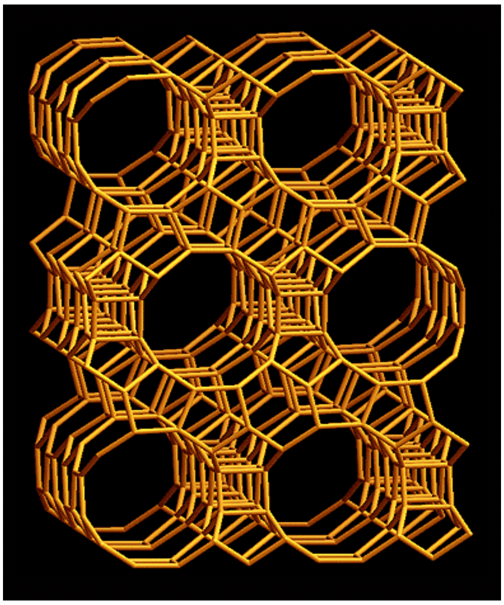

Figure 2.3: Structure of Beta zeolite.

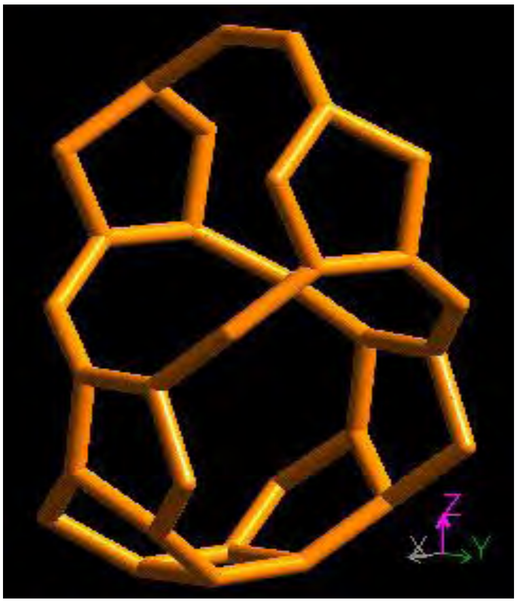

Figure 2.4: Beta zeolite pore structure.

The network of linked cavities or pores in zeolites form a system of channels throughout the structure. The cavities or void spaces in the crystalline structures of zeolites are of molecular dimensions and provide a high capacity for molecules small enough to gain access to them. It is these structural features of zeolites that enable them to function as molecular sieves i.e. selectively adsorb or reject molecules based upon molecular size, shape and other properties including polarity (Damjanovic et al., 2010).

Zeolites have been investigated as adsorbents because of their (i) high selectivity; (ii) high specific capacity; (iii) excellent resistance to chemical, biological and thermal stress (Perego et al., 2013). Synthetic and natural zeolites have been widely used as adsorbents, catalysts, ion exchangers, membranes, and molecular sieves (Damjanovic et al., 2010). Worldwide consumption of synthetic zeolites has been estimated at around 2Tg/year, with marginally higher values reported for natural zeolites (Yilmaz and Mueller 2009).

Numerous reports are cited in literature on the application of natural and synthetic zeolites for the removal of phenolic compounds from wastewater such as studies by Okolo et al., 2000; Khalid et al., 2004; Kawai and Tsutsmi 2004; Koubaissy et al., 2008 and Reungoat et al., 2007. Cosseron et al., reported pure silica Beta zeolite as a highly hydrophobic material, exhibiting significant physical interaction with organic molecules (Cosseron et al., 2013). Damjanovic et al., investigated the adsorptive propertied of various zeolites including Beta zeolite and ZMS-5 for the removal of phenols from aqueous solutions. In this study Damjanovic et al., report on the influence of Si/Al ratio of the zeolite on phenol adsorption. It is known that for adsorption of phenols from aqueous solutions, zeolite adsorbents must be hydrophobic, i.e. possess a high Si/Al ratio (Khalid et al., 2004; Reungoat et al., 2007 and Koubaissy et al., 2008).

Stelzer et al., carried out competitive sorption tests in water-toluene mixtures as a function of Si/Al ratio (Stelzer et al., 1998). They showed that the amount of adsorbed water decreases dramatically on increasing the Si/Al ratio in the Beta zeolite framework. While the adsorption of aromatic compounds (e.g. nitrophenol, nitroaniline, chlorophenol, chloroaniline) present in wastewater on Y zeolite (with Si/Al of 200 mol/mol) have been investigated by Koubaissy et al., (Koubaissy et al., 2011).

The potential adsorption capacities of zeolites for organic compounds has been cited in literature by O'Brien et al., who reported a maximum aniline adsorption capacity of 106 mg g^{-1} on Beta zeolite (O'Brien et al., 2008), while Yousef et al., investigated the use of zeolite tuff for the adsorption of phenol from aqueous solutions at different temperatures in a batch process and reported adsorption efficiencies of 96%, 88%, 76% and 84% for 10, 30, 59, 70 and 90 mg g^{-1} phenol solutions respectively (Yousef et al., 2011).

The aim of this work is to investigate the adsorptive properties of various Si/Al ratio Beta zeolites for the removal of 2-nitrophenol from aqueous solutions. The effectiveness of the adsorption process was evaluated by investigating the adsorption characteristics including isotherms (Langmuir and Freundlich), kinetics (pseudo-first-order and pseudo-second-order models), thermodynamics ($\Delta G°$, $\Delta H°$ and $\Delta S°$) and mechanism (intraparticle diffusion model).

2.2. Experimental

2.2.1 Preparation of 2-Nitrophenol Adsorption Isotherm

Four different Beta zeolites (Zeolyst International) with differing silica-to-alumina ratios (Si/Al) β(25), β(75), β(150), and β(300) were used in the adsorption studies. Accurately weighted portions of Beta zeolite adsorbent (0.2 g) were placed into a series of 50 ml vials. A series of 2-nitrophenol solutions of varying initial concentration (5 mg dm^{-3} to 1000 mg dm^{-3}) were prepared by dissolving appropriate amounts of 2-nitrophenol (Sigma Aldrich) in deionised water. From each flask, a 20 cm^3 aliquot was removed and added to each vial. The solutions were stirred continuously until equilibrium was reached. The contents of the adsorption vials were then separated by centrifugation for 20 min at 3,500 rpm using a Ritofix 32 centrifuge (Hettich Zentrifugen). An aliquot of the supernatant was then removed (10 cm^3) for analysis, for all samples.

The initial and final concentration of 2-nitrophenol before and after adsorption was determined spectrophotmetrically (λ_{max} 350 nm) by a Varian (Cary) UV-spectrophotometer. The amount adsorbed was calculated from initial and final concentrations of 2-nitrophenol in the liquid phase. Blank solutions were prepared containing equivalent initial concentrations of 2-nitrophenol but without the addition of the adsorbent. All samples and blanks were run in triplicate to ensure reproducibility and accuracy. Distilled water was used as the solvent. This initial adsorption isotherm was carried out at 24°C.

2.2.2. Evaluation of the Thermodynamics of Adsorption

Isotherms were prepared for 2-nitrophenol adsorption onto β(25), β(75), β(150) and β(300) at 6ºC, 24ºC and 40ºC using the batch technique described in section 2.2.1. The temperature was maintained using an ice bath and a thermostatically controlled water bath.

2.2.3. Kinetics of Adsorption

The equilibrium time for maximum adsorption was determined using the following procedure. Accurately weighed amounts of adsorbent (0.2 g) were added to vials containing 20 ml of 2-nitrophenol solutions where the initial 2-nitrophenol concentrations were 50 mg dm^{-3}, 100 mg dm^{-3} and 500 mg dm^{-3}. The solutions were stirred continuously at 24ºC for times ranging between 5 minutes and 2 hours. The contents of the adsorption flasks were then separated using a centrifuge at 3,500 rpm for 20 minutes. The supernatant was then analysed as in section 2.2.1. All experiments were run in triplicate and controls using 2-nitrophenol only were used to ensure reproducibility and accuracy. Distilled water was used as solvent.

2.2.4. Influence of Solution pH on Adsorption

A pH study was undertaken to investigate the effect of acidic and basic aqueous conditions on the uptake of 2-nitrophenol. Accurately weighed portions of zeolite adsorbent (0.2 g) were placed into a series of 50 ml vials. After the addition of 20 ml of 2-nitrophenol (adsorbate) solutions at an initial concentration of 100 mg dm^{-3}, the pH was adjusted appropriately using either NH_4OH or HCl. The vials were then sealed and the solutions were stirred continuously until equilibrium was reached.

2.3. Results and Discussion

2.3.1. Preparation of 2-Nitrophenol Adsorption Isotherm

The adsorption isotherms for 2-nitrophenol on β(25), β(75), β(150) and β(300) were undertaken at 24°C and are displayed in figure 2.5. It is evident from the figure that both the shape of the isotherm uptake and the maximum values of adsorbed 2-nitrophenol, are dependent on the SiO_2:Al_2O_3 ratio. The shape of the adsorption curves for β(25), β(75) β(150) and β(300) samples is similar to that of a Type I profile as defined by the Brunauer classification (Brunauer et al., 1940) where the isotherm approaches a limiting value. The Type I adsorption profile is interpreted in literature as an indication that there is no strong competition between the solvent and the adsorbate to occupy the adsorbent surface sites (Damjanovic et al., 2010).

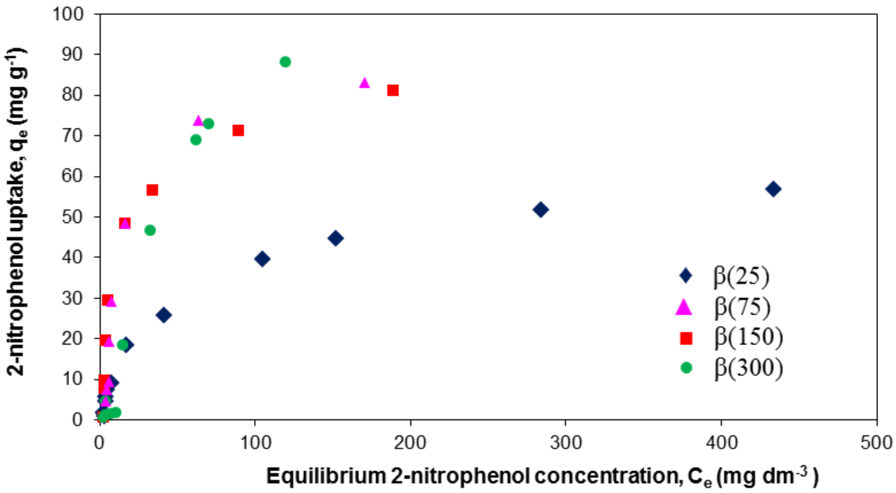

Figure 2.5: The adsorption isotherm for 2-nitrophenol on the indicated Beta zeolites, at varying initial concentrations between 10 mg dm^{-3} and 1000mg dm^{-3} at 24°C.

There is a strong uptake of 2-nitrophenol from aqueous solution at low adsorbate concentrations with an uptake plateau (limiting value) observed at higher 2-nitrophenol concentrations. The isotherms for β(75), β(150) and β(300) are steeper at low concentrations than that of β(25) indicating a higher efficiency of these adsorbents at low phenol concentrations. Maximum uptake of 2-nitrophenol of between 40 - 50 mg g^{-1}, 80 - 90 mg g^{-1}, 80 - 90 mg g $^{-1}$ and 90 - 100 mg g $^{-1}$ on β(25), β(75), β(150) and β(300) respectively, was achieved at 24°C, suggesting that at these uptake levels each zeolite is saturated. It is evident that the silica rich Beta zeolite samples have shown the highest adsorption capacity for 2-nitrophenol, while Beta zeolite with a lower Si:Al ratio (β(25)) has some potential for application as an adsorbent for dilute 2-nitrophenol solutions. The 2-nitrophenol adsorption levels achieved in this study are comparable with adsorption levels reported for phenolic compounds in literature such as studies are detailed in table 2.1.

Table 2.1: A comparison of the adsorption uptake levels of phenolic compounds by various adsorbents.

Adsorbent	Phenolic compound	Uptake mg g^{-1}	Reference
Jordanian zeolitic tuff	2-nitrophenol	75.6	Yousef et al., 2011
Macrocystis integrifolia Bory biomass crosslinked with CaCl2	2-nitrophenol	97.37	Navarro et al., 2009b
Lessonia nigrescens Bory biomass crosslinked with $CaCl_2$	2-nitrophenol	71.28	Navarro et al., 2009b
Bentonite chemically exchanged	2-nitrophenol	18.64 - 23.02	Navarro et al., 2009b
Coconut shell activated carbon	2-nitrophenol	32.94	Shao et al., 2013
Mansonia wood saw dust	4-nitrophenol	21.28	Ofomaja et al., 2011
Functional chitosan	Phenol p-chlorophenol p-nitrophenol	2.22 2.58 1.98	Li and Juang.2009

The adsorption capacity of a system cannot be easily predicted since it is highly dependent on factors such as properties of adsorbent (porosity, surface area, particle size), adsorbate (structure, water solubility, ionic charge, functional groups, pKa, polarity, functionality, molecular weight and size), solution conditions (solvent, pH, temperature, ionic strength, solute concentration and competition between solutes) and interactions at the solid–liquid interface (Soto et al., 2011). The interaction of the 2-nitrophenol molecule with the Beta zeolite structure is dependent on several factors such as the Beta zeolite, silica to alumina ratio, pore size, solution pH and the molecular size of 2-nitrophenol.

The adsorption isotherms for 2-nitrophenol on each of the beta zeolites, β(25), β(75), β(150) and β(300) and displayed in figure 2.5 illustrate the effect of varying the silica to alumina ratio of the Beta zeolite samples on the adsorption process. Zeolites with low Si/Al ratios are hydrophilic in nature, however, it is generally accepted that they turn more hydrophobic when the Si:Al ratio reaches 10 (Ruthven, 1984). Shu et al., and Khalid et al., have investigated the adsorption of phenol on various zeolite types and have noticed the improvement of adsorption capacity with increased hydrophobicity (Shu et al., 1997 and Khalid et al., 2004).

This adsorption study revealed that 2-nitrophenol uptake was influenced by the silica to alumina ratio with uptake levels increased with increasing Si:Al ratio above 25:1 as shown in figure 2.6. Increasing the silica to alumina ratio of the Beta zeolite from β(25) to β(75), results in a subsequent decrease in the H^+, which alters the Beta zeolite surface making it more hydrophobic in nature, thereby reducing the competition between the water and the 2-nitrophenol molecules. However increasing the $SiO_2:Al_2O_3$ ratio above 75:1, did not result in any significant increase in 2-nitrophenol adsorption levels at 24°C. Hence, the results presented in figure 2.6 are in general agreement with previous reports in relation to the adsorption of methylene blue and bisphenol-A by a synthesised zeolite increased with increasing $SiO_2:Al_2O_3$ ratios (Tsai et al., 2009), while others showed that the adsorption capacity of phenol onto HFAU zeolites increased in the range of 0.1 – 0.6 mmol/g with an increasing $SiO_2:Al_2O_3$ ratio from 5 to 500 (Khalid et al., 2004). They concluded that the $SiO_2:Al_2O_3$ ratio, rather than the pore size of the zeolite has the predominant effect on the adsorption capacity of phenol. The results obtained in this investigation confirm that the adsorption of 2-nitrophenol from aqueous solution is more pronounced on hydrophobic Beta zeolite samples. These results correlate with similar findings both on adsorption and microcalorimetric measurements by Damjanovic et al., 2010 who reported that the higher the Si/Al ratio, the higher the levels of adsorption of phenols from aqueous solutions.

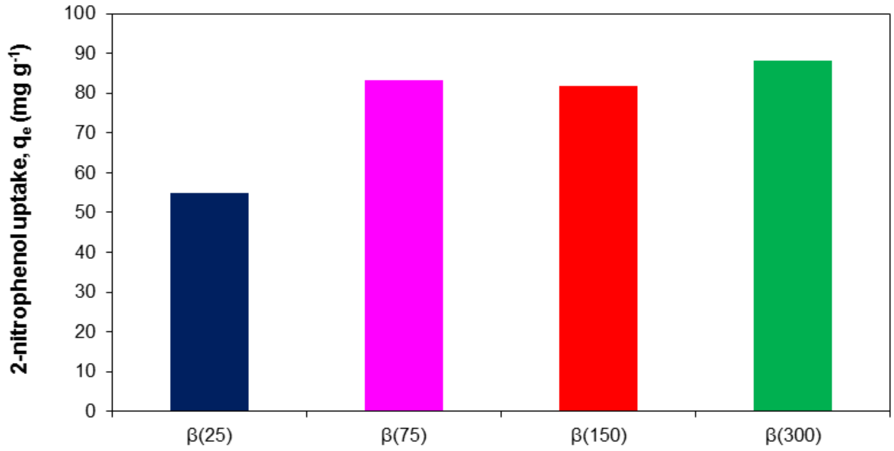

Figure 2.6: Comparison of 2-nitrophenol uptake on the indicated Beta zeolite samples. Initial 2-nitrophenol concentration of 1000 mg dm^{-3}.

It is well known that zeolites consist of three-dimensional framework with well defined, regular channels and cavities of molecular dimensions, specific to the type of zeolite. Zeolites are size selective adsorbents, molecules which are to be adsorbed should be smaller than the pore size of the adsorbent. Beta zeolite has a three-dimensional intersecting channel system, two mutually perpendicular straight channels each with a cross section of 6.6 Å x 6.7 Å and a sinusoidal channel with a cross section of 5.6 Å x 5.6 Å (Khalid et al., 2004). Pollutant molecules with sizes larger than the pore opening of the zeolite can only be adsorbed on the external surface of the zeolite. The molecular dimensions of 2-nitrophenol have been reported as 6.84 Å x 4.17 Å (Liu et al., 2010) and therefore it is close to pore size and may block the Beta zeolites channels during the adsorption process. This would restrict the adsorption of 2-nitrophenol to the outer surface of the Beta zeolite. It is also possible that the adsorption may occur through the insertion of the nitro group in the channel of the Beta zeolite, as the dimensions of the nitro group (3.58 Å) are smaller than that of the Beta zeolite channels. The adsorption of nitrobenzene by the insertion of the nitro group into the pore channel of zeolites has been reported by Yang et al., (2007).

An adsorption isotherm describes how solutes interact with adsorbents and is critical in optimizing the use of adsorbents. Adsorption isotherms reflect the relationship between the amount of solute adsorbed at constant temperature and its concentration in the equilibrium solution. It provides essential physiochemical data for assessing the applicability of the adsorption process as a complete unit operation. There are several isotherm equations available for analysing experimental adsorption equilibrium data. In this work two adsorption isotherms models: Langmuir and Freundlich, as defined in Equations 2.28 and 2.30 were applied to fit the equilibrium data of adsorption of 2-nitrophenol onto Beta zeolite (Langmuir, 1918, Freundlich, 1906).

The Langmuir isotherm is the most widely used two-parameter equation, and assumes the following hypotheses: uniform adsorption energies along the homogeneous adsorbent surface, equal solute affinities in all the adsorption sites, no interaction among adsorbed molecules, single adsorption mechanism, formation of a monolayer on the free surface (Soto et al., 2011). In the literature, the Langmuir isotherm has been widely applied to interpret the data obtained from the adsorption of liquid organic pollutants such as phenols and it has shown good agreement with a wide variety of experimental data (Yousef and El-Eswed 2009, and Ghiaci et al., 2004).
The Langmuir isotherm as shown in section 2.1.3 equation 2.28, where q_e is the amount of solute adsorbed per gram of adsorbent and C_e (mg dm^{-3}) is the equilibrium concentration of 2-nitrophenol and K_L and W_{max} are Langmuir constants related to the rate of adsorption and the adsorption capacity. A plot of C_e/q_e versus C_e, was constructed to determine the values $1/W_{max}K_L$ (intercept) and $1/W_{max}$ (slope).

The data obtained from the Langmuir plots for Beta zeolite samples β(25), β(75), β(150) and β(300) at the indicated temperatures are shown in table 2.2. Jaynes and Boyd (1991) proposed that the adsorption conforms to the Langmuir model when the value of the correlation coefficient (R^2) is greater than 0.89. Therefore based on the R^2 values obtained from the Langmuir plots the sorption of the 2-nitrophenol from aqueous solution onto β(25) and β(75) at all temperatures studied show a good fit to the Langmuir model approach of adsorption on a uniform surface, while it is evident that the adsorption of 2-nitrophenol on β(150) and β(300) only follow the Langmuir model of adsorption at temperatures of 24°C, 6°C (β(150)) and 24C° β(300). The decrease in Langmuir constant (K_L) values with increase in temperature indicate lower affinity of the 2-nitrophenol for β(25), β(75), β(150) and β(300) with increasing temperature, which would suggest that the adsorption is an exothermic process. Maximum 2-nitrophenol uptake on the zeolite adsorbent surface was then obtained as W_{max}, these theoretical uptake levels of 2-nitrophenol are slightly higher than the experimental uptake levels $W_{max\ exp}$, over the temperature ranges studied.

The separation factor (R_L) is a dimensionless equilibrium parameter which can be calculated from the Langmuir isotherm equation as defined by Hall et al., 1966. The R_L value indicates the favourability of the adsorption process as described by the Langmuir isotherm. The isotherm is described as favourable ($0<R_L<1$), unfavourable ($R_L> 1$) and irreversible ($R_L=0$). The calculated values of R_L at different initial 2-nitrophenol concentrations were found to be less than 1, indicating the favourable adsorption of 2-nitrophenol by Beta zeolite independent of the Si:Al ratio shown in table 2.2. The increase in the R_L value with increasing temperature further suggests that the adsorption of 2-nitrophenol by all the Beta zeolite samples is exothermic in nature (Mittal et al., 2007).

Table 2.2: **Langmuir constants for 2-nitrophenol adsorption onto different Beta zeolites at the indicated temperatures.**

Sample Name	Temperature (°C)	$W_{max, exp}$ (mg g^{-1})	K_L ($dm^3 g^{-1}$)	W_{max} (mg g^{-1})	R_L	R^2
β(25)	6	56.60	0.021	61.34	0.823	0.996
	24	54.80	0.015	61.34	0.864	0.989
	40	53.88	0.006	69.40	0.938	0.969
β(75)	6	108.83	0.022	121.95	0.699	0.962
	24	82.90	0.043	103.09	0.819	0.981
	40	80.10	0.027	90.90	0.787	0.909
β(150)	6	115.0	0.013	434.78	0.884	0.356
	24	74.60	0.046	90.90	0.714	0.983
	40	81.09	0.011	217.39	0.900	0.186
β(300)	6	87.75	0.015	135.13	0.869	0.957
	24	88.01	0.010	161.29	0.854	0.914
	40	87.36	0.006	212.76	0.900	0.767

Freundlich 1906 developed an empirical equation to describe the adsorption process. His development was based on the assumption that the adsorbent had a heterogeneous surface composed of different classes of adsorption sites. Freundlich demonstrated that the ratio of the amount of solute adsorbed onto a given mass of an adsorbent to the concentration of the solute in the solution was not constant at different solution concentrations (Zahir and Najwa 2006). In contrast to the Langmuir isotherm, this isotherm does not predict any saturation of the sorbent by the sorbate, thus infinite surface coverage is predicted mathematically, indicating multilayer sorption of the surface (Donat et al., 2005). The Freundlich isotherm has been widely applied to the removal of organic compounds from aqueous solution in heterogeneous systems. Dabrowski et al., 2005 reported on the Freundlich isotherm for the adsorption of phenolic compounds onto activated carbons.

The data obtained from the adsorption of 2-nitrophenol were fitted to the Freundlich model by plotting $\ell n C_e$ versus $\ell n q_e$. The linear plot obtained has a slope that has the value 1/n and y-intercept that is $\ell n K_F$, where K_F is a constant related to the extent of sorption or adsorption capacity, and n is a constant related to the intensity of sorption or the degree of dependence of sorption on concentration (Zahir and Najwa 2006). The values of K_F and n depend on temperature, the nature of the adsorbent, and the substance to be adsorbed. The values of 1/n imply the type of isotherm and can be classified as irreversible ($1/n = 0$), favourable ($0 < 1/n < 1$) and unfavourable ($1/n > 1$). A relatively slight slope (and hence a high value of n) indicates that the adsorption is good over the entire range of concentrations studied, while a steep slope (and hence a small n) means that the capacity of the sorbent is more susceptible to the 2-nitrophenol concentration (good adsorption at high concentrations but poorer at low concentrations). Based on the equilibrium equations for both isotherms, the requirement parameters were obtained and presented in table 2.3. The Freundlich constant n decreases as the temperature increases indicating that the adsorption process is mildly exothermic. The magnitude of the Freundlich constant n is greater than 1 indicating that the adsorption process is favoured. While Baocheng et al., reported that the adsorption isotherm follows L-type curves ($n > 1$) as classified by Giles et al., 1963 which indicates that the adsorption firstly occurs on the energetically more favourable sites of the adsorbent followed by the less energetically favourable sites (Baocheng et al., 2001). The initial slope of the L type adsorption curve shows that the adsorbate has a high affinity for the surface of the adsorbent. As more sites on the sorbent are occupied it becomes increasingly difficult for adsorbate molecules to find a vacant site.

The greater the value of the Freundlich constant, K_F, the greater the capacity for adsorption. Increasing the temperature of the adsorption solution results in a decrease in the K_F values, also indicating that the adsorption process is mildly exothermic in nature. Deviations of the results in Table 2.3 from these trends can be explained by the poorer fitting of the results to the adsorption model as indicated by the decrease in the R^2 values for example β(150).

Table 2.3: Freundlich constants for 2-nitrophenol adsorption onto different Beta zeoliles at the indicated temperatures.

Sample Name	Temperature (°C)	K_F ($dm^3\ g^{-1}$)	n	R^2
β(25)	6	3.672	2.089	0.939
	24	0.435	1.546	0.890
	40	0.533	1.239	0.870
β(75)	6	3.691	1.496	0.700
	24	3.644	1.439	0.764
	40	2.797	1.347	0.744
β(150)	6	1.280	0.626	0.900
	24	6.999	1.890	0.822
	40	2.464	1.043	0.925
β(300)	6	2.897	1.341	0.988
	24	0.112	0.696	0.916
	40	0.775	0.946	0.944

A poorer correlation (relative to the Langmuir approach) has been observed for the adsorption of 2-nitrophenol onto β(25) and β(75) as is evident from comparison of R^2 values in Table 2.2-2.3. However, the adsorption of 2-nitrophenol by β(150) at 6°C and 40°C appears to follow the Freudlich model of adsorption, as does the adsorption of 2-nitrophenol onto β(300) at all temperatures studied. The fitting of the Freudlich model for the adsorption process by β(300) at the indicated temperatures suggests that at these higher silica to alumina ratios the surface of the Beta zeolite becomes more heterogeneous possibly due to the decrease in the number of exchangeable cations, allowing for multilayer adsorption.

The Langmuir isotherm is therefore the more suitable equation to describe the adsorption equilibrium of 2-nitrophenol onto β(25) and β(75) at temperatures 6, 24 and 40°C, β(150) at 24°C. The applicability of the Langmuir model suggests that adsorption of one single adsorbate molecule takes place at specific active sites of an energetically homogeneous surface resulting in monolayer coverage of the adsorbate at the outer surface of the adsorbent. These findings correlate to works previously published by Yousef et al., 2011 who reported the Langmuir model for adsorption of phenols with a maximum adsorption capacity of 34.5, 24.9, 23.8 and 23.3 mg g^{-1} at temperatures 25, 35, 45, and 55 °C respectively.

2.3.2 Evaluation of the Thermodynamics of Adsorption

2-nitrophenol adsorption isotherms obtained at 6ºC, 24ºC and 40ºC are plotted in Figures 2.7 to 2.10 for β(25), β(75), β(150) and β(300) samples at initial concentrations (5 – 1000 mg dm^{-3}) after 1 hour. They correlate the amount of 2-nitrophenol adsorbed per unit weight of adsorbent, q_e, with the 2-nitrophenol equilibrium concentration, C_e.

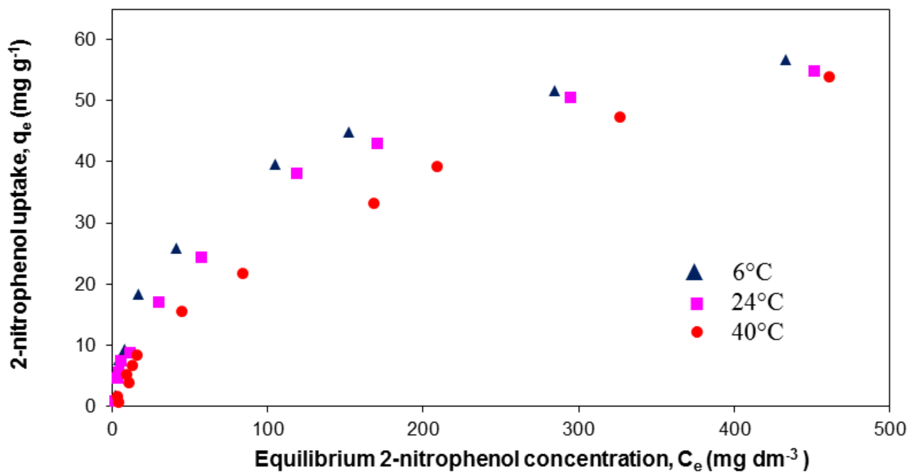

Figure 2.7: Thermodynamic plots displaying 2-nitrophenol adsorption on β(25), as a function of the 2-nitrophenol equilibrium concentration at the indicated temperatures.

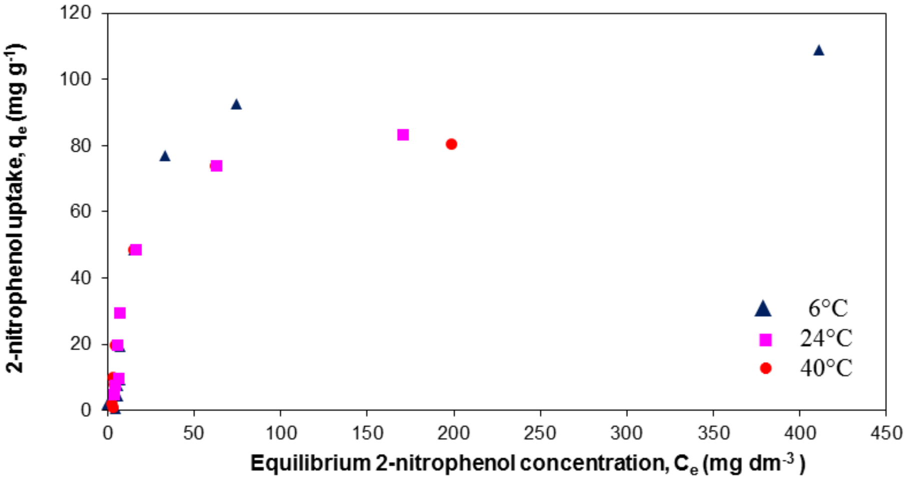

Figure 2.8: Thermodynamic plots displaying 2-nitrophenol adsorption on β(75), as a function of the 2-nitrophenol equilibrium concentration at the indicated temperatures.

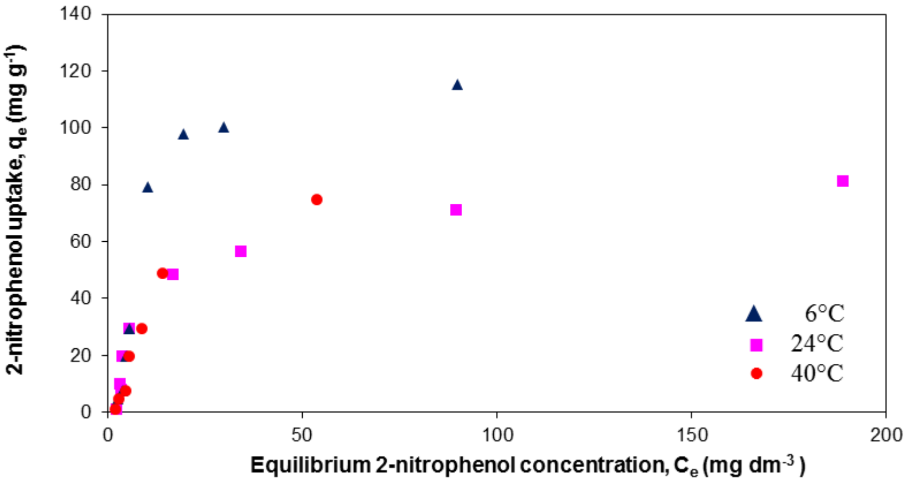

Figure 2.9: Thermodynamic plots displaying 2-nitrophenol adsorption on β(150) as a function of 2-nitrophenol equilibrium concentration at the indicated temperatures.

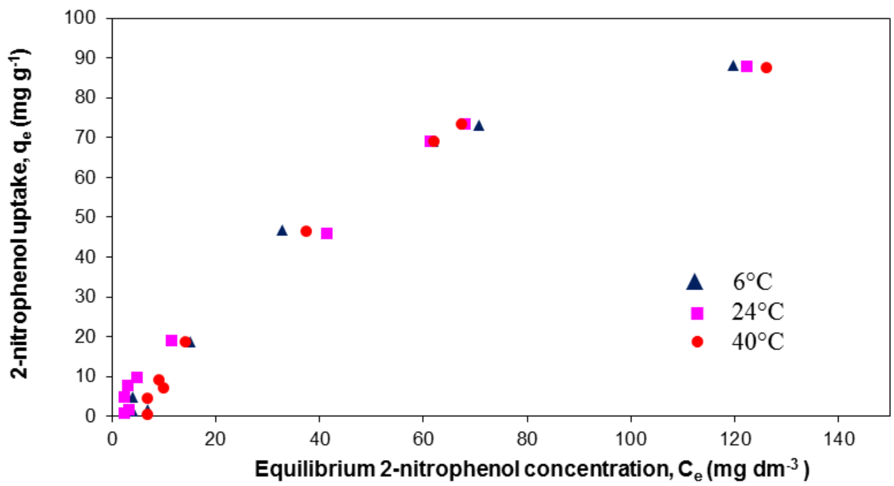

Figure 2.10: Thermodynamic plots displaying 2-nitrophenol adsorption on β(300) as a function of 2-nitrophenol equilibrium concentration at the indicated temperatures.

The 2-nitrophenol uptake was found to be mildly dependent on solution temperature from 6 to 40 ºC for β(25), β(75) and β(150) samples as illustrated in figures 2.7, 2.8 and 2.9. The decrease in the adsorption capacity of the Beta zeolite samples with increasing temperature suggests that the adsorption process is exothermic. The adsorption of 2-nitrophenol onto β(300) was found to be largely independent of temperature as shown in figure 2.10, as with increasing temperature the adsorption capacity of β(300) was approximately constant. Increasing the temperature of the adsorbing solution to 24°C and 40°C did not alter the shape of the isotherm curves for the adsorption of 2-nitrophenol onto β(25), β(75), β(150) and β(300) which is typical of type I adsorption curve (monolayer adsorption).

The thermodynamic parameters that must be considered to determine the adsorption processes are the changes in standard enthalpy (ΔH°), standard entropy (ΔS°), and standard free energy (ΔG°) due to the transfer of unit mole of solute from solution onto the solid –liquid interface. The thermodynamic parameters, Gibbs free energy, and enthalpy changes for 2-nitrophenol adsorption on β(25), β(75), β(150) and β(300) samples were calculated and are presented in Table 2.4. The Langmuir constant K_L can be related to the free energy ($\Delta G°_{ads}$) (Toppallar and Bayrak, 1999). The Gibbs free energy of adsorption was calculated using Equations 2.11 - 2.14. In this study the values of ln K_L were plotted against 1/T, where ΔH° and ΔS° values were calculated from the slope and the intercept of the plot. The obtained thermodynamic parameters are listed in Table 2.4.

Table 2.4: Thermodynamic parameters for 2-nitrophenol adsorption on the indicated Beta zeolite SiO_2:Al_2O_3 ratios.

Sample Name	(ΔG°) (kJ mol $^{-1}$)			(ΔH°) (kJ mol $^{-1}$)	(ΔS°) (J mol^{-1}K^{-1})
	6°C	24°C	40°C		
β(25)	9.131	11.21	13.061	-23.110	-115.58
β(75)	8.088	8.741	9.322	-2.039	-36.298
β(150)	8.542	10.147	11.573	-16.328	-89.142
β(300)	10.107	11.808	13.321	-16.269	-94.538

In this work the negative ΔH° values calculated for β(25), β(75), β(150) and β(300), indicate the adsorption of 2-nitrophenol onto each of the Beta zeolites is mildly exothermic in nature, which is in agreement with the experimental observations illustrated in figures 2.7 – 2.9. Similar findings on an adsorption process involving a solid–liquid system has been reported by Yousef et al., 2011. They reported on the adsorption characteristics of natural zeolites as solid adsorbents for phenol removal from aqueous solutions. The adsorption process was found to be exothermic in nature in the temperature range of 24 – 55°C.

Adsorption processes are divided into physical adsorption and chemical adsorption based on the magnitude of the adsorption enthalpy change (Jinbei et al., 2014). The adsorption process is defined as chemical when the adsorption enthalpy change is greater than, 42 kJ mol^{-1}, while physical adsorption is based on weaker interaction such as Van der Waals forces (Jinbei et al., 2014). Physical adsorption has been reported for the adsorption of phenols by natural zeolites (Yousef et al., 2011), for model phenolic compounds on a water compatible hypercrosslinked polymer resin (Lin et al., 2002a and Li et al., 2002b) and onto agro based adsorbents (Srihari and Das, 2008) and onto natural zeolites (Yousef et al., 2011).

The magnitude of ΔH° values suggests a physical and a mildly exothermic nature for the adsorption process. This physical nature of adsorption enhances the possibility of the reversibility of the adsorption process. Negative ΔS° values suggest that the organization of the adsorbate at the solid/solution interface becomes less random (Yousef et al., 2011). It has also been supposed that the change of ΔS° value is related to the displacement of the adsorbed water molecules by the adsorbate (Li et al., 2005). In this study, the negative values of ΔS° indicates that the adsorption process takes place through electrostatic interactions between the adsorbent surface and adsorbate species in solution (Rida et al., 2013). In addition the negative values of ΔS° reflects that no significant change occurs in the internal structure of the adsorbent during the adsorption process (Anirudhan and Radhakrishnan, 2008). Based on the values of both enthalpy and entropy, ΔG° is obtained to be positive by equations 2.11 and 2.14. The positive ΔG° values may be explained through the relationship between the standard Gibbs free energy and the equilibrium constant in equation 2.12 (Keeler and Wothers 2003). This equation implies that if ΔG° is negative then the equilibrium constant will be greater than 1 and the reaction will come to an equilibrium position which favours the formation of products however if ΔG° is positive the equilibrium constant will be less than 1 therefore the reaction will come to an equilibrium position which favours the reactants. Therefore the positive values for the Gibbs free energy change ($\Delta G°$) in table 2.4, suggest that the adsorption of 2-nitrophenol onto the Beta zeolite surface will come to an equilibrium position which will favour 2-nitrophenol in the aqueous phase. Under these conditions 2-nitrophenol is adsorbed on the surface of the Beta zeolites as shown in Figures 2.7 – 2.10. The magnitude of the values for ($\Delta G°$) detailed in Table 2.4 are small and are influenced by increasing temperatures which suggest that the adsorption process is less disfavoured at lower temperatures which is in agreement with the thermodynamic findings illustrated in Figures 2.7 - 2.9 and the negative values calculated for the entropy and the enthalpy.

These findings are similar to those reported by previous works on the thermodynamics of adsorption of phenol and chlorophenol by surfactant-modified natural zeolite by Kuleyin 2007. Based on experimental results the adsorption process was reported to be exothermic in nature with a reported decrease in adsorption levels for both phenol and 4-chlorophenol as temperature increased from 20°C to 40°C. The Gibbs free energy of adsorption was reported to be positive indicating the reaction was non-spontaneous at all temperatures studied.

Due to the relatively small magnitude of the thermodynamic parameters $\Delta°H$, $\Delta°S$ and $\Delta°G$ in this study it is only possible to say that the experimental results presented in figures 2.7 - 2.9 suggest that the adsorption of 2-nitrophenol by β(25), β(75), β(150) is mildly exothermic in nature while the adsorption of 2-nitrophenol by β(300) is independent of temperature (figure 2.10). Given the adsorption levels of 2-nitrophenol achieved in this study by Beta zeolites at 6°C it is evident that the adsorption process is thermodynamically feasible.

2.3.3 Kinetics of Adsorption

In order to apply the adsorption technique to larger scale processes, the elucidation of the kinetic parameters on the sorption characteristics of the adsorbent material is necessary. The two primary issues to be addressed are contact time for equilibrium adsorption and the influence of initial adsorbate concentration on uptake.

The contact time between the pollutant and the adsorbent is of significant importance in wastewater treatment by adsorption. A rapid uptake of pollutants and establishment of equilibrium in a short period signifies the efficacy of that adsorbent for its use in wastewater treatment. In physical adsorption most of the adsorbate species are adsorbed within a short interval of contact time. However, strong chemical bonding of the adsorbate with adsorbent requires a longer contact time for the attainment of equilibrium. In the initial stages of the adsorption process the uptake of adsorbate species is fast while it becomes slower as the equilibrium is reached. In between these two stages of the uptake, the rate of adsorption is found to be nearly constant. This is obvious from the fact that a large number of vacant sites are available for adsorption during the initial stage, and after a lapse of time, the remaining vacant sites are difficult to be occupied due to repulsive forces between the solute on the solid and bulk phases (Mall et al., 2006). This mechanism of adsorption has been observed by Azizian 2006, Bhatnagar 2007, Tsai et al., 2009 and Ofomaja 2011 during their adsorption studies.

The effect of contact time on the removal of 2-nitrophenol at 24°C is presented in figures 2.11 (A – D). The adsorption uptake was found to be rapid for all samples (β(25), β(75), β(150) and β(300)) irrespective of the initial 2-nitrophenol concentration (50, 100 and 500 mg dm^{-3}). At the equilibrium point, the amount of 2-

nitrophenol desorbing from the zeolite was in a state of dynamic equilibrium with the amount of 2-nitrophenol being adsorbed on the zeolite. The amount of 2-nitrophenol adsorbing at the equilibrium time reflected the maximum adsorption uptake of the adsorbent under the operating conditions applied. The plots show that the adsorption attains equilibrium faster for the solutions with lower initial concentrations, as initially, a large number of vacant surface sites are available for adsorption. The adsorption rate is very fast thus rapidly increases the amount of adsorbate accumulated on the zeolite surface mainly within 10 minutes of adsorption. This relatively short time requirement for adsorption of 2-nitrophenol is of strong significance and will be of considerable benefit in any future practical applications of this work.

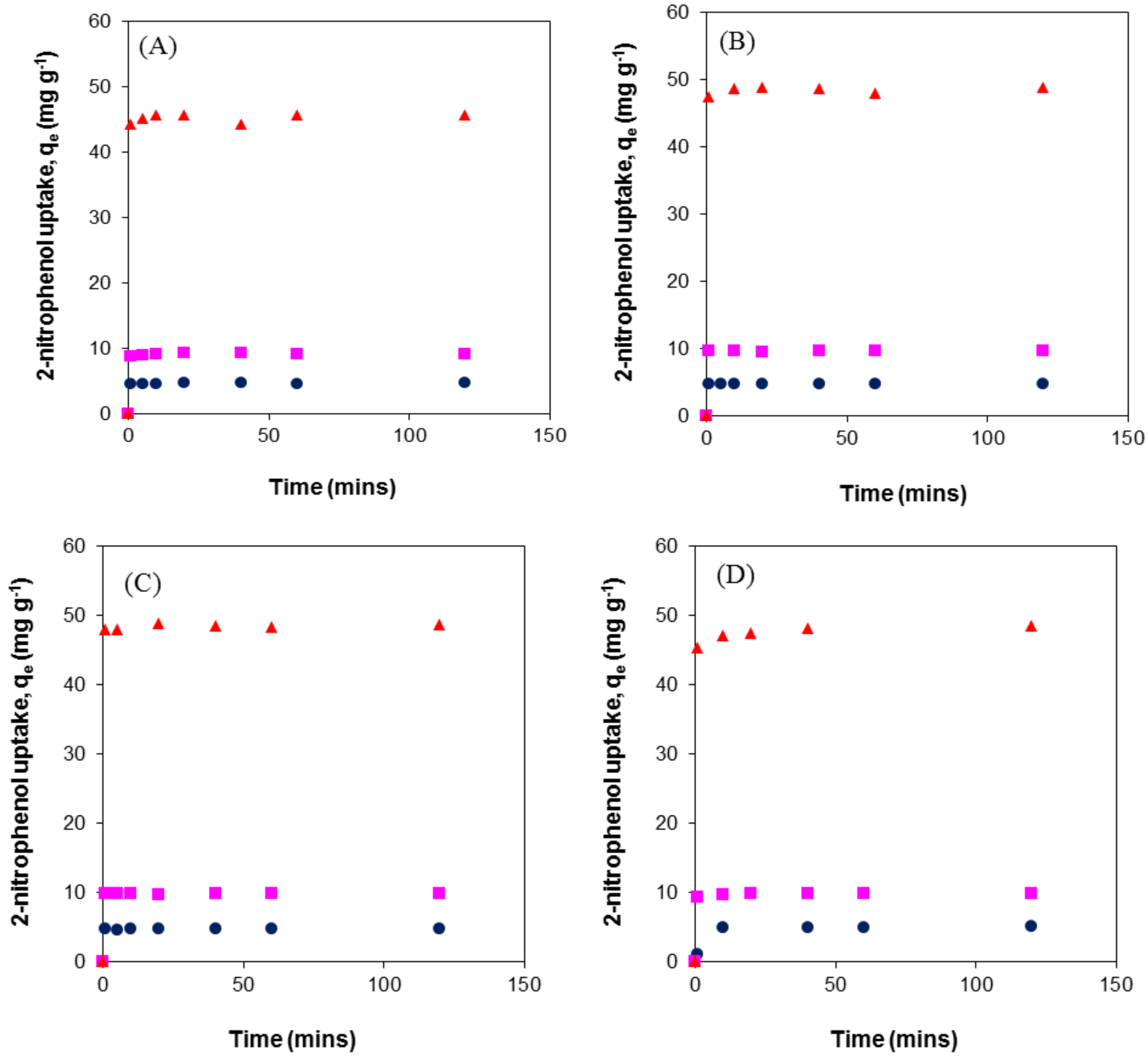

Figure 2.11: Kinetic plots displaying 2-nitrophenol adsorption on (A) β(25), (B) β(75), (C) β(150) and (D) β(300) at 24°C as a function of time and initial 2-nitrophenol concentration; ● 50 mg dm^{-3}; ■ 100 mg dm^{-3}; ▲ 500 mg dm^{-3}.

The curves of contact are single, smooth and continuous leading to saturation. These curves indicate the possible monolayer coverage of 2-nitrophenol on the Beta zeolite samples which corresponds to other accounts cited in literature who report the rapid rate of adsorption of *p*-nitrophenol on two typical Chinese soils namely Jiangxi and Heilongjiang soils (Pei et al., 2006), the kinetics and pseudo-isotherm of 4-nitrophenol adsorption onto mansonia wood sawdust (Ofomaja 2011) and the rapid uptake of aniline from aqueous solution onto Beta zeolite and onto its copper modified forms (O’Brien et al., 2008). It has been reported in literature that the remaining vacant surface sites are difficult to be occupied due to repulsion among adsorbate molecules such as phenol (on the surface and in the bulk phase) (Mall et al., 2006). This lead to a decrease of adsorption rate and was well exhibited by a plateau in the adsorption uptake curve after 10 minutes of adsorption; a confirmation that the process has reached the steady-state condition (Bhatnagar 2007).

Several kinetics models are available to describe the reaction order of sorption processes; pseudo first order (Lagergren, 1898); first order (Sobkowsk and Czerwinski, 1974); second order (Blanchard et al., 1984) and pseudo-second order (Ho, 1995). In order to assess the dependency of the process on the adsorbed 2-nitrophenol concentration, Lagergren's pseudo first order kinetic expression (equation 2.39) was applied to the kinetic data, where q_e and q_t (mg g^{-1}) are the amount of 2-nitrophenol absorbed at equilibrium and at any time t respectively. The adsorption rate constant, k_1 and the equilibrium sorption capacity, $q_{e\ cal}$ for the pseudo-first–order reaction were obtained from the pseudo-first-order model (equation 2.39). The pseudo-first-order model assumes that adsorption occurs due to a concentration difference between the adsorbate surface and solution (Gregorio and Badot 2008). This occurs only in adsorption and begins when the external mass transfer coefficient controls the process (Dotto and Pinto 2011). In this study the non-linear Chi-squared error analysis method was used to test the best fit of the kinetic model to the experimental data (equation 2.49). If the data from the model are similar to the experimental data, χ^2 will be a small number and if they are different, χ^2 will be a bigger number. The pseudo-first- order rate constant, k_1, the equilibrium sorption capacity, $q_{e\ cal}$, the experimental equilibrium sorption capacity $q_{e\ exp}$, (obtained from figures 2.11 (A - D)) correlation co-efficient, R^2 and the co-efficient of Chi-squared,

χ^2 at 24ºC are tabulated in tables 2.5 - 2.8. Low R^2 values and notable variances between the experimental uptakes ($q_{e, exp}$) and the theoretical uptakes ($q_{e, cal}$) and the large values obtained from the chi square test (χ^2) reveal the poor fitting of the pseudo-first-order model. Thus the adsorption of 2-nitrophenol β(25), β(75), β(150) and β(300) does not follow pseudo-first-order reaction kinetics.

Table 2.5: Effect of initial 2-nitrophenol concentration on sorption data on β(25) using pseudo-first-order approach.

C_0 (mg dm^{-3})	$q_{e, exp}$ (mg g^{-1})	$q_{e, cal}$ (mg g^{-1})	k_1 (min^{-1})	(R^2)	χ^2
50	4.61	99.31	0.056	0.2769	90.303
100	8.795	27.61	0.044	0.1715	12.821
500	42.9	178.64	0.188	0.7064	103.142

Table 2.6: Effect of initial 2-nitrophenol concentration on sorption data on β(75) using pseudo-first-order approach.

C_0 (mg dm^{-3})	$q_{e, exp}$ (mg g^{-1})	$q_{e, cal}$ (mg g^{-1})	k_1 (min^{-1})	(R^2)	χ^2
50	4.37	18.793	0.045	0.2874	11.069
100	9.29	22.130	0.117	0.1085	7.449
500	48.44	6.306	0.072	0.1265	281.521

Table 2.7: Effect of initial 2-nitrophenol concentration on sorption data on β(150) using pseudo-first-order approach.

C_0 (mg dm^{-3})	$q_{e, exp}$ (mg g^{-1})	$q_{e, cal}$ (mg g^{-1})	k_1 (min^{-1})	(R^2)	χ^2
50	7.64	20.09	0.007	0.002	7.70
100	9.67	4.36	0.055	0.237	6.43
500	48.32	4.46	0.187	0.445	431.09

Table 2.8: Effect of initial 2-nitrophenol concentration on sorption data on β(300) using pseudo-first-order approach.

C_0 (mg dm^{-3})	$q_{e, exp}$ (mg g^{-1})	$q_{e, cal}$ (mg g^{-1})	k_1 (min^{-1})	(R^2)	χ^2
50	4.75	1.35	0.165	0.453	8.47
100	9.50	4.38	0.055	0.236	6.00
500	45.85	1.71	0.132	0.637	1137.22

Since the data do not appear to fit the pseudo first order kinetics, a pseudo second order reaction model, as developed by Ho et al., (Ho et al., 2000), was applied to the overall rate of this adsorption process as described by equations 2.41 and 2.42, where q_e and q_t (mg g^{-1}) are the amounts of 2-nitrophenol adsorbed at equilibrium and at any time, t (min), respectively. The constant k_2 (g mg^{-1} min^{-1}) is the adsorption rate constant of pseudo-second-order adsorption and h is the initial sorption capacity. The values of t/q_t plotted against t for β(25), β(75), β(150) and β(300) samples are shown in figure 2.12 (A - D). Figures 2.12 (A - D) show the appropriate second order plots for 2-nitrophenol on beta zeolite. The plots show high correlation co-efficient (R^2) and good compliance with the proposed pseudo-second-order equation.

The pseudo-second-order kinetic expression described by Ho (1995) is by far the most widely applied kinetic model for sorption systems in recent years (Ofomaja 2011). This kinetic expression was initially used to model bimetal solutions (Ho et al., 1996). The application of Ho's pseudo-second-order kinetic expression to several adsorption systems has been reported in literature, metal adsorption (Ho, 2003 and Ho and McKay 2000), dye adsorption (Ho and McKay, 1998a,b, 1999a, Ho et al., 2005, Ofomaja 2007a,b) and organic pollutant adsorption (Ho and McKay, 1999b and Kelleher et al., 2001). The pseudo-second-order equation has the following advantages: (i) it does not have the problem of assigning an effective sorption capacity, and (ii) the sorption capacity, rate constant of pseudo-second-order and the initial sorption rate can all be determined from the equation without knowing any of the parameters beforehand (Ofomaja 2011).

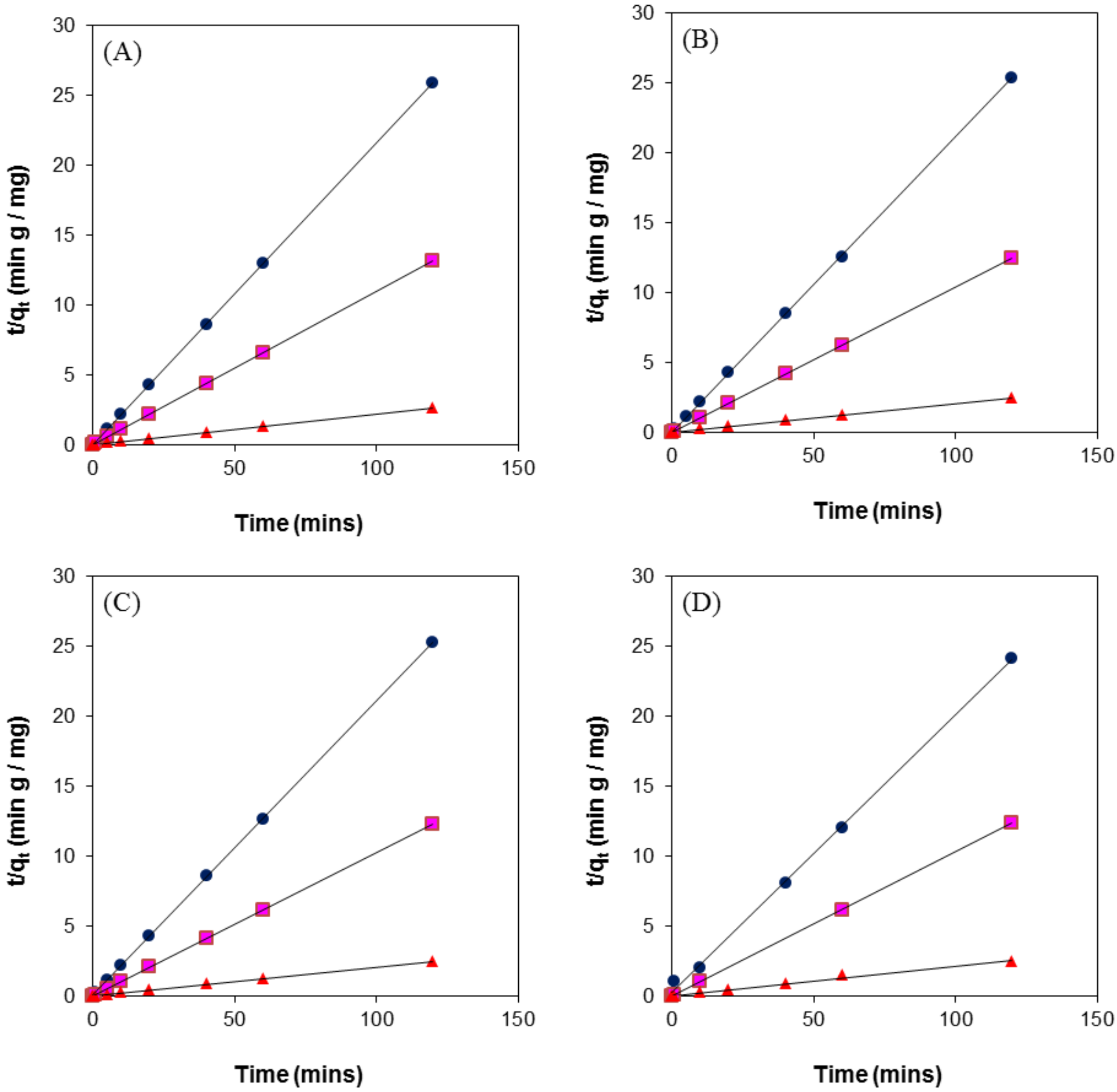

Figure 2.12: **Pseudo-second-order sorption kinetics of 2-nitrophenol on (A) β(25), (B) β(75), (C) β(150) and (D) β(300) at initial concentrations; ● 50 mg dm^{-3}, ■ 100 mg dm^{-3}, and ▲ 500 mg dm^{-3}.**

The pseudo-second-order kinetic model assumes that adsorption is a pseudo–chemical reaction and that the adsorption reaction on the surface of adsorbent is the rate controlling step (Yu 2008). The pseudo-second-order rate constant, k_2, the equilibrium sorption capacity, $q_{e,cal}$, the experimental equilibrium sorption capacity $q_{e\ exp}$, (obtained from figures 2.11 (A - D)), the percentage 2-nitrophenol removal, R_e, the correlation co-efficient, R^2 and the co-efficient of Chi-squared, χ^2, with respect of initial 2-nitrophenol concentrations, C_0, at 24°C are tabulated in tables 2.9 – 2.10.

Table 2.9: Effect of initial 2-nitrophenol concentration on sorption data on β(25) using pseudo-second-order approach.

C_0 (mg dm^{-3})	$q_{e,\,exp}$ (mg g^{-1})	$q_{e,\,cal}$ (mg g^{-1})	Re (%)	k_2 (g mg^{-1}min^{-1})	h (mg g^{-1} min^{-1})	R^2	χ^2
50	4.61	4.63	92.76	5.60	120.48	1	0.0001
100	8.79	9.19	91.99	3.28	277.70	1	0.0177
500	42.90	45.45	90.90	0.13	285.71	0.99	0.1430

Table 2.10: Effect of initial 2-nitrophenol concentration on sorption data on β(75) using pseudo-second-order approach.

C_0 (mg dm^{-3})	$q_{e,\,exp}$ (mg g^{-1})	$q_{e,\,cal}$ (mg g^{-1})	Re (%)	k_2 (g mg^{-1}min^{-1})	h (mg g^{-1} min^{-1})	(R^2)	χ^2
50	4.37	4.73	94.78	2.74	61.72	1	0.0280
100	9.29	9.65	96.52	0.71	66.22	1	0.0135
500	48.44	48.54	97.08	0.30	714.28	0.99	0.0002

Table 2.11: Effect of initial 2-nitrophenol concentration on sorption data on β(150) using pseudo-second-order approach.

C_0 (mg dm^{-3})	$q_{e,\,exp}$ (mg g^{-1})	$q_{e,\,cal}$ (mg g^{-1})	Re (%)	k_2 (g mg^{-1}min^{-1})	h (mg g^{-1} min^{-1})	(R^2)	χ^2
50	7.64	4.73	94.60	1.51	33.89	0.999	0.001
100	9.67	9.79	97.94	1.42	136.98	1	0.001
500	48.32	48.78	97.56	0.11	270.27	0.999	0.004

Table 2.12: Effect of initial 2-nitrophenol concentration on sorption data on β(300) using pseudo-second-order approach.

C_0 (mg dm^{-3})	$q_{e,\,exp}$ (mg g^{-1})	$q_{e,\,cal}$ (mg g^{-1})	Re (%)	k_2 (g mg^{-1}min^{-1})	h (mg g^{-1} min^{-1})	(R^2)	χ^2
50	4.75	5.05	100.0	0.15	3.87	0.998	0.010
100	9.50	9.71	97.18	5.05	500	0.992	0.004
500	45.85	47.39	94.78	0.018	40.48	1	0.050

The overall sorption rate constants, k_2, were generally found to decrease with increasing initial 2-nitrophenol concentration, while the initial sorption capacity, h, increases with increasing 2-nitrophenol concentration. The linear relationship between the initial 2-nitrophenol concentration and the initial sorption rate suggests that the rate of adsorption of 2-nitrophenol onto Beta zeolite is initially dependent on the adsorbate concentration in solution (which is in agreement with figures 2.11 (A - D) where there is an initial rapid uptake of 2-nitrophenol by all Beta zeolites), and is related to the hydrophobic nature of the Beta zeolites. However the inverse relationship between the initial 2-nitrophenol concentration and the overall sorption rate constant suggests that as the initial concentration increases the overall sorption rate k_2 ultimately becomes dependent on the availability of adsorption surface sites rather than on the adsorbate concentration in solution (which is in agreement with figures 2.11 (A - D) where after an initial rapid uptake of 2-nitrophenol a plateau is reached).

The calculated values of q_e ($q_{e,\ cal}$) obtained from the pseudo-second-order model are in agreement with the experimental values of q_e, ($q_{e,\ exp}$). This indicates the applicability of the second order kinetic model in describing the adsorption process of 2-nitrophenol onto β(25), β(75), β(150) and β(300). As can be seen by the values of R^2 and the χ^2 the pseudo second order kinetic model fits the experimental results more accurately than the pseudo-first-order kinetic model which assumes that adsorption occurs due to a concentration difference between adsorbate surface and solution. This suggests that the sorption system is not a pseudo-first-order reaction and that the pseudo-second-order model provides the best correlation of the data. Figures 2.13 (A - D) show the variation in the equilibrium 2-nitrophenol uptake (q_e) and the % removal 2-nitrophenol removal in relation to the initial 2-nitrophenol concentration.

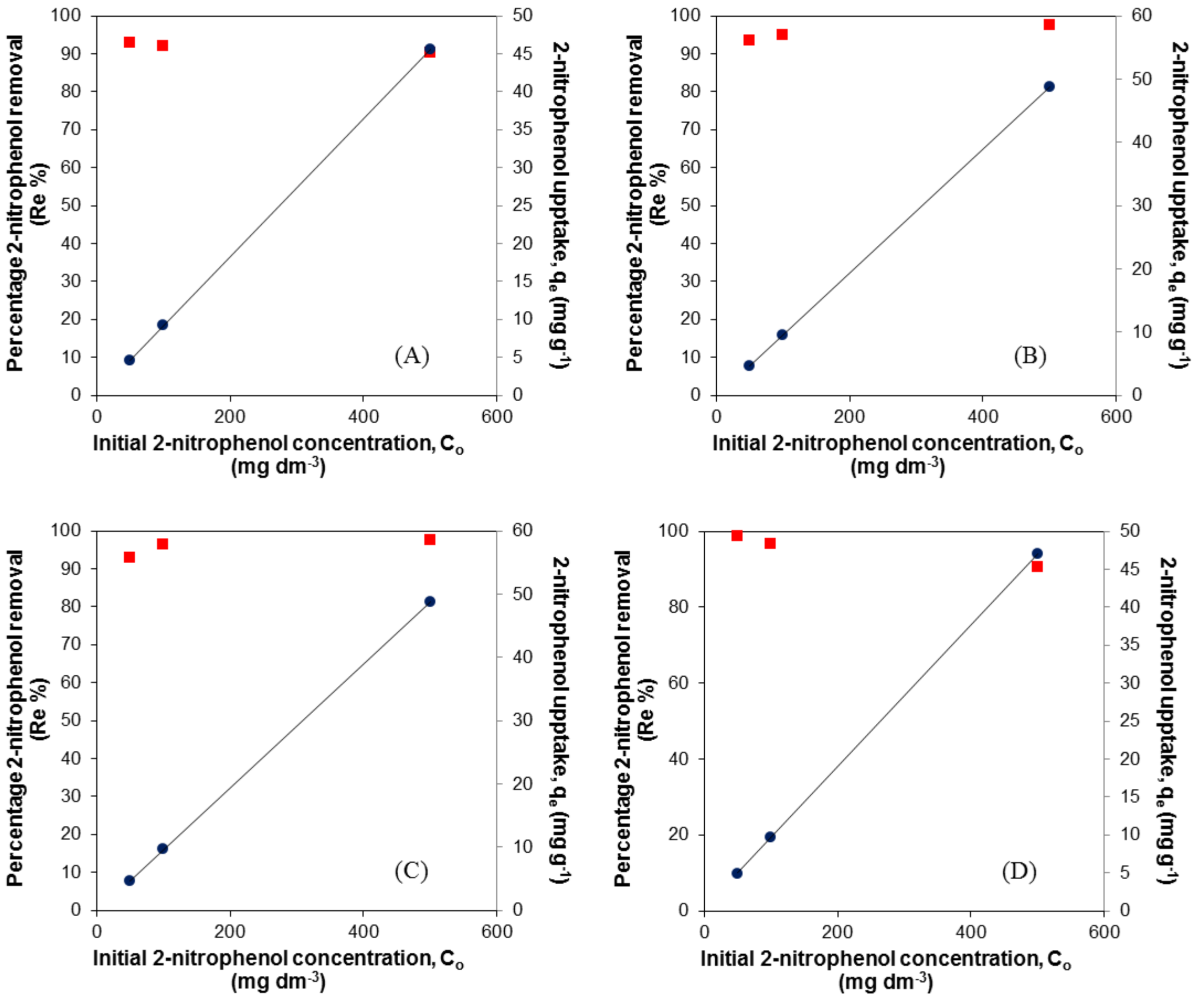

Figure 2.13 (A - D): Variation in the 2-nitrophenol uptake (q_e) and the percentage 2-nitrophenol removal (Re%) in relation to the initial 2-nitrophenol concentration C_0; (A) β(25), (B) β(75), (C) β(150) and (D) β(300).

As the 2-nitrophenol concentration is increased from 50 – 500 mg dm^{-3}, the equilibrium 2-nitrophenol uptake $q_{e\ cal,}$ increases for all Beta zeolite samples, while the % 2-nitrophenol removal appears to be independent of the initial 2-nitrophenol concentration when it is increased from 50 to 500 mg dm^{-3} (also reported in tables 2.9 – 2.12). The independence of % 2-nitrophenol removal on the initial 2-nitrophenol concentration demonstrated the efficiency of Beta zeolite to adsorb 2-nitrophenol from aqueous solutions at initial concentrations between 50 - 500 mg dm^{-3}. These findings support the adsorption isotherms displayed in figure 2.5 which demonstrate the ability of all Beta zeolite samples to adsorbed 2-nitrophenol from aqueous solution with varying initial concentrations of 10 – 1000 mg dm^{-3}. Provided there are vacant surface sites available, the adsorption of 2-nitrophenol by all Beta zeolite samples is favoured which supports the thermodynamic study that was previously reported in section 2.3.2 table 2.4.

The fitting of the pseudo-second-order reaction model to the kinetic data suggests that the adsorption of 2-nitrophenol was dependent on the availability of adsorption sites rather than on the adsorbate concentration in solution therefore as time elapses most of the adsorption sites have been occupied, thus limited free sites are available for further adsorption to occur. These findings also suggest that the adsorption of 2-nitrophenol is limited to the Beta zeolite surface as the Beta zeolite linear beta channels (0.57 nm x 0.65nm) (Smirniotis and Ruckenstein 1993) are too small to accommodating the 2-nitrophenol molecules into its internal pore structure.

The rate controlling step of an adsorption process may not be described by kinetic models alone, especially with porous materials. It is important to have information relating to the rate of pollutant removal from the liquid phase to the various mass and diffusion coefficients of the system. Several authors have shown that the kinetics of large organic compound adsorption onto untreated sawdust may be limited by the diffusion through micro and mesopores. Ahmada et al., 2009 reported that the intrapacticle diffusion plots for the adsorption of methylene blue onto untreated meranti sawdust could be divided into three stages representing micro and mesopore diffusion. Hameed and El-Khaiary (2008) also reported similar findings for the biosorption of malachite green onto rattan sawdust. Both authors however noted that pore diffusion was not the sole limiting step but was important in the adsorption kinetic process.

Prediction of the rate limiting step is an important factor to be considered in the adsorption process. An adsorption reaction is said to be intra-particle diffusion controlled if the reaction sites are internally located in the porous adsorbents and the external resistance to diffusive transport process is much less than the internal resistance (Tsai et al., 2009). Therefore, the intraparticle diffusion model proposed by Weber and Morris (Weber and Morris, 1963) shown in equation 2.45 was applied to the kinetic data of 2-nitrophenol adsorption on Beta zeolite in order to assess if the adsorption reaction was controlled by intraparticle diffusion, where k_{id} (mg/g $h^{0.5}$) is the intraparticle diffusion constant and C_i is associated to the boundary layer thickness. The values of q_t are plotted against $t^{0.5}$ for β(25), β(75), β(150) and β(300) samples are shown in figure 2.14 (A - D).

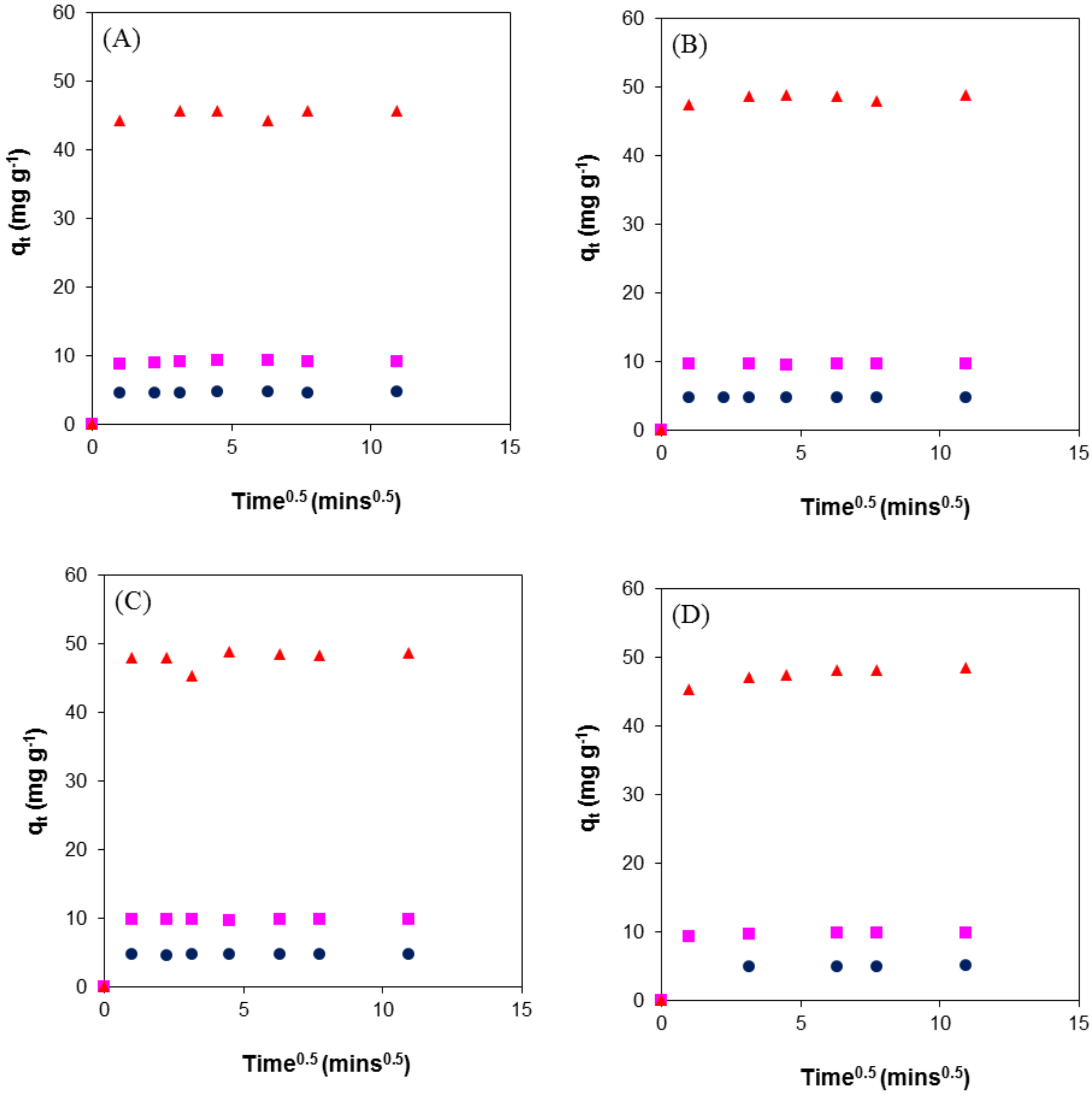

Figure 2.14: Intraparticle diffusion plots for the adsorption of 2-nitrophenol onto (A) β(25), (B) β(75), (C) β(150) and (D) β(300) at initial concentrations ● 50 mg dm^{-3}, ■ 100 mg dm^{-3}, and ▲ 500 mg dm^{-3}.

Table 2.13: Effect of initial 2-nitrophenol concentration on sorption data on β(25) using the intraparticle diffusion model.

C_0 (mg dm^{-3})	R^2	k_{id} (mg/g min$^{0.5}$)	C_i
50	0.25	0.22	3.03
100	0.27	0.45	5.90
500	0.28	2.29	28.65

Table 2.14: Effect of initial 2-nitrophenol concentration on sorption data on β(75) using the intraparticle diffusion model.

C_0 (mg dm^{-3})	R^2	k_{id} (mg/g min$^{0.5}$)	C_i
50	0.26	0.23	3.05
100	0.30	0.51	5.72
500	0.31	2.66	28.64

Table 2.15: Effect of initial 2-nitrophenol concentration on sorption data on β(150) using the intraparticle diffusion model.

C_0 (mg dm^{-3})	(R^2)	k_{id} (mg/g min$^{0.5}$)	C_i
50	0.25	0.22	3.08
100	0.26	2.37	31.26
500	0.24	0.46	64.42

Table 2.16: Effect of initial 2-nitrophenol concentration on sorption data on β(300) using the intraparticle diffusion model.

C_0 (mg dm^{-3})	(R^2)	k_{id} (mg/g min$^{0.5}$)	C_i
50	0.65	0.44	1.29
100	0.35	0.55	5.32
500	0.30	2.53	27.42

As seen from figures 2.14 (A - D) the plots were not linear over the whole time range. The values of k_{id} and C_i obtained from the plot in table 2.13 - 2.16 indicated that the intraparticle diffusion model is not applicable. Since the plots of q_t versus $t^{0.5}$ (figures 2.14 (A - D)) do not produce a straight line and the poor R^2 values of the plots (table 2.13-2.16) intraparticle diffusion is not the rate determining step in the adsorption mechanism. It has been reported by Cheung et al., 2007, that if the intraparticle diffusion was the only rate controlling step the plots would pass through the origin, if not the boundary layer diffusion may control the adsorption to some degree (Cheung et al., 2007). However, the plot of this model often has a multi-linear nature which indicates that there are two or more steps with different rate constants affecting the adsorption process. As illustrated in figures 2.14 (A - D) the diffusion in bulk phase to the exterior surface of adsorbent, which started the onset of the process was the fastest, leading rapidly to an equilibrium phase where a low slope corresponded to a slower adsorption process during which period the rate of adsorption started to slow down due to the decrease in availability of adsorption sites. These finding correspond to the fitting of the pseudo-second-order kinetic model to the adsorption data as the adsorption rate was found to be controlled by the availability of adsorbent surface sites rather than adsorbate solution concentration.

Similar plots were obtained for the adsorption of 2-nitrophenol at all three initial concentrations onto Beta zeolite independent of the Si/Al. The adsorption characteristics of 2-nitrophenol onto Beta zeolite reported in this study are supported by previous works in this area by Yousef et al., 2011 who investigated the adsorption characteristics (kinetics and mechanism) of natural zeolites as solid adsorbents for phenol removal from aqueous solutions. The kinetics of the adsorption was found to follow pseudo-second-order model and the intraparticle diffusion model was not the rate determining step in the phenol adsorption mechanism, this was further supported by the authors previous study on pH dependent adsorption of phenol onto natural zeolites (Yousef et al., 2009), which indicated that phenols are adsorbed on the outer surface of the zeolite rather than in the pores. Similar findings were also reported by Kamel et al., 2013 who investigated the mechanism of adsorption of methylene blue from aqueous solutions by kaolin and zeolite. They also reported that the rate of adsorption was not controlled by intraparticle diffusion processes.

In order to investigate the contribution of film resistance to the kinetics of 2-nitrophenol adsorption, the Boyds film-diffussion model was employed (Boyd et al., 1947). This model has the assumption that the boundary layer surrounding the adsorbent particle is the main resistance to diffusion. According to this model, the plot of Bt against time (section 2.1.5 equation 2.45) should be linear and pass through the origin if the intra-particle diffusion controls the rate of mass transfer. If the plot is nonlinear or linear but does not pass through the origin, then it can be concluded that the adsorption rate is controlled by film-diffusion or chemical reaction. Due to the rapid attainment of equilibrium Boyds film diffusion model was found to have minimal influence on the overall adsorption process. These results are in agreement with reports by Dutta et al., 2001 that suggest when adsorption is preceded by diffusion through a boundary layer the kinetics data follows that of a pseudo-first order reaction.

Since the adsorption of 2-nitrophenol onto Beta zeolite did not follow the pseudo-first-order reaction model which suggest that the adsorption process is due to a concentration difference between the adsorbate surface and solution, nor was it controlled by either the intraparticle diffusion model or the film diffusion model it suggests that the rate limiting step is the availability of adsorption sites on the Beta zeolite surface as predicted by the pseudo-second-order kinetic model. The adsorption of 2-nitrophenol is therefore found to take place on outer surface adsorption sites of the Beta zeolite.

2.3.4 Influence of Solution pH on Adsorption

It has been cited in literature that the factors affecting phenols–zeolite interactions are repulsion between phenolate anions and the negative charged zeolite, solubility of phenols in water, hydrogen bonding between hydroxyl groups of phenols and zeolite surface and complexation of phenolate anions with zeolite surface metals (Si, Al, Fe, Ti, Mn, Na, K, Ca, Mg, etc) (Damjanovic et al., 2010 and Yousef and El-Eswed 2009). Therefore a pH study was undertaken to investigate the effect of acidic and basic solution conditions (which effects the surface charge of the adsorbent and the degree of ionization of the adsorbent) on the uptake of 2-nitrophenol and is illustrated in figure 2.15.

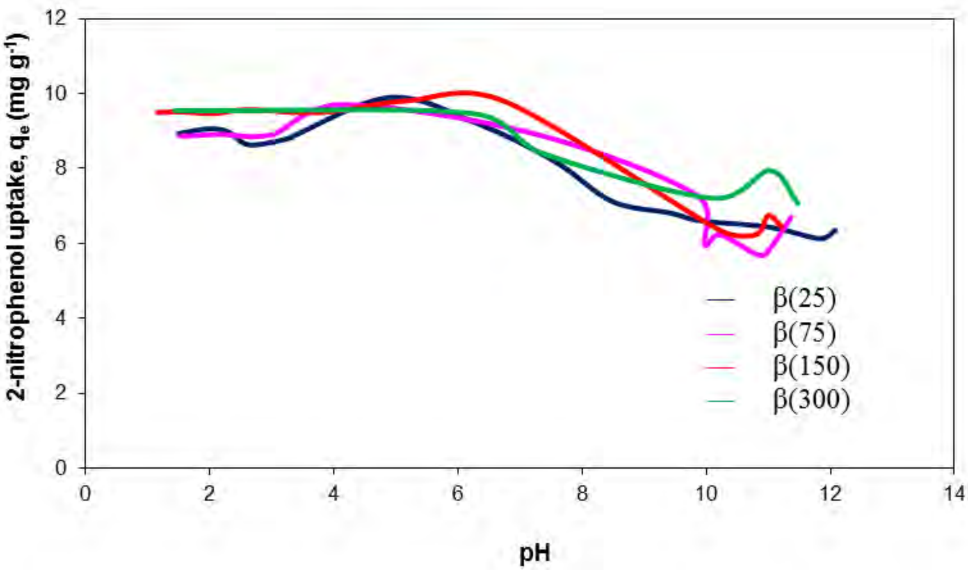

Figure 2.15: Effect of varying pH on the adsorption of 2-nitrophenol on Beta zeolite. At initial 2-nitrophenol concentration of 100 mg g^{-1}.

The surface charge on the zeolite remained slightly negative over a wide pH range (i.e., 3 – 9) (Tsai et al., 2009). While the degree of ionization of 2-nitrophenol is influenced by the pH of the solution. Based on the Henderson–Hasselbach equation and the pKa of 2-nitrophenol (pKa=7.23, 25°C) at solution pHs below pH 6, greater than 90% of the 2-nitrophenol exist in the unionised form, as the pH increases above pH 6 the percentage ionisation of 2-nitrophenol increases for example above pH 8, 85% is ionised. As evident in figure 2.15 the adsorption capacity of Beta zeolite was higher at pH values < 6 due to the electrostatic interaction with Beta zeolites negatively charged surface sites which favour the uptake of the unionised 2-

nitrophenol molecule under acidic conditions. Increasing the solution pH resulted in the dissociation of the 2-nitrophenol molecules forming phenolate anions and increased the solubility of 2-nitrophenol. The electrostatic repulsion between the identical charges (negatively charged Beta zeolite surface and phenolate anions) therefore lowers the adsorption of 2-nitrophenol by the Beta zeolite at increasing pH values. A similar trend in 2-nitrophenol uptake was observed for all Beta zeolite samples, β(25), β(75), β(150) and β(300). These findings are supported by works published by Li et al., 2009 and Li et al., 2011 who reported that adsorption of phenols from wastewater decreased with increasing pH values of the solution due to its effect on the surface charge of the adsorbent and the degree of ionization of phenol molecules.

2.3.5 Conclusion

Beta zeolite with varying silica to alumina ratios, 25:1, 75:1, 150:1 and 300:1, adsorbed 40 - 50 mg g^{-1}, 80 - 90 mg g^{-1}, 80 - 90 mg g^{-1} and 80 - 90 mg g^{-1} of 2-nitrophenol from aqueous solution, respectively. The adsorption of 2-nitrophenol was found to be influenced by Si/Al ratio of the Beta zeolite which determined the hydrophobic nature of the Beta zeolite. The highest adsorption levels being attained on the higher Si/Al ratio and hydrophobic Beta zeolites. It has been reported that adsorption of 2-nitrophenol from aqueous solution depended not only on the pore structure, but also on the competition between the 2-nitrophenol molecules and water for the adsorption site (Khalid et al., 2004). Increasing the silica to alumina ratio of the Beta zeolite from 25:1 to 300:1, results in a subsequent decrease in the H^+, which alters the Beta zeolite surface making it more hydrophobic in nature, thereby reducing competition between water and 2-nitrophenol molecules.

Equilibrium adsorption data were best represented by the Langmuir isotherm models for β(25), β(75) at 6°C and 24°C and β(150) at 24°C, while the Freundlich model fitted the adsorption data of β(150) at 6 and 40°C and β(300) at all temperatures studied. Fitting of the Langmuir adsorption isotherm to the experimental data suggests that the adsorption of 2-nitrophenol results in the formation of a monolayer on the Beta zeolite surface. The fitting of the adsorption data to the Langmuir model is in agreement with the shapes of the adsorption curves for all samples which were similar to that of a Type I profile as defined by the Brunauer classification (Brunauer et al., 1940) where the isotherm approaches a limiting value. The adsorption of 2-nitrophenol itself was rapid with equilibrium being attained in 10 minutes. In order to investigate the dependency of the adsorption process on the adsorbed 2-nitrophenol concentration both Langergen's pseudo-first order kinetic expression (Lagergen, S. 1898) and the pseudo-second order reaction model as developed by Ho et al., (Ho et al., 2000) were both applied to the kinetic data. The kinetic data of adsorption of 2-nitrophenol by β(25), β(75), β(150) and β(300) was found to follow the pseudo-second-order reaction model based on the values of the correlation coefficients (R^2) and the Chi squared test χ^2. The fitting of the pseudo-second-order reaction model over the pseudo-first-order model suggests that the rate of adsorption was dependent on both the availability of adsorption surface sites and on the adsorbate concentration.

In order to investigate other possible rate limiting steps to the adsorption process the kinetic data were further analysed by applying the intraparticle diffusion model proposed by Weber and Morris (Webber and Morris 1963). However it was found that the intraparticle diffusion process was not the rate determining step in the adsorption mechanism as plots of this model revealed that diffusion in bulk phase to the exterior surface of adsorbent, which started the onset of the process was the fastest, leading rapidly to an equilibrium phase where a lower slope corresponded to a slower adsorption process during which period the intraparticle diffusion started to slow down due to the decrease in availability of adsorption sites. The data were also analysed by Boyd's film diffusion mechanism which was found not to be a rate controlling step due to rapid diffusion of 2-nitrophenol in the bulk to the exterior phase. These findings suggest that the adsorption rate is controlled by the availability of monolayer adsorption sites on the outer surface of the Beta zeolite involving weak interaction between 2-nitrophenol and the Beta zeolite surface sites such as Van der Waals forces and hydrogen bonding. This further support the fitting of the pseudo-second-order kinetics model to the adsorption data.

The thermodynamic parameters show that the adsorption process is mildly exothermic in nature with negative enthalpy values obtained from the experimental data. The magnitude of the negative values of the enthalpy change indicate that the adsorption is physical in nature involving weak forces of attraction which would further support the fitting of the pseudo-second-order kinetic model. The Gibbs free energy was found to be small and positive in magnitude which suggests that the equilibrium adsorption position favours 2-nitrophenol in the aqueous solution. The Gibbs free energy for the adsorption process was reported to become less positive with decreasing temperature which suggests that the adsorption will be more spontaneous at lower temperatures as predicted by the negative values of $\Delta H°$ and $\Delta S°$. However based on the magnitude of the thermodynamic parameters $\Delta G°$, $\Delta H°$ and $\Delta S°$, it is only possible to say that the experimental data suggests that the adsorption of 2-nitrophenol is mildly exothermic in nature in the temperature range of 6 – 40°C for β(25), β(75) and β(150) samples, while that adsorption process is largely independent of temperature for β(300) sample.

The adsorption process for 2-nitrophenol on β(25), β(75), β(150) and β(300) is largely independent of the pH of the adsorbate solution below pH 7. As the pH of the adsorbate solution increases above pH 7 there is a noticeable decrease in 2-nitrophenol uptake. An increase in pH values results in the 2-nitrophenol molecules being ionized into 2-nitrophenolate anions and also increases the solubility of the 2-nitrophenolate anion which can account for the observed decrease in uptake.

The findings of step one of this work suggest that in a controlled aqueous pH environment, Beta zeolites have significant potential as adsorbents for certain types of industrial wastewaters due to their large surface area and favourable electrostatic characteristics of their framework in the removal of low concentrations of 2-nitrophenol and possibly other organics. Subsequent chapters of this thesis focus on the modification of the Beta zeolite to incorporate a catalytic component, adsorption studies on the modified Beta zeolite and the catalytic oxidation of the adsorbed 2-nitrophenol.

2.3. References

Al-Duri, B., Khader, Y. and G. McKay (1992) 'Prediction of binary components isotherms for adsorption on heterogeneous surface', *Chemical Technology and Biotechnology*. **53**, 345-352.

Ahmad, A., Rafatullah, M., Sulaiman, O., Ibrahim, M. H. and R. Hashim (2009) 'Scavenging behaviour of meranti sawdust in the removal of methylene blue from aqueous solution',*Journal of Hazardous Materials*, **170**, 357-365.
.
Anirudhan, T. S. and P. G. Radhakrishnan (2009) 'Improved performance of a biomaterial – based cation exchanger for the adsorption of uranium (VI) from water and nuclear industry wastewater' *Journal of Environmental Radioactivity*, **100**, 250-257.

Arasteh, R., Masoumi, M., Rashidi A.M., Moradi, L., Samimi, V., S.T.Mostafavi (2010) 'Adsorption of 2-nitrophenol by multi-wall carbon nanotubes from aqueous solutions', Applied Surface Science, **256**, 4447-4455.

Atkins, P. W. (1994) Physical Chemistry, Oxford University Press, Oxford.

Azizian, S. (2006) 'A novel and simple method for finding the heterogeneity of adsorbents on the basis of adsorption kinetic data', *Journal of Colloid and Interface Science*,**302**,76-81.

Baerlocher, C., Meier, W. M. and D. H. Olson (Eds.) (2001) Atlas of Zeolite Framework Types Elsevier, Amsterdam.

Baocheng, Q. U., Jiti, Z., Xuemin, X., Chunli, Z., Hongxia, Z. and Z. Xiaobai (2008) ' Adsorption behaviour od azo dye C. I. acid red 14 in aqueous solution on surface soils', *Journal of Environmental Science*, **20**, 704-709.

Barrer, R. M. (1978) Zeolites and Clay Material, Academic Press, London.

Bhattacharya, A. K. and C. Venkobachar (1984) 'Removal of cadmium (II) by low cost adsorption', *Environmental Engineering Journal*, **110**, 110-122.

Bhatnagar, A. (2007) 'Removal of bromophenols from water using industrial wastes as low cost adsorbents', *Journal of Hazardous Materials*, **B139**, 93-102.

Boyd, G. E., Adamson, A. W. and L. S. Jr. Myers (1947) 'The exchange adsorption of ions from aqueous solutions by organic zeolites. II. Kinetics', *Journal of the American Chemical Society*, **69**, 2836-2848.

Breck, D. (1974) Zeolite Molecular Sieves: Structure, Chemistry and Uses Wiley, New York

Brunauer, S., Demming, L .S., Demming, W. E. and E. Teller (1940) 'On a theory of the Van der Waals adsorption of gas', *Journal of American Chemical Society*, **62**, 172-1732.

Campbell, I. M. (1988) Catalysis at Surfaces, Chapman and Hall London; New York.

Cejka, J., Bekkum, H. V., Corma, A. and F. Schueth (Eds.), Introduction to zeolite science and practice, Studies in Surface Science and Catalysis, 168, third ed., Elsvier, The Netherlands, 2007.

Cheung, W. H., Szeto, Y. S. and G. McKay (2007) 'Intraparticle diffusion processes during acid dye adsorption onto chitosan', *Bioresource Technology*, **98**, 2897-2904.

Cosseron, A. F., Daou, T. J., Tzanis, L., Nouali, H., Deroche, I., Coasne, B. and V. Tchamber (2013) 'Adsorption of volatile organic compounds in pure silica CHA, *BEA, MFI and STT-type zeolites', *Microporous and Mesoporous Material*, **173**, 147-154.

Dabrowski, A., Podkoscielnv, P., Hubicki, Z. and M. Barczak (2005) 'Adsorption of phenolic compounds by activated carbon – a critical review', *Chemosphere*, **58**, 1049-1070.

Damjanovic, L., Rakic, V., Rac, V., Stosic, D., and A. Auroux (2010)'The investigation of phenol removal from aqueous solutions by zeolites as solid adsorbents', *Journal of Hazardous Material*s, **184**, 477-484.

Donat, R., Akdogan, A., Erdem, E. and H. Cetisli (2005) 'Thermodynamics of Pb^{2+} and Ni^{2+} adsorption onto natural bentonite from aqueous solutions', *Journal of Colloid Interface Science*, **286**, 43-52.

Dotto, G. L. and L. A. A. Pinto (2011) 'Adsorption of food dyes acid blue 9 and food yellow 3 onto chitosan: Stirring rate effect in kinetics and mechanism', *Journal of Hazardous Material*, **187**, 164-170.

Dutta, P. K., Durga Bhavani, K. and N. Sharma (2000) 'Adsorption for dyehouse effluent by low cost adsorbent (chitosan)', *Asian Textile Journal*, **10**, 57-63.

Ersoy, B.and M. S.Celik (2004), *Environmental Technology*, **25,**341.
Freundlich, H. A. (1906) 'Uber die Adsorption in Losungen', Z.Phys.Chem. **A57**,385.

Giles, C. H., D. Smith and A. Huitson (1974) 'A general treatment and classification of the solute adsorption isotherm. I: Theoretical', *Journal of Colloid Interface Science*, **47**, 755-765.

Gregg, S. J. and Sing K. S. W. (1982) Adsorption Surface Area and Porosity. London Academic Press Inc.

Ghiaci, M., Abbaspur, A., Kia, R. and F. Seyden – Azad (2004) 'Equilibrium isotherms studies for the sorption of benzene, toluene and phenol onto organo-zeolites and as-synthesized MCM-41', *Separation and Purification Technology*, **40**, 217-229.

Gregg, S. J. and K. S. W. Sing, (1982), *Adsorption, surface area and porosity, 2 Edition*, Academic Press, London.

Gregorio, C. and P. M. Badot (2008) 'Application of chitosan, a nutral aminopolysaccharide, for dye removal from aqueous solutions by adsorption processes using batch studies: A review of recent literature', *Progress in Polymer Science*, **33**, 399-447.

Hall, R., Eagleton, L. C., Acrivos, A. and T. Vermeulen (1966) 'Pore and solid diffusion kinetics in fixed-bed adsorption under constant pattern conditions', *Industrial and Engineering Chemistry Fundamentals*, **5**, 212-231.

Hameed, B. H. and M. I. El-Khaiary (2008) 'Malachite green adsorption by rattan sawdust: Isotherm, kinetic and mechanism modelling', *Journal of Hazardous Materials*, **159**, 574-579.

Ho, Y. S. and G. Mckay (1999) 'A kinetic study of dye adsorption by bisorbent waste pith', *Resources, Conservation and Recycling*, **25**, 171-193.

Ho, Y. S. and G. Mckay (1999) 'Pseudo-second order model for sorption processses',*Process Biochemistry*, **34**, 451-465.

Ho, Y. S. (2003) 'Removal of Metal Ions from Sodium Arsenate Solution using tree fern', *Process Safety and Environmental Protection*, **81**, 352-356.

Ho, Y. S. (1995) 'Adsorption of heavy metals from waste streams by peat', Ph.D Thesis, University of Birmingham, Birmingham, UK.

Ho, Y. S. and G. McKay (1999) 'The Sorption of lead (II) ions on peat', *Water Research,* **33**, 578-584.

Ho, Y. S. and G. Mckay (1998) 'Kinetic models for the sorption of dye from aqueous solution by wood', *Process Safety and Environmental Protection*, **76**, 183-191.

Ho, Y. S. and G. Mckay (1998) ' A comparison of chemisorption kinetic models applied to pollutant removal on various sorbents', *Process Safety and Environmental Protection*, **76**, 332-340.

Ho, Y. S. and G. Mckay (2000) 'Correlative biosorption equilibria model for a binary batch system', *Chemical Engineering Science*, **55**, 817-825.

Ho, Y. S., Mckay, G., Wase, D. A. J. and C. F. Forster (2000) 'Study of the sorption of diavalent metal ions onto peat', *Adsorption Science and Technology*, **18**, 639-650.

Ho, Y. S., Wang, C. B. and C. T. Yeh (1996) 'Calorimetric study on interaction of dioxygen with alumina supported palladium', *Journal of Molecular Catalysis A: Chemical*, **112**, 287-294.

Jaynes, W. F. and S. A. Boyd (1991) ‘Hydrophobicity of siloxane surfaces in smectities as revealed by aromatic hydrocarbon adsorption from water’ *Clays and Clay Minerals*, **39**, 428-436.

Li, J. M., Xiang-Guang, M., Chang-Wei, H. and D. Juan (2009) ‘Adsorption of phenol, p-chlorophenol and p-nitrophenol onto functional chitosan’, *Bioresource Technology*, **100**, 1168-1173.

Jinbei, Y., Meiqiong, Y. and Q. Ting (2014) ‘Adsorption thermodynamics and kinetics of Cr (VI) on KIP 210 resin’, *Journal of Industrial and Engineering Chemistry*,**20**, 480-486.

Kamel, R., Sarra, B. and H. Selma (2013) ‘Adsorption of methylene blue from aqueous solution by kaolin and zeolite’, *Applied Clay Science*, **83-84**, 99-105.

Kawai, T. and K. Tsutsmi (2004) ‘Adsorption characteristics of surfactants and phenol on modified zeolites from their aqueous solutions’, *Colloid Polymer Science*, **273**, 787-792.

Keeler, J. and P.Wothers (2003) ‘Why Chemical Reactions Happen’ Oxford University Press.

Kelleher, B. P., A. M. Doyle, T. F. O 'Dwyer and B. K. Hodnett, (2001) ‘Preparation and Use of a Mesoporous Silicate Material for the Removal of Tetramethyl Ammonium Hydroxide (TMAH) from Aqueous Solution’, *Journal of Chemical Technology and Biotechnology.* **76**, 1216-1222.

Khalid, M., Joly, G., Renaud, A. and P. Magnoux (2004) ‘Removal of phenol from water by adsorption using zeolites’, *Industrial Engineering Chemistry Resource*, **43**, 5275.

Knaebel, K. S., (1995) ‘For your next separation consider adsorption’, *Chemical Engineering*, **102**, 92-102.

Koubaissy, G., Joly, P. and P. Magnoux (2008) ‘Adsorption and competitive adsorption on zeolites of nitrophenol compounds present in wastewaters’, *Industrial Engineering Chemistry Resource*,**47**,9558-9565.

Koubaissy, B., Toufaily, J., El-murr, M., Hamieh, T., Magnoux, P. and G. Joly (2011) ‘Elimination of aromatic pollutants present in wastewater by adsorption over zeolites’, *Physics Procedia*, **21**, 220-227.

Kuleyin, A. (2007)’ Removal of phenol and 4-chlorophenol by surfactant-modified natural zeolite’, *Journal of Hazardous Materials*, **144**,307-315.

Langmuir, I. (1918) ‘The adsorption of gases on plane surfaces of glass, mica and platinum’, Journal of American Chemical Society, **40,** 1361-1403.

Lagergen, S. (1898) ‘Zur The Theorie der Sogenannten Adsorption Geloster Stoffe’, Kungliga Svenska Vetenskapademiens Handlinger, **24**, 1-39.

Li, Z., Li, X., Xi, H. and B. Hua (2002) 'Effects of ultrasound on adsorption equilibrium of phenol on polymeric adsorption resin', *Chemical Engineering Journal*, **86**, 375-379.

Li, X., Zhao, B., Zhi, K. and X. Hao (2011)' Removal of Nitrophenols using β-cyclodextrin modified zeolites', *Chinese Journal of Chemical Engineering*,**19**,938-943.

Lin, S. H. and R. S. Juang (2009) 'Adsorption of phenol and its derivatives from water using synthetic resins and low-cost natural adsorbents: a review', *Journal of Environmental Management*, **90**,1336-1349.

Lin, S. Y., Dong, C., Hsu, T. J. and C. T. Hsu (2002) 'Determination of adsorption of an ionic surfactant on latex from surface tension measurements', *Colloids and Surfaces A: Physicochemical and Engineering Aspects,* **196**, 189-198.

Liu, Y., Zheng, Y. and A. Wang (2010) 'Enhanced adsorption of Methylene Blue from aqueous solutions by chitosan –g- poly (acrylic acid)/ vermiculite hydrogel composites', **22**, 486-493.

Liu, Y. H., Di, Z., Ding, J., Wu, D., Luan, Z., Zhu, Y., (2005) 'Adsorption Thermodynamic, Kinetic and Desorption Studies of Pb^{2+} on Carbon Nanotubes', *Water Resources*, **39**, 605-609.

Lowell, S. and J. E. Shields (1991) Powder Surface and Porosity, Chapman and Hall, London.

Mall, I. D., Srivastava, V. C. and N. K. Agarwal (2006) 'Removal of Orange – G and Methyl Violet dyes by adsorption onto bagasse fly ash-kinetic study and equilibrium isotherm analyses', *Dyes and Pigments*, **69**, 210-223.

Martucci, A., Pasti, L., Marchetti, N., Cavazzini, A., and F. Dondi (2012)' Adsorption of pharmaceuticals from aqueous solutions on synthetic zeolites', *Microporous and Mesoporous Materials*, **148**, 174-183.

Mittal, A., Kurup, L. and Mittal, J. (2007) ' Freundlich and Langmuir adsorption isotherms and Kinetics for the removal of tartazine from aqueous solutions using hen feathers', *Journal of Hazardous Materials*, **146**, 243-248.

Navarro, A. E., Cuizano, N. A., Lazo, J. C., Sun-Kou, M. R. and B. P. Llanos (2009) 'Comparative study of the removal of phenolic compounds by biological and non-biological adsorbents', *Journal of Hazardous Materials*,**164**, 1439-1446

Ng, J. C. Y., Cheung, W. H. and G. McKay (2003) 'Equilibrium studies for the sorption of lead from effluents using chitosan', *Chemosphere*, **52**, 1021-1030.

O' Brien, J., Curtin, T and T. F. O'Dwyer (2008) 'A Novel Process for the removal of aniline from wastewaters', *Journal of Hazardous Materials*, **159**, 476-482.

Ofomaja, A. E. (2007) ‘Sorption dynamics and isotherm studies of methylene blue uptake onto palm kernel fibre’, *Chemical Engineering Journal*, **126**, 35-43.

Ofomaja, A. E. (2007) ‘Kinetics and mechanism of methylene blue sorption onto palm kernel fibre’, *Process Biochemistry*, **42**, 16-24.

Ofomaja, A. E. (2011) ‘Kinetics and pseudo-isotherm studies of 4-nitrophenol adsorption onto mansonia wood sawdust’, *Industrial Crops and Products*, **33**, 418-428.

Okolo, B., Park, C. and M. A. Keane (2000) ‘Interaction of phenol and chlorophenols with activated carbon and synthetic zeolites in aqueous media’, *Journal of Colloidal Interface Science*, **226**, 308-317.

Pei, Z. G., Shan, X. Q., Wen, B., Zhang, S., Yan, L. and S. U. Khan (2006) ‘Effect of copper on the adsorption of *p*-nitrophenol onto soils’ *Environmental Pollution*, **139**, 541-549.

Perego, C., Bagatin, R. Tagliabue, M. and R. Vignola (2013) ‘Zeolites and related mesoporous materials for multi-talented environmental solutions’ *Microporous and Mesoporous Materials*, **166**, 37-49.

Poots, V. J. P. and G. McKay (1977) Proceeding s Royal Irish Academy, **47**,539.

Reichenberg, D. (1953) ‘Properties of ion exchange resins in relation to their structure. III. Kinetics of exchange’, Journal of the American Chemical Society, **75**, 589-598.

Reungoat, J., Pic, J. S., Manero, M. H. and H. Debellefontaine (2007) ‘Adsorption of nitrobenzene from water onto high silica zeolites and regeneration by ozone’, *Separation Science and Technology*, **42**, 1447-1463.

Rida, K., Bouraoui, S. and S. Hadnine (2013) ‘Adsorption of methylene blue from aqueous solution by kaolin and zeolite’, *Applied Clay Science*, **83-84**, 99-105.

Ruthven, D. M. (1984), ‘Principles of Adsorption and Adsorption Processes’, First Ed., Wiley Interscience., New York.

Singh, A. K., Singh D. P., Panday K. K. and V. N. Singh (1988) ‘Wollastonite as Adsorbent for Removal of Fe (II) from Water’*, Journal of Chemical Technology and Biotechnology*, **42**, 39-49.

Shao, Y., Zhang, H. and Y. Yan (2013) ‘Adsorption dynamics of p-nitrophenol in structured fixed bed with microfibrous entrapped activated carbon’, *Chemical Engineering Journal*, **225**, 481-488.

Shu, H. T., Li, D., Scala, A. A. and Y. H. Ma (1997) ‘Adsorption of small organic pollutants from aqueous streams by aluminosilicate-based microporous materials’, *Separation and Purification Technology*, **11,** 27-36.

Smirniotis, P. G. and E. Ruckenstein (1993) ‘Comparison between zeolite β and Al_2O_3 supported Pt for reforming reactions’, *Journal of Catalysis*, **140**, 526-542.
Sobkowski, J. and A. Czerwinski (1974) ‘Kinetics of carbon dioxide adsorption on a platinum electrode’, *Journal of Electronanalytical Chemistry and Interfacial Electrochemistry*, **55**, 391-397.

Soto, L. M., Moure, A., Dominguez, H. and J. C. Parajo (2011) ‘Recovery, concentration and purification of phenolic compounds by adsorption: A review’, *Journal of Food Engineering*, 105, 1-27.

Srihari, V. and A. Da (2008) ‘Comparative studies on adsorptive removal of phenol by three agro-based carbons: equilibrium and isotherm studies’, *Ecotoxicology Environmental Safety*, **71**, 274-283.

Stelzer, J., Paulus, M., Hunger, M., and J. Weitkamp (2008) ‘Hydrophobic properties of all silica zeolite beta’, *Microporous Mesoporous Materials*, **22**, 1-8.

Treacy, M. M. J. and J. M. Newsam (1988) ‘Two new three-dimensional twelve-ring zeolite frameworks of which zeolite beta is a disordered intergrowth’, *Nature*, **332**, 249-251.

Topallar, H. and Y. Bayrak (1999) ‘Investigation of adsorption isotherms of myristic, palmitic and stearic acids on rice hull ash’, Turkish Journal of Chemistry, **23,** 193-198.

Tsai, W. T., Hsien, K. J. and H. C. Hsu (2009) ‘Adsorption of organic compounds from aqueous solution onto the synthesized zeolite’, *Journal of Hazardous Material*, **166**,635-641.

Wadlinger, R. L., Oneonta, N. Y. and G. T. Kerr (1967) In US Patent No. 3308069, Mobil Oil Corporation, New York. USA.

Webber, W. J. and J. C. Morris (1963) ‘Kinetics of adsorption on carbon from solution’ *Journal of Sanitary Engineering Division*, **89**, 31-59.

Weitkamp, J. (2000) ‘Zeolites and Catalysis’ Solid State Ionics,**131**, 175-188.

Yilmaz, B. and U. Muller (2009) ‘Catalytic Applications of Zeolites in Chemical Industry’, *Topics in Catalysis,***52**, 888-895.

Yang, Y., Ma, J., Qin, Q. and X. Zhai (2007) ‘Degradation of nitrobenzene by nano-TiO_2 catalyzed ozonation’ *Journal of Molecular Catalysis A: Chemical*, **267**, 41 – 48.

Yousef, I. R. and B. El-Eswed (2009) ‘The effect of pH on the adsorption of phenol and chlorophenol onto natural zeolite’, *Colloids and Surfaces A: Physicochemical Engineering Aspects*, **334**, 92-99.

Yousef, R. I., El-Eswed, B. and A. H. Al-Muhtaseb (2011) ‘Adsorption characteristics of natural zeolites as solid adsorbents for phenol removal from aqueous solutions:

Kinetics, mechanism, and thermodynamics studies', *Chemical Engineering Journal*, **171**, 1143-1149.

Yu, L. (2008) 'New insights into pseudo-second –order kinetic equation for adsorption', *Colloids and Surfaces A: Physicochemical and Engineering Aspects*, **320**, 257-278.

Zahir, R. and N. Najwa (2006) 'Characteristic of phenol and chlorinated phenols sorption onto surfactant modified bentonite' *Journal of Colloid and Interface Science*, **298**, 39-49.

Chapter 3

Modification of Beta Zeolite with a Catalytic Component

3.1 Introduction

The rising problem of water pollution has posed a big challenge to both industry and society in terms of their economic growth and sustainability. Pollutants such as phenol and nitrophenols arising from refineries are highly toxic and comparatively more refractory to natural degradation, thereby causing a potential threat to land and surface waters, even if discharge is in a minute quantity (Shukla et al., 2010). Various treatment techniques and processes discussed in chapter 1 section 1.5 have been used to remove pollutants from contaminated water. Among all the approaches proposed, adsorption is one of the most popular methods and is currently considered as an effective, efficient and economic method for water purification (Jiuhui, 2008). Among inorganic adsorbents, it has been proven that zeolites are efficient in removing small organic compounds from an environmental matrix (Martucci et al., 2012).

However, adsorption processes just transfer pollutants from one phase to another, rather than eliminating them from the environment. Recently, numerous approaches have been investigated for the development of cheaper and more effective novel composite adsorbents (Machado et al., 2006, Guillemot et al., 2007 and Zhang et al., 2007). Dual functional adsorbents / catalysts with both adsorption and catalytic functions has been reported as a proper control method for treating low concentration levels of volatile organic compounds (VOCs) in waste gases (Baek et al., 2004 and Brazlauskas and Kitrys 2008). The dual function sorbent–catalysts medium is reported to be efficient for trapping volatile organic compounds at ambient temperatures, while also catalysing their destruction and desorbing the products at elevated temperatures (~ 350°C). Such a system eliminates the need for separate adsorption beds and significantly reduces energy consumption (Brazlauskas and Kitrys 2008). Such sorbent–catalysts can be a metal impregnated or metal exchanged zeolite.

Zeolites have gained interest as potential active catalysts for the oxidation of volatile organic compounds because of their ease of synthesis, pore structure, high surface area, pore widths in the order of molecular dimensions, good thermal stability, ion exchange properties and their regeneration capabilities (Brazlauskas and Kitrys 2008, Khalid et al., 2004). Various types of zeolites have been used as adsorbents, catalysts supports and catalysts. Guisnet and Gilson and O' Brien et al. have studied the dual function of zeolites as both adsorbents and catalysts (Guisnet and Gilson, 2002, O'Brien et al., 2008).

A variety of zeolite modification techniques has been cited in literature such as ion exchange (Alver and Metin 2012, Leyva–Ramos et al., 2010, Ohman et al., 2002) and impregnation (Lindmark et al., 2010, Hajimirzaee et al., 2012, Brooks et al., 2012; De Lucas et al 2005). Among various N_2O decomposition catalysts, cobalt zeolites have gained much attention for their high activities (Zhang et al., 2011). Various preparation methods were developed to prepare Co-zeolite catalysts, such as ion exchange (Abu-Zied et al 2008 and Smeets et al., 2008), impregnation, semi-continuous methods (Smeets et al., 2008), and sublimation (Wang et al., 2001).

During the modification process, zeolites may act as a support for the catalytic component. Supported catalysts are often applied because they combine a relatively high dispersion (amount of active surface) with a high degree of thermostability of the catalytic component. Zeolites function as a support enabling the formation of a large particle or tablet of catalyst composed of very small readily sinterable crystals of catalysts which are prevented from coalescing by being separated from each other by the support component. The support component clearly has to be much more resistant to sintering than the catalytic species.

Impregnation can be used to load a metal onto the surface of a zeolite. This method involves three steps (Perego and Villa 1997):

1. Contacting the support with the impregnating solution for a certain period of time
2. Drying the support to remove the imbibed liquid
3. Activating the catalysts by calcination, reduction or other appropriate treatment.

Two methods of contacting may be distinguished depending on the total amount of solution. One involves treating the support with excess solution. The support is placed on a screen and dipped into an excess quantity of solution for the time necessary for total impregnation. The solid is then drained, dried and calcined. The second involves treating the support with repeated application of a solution. A more precise control is achieved by this technique, termed dry impregnation or impregnation to incipient wetness. The support is contacted with a solution of appropriate concentration, corresponding in quantity to the total known pore volume or slightly less. The solid is then dried and calcined (Perego and Villa 1997).

Ion-exchange is also an effective and commonly used approach to modify zeolites with a range of different cations. With their negatively charged porous framework and mobile cations sitting in the pores, metals can easily be introduced into the zeolite pores by ion exchange with cationic forms of metals such as copper nitrate trihydrate ($Cu(NO_3)_2.3H_2O$) followed by thermal removal of the anionic ligands. The presence of highly charged metal cations introduced into the zeolite channels and/or cages, through ion exchange, leads to a change in zeolite acidity (Martins et al., 2005), which can be exploited for several important acid-catalysed reactions (Perego et al., 2013).

It has been reported in literature that there is an enhancement of the adsorption capacity of zeolites when they have been modified by transition metals via an ion exchange procedure. Damjanovic et al. reported an increase in adsorption of phenol from aqueous solution after the introduction of copper into the zeolite framework by ion exchange (Damjanovic et al., 2010). There are numerous reports in literature citing ion exchange as the method of enhancing the catalytic performance of zeolites such as the activity of Cu-ZSM-5 zeolite in the selective catalytic reduction (SCR) of NO by hydrocarbons (Iwamoto et al., 1993), oxidation of phenols by copper-modified zeolite (ZSM-5) in wet hydrogen peroxide (Maduna et al., 2007), the catalytic oxidation of aniline by Cu-Beta zeolite (O'Brien et al., 2008) and Fe/ZSM-5, which has been reported as a promising system for the treatment of phenolic aqueous wastes in the presence of H_2O_2, allowing for total elimination of phenol under milder working conditions (Kuznetsova et al., 2004). Compared with other methods, the ion exchange process is simpler and more feasible for industrial applications because it involves fewer steps, and the process parameters are easily controlled. Moreover, the ion exchange method can efficiently introduce mono-atomic Co^{2+} species into the zeolite exchanged sites, which is suggested to be more active for N_2O decomposition that the loaded cobalt oxides obtained by other methods (Smeets et al., 2008).

The method of ion exchange was chosen in this work to prepare a series of copper loaded Beta zeolite catalysts, as it has the advantage of producing a highly dispersed catalytic component within the zeolite carrier (Heck and Farrauto 2002). Ion exchange is the exchange of ions between a liquid and a solid phase. The solid phase is charged, as is the case with Beta zeolite, and this charge is balanced by ions of the opposite charge, named counter ions. When the Beta zeolite is immersed in a liquid phase containing a solution of ions of the opposite charge, then a diffusion process is established where ions diffuse out from the zeolite and ions diffuse into the solid Beta zeolite structure from the exchange solution. This diffusion is a result of the considerable concentration difference between the two phases. If the ions carried no electric charges, these concentration differences would be levelled out by diffusion. However, such a process would disturb electroneutrality since, actually the ions are charged. Eventually, an equilibrium is established in which the tendency of the ions to level out the existing concentration difference is balanced by the action of the solids electric field.

The adjustment of the solution to neutral and alkaline pH values is favourable, as at a low pH a higher concentration of H^+ cations exists, these H^+ have been reported to compete against the incoming cation and thus the exchange of the latter will be hindered (Inglezakis 2005).

While this procedure is very versatile, it has its limitations. Sometimes, the cation with its hydrated shell is too bulky to enter the pores of the zeolite, or the salt with cation in the desired valence state is unstable or insoluble in water. These limitations can however be overcome by solid–state ion exchange. The zeolite, in the H^+- form and a compound containing the in-going cation, e.g. a halide, are intimately mixed, whereupon this physical mixture of solids is heated in an inert gas stream (Weitkamp 2000). The obtained ion exchanged zeolites are then calcined to remove physisorbed water (Vanelderen et al., 2013). There are many literature reports illustrating the use of zeolites functioning as catalysts for the removal of contaminants from the gas phase. Transition metal–exchanged zeolite catalysts are effective catalysts for the reduction of nitrogen oxide and VOC emissions (Metkar et al., 2012, De La Torre et al., 2012, Zhang et al., 2011, Janas et al., 2009 and Lenihan and Curtin 2009). Iwamoto et al (Iwamoto et al 1986) found that copper exchanged ZMS-5 had a very high activity for the gaseous decomposition of nitrogen monoxide to nitrogen and oxygen. Copper exchanged zeolites were found to be active in a wide range of reactions, such as the selective catalytic reduction of NO with ammonia (Centi et al 1993, Wang and Hwang 1995), photocatalytic NO destruction (Anpo et al 1994) and the selective reduction of NO with hydrocarbons in the presence of excess oxygen (HC-SCR). The decomposition of N_2O has been studied using iron modified ZSM-5 zeolites (Waclaw et al 2004). While rhodium and ruthenium supported on ZSM-5 and cobalt exchanged zeolites were also reported to be active catalysts for the decomposition of nitrous oxide (Li and Armor 1992).

In this work a one-step ion exchange procedure was used to incorporate a catalytic component within the Beta zeolite framework. Copper was chosen as the catalytic component in this work due to its reported efficient activity for the catalytic oxidation of aniline by O'Brien et al, (O'Brien et al., 2008).

3.2 Experimental

3.2.1 Catalyst Preparation

A series of copper exchanged zeolites was prepared using a one-step exchange procedure. The exchange step involved the addition of approximately 10 g of zeolite to 500 ml of copper nitrate trihydrate ($Cu(NO_3)_2.3H_2O$, Sigma Aldrich) solution and stirring of this suspension at ambient temperature for 24 hours after which time the pH was adjusted to pH 7.0 using an 8% (v/v) NH_3 solution and the suspension was stirred for a further hour. The Beta zeolite supports used throughout the course of this work were supplied by Zeolyst International. After exchange, the sample was filtered and the filter cake was washed with distilled water in order to remove any non-exchanged ions. The sample was then dried overnight at 80°C and finally calcined at 450 ºC in air for 5 hours. The drying stage was necessary to remove any excess water or any other volatile species present in the samples. The calcination step ensured the removal of all traces of adsorbed water and decomposable salts used as metal precursors in the preparation of each catalyst. Variations of this ion exchange procedure were also investigated with a view to preparing the most stable catalyst. These variations included exchanging the samples for 24 hours after which, the pH of the suspensions was adjusted to pH 7 - 10. The Beta zeolite samples used were β(25), β(75), β(150) and β(300), which were zeolite β samples with SiO_2/Al_2O_3 ratios of 25, 75, 150 and 300, respectively.

3.2.2. Characterisation of Catalytic Adsorbent

3.2.2.1 Atomic Absorption Spectroscopy

The copper content of the metal exchanged Beta zeolite was measured by atomic absorption spectroscopy using a Varian SpectrAA atomic absorption (AA) spectrophotometer. Approximately 100 mg of the sample was dissolved in 3 ml of concentrated hydrofluoric acid (8%v/v) Merck) in a 50 ml Telflon flask and diluted to 50 ml with distilled water. The solution was then transferred to a 100 ml Teflon volumetric flask and diluted to 100 ml with distilled water. Further dilutions were made so that the sample concentration lay within the calibration range. The copper standards were prepared from 1000 mg L^{-1} metal AAS standard solution. A solution comprising of distilled water only was used as a blank. The absorbance of the standards was measured and a calibration plot of copper concentration versus absorbance was obtained.

3.2.2.2 X-Ray Diffraction

The crystallinity of the prepared copper exchanged Beta zeolites was studied using X-ray diffraction (XRD). Before analysis, all the samples were dried overnight at 80°C. The XRD patterns were recorded for both the unmodified Beta zeolites samples and for the Beta zeolite samples exchanged with copper, to evaluate mineralogical and structural changes, using a Philips X'pert PRO MPD (multi-purpose diffractometer) X–ray diffractometer PW3050/60 $\theta - \theta$ with a scan range of 5 – 60° (2θ) using a Cu Kα line at 1.543Å. A step size and scan speed of 0.017°(2θ) and 0.2°/s, respectively were implemented. The Cu Kα diffractometer anode was operated at 40 kV with a current of 35 mA.

3.2.3 Catalyst Leaching

The following procedure was used to assess the aqueous leachability of the exchanged copper cation from the zeolite under varying pH conditions. The pH of 20 ml distilled water was adjusted appropriately using either ammonium hydroxide (NH_4OH) or hydrochloric acid (HCl) and approximately 200 mg of catalyst was added to the solution. The solution was stirred continuously for 2 hours. The sample solution was separated from the adsorbent material by vacuum filtration (Whatman GFA filter paper). In order to ensure complete separation, the filtrate solution was then centrifuged at 3,500 rpm for 10 min using a Sigma 2 - 4 centrifuge and the supernatant was analysed for the leached cation by atomic absorption spectroscopy.

3.2.4 Dealumination of the Beta Zeolite

The aqueous stability of aluminium within the Beta zeolite framework was also investigated using the procedure outlined in section 3.2.3. However, for the atomic absorption spectroscopy analysis of aluminium, standards containing the relevant concentrations of aluminium were prepared from 100 mg L^{-1} metal AAS standard solutions. For analysis of aluminium, 40 mg of potassium chloride was added to 10 ml of each of the samples in an effort to suppress ionisation. The absorbance of the standards was measured and a calibration plot of aluminium concentration versus absorbance was obtained.

3.3. Results and Discussion

3.3.1 Characterisation of Catalytic Adsorbents Prepared

A series of copper exchanged zeolites was prepared using the one-step exchange procedure outlined in section 3.2.1. Table 3.1 lists all the catalysts prepared. The table includes the theoretical copper loadings, the actual copper loadings, the percentage copper exchanged, the pH of the exchange solution and the Si/Al ratio of the zeolite. The amount of copper nitrate in the exchanging solution was the same for all samples, and was enough to result in a 2.0 wt% Cuβ catalyst assuming that all the copper was exchanged onto the zeolite. The actual copper content of the exchanged zeolites was measured by atomic absorption. The pH of the exchange solution ranged from pH 3 to pH 10 for the indicated Beta zeolite samples. The catalyst naming system employed for each of the copper modified Beta zeolite samples included the actual weight percentage loading of copper on the indicated Beta zeolite of a given Si/Al ratio. For example 1.2%Cuβ(25) represents a solid prepared using a Beta zeolite of a Si/Al ratio of 25 and containing 1.2wt% copper (measured by A.A.).

Table 3.1. Summary of catalysts prepared using the indicated Beta zeolite samples.

Sample Name	**Theoretical Cu wt.% loading**	**Actual wt.% loading of Cu**	**% Cu exchanged**	**pH of exchange solution**	**SiO_2:Al_2O_3 ratio**
0.85% Cuβ(25)	2	0.85	7	3.5	25:1
1.20%Cuβ(25)	2	1.20	10	7.0	25:1
1.95%Cuβ(25)	2	1.95	16	10.0	25:1
0.19%Cuβ(75)	2	0.19	5	3.5	75:1
0.10%Cuβ(150)	2	0.08	4	3.5	150:1
1.02%Cuβ(150)	2	1.02	50	7.0	150:1
2.00%Cuβ(150)	2	1.98	97	8.2	150:1
0.02%Cuβ(300)	2	0.02	2	3.5	300:1
1.30%Cuβ(300)	2	1.30	126	9.5	300:1

The cation-exchange behaviour of natural zeolites depends on several factors such as the framework structure, contacting solution composition, contacting solution pH (protons are also exchangeable cations) and operating conditions (temperature, contacting time) (Perego et al., 2013). In this work both the influence of the Si/Al ratio of the Beta zeolite and the pH of the exchange solution on the overall copper loading achieved during catalysts synthesis, was studied. As evident in Table 3.1 the Si/Al ratio of the Beta zeolite can have a major influence on the Cu exchange level since the ion exchange capacity is based on the concentration of Al^{3+} ions in the zeolite framework. In the ion exchange procedure, copper exchanges for two exchangeable protons. Therefore, structures with low Si/Al ratios, such as β(25) have a potentially higher cation exchange capacity. The % of the total exchangeable sites exchanged with copper (% exchange) increases in general, with increasing Si/Al ratio. Indeed for the 1.3Cu β(300), the % exchange is over 100% this can be explained by the fact that the β(300) have fewer exchangeable sites and a relatively low laoding of copper would be required for complete exchange (100% exchange). Zeolite catalysts exceeding 100% exchange levels, can be attributed to either the formation of copper dimers in solution $(Cu^{2+}OH^{-})_2$, which would result in the anchoring of two Cu (II) ions per exchangeable site (Ohman et al., 2002), and/or to the formation of extraframework copper oxide species (Yashnik, et al., 2005). Also it has been reported by Centi and Perathoner that during the ion exchange process, local changes in pH could promote copper hydroxide precipitation (Centi and Perathoner 1995). This would result in an increase in the calculated ion exchange level and lead to stabilization of some copper ions in positions different from the zeolite cation-exchange sites (Yashnik, et al., 2005).

Figure 3.2 shows the influence of Si/Al ratio on the copper content of the synthesised Cu exchanged Beta zeolites which were prepared at pH 3.5 (without pH adjustment). When the pH and the copper concentration of the exchange solutions are held constant while the Si/Al ratio of the Beta zeolite increases there is a significant fall in the amount of copper loading. For example at an exchanged solution pH of 3.5 and a theoretical 2 wt.% Cu loading there is a decrease in the actual Cu wt.% loading, 0.85wt%, 0.19wt%, 0.08wt%, 0.02wt% as the Si/Al ratio of the Beta zeolite increases from 25, 75, 150 and 300 respectively as shown in Table 3.1. This is due to the decrease in cation exchange sites with increasing Si/Al ratio. This reported influence of Si/Al ratio on the percentage copper loadings has been cited in literature by works from O'Brien et al., Janas et al. and De La Torre et al., (O'Brien et al., 2008, Janas et al., 2009 and De La Torre et al., 2012).

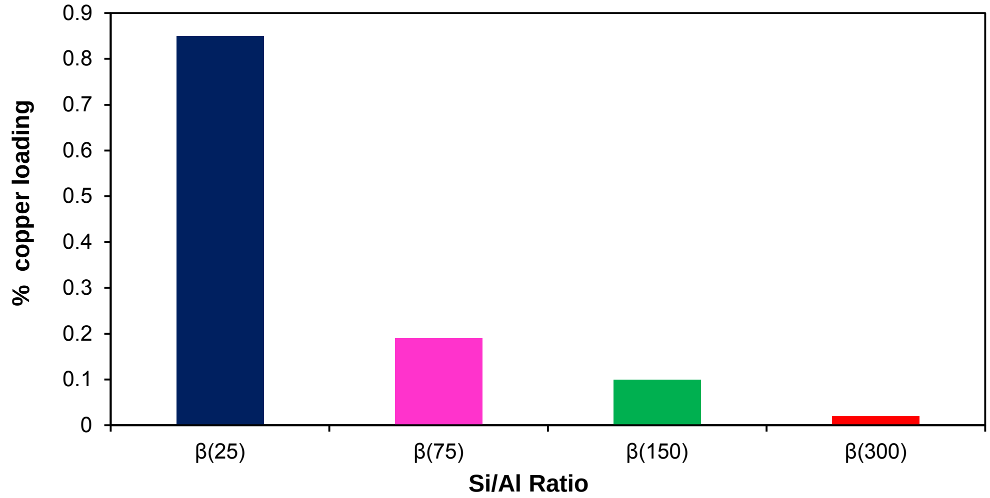

Figure 3.2: Influence of Si/Al ratio on the % copper loadings of the synthesised Cu exchanged Beta zeolite. (pH of exchange solution at 3.5).

It is well known that natural zeolites tend to elevate solution acidity (Inglezakis et al., 2003). However, acidity of solutions is expected to change during ion exchange, as copper cations are exchanged with the protons present in the zeolite structure (Chang, R. 1988). Figure 3.3 shows the influence of the pH of the exchange solution on the % copper loadings of the Beta zeolites. When the copper concentration of the exchange solution and the Si/Al ratio of the Beta zeolite are both held constant while the pH of the exchange solution is increased from acidic to alkaline there is an increase in the % Cu loading as increasing the pH (decreases the H^+ concentration) promotes the exchange process.

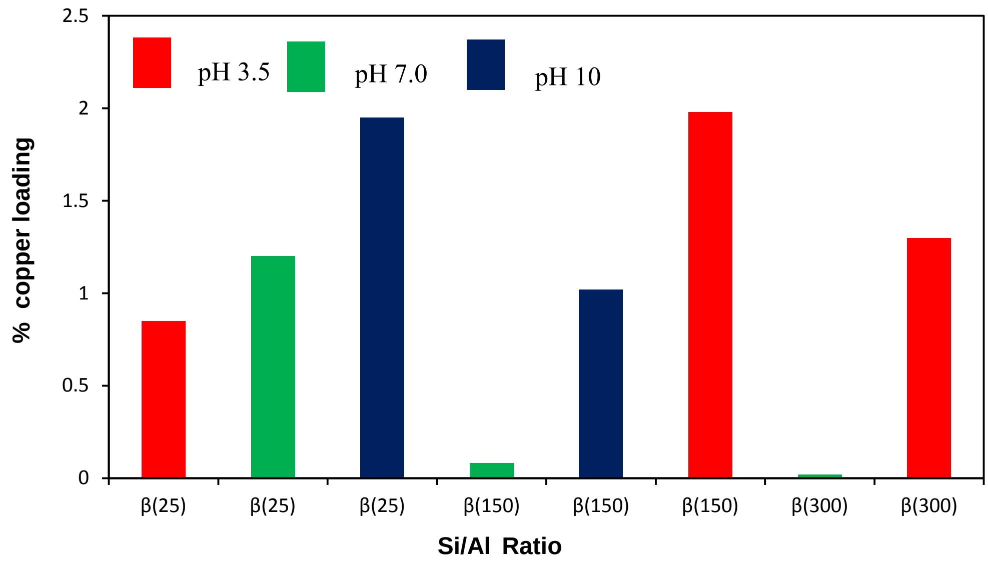

Figure 3.3: Influence of the pH of exchange solution on the % copper loading of the synthesised Cu exchanged Beta zeolite.

This would indicate that a modification in pH from acidic to more neutral and alkaline conditions pushes the equilibrium towards the exchange of protons on the zeolite for cations in solution. Thus the highest % copper loading occurred under more alkaline conditions for all Beta zeolite samples, such as 1.95%Cuβ(25) and 2.0%Cuβ(150). The observed increase in copper loading levels at higher pH values maybe also related to precipitation of the copper within the pores of the Beta zeolite. At high pH, copper may precipitate in the pores and over exchanged zeolites are obtained (Vanelderen et al., 2013). These zeolites contain more copper than needed for neutralization of the cation exchange capacity. Without pH adjustment of the exchange solution, lower percentage copper loadings were reported for all Beta zeolite sample such as 0.1%Cuβ(150) and 0.02%Cuβ(300) as under acidic conditions the equilibrium is unfavourable as a result of H^+ ions competing with the copper cations for exchange sites in the Beta zeolite framework. The lower uptakes observed under acidic conditions has been investigated by Kesraoui–Ouki and Kavannagh, Feng et al. and

Panayotova who reported on the influence of acidity on the uptake rates of heavy metal by clinoptilolite especially in the case of Cr^{3+} and Cu^{2+} (Kesraoui-Ouki and Kavannagh 1999; Feng et al., 2000, Panayotova 2001). Under acidic conditions, H^{+} cations are considered as competitive ions in the ion-exchange processes, and consequently ion exchange of metals is favoured at higher pH values (Inglezakis et al., 2003). According to these studies, there is no significant change in Pb^{2+} uptake in the range of acidity between 3 and 12, while a considerably lower uptake, up to 50%, is observed in the case of Cu^{2+} at pH 3 in comparison to higher pH values. An intense influence of acidity on Cu^{2+} removal has been reported for ion exchange using similar materials, such as kyanite, where adsorption increases from 44 to 88 % as the pH is increased from 1 to 6 (Ajmal et al., 2001).

XRD analysis of each of the copper exchanged Beta zeolite samples listed in Table 3.1 was performed. XRD was also carried out on the unmodified Beta zeolite samples (β(25), β(75), β(150) and β(300) as comparators to assess the effect of the introduction of copper on each of the Beta zeolites framework. The XRD patterns for Beta zeolite (β(25) and 1.95%Cuβ(25) are displayed in Figure 3.1. Both were almost identical which means that the crystalline nature of the zeolites was not modified after the incorporation of copper. All of the other copper modified samples prepared presented similar patterns.

During ion exchange, copper ions are generally introduced into the zeolite as exchangeable cations, which are dispersed and isolated Cu ions interacting with the zeolite framework via one or two oxygen-bridging bonds. Consequently no peaks corresponding to copper is expected, as these species are undetectable by XRD. However, it is also likely local precipitation of copper hydroxide inside the zeolite channels is possible due to local changes in pH. It is therefore important to investigate the zeolite support for the presence of both CuO and Cu cluster/species. CuO generally exist as monoclinic crystals with maximum intense diffraction peaks at 35.5° and 38.7° (referred to 2θ scale) corresponding to the [1,1,-1] and [1,1,1] planes, whereas Cu generally exist in the cubic crystal system with the maximum intense diffraction peak at 43.3°, corresponding to [1,1,1] plane (De La Torre et al., 2012). No peaks were observed that would indicate the presence of CuO or Cu°. This may be because the concentration of these species were not high enough to observe well defined diffraction peaks. Therefore the presence of the CuO and Cu cannot be ruled out in the Beta zeolite especially those with high % Cu exchange levels, such as the 1.30%Cuβ(300) which presented a copper exchanged level of 125.71%.

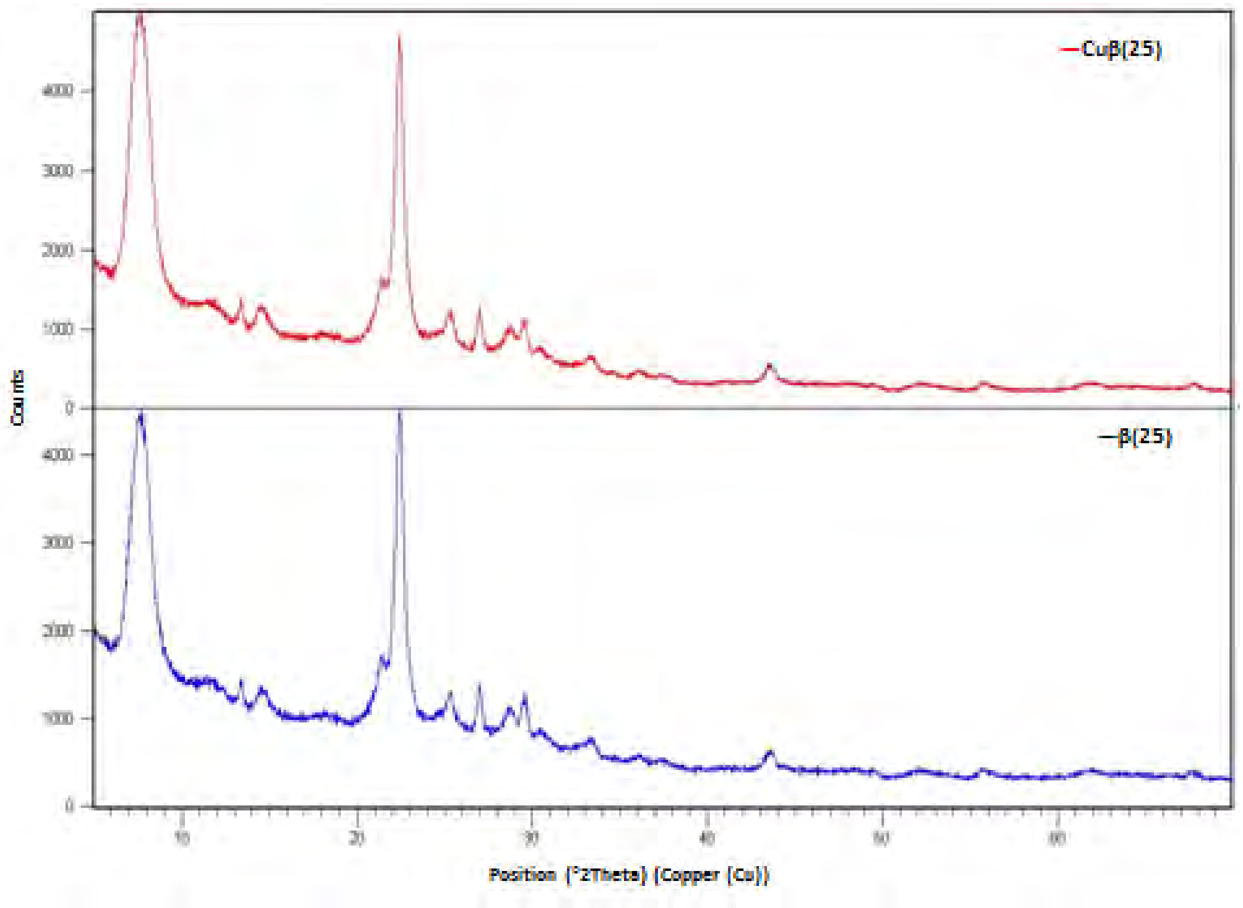

Figure 3.1: XRD pattern for unmodified Beta zeolite β(25) and 1.95%Cuβ(25).

3.3.2 Copper Leachability and Framework Dealumination

Leaching test were conducted on all copper modified Beta zeolite samples in order to assess the extent of copper leaching as a function of pH. Table 3.2 shows the results of the leaching experiments for 1.20%Cuβ(25), 1.95%Cuβ(25), 0.10%Cuβ(150) and 2.0%Cuβ(150) which were taken as representative samples for all prepared copper exchanged Beta zeolites.

Table 3.2: Summary of leaching tests undertaken on the indicated copper modified Beta zeolite over pH range 1 – 11.

Sample	SiO_2:Al_2O_3 ratio	pH	Aqueous Copper Concentration (mg dm^{-3})	Aqueous Aluminium Concentration (mg dm^{-3})
1.20%Cuβ(25)	25:1	1	25.0	40.0
		3	14.0	28.0
		5	0.9	5.0
		7	0.8	0.0
		10	0.6	0.0
		11	0.3	0.0
1.95Cuβ(25)	25:1	1	49.0	46.0
		3	38.0	32.0
		5	1.0	7.53
		7	0.2	0.0
		10	0.3	0.0
		11	0.1	0.0
0.1%Cuβ(150)	150:1	1	11.2	32.0
		3	10.2	15.0
		5	1.9	2.0
		7	0.3	0.0
		10	0.2	0.0
		11	0.1	0.0
2.00%Cuβ(150)	150:1	1	42.5	25.0
		3	15.1	18.0
		5	2.0	10.0
		7	0.3	0.0
		10	0.2	0.0
		11	0.1	0.0

At pH values less than pH 5, considerable leaching of the extra-framework copper into solution is evident, while minimal copper leaching was reported at neutral to alkaline pH ranges for all copper exchanged Beta zeolite samples. The highest copper leaching levels were reported at pH 1 for all copper exchanged Beta zeolites and this can also be attributed to dealumination of the zeolite at strongly acidic pHs which has previously been reported in literature (O'Dwyer 1993, Oumi et al., 2001, Janas et al., 2009 and Shukla et al., 2010).

It has been reported that natural zeolites tend to elevate the solution acidity, acting as amphoteric materials (Kesraoui-Ouki and Kavannagh 1999). In acidic solutions zeolites may exchange some of their exchangeable cations with H_3O^+ ions and Al can be progressively removed from the aluminosilicate framework (Inglezakis et al., 2003). Dealumination is the removal of the tetrahedral Al^{3+} ions from the zeolite lattice. Loss of framework aluminium reduces the cation exchange capacity of the Beta zeolite resulting in loss of isolated cupric ions as these ions replace the protons, which neutralise the excess negative charge with Al^{3+} within the framework (Janas et al., 2009).

The extent of dealumination of the 1.20%Cuβ(25), 1.95%Cuβ(25), 0.1%Cuβ(150) and 2.0%Cuβ(150) was investigated by atomic absorption analysis as described in section 3.2.4 and Table 3.2 shows the reported level of aluminium in mg g^{-1} that was lost from each of the Cu Beta zeolite samples as a function of pH. Loss of the aluminium from the Beta zeolite framework under strong acidic conditions was most pronounced with the lower Si/Al ratio solids such as 1.95%Cuβ(25) as illustrated in Table 3.2. Lower levels of Al leaching was observed from the higher Si/Al ratio 2.0%Cuβ(150) solids. This agrees with studies by Oumi et al. and Muller et al. who reported that Beta zeolite could be very easily dealuminated by HCl treatment (Oumi et al., 2003, Muller et al., 2000). As Beta zeolite has a three-dimensional 12-ring pore system, the framework is very flexible and was found to undergo dealumination easier than other less flexible zeolite structures such as mordenite, which has a one-dimensional 12-ring pore system and ZSM-5, which has a three-dimensional 10-ring pore system (Muller et al., 2000). Beta zeolite crystallizes with many stacking faults and these may increase the probability of the presence of defect sites in the framework (Meier 1961). Ultimately, it is deduced that acid treatment will reduce the cation-exchange capacity due to dealumination (Wang and Peng 2010). This supports the findings presented in Figure 3.3 which shows that the lowest % Cu loadings and exchange levels were obtained at a pH of 3.5.

Table 3.2 shows that copper modified samples β(25) and β(150) were most stable over the range of pH 5 – 11. Over this pH range, there was minimal leaching of framework aluminium while copper leached from 1.20%Cuβ(25) and 1.95%Cuβ(25) corresponds to an aqueous solution concentration of less than 0.9 mg dm^{-3} and 1.0 mg dm^{-3}, respectively. While for 0.1%Cuβ(150) and 2.0%Cuβ(150) the level of copper leaching corresponds to an aqueous solution concentration of less than 1.9 mg dm^{-3} and 2.0 mg dm^{-3}, respectively.

Typical emission limit values (ELVs) for copper concentration in various industrial effluents range from 0.5 mg dm^{-3} to 2.0 mg dm^{-3} (EPA, 1997). Over the pH range 5 – 11, the copper leached from the metal exchanged beta samples lies close to but within these typical industrial emission limits. It is envisaged that 2-nitrophenol adsorption experiments carried out in this pH range will lead to minimal aluminium leaching and consequently minimal loss of catalytic activity. Therefore under these pH conditions Beta zeolites may prove suitable adsorbents for the removal of 2-nitrophenol from an aqueous environment.

3.4 Conclusion

The unmodified Beta zeolite has shown strong and rapid uptake of 2-nitrophenol (Chapter 2 section 2.3.1). This work sought to modify the Beta zeolite by incorporating a catalytic component (copper) into the Beta zeolite, which would enhance and promote its potential catalytic activity in step 2 while maintaining its adsorption capacity achieved in step one.

During the modification of the Beta zeolite the effects of Si/Al ratio of the Beta zeolite, the exchange solution pH and ultimately the stability of the catalytically modified Beta zeolites were investigated.

A series of copper-exchanged Beta zeolites (β(25), β(75), β(150) and β(300)) was prepared at varying exchange solution pHs. An adjustment of the exchange pH over the range pH 3.0 – pH 10 revealed that the % Cu exchanged was influenced by the pH of the exchange solution, with neutral to alkaline pHs providing the optimum copper exchange conditions on all Beta zeolite samples prepared. It was observed that acidic pHs resulted in the potential destabilization of the Beta zeolite framework structure due to dealumination of framework aluminium ions, which ultimately resulted in a corresponding leaching of associated copper ions from the Beta zeolite framework.

The effect of Si/Al ratio also had an influence on the copper loading of the Beta zeolite, as decreasing the Si/Al ratio resulted in an increase in the extra framework cations which were readily replaced by copper under alkaline conditions such as with the β(25) which reported a 1.95% wt copper loading during the exchange procedure. While increasing the Si/Al ratio of the Beta zeolite resulted in a corresponding decrease in cation exchange capacity of the Beta zeolite for example with the β(300) which reported a 1.30% wt. copper loading during the exchange procedure.

The XRD spectra of both β(25) and 1.95%Cuβ(25) were almost identical as shown in Figure 3.1, which means that the crystalline nature of the Beta zeolite was not modified after the incorporation of copper. These XRD spectra were found to be representative of all the Beta zeolite samples. However, the presence of the CuO within the framework cannot be ruled out especially among the samples that reported high or over 100% Cu exchange levels such as 1.30%Cuβ(300).

The aim of this work was to catalytically modify the Beta zeolite. This was achieved as a series of copper exchanged Beta zeolite samples with varying loadings of copper was successfully prepared. These solids were shown to be resistant against leaching in aqueous solution if the pH range was maintained between 5 - 11.

3.5 References

Abu-Zied, B. M., Schwieger, W. and A. Unger (2008) 'Nitrous oxide decomposition over transition metal exchanged ZSM-5 zeolites prepared by the solid-state ion exchange method', *Applied Catalysis B:Environmental*, **84**, 277-288.

Ajmal, M., Rao, R., Ahmad, R. and A. J. Rao (2001) 'Removal and recovery of heavy metals from electroplating wastewater by using kynite as an adsorbent', *Journal of Hazardous Materials*, **87**, 127-137.

Alver, E. and A. U. Metin (2012) 'Anionic dye removal from aqueous solutions using modified zeolite: Adsorption kinetic and isotherm studies', *Chemical Engineering Journal*, **200-202**, 59-67.

Anpo, M., Matsuoka, M., Shioya, Y., Yamashita, H., Giamello, E., Morterra, C., Che, M., Patterson, H. H., Webber, S. Ouelletter, S. and M. A. Fox (1994) 'Preparation and characterisation of the Cu^{+} / ZSM-5 catalysts and its reaction with NO under UV irradiation at 275K. In situ photoluminescence, EPR and FTIR investigation', *Journal of Physical Chemistry,* **98**, 5744-5750.

Baek, S. W., Kim, J. R. and S. K. Ihm (2004) 'Design of dual functional adsorbent/catalyst system for the control of VOCs by using metal-loaded hydrophobic Y-zeolites', *Catalysis Today*, **93-95**, 575-581.

Brazlauskas, M. and S. Kitrys (2008) 'Synthesis and properties of CuO/zeolite sandwich type adsorbent – catalyst', *Chinese Journal of Catalysis*, **29**, 25-30.

Brooks, C. A., France, L., Gayot, C., Li, P. J., Sault, R.,Stafford, A., Wallis, D. J. and M. Stockenhuber (2012) 'A designed organic-zeolite hybrid acid-base catalysts', *Journal of Applied Catalysis*, **285**, 10-18.

Centi, G. C., Nigro, S., Perathoner and G. Stella (1993) 'Role of the support and adsorbed species on the behaviour of Cu-Based catalysts for NO conversion', *Catalysis Today*, **17**, 159-166.

Centi, G. and S. Perathoner (1995) 'Nature of active species in copper-based catalysts and their chemistry of transformation of nitrogen oxides', *Applied Catalysis A: General*, **132**, 179-259.

Chang, R. 'Chemistry' Third Edition, McGraw – Hill 1988.

Damjanovic, L., Rakic, V., Rac, V., Stosic, D., and A. Auroux (2010) 'The investigation of phenol removal from aqueous solutions by zeolites as solid adsorbents', *Journal of Hazardous Materials*, **184**, 477-484.

De La Torre, U., Pereda-Ayo, B. and J. R. Gonzalez-Velasco (2012) 'Cu-zeolite NH_3-SCR catalysts for NO_x removal in the combined NSR-SCR technology', *Chemical Engineering Journal*, **207-208**, 10-17.

De Lucas, A., Sánchez, P., Dorado, F., Ramos, M. J. and J. L. Valverde (2005) 'Effect of the metal loading in the hydroisomerization of *n*-octane over beta agglomerated zeolite based catalysts', *Applied Catalysis A*, **294**, 215-225.

Feng, D., Aldrich, C. and H. Tan (2000) 'Removal of heavy metal ions by carrier magnetic separation of adsorption of adsorptive particulates', *Hydrometallurgy*, **56**, 359-368.

Guillemot, M., Mijoin, J., Mignard, S. and P. Magnoux (2007) 'Volatile organic compounds (VOCs) removal over dual functional adsorbent/catalysts system', *Applied Catalysis B*: **75**, 249-255.

Guisnet, M. and J. P. Gilson (2002) 'Zeolites for cleaner technologies catalytic science series', 3, Imperial College Press, London.

Hajimirzaee, S., Leeke, A. G. and J. Wood (2012) 'Modified zeolite catalyst for selective dialkylation of naphthalene', *Chemical Engineering Journal*, **207-208**, 329-341.

Heck, R. M. and R. J, Farrauto (2002) Catalytic air pollution control commercial technology, John Wiley & Sons Inc, New York.

Inglezakis, V. J. 'The concept of capacity in zeolite ion-exchange system' (2005) *Journal of Colloid and Interface Science*, **281**, 68-79.

Inglezakis, V., Loizidou, D.. M. and H. P. Grigoropoulou (2003) 'Ion exchange of Pb^{2+}, Cu^{2+}, Fe^{3+} and Cr^{3+} on natural clinoptilolite: selectivity determination and influence of acidity on metal uptake', *Journal of Colloid and Interface Science*, **261**, 49-54.

Iwamoto, M. Furukawa, H., Mine, Y., Uemara, F., Mikuriya, S. and S. Kagawa (1986) 'Copper (II) ion-exchange ZSM-5 zeolites as highly active catalysts for direct and continuous decomposition of nitrogen monoxide', *Journal of Chemical Society, Chemical Commications,* **16** 1272-1273.

Janas, J., Gurgul, J., Socha, R. P. and S. Dzwigaj (2009) 'Effect of Cu on the catalytic activity of CuSiBEA zeolite in the SCR of NO by ethanol: Nature of the copper species', *Applied Catalysis B*: **91**, 217-224.

Jiuhui, Q. (2008) 'Research progress of novel adsorption processes in water purification: A review', *Journal of Environmental Sciences*, **20**, 1-13.

Kesraoui - Ouki and Kavannagh (1999) 'Treatment of metals-contaminated wastewaters by use of natural zeolites', *Water Science and Technology*, **39**, 115-122.

Khalid, M., Joly, G., Renaud, A. and P. Magnoux (2004) 'Removal of phenol from water by adsorption using zeolites', *Industrial Engineering Chemistry Resource*, **43**, 5275-5280.

Kuznetsova, E. V., Savinov, E. N., Vostrikova, L. A. and V. N. Parmon (2004) ' Heterogeneous catalysis in the Fenton-type system FeZSM-5/H_2O_2', *Applied Catalysis B: Environmental*, **51**, 165-170.

Lenihan, S. and T. Curtin (2009) 'The selective oxidation of ammonia using copper-based catalysts: The effects of water', *Catalysts Today*, **145**, 85-89.

Leyva – Ramos, R., Monsivais – Rocha, J. E., Aragon – Pina, A., Berber – Mendoza, M. S., Guerrero – Coronado, R. M., Alonso – Davila, P. and J. Mendoza – Barron (2010) 'Removal of ammonium from aqueous solution by ion exchange on natural and modified chabazite', *Journal of Environmental Management,* **91**, 2662-2668.

Li, Y. and J. N. Armor (1992) 'Catalytic decomposition of nitrous oxide on metal exchanged zeolites', *Applied Catalysis B: Environmental*, **1**, L21-L29.

Lindmark, J., Hedlund, J., Wirawan, K. S., Creaser, D., Li, M., Zhang, D. and X. Zou (2010) 'Impregnation of zeolite membranes for enhanced selectivity', *Journal of Membrane Science*, **365**, 188-197.

Machado, L. C. R., Torchia, C. B. and R. M. Lago (2006) 'Floating photocatalysts based on TiO_2 supported on high surface area exfoliated vermiculite for water decontamination', *Catalysis Communications*, **7**, 538-541.

Maduna Valkaj, K., Katovic, A. and S. Zrncevic (2007) 'Investigation of the catalytic wet peroxide oxidation of phenol over different types of Cu/ZSM-5 catalysts', *Journal of Hazardous Materials*, **144**, 663-667.

Martins, A., Silva, J. M., Henriques, C., Ribeiro, F. R. and M. F. Ribeiro (2005) 'Influence of rare earth elements La, Nd and Yb on the acidity of H-MCM-22 and H-Beta zeolites', *Catalysis Today*, **107-108**, 663-670.

Martucci, A., Pasti, L., Marchetti, N., Cavazzini, A. and F. Dondi (2012) 'Adsorption of pharmaceuticals from aqueous solutions on synthetic zeolites', *Microporous and Mesoporous Materials*, **148**, 174-183.

Meier, W. M. and D.H. Olson: *Atlas of Zeolite Structure Types*, 4th edition by Structure Commission of the International Zeolite Association (Elsevier, London 1996).

Metkar, P. S., Harlod, M. P. and V. Balakotaiah (2012) 'Selective catalytic reduction of NOx on combined Fe- and Cu- zeolite monolithic catalysts: Sequential and dual layer configurations', *Applied Catalysis B: Environmental*, **111-112**, 67-80.

O'Brien, J., O' Dwyer, T. F. and T. Curtin (2008) 'A novel process for the removal of aniline from industrial wastewaters', *Journal of Hazardous Materials*, **159**, 476-482.

O'Dwyer, T. F. (1993) PhD Thesis. 'Recovery of Chromium from Tannery Effluents Using a Redox Adsorption Approach', University of Limerick.

Ohman, O. L., Ganemi, B., Bjornbom, E., Rahkamaa, K., Keiski, R. L. and J. Paul (2002) 'Catalysts preparation through ion-exchange of zeolite Cu-, Ni-, Pd-, CuNi- and CuPd- ZSM-5', *Materials Chemistry and Physics*, **73**, 263-267.

Oumi, Y., Mizuno, R., Azuma, K., Nawata, S., Fukushima, T. Uozumi, T., and T. Sano (2001) 'Reversibility of dealumination-realumination process of BEA zeolite', *Microporous and Mesoporous Materials*, **49**, 103-109.

Panayotova, M. I., (2001) 'Kinetics and thermodynamics of copper ions removal from wastewater by use of zeolite' *Waste Management*, **21**, 671-676.

Perego, C. and P. Villa (1997) 'Catalysts preparation methods', *Catalysts Today*, **34**, 281-305.

Shukla, P., Wang, S., Singh, K., Ang, H. M. and M. O. Tade (2010) 'Cobalt exchange zeolites for heterogeneous catalytic oxidation of phenol in the presence of peroxymonosulphate', *Applied Catalysis B: Environmental*, **99**, 163-169.

Smeets, P. J., Meng, Q. G., Corthals, S., Leeman, H. and R. A. Schoonheydt (2008) 'Co-ZSM-5 catalysts in the decomposition of N_2O and the SCR of NO with CH_4: influence of preparation method and cobalt loading', *Applied Catalysis B*: **84**, 505-513.

Vanelderen, P., Vancauwenbergh, J., Sels, F. B. and R. A. Schoonheydt (2013) 'Coordination chemistry and reactivity of copper in zeolites', *Coordination Chemistry Reviews*, **257**, 483-494.

Waclaw, A., Nowinska, K., Schwieger, W. and A. Zielinska (2004) 'NO_2 decomposition over iron modified zeolites ZSM-5', *Catalysis Today*, **90**, 21-25.

Wang, X., Chen, H. and W. M. H. Sachtler (2001) 'Selective reduction of NO_x with hydrocarbons over Co/MFI prepared by sublimation of $CoBr_2$ and other methods', *Applied Catalysis B:Environmental*, **29**, 47-60.

Wang, S. and Y. Peng (2010) 'Natural zeolites as effective adsorbents in water and wastewater treatment', *Chemical Engineering Journal*, **156**, 11-24.

Wang, W. and S.J. Hwang (1995) 'Effects of the pretreatment of Cu-Y zeolite catalysts on the reduction of nitric oxide with ammonia', *Applied Catalysis B: Environmental*, **5**, 187-197.

Weitkamp, J. (2000) 'Zeolites and catalysis', *Solid State Ionics*, **131**, 175-188.

Yashnik, A. S., Ismagilov, Z. R., and V. F. Anufrienko (2005) 'Catalytic properties and electronic structure of copper ions in Cu–ZSM–5', *Catalysis Today*, **110**, 310–322.

Zhang, X., Shen, Q., He, C., Wang, Y., Cheng, J. and Z. Hao (2011) 'CoMOR zeolite catalyst prepared by buffered ion exchange for effective decomposition of nitrous oxide', *Journal of Hazardous Materials*, **192**, 1756-1765.

Chapter 4

Adsorption of 2-Nitrophenol onto Copper Modified Beta Zeolite

4.1 Introduction

The findings from chapter 2 sections 2.3.1 – 2.3.4 of this work suggest that in a controlled aqueous pH environment, unmodified Beta zeolite has significant potential as an adsorbent in the removal of low concentrations of 2-nitrophenol from aqueous streams. There are numerous reports cited in literature on the benefits of modification of adsorbent materials in order to enhance their adsorption and catalytic properties. Damjanovic et al., 2010 investigated the removal of phenol from aqueous solutions by zeolites as solid adsorbents. They reported that HZSM-5(15) had the lowest adsorption capacity for phenol from aqueous solution and they subsequently performed ion exchange of H^+ ions with Cu^{2+} in order to investigate the influence of extraframework cations on phenol adsorption. They reported that the ion exchange procedure resulted in an increase in adsorption level over the whole range of applied phenol concentrations, while the adsorption of nitrophenols from aqueous solutions was reported to be enhanced using cationic β-cyclodextrin modified zeolites by Xiaohong et al., 2011. Lopez- Fonseca et al., 2005 investigated the catalytic oxidation of aliphatic chlorinated organic compounds over Pt/H-Beta zeolite catalysts under dry and humid conditions. They compared the chlorinated VOC conversion using Pt/H-Beta and only the supported material, H-Beta, it was clear that Pt reduced the destructive temperatures, although they found H-Beta to be active due to it acidic properties, however it was reported that with H-Beta the CO production was much higher.

Lenihan and Curtin (2003) investigated the selective oxidation of ammonia using both a copper oxide supported on alumina and a copper exchanged beta zeolite catalyst. The introduction of copper into both of these supports resulted in a dramatic increase in the conversion of ammonia to nitrogen and water especially for copper exchanged beta zeolite. Modification of the zeolite adsorbent in chapter 3 section 3.3.1 of this thesis was performed with the aim of enhancing the dual function of Beta zeolite as an adsorbent and a catalyst.

The aim of this work was to investigate the influence of the introduction of extra-framework copper cations into β(25), β(75), β(150) and β(300) with respect of 2-nitrophenol adsorption capacity, adsorption equilibrium, thermodynamics, kinetics and mechanism.

4.2 Experimental

4.2.1 Preparation of 2-Nitrophenol Adsorption Isotherm

Adsorption isotherms were prepared to evaluate the effectiveness of the modified Beta zeolites in removing low concentrations of 2-nitrophenol from water. Accurately weighed portions of the modified beta zeolite (0.2 g) were placed into a series of 50 ml vials. A series of 2-nitrophenol solutions of varying initial concentration (5 mg dm^{-3} to 1000 mg dm^{-3}) were prepared by dissolving appropriate amounts of 2-nitrophenol, (Sigma Aldrich) in deionised water. From each flask, a 20 cm^3 aliquot was removed and added to each vial. The solutions were stirred continuously until equilibrium was reached. The contents of the adsorption vials were then separated by centrifugation for 20 min at 3,500 rpm using a Rotofix 32 centrifuge (Hettich Zentrifugen). An aliquot of each of the supernatants was then removed (10 cm^3) for analysis.

The concentration of 2-nitrophenol before and after adsorption was determined spectrophotmetrically (λ_{max} 350 nm) by a Varian (Cary) UV-spectrophotometer. The amount adsorbed was calculated from initial and final concentrations of 2-nitrophenol in the liquid phase. Blank solutions containing equivalent initial concentration of 2-nitrophenol but without the addition of the adsorbent were also prepared. All samples and blanks were run in triplicate to ensure reproducibility and accuracy. Distilled water was used as the solvent. Adsorption isotherms were carried out at 24^{o}C.

4.2.2. Evaluation of the Thermodynamics of Adsorption

Isotherms were prepared for 2-nitrophenol adsorption onto copper modified Beta zeolite (Si/Al of 25:1, 75:1 150:1 300:1) at 6ºC, 24ºC and 40ºC using a batch technique. The same procedure as outlined in chapter 2 section 2.2.2 was used to determine the amount of 2-nitrophenol adsorbed as a function of temperature.

4.2.3 Kinetics of Adsorption

The equilibrium time for maximum adsorption on the copper modified Beta zeolite catalysts was determined using the following procedure.

Accurately weighed amounts of the modified adsorbent (0.2 g) were added to vials containing 20 ml of 2-nitrophenol solutions where the initial 2-nitrophenol concentrations were 50 mg dm^{-3}, 100 mg dm^{-3} and 500 mg dm^{-3}. The solutions were stirred continuously at 24ºC for times ranging between 5 minutes and 2 hours. The contents of the adsorption flasks were then separated using a centrifuge at

3,500 ramps/minute for 20 minutes. The supernatant was then analysed as in the procedure outlined in chapter 2 section 2.2.2. All experiments were run in triplicate and controls using 2-nitrophenol only were used to ensure reproducibility and accuracy. Deionised water was used as solvent.

4.3. Results and Discussion

4.3.1 Preparation of 2-Nitrophenol Adsorption Isotherm on modified Beta zeolite

To date the unmodified Beta zeolite has shown strong and rapid uptake of the 2-nitrophenol as reported in chapter 2 section 2.3.1 of this thesis. In chapter 3 the Beta zeolite was modified by the introduction of a catalytic component (copper) by an ion exchange procedure as described in chapter 3 section 3.2.1. The aim of this work was to investigate the influence of extra-framework copper cations into β(25), β(75), β(150) and β(300) with respect to 2-nitrophenol adsorption capacity, adsorption equilibrium, thermodynamics, kinetics and mechanism. The adsorption isotherms for 2-nitrophenol uptake onto each of the copper modified and unmodified Beta zeolite samples at 24°C are shown in Figures 4.1 - 4.4.

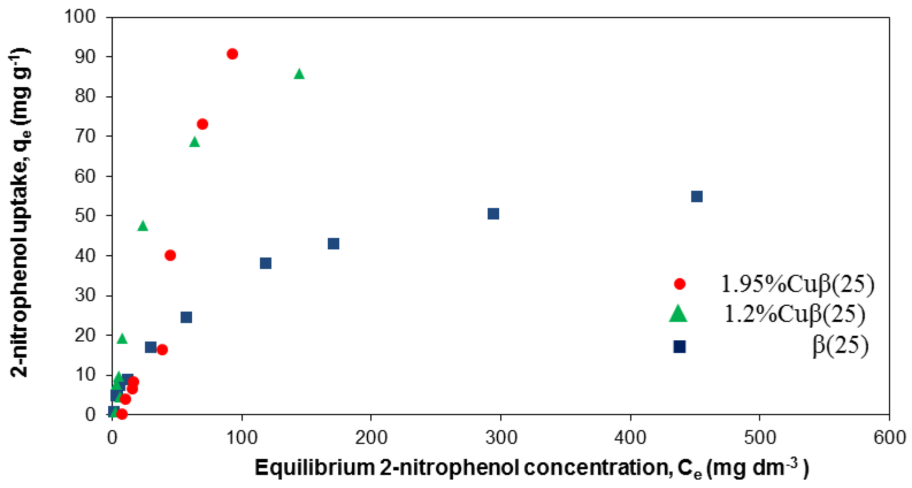

Figure 4.1: Adsorption isotherm for 2-nitrophenol onto the indicated copper exchanged Beta zeolite and unmodified Beta zeolite samples, at varying initial 2-nitrophenol concentrations between 10 mg dm^{-3} and 1000 mg dm^{-3} at 24°C.

The unmodified Beta zeolite sample β(25) showed the lowest adsorption of 2-nitrophenol with adsorption uptake levels of 40 - 50 mg g^{-1} being reported in chapter 2 section 2.3.1. However it is evident in Figure 4.1 that the introduction of extra-framework copper cations in the Beta zeolite has resulted in a significant increase in adsorption levels over the applied 2-nitrophenol concentration range. It is also clearly shown in Figure 4.1 that Beta zeolites adsorption capacity increases with increasing percentage copper loading with maximum 2-nitrophenol uptake of between 80 - 90 mg g^{-1} and 90 - 100 mg g^{-1} being achieved on the 1.2%Cuβ(25) and 1.95%Cuβ(25) samples respectively.

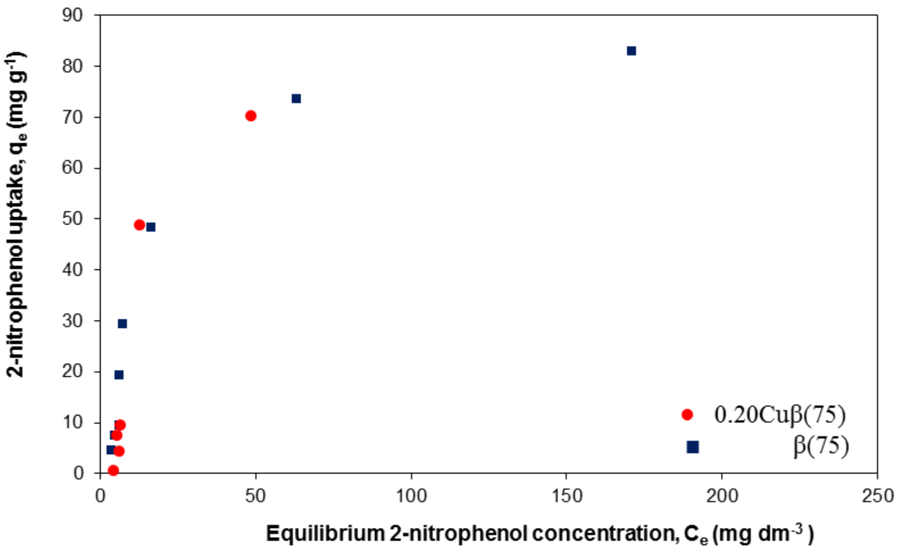

Figure 4.2: Adsorption isotherm for 2-nitrophenol onto the indicated copper exchanged Beta zeolite and unmodified Beta zeolite samples, at varying initial 2-nitrophenol concentrations between 10 mg dm^{-3} and 1000 mg dm^{-3} at 24°C.

The presence of copper in the β(75) framework is also observed to positively influence the adsorption level of 2-nitrophenol, however it does not significantly increase the adsorption level of 80 – 90 mg g^{-1} achieved by the unmodified sample as shown in Figure 4.2. This may be due to saturation of the adsorption sites or be related to the relatively low percentage copper loadings on the β(75) sample.

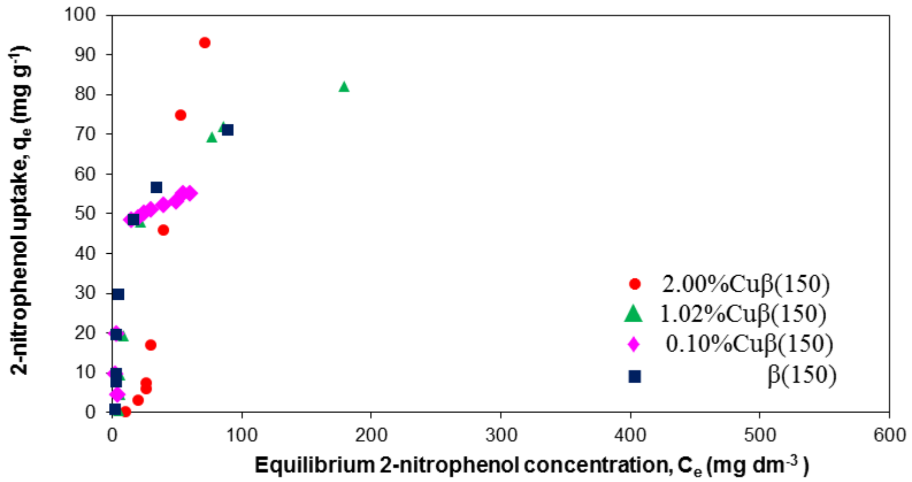

Figure 4.3: Adsorption isotherm for 2-nitrophenol onto the indicated copper exchanged Beta zeolite and unmodified Beta zeolite samples, at varying initial 2-nitrophenol concentrations between 10 mg dm^{-3} and 1000 mg dm^{-3} at 24°C.

A similar trend to the copper modified β(25) and β(75) samples is observed for β(150) samples where the introduction of extra-framework copper cations enhances the 2-nitrophenol adsorption level achieved by the β(150) sample from 70 - 80 mg g^{-1} to between 80 - 90 and 90 - 100 mg g^{-1} for the 1.02%Cuβ(150) and the 2.0% Cuβ(150) samples respectively, while the lowest percentage copper loading sample 0.10 %Cuβ(150) did not increase the adsorption level achieved by the unmodified sample as shown in Figure 4.3.

Finally the most hydrophobic Beta zeolite sample β(300) achieved one of the highest adsorption levels of 2-nitrophenol of 80 - 90 mg g^{-1} (Figure 4.4), it is evident that the presence of extraframe work copper cations positively influences the adsorption of 2-nitrophenol however similar to the 0.2%Cuβ(75) sample it did not significantly increase the adsorption levels achieved by the unmodified sample.

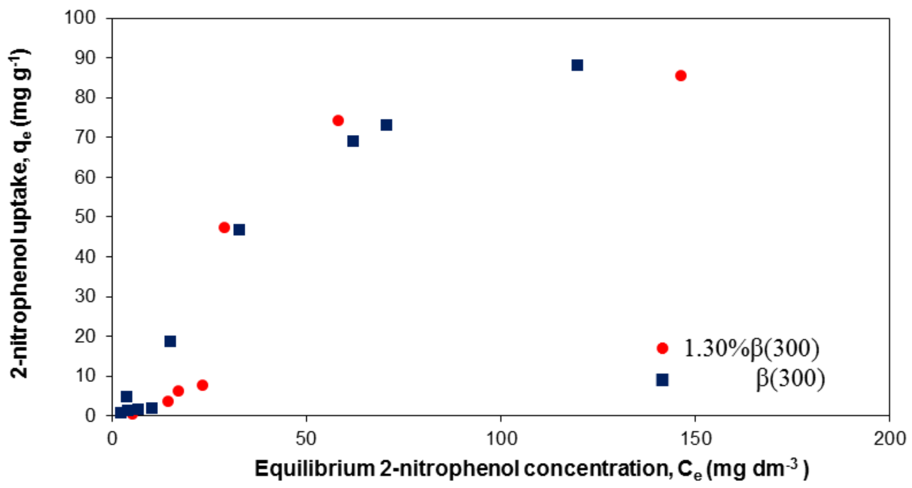

Figure 4.4: **Adsorption isotherm for 2-nitrophenol onto the indicated copper exchanged Beta zeolite and unmodified Beta zeolite samples, at varying initial 2-nitrophenol concentrations between 10 mg dm^{-3} and 1000 mg dm^{-3} at 24°C.**

The results showed that 2-nitrophenol uptake was positively influenced by the presence of extra-framework copper, with a reported increase in uptake levels on the copper modified Beta zeolite over the unmodified Beta zeolites. It is also evident that increasing the percentage copper loadings in the Beta zeolite framework further increases its adsorption affinity for 2-nitrophenol molecules, this is clearly shown in Figure 4.3 where the adsorption level of 2-nitrophenol increases from 50 – 60, to 90 – 100 mg g^{-1} with increasing the percentage of copper loadings from 0.10 to 2.0% for the copper modified β(150) samples.

The findings reported in this initial study are supported by works published in this area by a number of researchers who all reported an increase in the affinity of mineral adsorbents such as bentonite clay (Anirudhan and Ramachandran, 2006), zeolites (Damjanovic et al., 2010) and clinoptilolite (Hong- Yu et al., 2011) for the adsorption of phenolic compounds after chemical modification. Damjanovic et al., investigated the removal of phenols from aqueous solution using zeolites as solid adsorbents (Damjanovic et al., 2010). They reported that HZSM-5(15) zeolite showed the lowest adsorption of phenol from aqueous solution at ~ 13.95 mg g^{-1}. In order to investigate the influence of extra-framework cations on the adsorption of phenol they performed ion exchange of H^+ ions with Cu^{2+} ions. The ion exchange procedure resulted in an increase of phenol adsorption over the whole range of applied phenol concentration with a maximum adsorption level of ~ 18.6 mg g^{-1} being achieved (Damjanovic et al., 2010).

To optimize the design of an adsorption system for the adsorption of adsorbates, it is important to establish the most appropriate correlation for the equilibrium curves. Various isotherm equations have been reported in literature to describe the equilibrium nature of adsorption (Mall et al 2006). Langmuir and Freundlich plots, as defined in Equations 2.28 and 2.31 in chapter 2 section 2.1.3 were applied to the equilibrium data for adsorption of 2-nitrophenol onto copper modified Beta zeolite (Langmuir, 1918, Freundlich, 1906).

A basic assumption of the Langmuir model is that sorption takes place at specific homogeneous sites within the adsorbent. It is assumed that once a molecule occupies a site no further adsorption can take place at that site. Theoretically, therefore, a saturation value is reached beyond which no further sorption can take place (Mall et al 2006). In chapter 2 section 2.3.1 the adsorption of 2-nitrophenol from aqueous solutions onto unmodified Beta zeolite (β(25), β(75) and β(150) samples was found to follow the Langmuir model of adsorption, with a plateau or maximum adsorption of 2-nitrophenol being achieved over the applied concentration ranges. The data obtained from the Langmuir plots at the indicated temperature for copper modified Beta zeolite samples are shown in Table 4.1 such as maximum 2-nitrophenol uptake on the copper modified Beta zeolite samples W_{max}, the adsorption equilibrium constant K_L. Also listed in Table 4.1 are the experimentally determined maximum 2-nitrophenol uptake on the copper modified Beta zeolite samples $W_{max\ exp}$, the separation factor, R_L and the correlation coefficient, R^2 value.

Table 4.1: Langmuir constants for 2-nitrophenol adsorption onto copper exchanged Beta zeolites with varying SiO_2:Al_2O_3 ratios, at the indicated temperatures.

Sample Name	Temperature (°C)	$W_{max, exp}$ (mg g^{-1})	K_L (dm^3 g^{-1})	W_{max} (mg g^{-1})	R_L	R^2
1.95%Cuβ(25)	6	92.80	-0.013	-15.38	1.149	0.583
	24	90.72	-0.007	-47.61	1.075	0.725
	40	66.06	-0.007	-31.05	1.075	0.536
0.20%Cuβ(75)	6	94.54	0.060	123.45	0.819	0.985
	24	70.13	0.109	92.592	1.075	0.839
	40	85.77	1.000	113.68	0.95	0.979
2.00%Cuβ(150)	6	115.0	-0.009	-53.47	1.176	0.551
	24	74.60	-0.015	-10.25	1.194	0.574
	40	85.77	-0.016	-14.12	1.098	0.116
1.30%Cuβ(300)	6	85.5	-0.002	-131.57	1.020	0.124
	24	84.96	-0.006	-32.05	1.063	0.190
	40	84.96	-0.007	-8.17	1.075	0.254

As discussed in chapter 2 section 2.3.1, the separation factor, R_L, classifies the nature of adsorption isotherm to be unfavourable ($R_L > 1$), linear ($R_L = 1$), favourable ($0 < R_L < 1$) and irreversible ($R_L = 0$) (Almeida et al., 2009). While the value of the correlation coefficient (R^2) was also discussed in that chapter with reference to Jaynes and Boyd (1991) who proposed that the adsorption conforms to the Langmuir model of adsorption when its value is greater than 0.89. Therefore the low R^2 values, unfavourable R_L values and notable variances between the experimental ($W_{max,exp}$) and theoretical uptakes (W_{max}) shown in Table 4.1 and Figures 4.1, 4.3 and 4.4, indicated the unsuitability of the Langmuir model to describe the adsorption of 2-nitrophenol on the 1.95%Cuβ(25), 2.0%Cuβ(150) and 1.30%Cuβ(300) samples. However, based on the higher R^2 and favourable R_L values the adsorption of 2-nitrophenol on 0.2%Cuβ(75) was found to follow the Langmuir model of adsorption.

Modification of the Beta zeolite samples with copper in chapter 3 section 3.2.1 has resulted in the alteration of the homogeneous surface sites of the Beta zeolite samples (β(25), β(150), β(300)) which is the basic feature of the Langmuir adsorption model. The Langmuir isotherm is the most widely used two parameter equation (Soto et al., 2011) with its characteristic features, of uniform adsorption energies, equal solute affinity in all the adsorption sites, no interaction among adsorbed molecules, a single adsorption mechanism and the ultimate formation of a monolayer on the free surface. In practice however, several types of adsorption sites exist, and the mechanism is not the same for the first and for the last molecules adsorbed, and models based on monomolecular surface layer without interaction may not be realistic under some experimental conditions (Bretag et al., 2009b).

The Freundlich isotherm is an empirical equation suited for non-ideal systems with highly heterogeneous surfaces and a non-uniform distribution of heat of adsorption. It does not imply the formation of a monolayer, and frequently gives good interpretation of data over a restricted concentration range (Mall et al 2006 and Soto et al., 2011). The Freundlich model was also applied to the adsorption data, Table 4.2 shows the resulting correlations which were obtained by plotting the linearized form of equation 2.31 in chapter 2 section 2.3.1. As discussed in chapter 2 section 2.3.1 the Freundlich parameters listed, including n and K_F, assigned to the measurement of the adsorption strength of 2-nitrophenol and the binding affinity constant provide more substantial information on the adsorption mechanism.

Table 4.2: Freundlich constants for 2-nitrophenol adsorption onto the copper modified Beta zeolite samples, at the indicated temperatures.

Sample Name	Temperature (°C)	K_F ($dm^3 g^{-1}$)	n	R^2
1.95%Cuβ(25)	6	0.110	0.670	0.976
	24	0.018	0.535	0.874
	40	0.007	0.444	0.820
0.20%Cuβ(75)	6	2.708	1.028	0.850
	24	1.749	1.000	0.845
	40	3.894	1.482	0.938
2.00%Cuβ (150)	6	0.146	0.650	0.943
	24	0.006	0.347	0.912
	40	1.672	1.083	0.961
1.30%Cuβ(300)	6	0.043	0.612	0.979
	24	0.287	0.848	0.941
	40	0.777	0.946	0.943

Based on the R^2 values presented in Table 4.2 it is evident that the adsorption data for 1.95%Cuβ(25), 2.0%Cuβ(150) and 1.20%Cuβ(300) may be described by the Freundlich adsorption model. However this model is a slightly poorer fit to the adsorption data of 2-nitrophenol by 0.20%Cuβ(75) sample as indicated by the lower R^2 values in comparison to the Langmuir model. When the calculated n value for the adsorption of 2-nitrophenol is greater than 1 ($n > 1$) it indicates that the adsorption is good over the entire range of concentrations studies. However the value of n is less than 1 ($n < 1$) for the adsorption of 2-nitrophenol by the 1.95%Cuβ(25), 2.0%Cuβ(150) and 1.20%Cuβ(300) samples which indicates that the adsorption process is more favourable at higher concentrations but much poorer at low concentrations which is indicative of multilayer adsorption isotherms where an inflection point occurs at higher concentrations. The value of the binding affinity constant (K_F), indicates the capacity of the adsorbent with higher values indicative of greater adsorption capacities. The values of K_F are found to decrease with increasing temperature for 1.95%Cuβ(25) suggesting an exothermic adsorption process, however the K_F values were found to be independent of temperature for 0.20%Cuβ(75), 2.0%Cuβ(150) and 1.30%Cuβ(300) samples.

The Freundlich isotherm is widely applied in heterogeneous systems, especially in the removal of organic compounds from aqueous solution, a higher correlation, R^2 (relative to the Langmuir approach) has been observed in this study as is evident in Tables 4.1 and 4.2. In chapter 2 section 2.3.1, the adsorption of 2-nitrophenol from aqueous solutions onto unmodified Beta zeolite (β(25), β(75) and β(150)) samples was reported to follow a Langmuir model of adsorption due to the apparent homogeneous nature of the surface sites. In contrast to monolayer adsorption which is characteristic of the Langmuir model, the Freundlich isotherm does not predict any saturation of the adsorbent by the sorbate thus infinite surface coverage is predicted, indicating multilayer sorption of the surface (Zahir and Najwa 2006).

As reported by XRD analysis of the unmodified and copper modified Beta zeolite samples in chapter 3 section 3.3.1, the introduction of extra-framework cations by ion exchange did not alter the crystalline nature of the Beta zeolites. However, the presence of the CuO within the framework cannot be ruled out. The presence of copper species on the outer surface adsorption sites of the Beta zeolites has increased the heterogeneous nature of the Beta zeolite. This increase in surface heterogeneity of the Beta zeolite resulted in the change from the monolayer adsorption isotherm of the Langmuir model reported in chapter 2 section 2.3.1 to a multilayer adsorption isotherm of the Freundlich model.

Kuleyin (2007) reported the Freundlich isotherm to describe the adsorption characteristics of phenol and 4-chlorophenol by surfactant modified zeolite. While Damjanovic et al., investigated the adsorption of phenol from aqueous solutions by zeolites as solid adsorbents, they reported that adsorption from aqueous solutions is a complex phenomenon and in order to clarify the process of phenol adsorption they performed microcalorimetric experiments in order to assess the strength of phenol-adsorbent surface interaction (Damjanovic et al., 2010). The evolved heats measured upon adsorbate (phenol) adsorption from aqueous solutions, originated from the exothermic enthalpy of adsorption on the active sites and the endothermic enthalpy of the solvent displacement. In the case of HZSM-5(15), the profile for differential heats versus adsorbed amount of phenol decreased slightly at the beginning, it then presented a plateau like part, followed by an abrupt decrease, indicating that all the available sites for phenol adsorption had been covered. For the copper exchanged forms of HZSM-5(15), again decreasing differential heats were observed on increased adsorption, however, the heats of adsorption had higher values for the Cu-ZSM-5(15) over the whole range of coverage. The reported higher values of differential heats from the copper exchanged form of ZSM-5(15) indicated the existence of stronger active sites on the Cu-ZSM-5(15) sample. It was inferred from these microcalorimetric results that all investigated systems expressed energetic heterogeneity in the process of phenol adsorption with surface heterogeneity increasing with increasing differential heats of adsorption (Damjanovic et al., 2010). The results of Damjanovic et al., 2010 support the findings reported in this work in relation to adsorbent surface heterogeneity increasing after ion exchange with copper.

4.3.2 Evaluation of the Thermodynamics of Adsorption

2-nitrophenol adsorption isotherms obtained at 6ºC, 24ºC and 40ºC, are plotted in Figures 4.5 to 4.8 for the copper modified Beta zeolite. They correlate the amount of

2-nitrophenol adsorbed per unit weight of adsorbent, q_e, with the 2-nitrophenol equilibrium concentration, C_e.

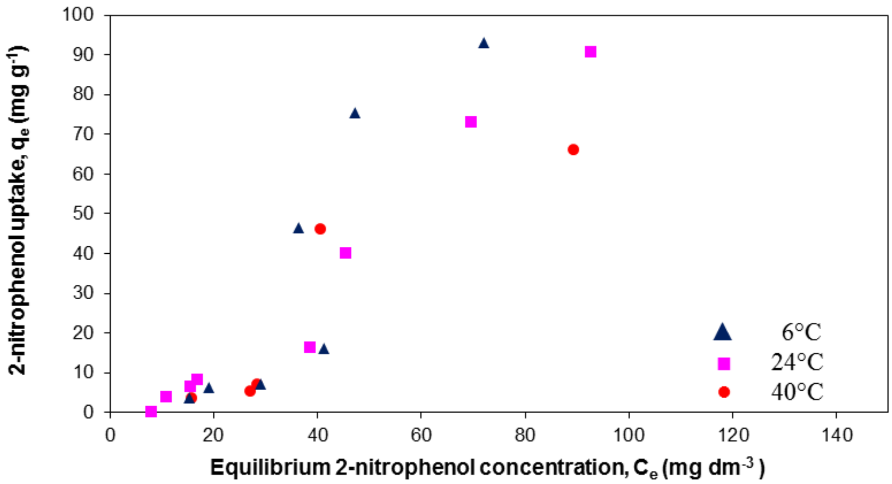

Figure 4.5: Thermodynamic plots displaying 2-nitrophenol adsorption onto 1.95 %Cuβ(25) at varying 2-nitrophenol concentrations after 1 hour. Initial 2-nitrophenol concentrations varied between 10ppm and 1000ppm, at the indicated temperatures.

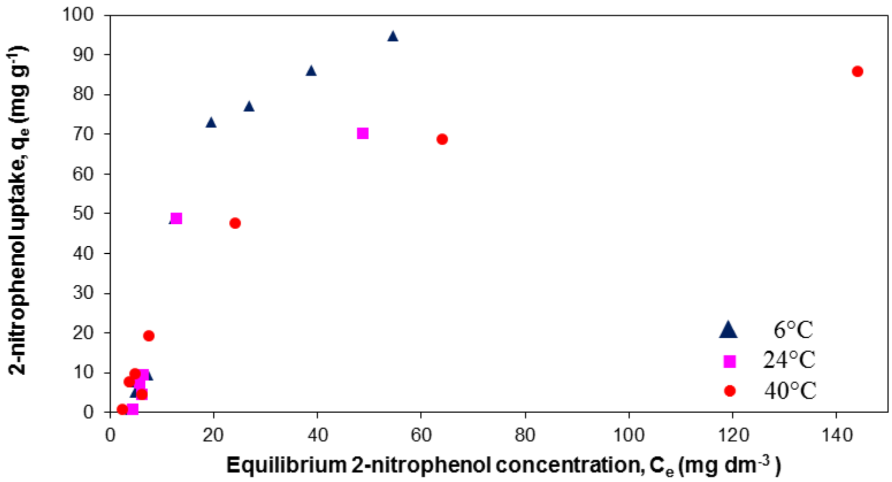

Figure 4.6: Thermodynamic plots displaying 2-nitrophenol adsorption onto 0.20%Cuβ(75) at varying 2-nitrophenol concentrations after 1 hour. Initial 2-nitrophenol concentrations varied between 10ppm and 1000ppm, at the indicated temperatures.

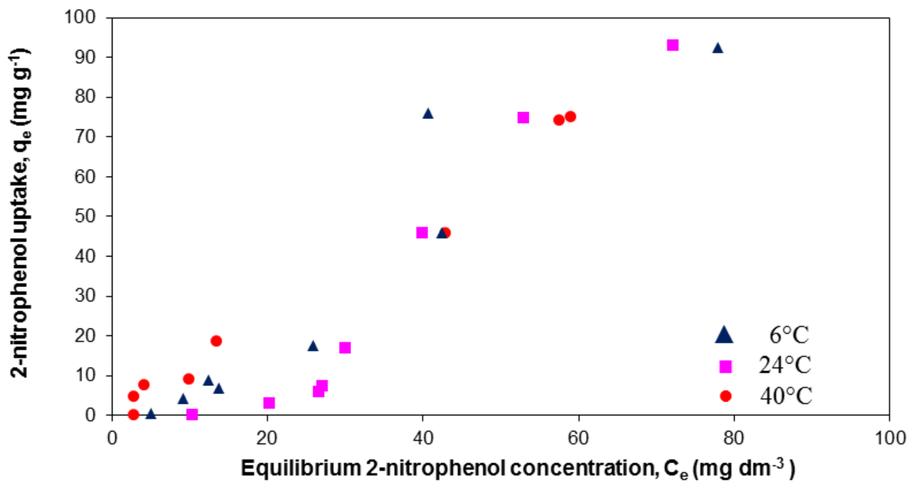

Figure 4.7: Thermodynamic plots displaying 2-nitrophenol adsorption onto 2.0%Cuβ(150) at varying 2-nitrophenol concentrations after 1 hour. Initial 2-nitrophenol concentrations varied between 10ppm and 1000ppm, at the indicated temperatures.

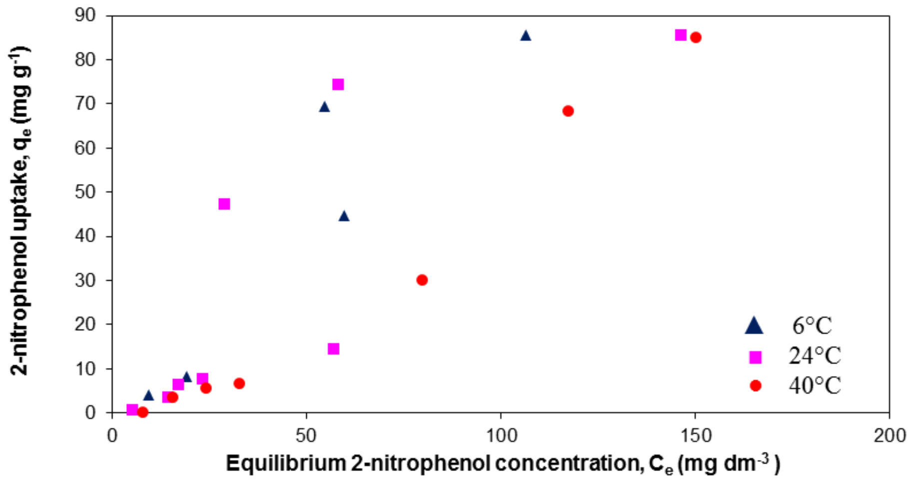

Figure 4.8: Thermodynamic plots displaying 2-nitrophenol adsorption on 1.30%Cuβ(300) at varying 2-nitrophenol concentrations after 1 hour. Initial 2-nitrophenol concentrations varied between 10ppm and 1000ppm, at the indicated temperatures.

The 2-nitrophenol adsorption on copper exchanged Beta zeolites 1.95%Cuβ(25) was found to be largely independent of the temperature of the adsorption solution at low equilibrium 2-nitrophenol concentrations however with increasing 2-nitrophenol equilibrium concentration the adsorption process becomes mildly exothermic in nature as shown in Figure 4.5. Other reports cited in literature report the exothermic nature of the adsorption of phenols onto copper exchanged ZSM-5(15) by microcalorimetric experiments (Damjanovic et al., 2010) and thermodynamic studies on phenol adsorption on zeolites (Yousef et al., 2011). The adsorption process for 0.2%Cuβ(75) was found to be mildly exothermic in nature over the applied temperature ranges of 6 – 40°C as shown in Figure 4.6. Similar to the 1.95%Cuβ(25) sample the adsorption of 2-nitrophenol on the 2.0%Cuβ(150) sample was found to be largely independent of the temperature of the adsorption solution at low equilibrium 2-nitrophenol concentrations however with increasing 2-nitrophenol equilibrium concentration the adsorption process becomes mildly exothermic in nature as shown in Figure 4.7, while the thermodynamic plots for 1.30%Cuβ(300) sample is observed to be independent of temperature as evident in Figure 4.8.

It is evident in figures 4.5, 4.7 & 4.8 that the introduction of framework copper cations into the Beta zeolites (β(25), β(150) and β(300)) has altered the shape of the adsorption isotherms that was reported in chapter 2 section 2.1 from a type I adsorption profile where the isotherm approaches a limiting value to a type V adsorption profile, which is characterised by a point of inflection at high relative concentrations so that the isotherm bends over and reaches a plateau in the multilayer region of the isotherm as defined by the Brunauer classification (Brunauer et al., 1940). The introduction of framework cation results in the continuous progression from monolayer to multilayer adsorption as the adsorbate concentration increases. The inflection point in the isotherm usually occurs near the completion of the first fully adsorbed monolayer, with increasing concentration second and higher layers are completed, until at saturation when the number of adsorbed layers becomes infinite. These multilayer adsorption isotherms support the findings previously stated in section 4.1 that the modification of Beta zeolite with copper altered the surface sites of Beta zeolite from the uniform Langmuir model of adsorption which was reported in chapter 2 section 2.3.1 to a more heterogeneous adsorption surface which is a characteristic of the Freundlich adsorption isotherm. While the introduction of extra-framework copper cations into the β(75) sample did not result in a significant change in its adsorption isotherm shape as illustrated in Figure 4.6, which supports the findings in section 4.1 where its adsorption data was found to follow that of a Langmuir adsorption model. In contrast to the Langmuir model of adsorption which is characteristic of monolayer adsorption, the Freundlich model does not predict any saturation of the adsorbent by the sorbate thus infinite surface coverage is predicted, indicating multilayer sorption of the surface (Zahir and Najwa 2006).

The thermodynamic parameters, Gibbs free energy, and enthalpy changes for 2-nitrophenol adsorption on 1.95%Cuβ(25), 0.20%Cuβ(75), 2.00%Cuβ(150) and 1.30%Cuβ(300) samples were calculated and are presented in Table 4.3. The Langmuir constant K_L can be related to the free energy ($\Delta G°_{ads}$) (Toppallar and Bayrak, 1999). The Gibbs free energy of adsorption was calculated using Equation 2.11 - 2.14. In this study the values of ln K_L were plotted against 1/T, where $\Delta H°$ and $\Delta S°$ values were calculated from the slope and the intercept of the plot. The obtained thermodynamic parameters are listed in Table 4.3.

Table 4.3: Thermodynamic parameters for 2-nitrophenol adsorption on the indicated copper modified Beta zeolite samples.

Sample Name	($\Delta G°$) (kJ mol $^{-1}$)			($\Delta H°$) (kJ mol $^{-1}$)	($\Delta S°$) (J mol $^{-1}$ K^{-1})
	6°C	24°C	40°C		
1.95%Cuβ(25)	-10.532	-11.810	-12.947	9.282	71.02
0.20%Cuβ(75)	5.696	7.834	9.735	-27.461	-118.84
2.00%Cuβ(150)	-10.332	-10.509	-10.667	-7.581	9.864
1.30%Cuβ(300)	-12.740	-12.663	-12.596	-13.920	-4.229

Negative values for enthalpy change ($\Delta H°$) suggest an adsorption process is exothermic and conversely positive values suggest an endothermic process. The $\Delta H°$ values are negative for 1.20%Cuβ(75), 2.0%Cuβ(150) and 1.30%Cuβ(300) samples demonstrating the exothermic nature of these adsorption processes. While the $\Delta H°$ value was found to be positive for 1.95%Cuβ(25), this suggests that the adsorption process is mildly endothermic. The adsorption process was found to be largely independent of temperature at low 2-nitrophenol concentration and mildly exothermic at higher 2-nitrophenol concentrations as shown in Figure 4.5 for the 1.95%Cuβ(25) sample, which resulted in the overall adsorption process being endothermic. The $\Delta H°$ values obtained for 1.95%Cuβ(25), 0.2%Cuβ(75), 2.0%Cuβ(150) and 1.30%Cuβ(300) respectively, indicate the physical nature of the adsorption process. The adsorption of 2-nitrophenol by copper modified Beta zeolite involves weak interaction forces such as van der Waals, with more than one layer of adsorption occurring as seen in Figures 4.5, 4.7 - 4.8 and with the fitting of the Freundlich isotherm to the adsorption data on copper modified β(25), β(250) and β(300) in section 4.3.1. Physical adsorption has been reported for model phenolic compounds on water-compatible hypercrosslinked polymeric resin (Li et al., 2002a and Li et al., 2002b). Exothermic adsorption was reported for pure phenolics onto activated carbons and polymeric resins (Pan et al., 2008 and Huang et al., 2009a) and for phenolics from industrial effluents onto fly ash (Ugurlu et al., 2005) and onto modified macroalgae (Aravindhan et al., 2009).

Negative values of ΔG° were calculated for Cu modified Beta zeolites β(25), β(150) and β(300) indicating the spontaneous nature of the adsorption process in the presence of copper species. The small magnitude of the ΔG° values suggest that the equilibrium position for the adsorption process favours the adsorption of 2-nitrophenol onto the copper modified Beta zeolites β(25), β(150) and β(300). Similar to the ΔG° values calculated for unmodified β(75) sample in table 2.4 in section 2.3.2 in chapter 2, the ΔG° values were found to be small and positive for the 0.20%Cuβ(75) sample. It is evident from Figure 4.6 that 2-nitrophenol is adsorbed onto 0.20%Cuβ(75), however positive ΔG° values imply that the equilibrium position for the adsorption of 2-nitrophenol onto 0.20%Cuβ(75) favours 2-nitrophenol in aqueous solution. The ΔG° values were found to become more positive with increasing temperatures for the 0.20%Cuβ(75) and the 1.30%Cuβ(300) samples indicating the adsorption process is favoured at lower temperatures sample which is predicted by the negative ΔH° and ΔS° values.

The ΔG° values were found to become more negative with increasing temperatures for the 1.95%Cuβ(25) and the 2.0%Cuβ(150) samples indicating the adsorption process becomes marginally more spontaneous at higher temperatures. The introduction of framework cations into the Beta zeolite structure has increased the spontaneous nature of the adsorption process, which suggests that the presence of copper species alters the nature of the adsorption process as can be seen by the change in the shape of the adsorption isotherms presented in Figures 4.5, 4.7 and 4.8. The negative $\Delta G°$ values and the fitting of the Freundlich adsorption isotherm to the data support the theory that the adsorption of 2-nitrophenol on copper modified Beta zeolites involves a multilayer coverage on the outer surface of the copper modified Beta zeolite samples (β(25), β(150) and β(300)). Positive $\Delta S°$ values were obtained for 1.95%Cuβ(25) and 2.0%Cuβ(150), while negative values were obtained for 0.20%Cuβ(75) and 1.30%Cuβ(300). In the case of 1.95%Cuβ(25) the adsorption process was found to be endothermic and the adsorption of 2-nitrophenol on the surface sites of the 1.95%Cuβ(25) resulted in an overall increase in entropy of the adsorption process. As for 2.0%Cuβ(150), 0.20%Cuβ(75) and 1.30%Cuβ(300) samples the adsorption process was found to be exothermic but the entropy was found to be positive for the 2.0%Cuβ(150) sample while negative for the 0.20%Cuβ(75) and 1.30%Cuβ(300) samples. In the case of the 2.0%Cuβ(150) sample the adsorption process is physical and exothermic in nature, therefore the adsorption process involves weak interactions at the copper modified Beta zeolite surface, the associated positive entropy value suggests that the increase in entropy of the surrounding is sufficient to compensate for the decrease in entropy at the adsorption surface sites so that the overall entropy of the adsorption process is positive. As for the 0.20%Cuβ(75) and 1.30%Cuβ(300) samples, similar to the 2.0%Cuβ(150) sample the adsorption process were found to be exothermic and physical in nature, with negative entropy values of adsorption of -118.84 J mol^{-1} $K^{-1}$and -4.229 J mol^{-1} K^{-1}respectively. The negative enthalpy values suggest that there is an increase in the entropy of the adsorbing solution however the overall decrease in the entropy of the adsorption process suggests that the increase in entropy of the adsorbing solution is not sufficient to compensate for the decrease in entropy at the adsorption surface sites and therefore the entropy for the overall adsorption process is negative. Positive entropy change values suggest the affinity of the copper modified Beta zeolites for 2-nitrophenol and that organization of the adsorbate at the solid/solution interface becomes more random which has previously been reported by other authors in the study of adsorption of organics by zeolites (Alver and Metin 2012 and Yousef et al., 2011).

The small magnitude of the calculated thermodynamic parameters involved ($\Delta G°$, $\Delta H°$, $\Delta S°$) and the experimental thermodynamic data which is based on three temperatures (6°C, 24°C and 40°C) shown in Figures 4.5 – 4.8 suggests that the adsorption of 2-nitrophenol involves weak physical surface interactions on the copper modified Beta zeolite samples.

4.3.3 Kinetics of Adsorption

The adsorption of 2-nitrophenol onto copper modified Beta zeolite at various initial 2-nitrophenol concentrations was studied as a function of contact time in order to determine the necessary equilibrium time. The effect of contact time on the removal of 2-nitrophenol at 24°C is presented in Figure 4.9 (A & B) for 1.95%Cuβ(25) and 1.30%Cuβ(300) respectively. All the adsorption isotherms were studied at a contact time of 1 hour to ensure equilibrium has been reached.

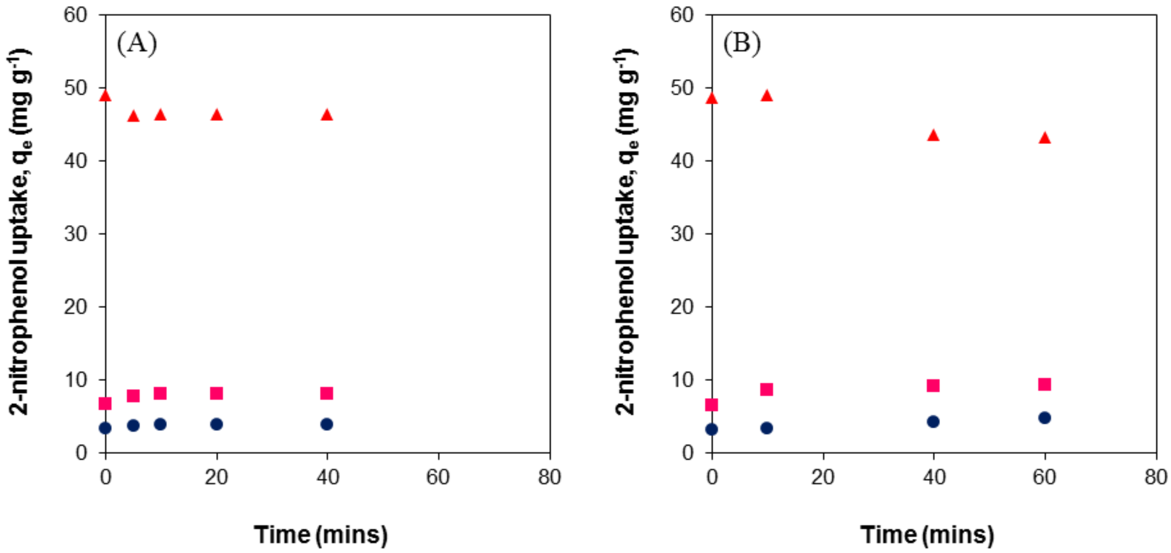

Figure 4.9: Kinetic plots displaying 2-nitrophenol adsorption on (A) 1.95%Cuβ(25) and (B) 1.30%Cuβ(300) samples at 24ºC as a function of time and initial 2-nitrophenol concentration ; ● 50 mg dm^{-3}; ■100 mg dm^{-3}; ▲500 mg dm^{-3}.

The amount of 2-nitrophenol adsorbed at the equilibrium time reflected the maximum adsorption uptake capacity of the adsorbent under the operating conditions applied. The plots show that the adsorption attains equilibrium rapidly for all initial concentrations of 2-nitrophenol. Initially there are a large number of vacant sites available for adsorption. The adsorption rate was fast thus rapidly increases the amount of adsorbate accumulated on the copper modified zeolite surface mainly within 5 minutes of adsorption. It was reported by Soto et al., 2011 that the remaining vacant surface sites are difficult to occupy due to repulsion among 2-nitrophenol molecules (on the surface and in the bulk phase). This leads to a decrease of the adsorption rate as illustrated by plateau lines in Figures 4.9 (A & B) after 5 minutes of adsorption and this confirms that the adsorption of 2-nitrophenol from aqueous solution onto 1.95%Cuβ(25) and 1.30%Cuβ(300) has reached a steady-state condition.

The kinetics of adsorption describes the rate of adsorbate uptake on adsorbent and it controls the equilibrium time. The kinetic parameters are helpful for the prediction of adsorption rate, which gives important information for designing and modelling the process. A number of kinetic models have been proposed to assess the adsorption of aromatic solutes (Soto et al., 2011). It has been reported that the adsorbate transport occurs in a series of consecutive steps: transport of the adsorbate from the bulk solution to the boundary layer surrounding the adsorbent particles, transport of the solute across the boundary layer, intraparticle solute diffusion into the pores and adsorption and desorption of adsorbate. The overall process may be controlled by one of the above or a combination of them. The characteristics of the adsorbent, adsorbate and solution are influential on the rate limiting step (Soto et al., 2011). The most popular models used to establish the controlling adsorption mechanism are those assuming that the controlling step is mass transfer and those assuming that adsorption is governed by surface phenomena (Soto et al., 2011).

In this study, the kinetics of the adsorption data was analysed using two different kinetic models, the pseudo-first-order and the pseudo-second-order models which are extensively used in kinetics studies (Yousef et al., 2011). The pseudo-first-order model considers reversible equilibrium of organic molecules between a liquid and a solid phase. The pseudo-first-order model assumes that adsorption occurs due to a concentration difference between the adsorbate surface and solution (Gregorio and Pierre-Maire 2008). The pseudo-first-order rate constant, k_1, the calculated equilibrium sorption capacity, $q_{e,cal}$ the experimental equilibrium sorption capacity, $q_{e\ exp}$, the correlation co-efficient, R^2 and the co-efficient of Chi-squared, χ^2 at 24ºC are tabulated in Tables 4.5 - 4.6.

However the adsorption data showed a poor correlation with the pseudo-first-order kinetic expression with low R^2 values and notable variances between the experimental uptakes ($q_{e\ exp}$) and the theoretical uptakes ($q_{e\ cal}$)shown in tables 4.5 - 4.6 and by the large values obtained from the chi squared test (χ^2) reveal the poor fitting of the pseudo-first-order model. Thus the adsorption of 2-nitrophenol onto 1.95%Cuβ(25) and 1.30%Cuβ(300) samples is not a pseudo-first-order process.

Table 4.5: Effect of initial 2-nitrophenol concentration on sorption data on 1.95%Cuβ (25) using pseudo-first-order approach.

C_0 (mg dm^{-3})	$q_{e,\ exp}$ (mg g^{-1})	$q_{e,\ cal}$ (mg g^{-1})	k_1 (min^{-1})	R^2	χ^2
50	3.88	1.0073	5.51	0.613	8.192
100	7.98	1.008	6.63	0.425	48.223
500	46.38	0.987	-6.534	0.220	2087.66

Table 4.6: Effect of initial 2-nitrophenol concentration on sorption data on 1.30%Cuβ (300) using pseudo-first-order approach.

C_0 (mg dm^{-3})	$q_{e,\ exp}$ (mg g^{-1})	$q_{e,\ cal}$ (mg g^{-1})	k_1 (min^{-1})	R^2	χ^2
50	4.216	0.996	3.576	0.064	10.410
100	13.75	0.975	3.085	0.198	166.86
500	43.45	1.075	1.946	0.334	1670.36

Since the data do not appear to fit the pseudo-first-order kinetics a pseudo-second-order reaction model as developed by Ho et al., (Ho et al., 2000), was applied to the overall rate of this adsorption process which assumes that the sorption capacity is proportional to the number of active sites occupied on the adsorbent. The pseudo-second-order kinetic model also assumes that adsorption is a pseudo-chemical reaction and that adsorption reaction on the surface of adsorbent is the rate controlling step (Yu 2008). The values of t/q_t are plotted against t for 1.95%Cuβ(25) and 1.30%Cuβ(300) samples and are shown in Figure 4.10 (A & B).

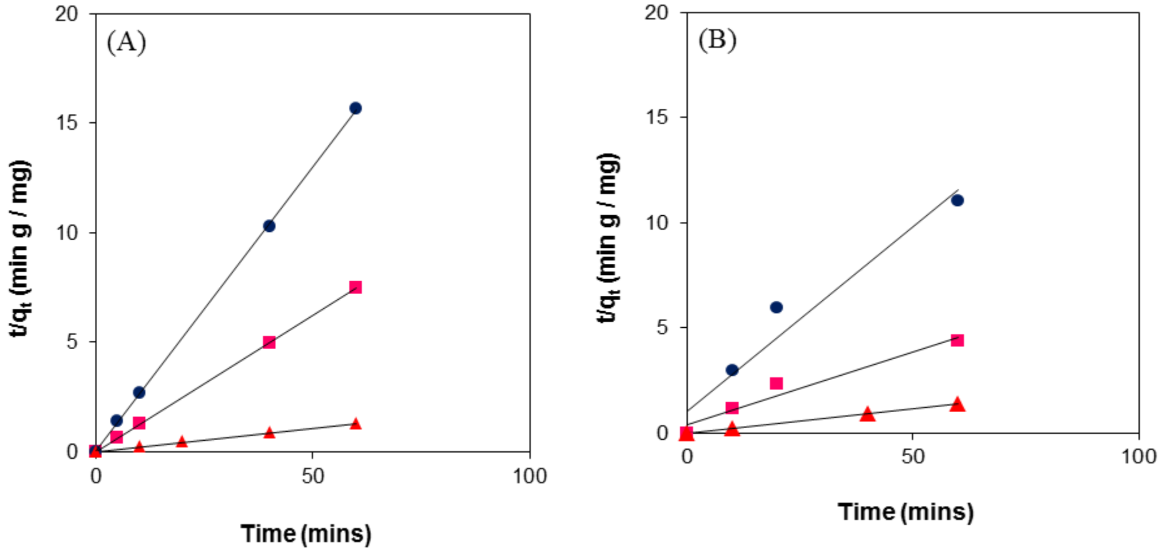

Figure 4.10: Pseudo-second-order sorption kinetics of 2-nitrophenol on (A) 1.95%β(25) and (B) 1.30%β(300) at 2-nitrophenol concentrations of ; (● 50 mg dm^{-3}; ■ 100 mg dm^{-3}; ▲ 500 mg dm^{-3}).

The pseudo-second-order rate constant, k_2, the equilibrium sorption capacity, $q_{e\ cal}$, the experimental equilibrium sorption capacity $q_{e\ exp}$, (obtained from Figures 2.11 (A - D)), the percentage 2-nitrophenol removal, R_e, the correlation co-efficient, R^2 and the co-efficient of Chi-squared, χ^2, with respect of initial 2-nitrophenol concentrations, C_0, at 24°C are tabulated in Tables 4.7 – 4.8 for the 1.95%Cuβ(25) and 1.30%Cuβ(300) samples respectively.

Table 4.7: Effect of initial 2-nitrophenol concentration on sorption data on 1.95%βCu(25) using pseudo-second-order approach.

C_0 (mg dm^{-3})	$q_{e\ exp}$ (mg g^{-1})	$q_{e\ cal}$ (mg g^{-1})	Re (%)	k_2 (g mg^{-1}min^{-1})	h (mg g^{-1} min^{-1})	(R^2)	χ^2
50	3.88	3.856	67.0	1.842	27.397	0.99	0.0001
100	7.98	8.019	80.3	1.943	125	1	0.0001
500	46.38	46.511	92.3	0.942	2000	1	0.0003

Table 4.8: Effect of initial 2-nitrophenol concentration on sorption data on 1.30%Cuβ (300) using pseudo-second-order approach.

C_0 (mg dm^{-3})	$q_{e\,exp}$ (mg g^{-1})	$q_{e\,cal}$ (mg g^{-1})	Re (%)	k_2 (g $mg^{-1}min^{-1}$)	h (mg g^{-1} min^{-1})	(R^2)	χ^2
50	4.216	5.72	84.33	0.0287	0.940	0.950	0.395
100	13.75	14.49	93.40	0.0117	2.461	0.953	0.037
500	43.45	44.05	97.30	0.0109	21.276	0.967	0.0081

The value of the pseudo-second-order adsorption rate constant decreases while the initial sorption rate (h) increases as the initial 2-nitrophenol concentration increases from 50 – 500 mg dm^{-3}. This suggests that the mass transfer rate improves with increasing initial concentration however the fitting of the pseudo-second order reaction model to the kinetic data suggests that the adsorption of 2-nitrophenol was dependent on the availability of adsorption sites in addition to the adsorbate concentration in solution therefore as time elapses most of the adsorption sites have been occupied, thus limited free surface sites are available therefore the adsorption of additional 2-nitrophenol molecules may occur with the formation of multilayers, therefore the rate of adsorption decreases (k_2). The adsorption capacity ($q_{e\ cal}$) increases with the increase in initial concentration. This can be explained as follows: the increase in initial concentration of 2-nitrophenol has led to a reduction in resistance of 2-nitrophenol mass transfer from solution bulk onto the adsorbent, hence a greater amount of 2-nitrophenol molecules being adsorbed onto the copper modified Beta zeolite surface, once the surface adsorption sites become saturated, additional 2-nitrophenol molecules are adsorbed as the adsorption is not restricted to the formation of monolayer at the sorbent surface.

The correlation coefficients for the linear plots of t/q_t are plotted against t for the pseudo-second order model, are 0.999 for all copper modified samples as shown in

Table 4.7 - 4.8 and reflect the suitability of the pseudo-second- order model to the adsorption of 2-nitrophenol. However as indicated by the magnitude of the ΔH° values for the adsorption process in Table 4.3 section 4.3.4 the reaction is of a physical nature and the kinetics of the adsorption of 2-nitrophenol is better described as being dependent on the availability of adsorption surface sites and weak physical interaction such as Van der Waals forces and electrostatic interactions rather than chemisorption processes. The introduction of framework cations into the Beta zeolite structure in chapter 3 section 3.2.1 did not alter the type of kinetics of the adsorption process as a pseudo-second-order model was also reported for the adsorption process on unmodified Beta zeolite samples in chapter 2 section 2.3.3 Tables 2.9 – 2.12.

Figures 4.11 (A - B) shows the relationship between the equilibrium 2-nitrophenol uptake (q_e) and the % removal 2-nitrophenol removal with the initial 2-nitrophenol concentration. As the 2-nitrophenol concentration is increased from
50 – 500 mg dm^{-3}, the equilibrium 2-nitrophenol uptake $q_{e\ cal,}$ increases from ~ 4 to 47 mg g^{-1}, while the % 2-nitrophenol removal increases from 67 to 92% and 84 to 97% for 1.95%Cuβ(25) and 1.30%Cuβ(300) respectively. The increase in the % 2-nitrophenol removal as the initial 2-nitrophenol concentration increases supports the finding from fitting the Freundlich adsorption model to the data where the value of n suggested that the adsorption is good at high concentrations but is much poorer at lower concentrations for 1.95%Cuβ(25), 2.0%Cuβ(150) and 1.30%Cuβ(300) as shown in Table 4.2.

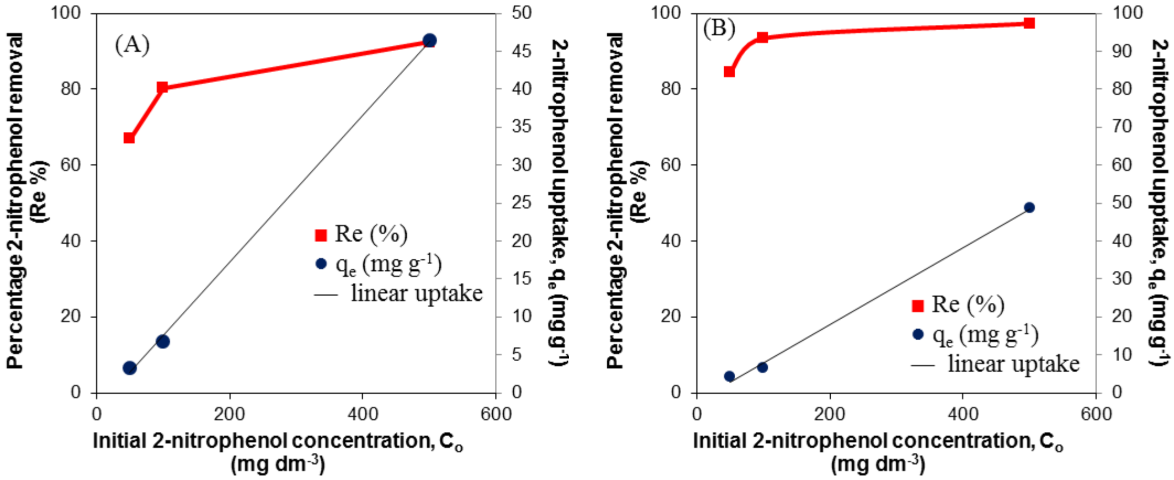

Figure 4.11 (A - B): Variation in the 2-nitrophenol uptake (q_e) and the percentage 2-nitrophenol removal (Re%) in relation to the initial 2-nitrophenol concentration C_0; (A) 1.95%Cuβ(25) and (B) 1.30%Cuβ(300).

Sorption processes onto porous particles include mass transport phenomena like: solute transfer from the solution to the boundary film surrounding the particles (bulk diffusion), diffusion from the film to the surface of the sorbent (boundary layer or film diffusion) and diffusion from the surface to the internal sites (pore or intra-particle) diffusion (Guibal et al., 1998). As bulk diffusion is always neglected for the stirred systems, the significance of film and intra-particle diffusion was examined for investigated sorption processes (Ivanovic et al., 2013).

The intraparticle diffusion model proposed by Weber and Morris (Weber and Morris, 1963) described in chapter 2 section 2.15 equation 2.44 was applied to the kinetic data of 2-nitrophenol adsorption on copper modified Beta zeolite samples in order to assess if the adsorption reaction was controlled by intraparticle diffusion, where k_{id} (mg/g $h^{0.5}$) is the intraparticle diffusion constant and C_i is associated with the boundary layer thickness (i.e., the larger the intercept the greater is the boundary layer effect) (Mall et al., 2006). The values of q_t are plotted against $t^{0.5}$ for 1.95%Cuβ(25) and 1.30%Cuβ(300) samples are shown in Figures 4.12 (A & B). If intraparticle diffusion is rate limiting, then q_t versus $t^{0.5}$ will be linear and if the plot passes through the origin then the rate limiting process is only due to the intraparticle diffusion. Otherwise some other mechanism along with intraparticle diffusion is also involved (Yousef et al., 2011).

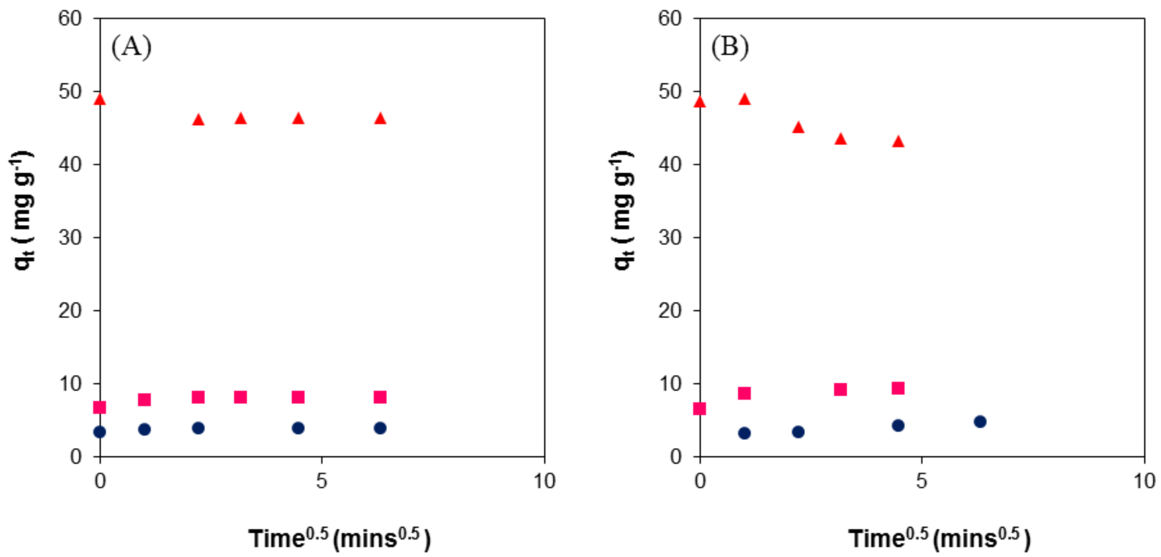

Figure 4.12: Intraparticle diffusion plots for the adsorption of 2-nitrophenol onto (A) 1.95%Cuβ(25) and (B) 1.30%Cuβ(300). At initial 2-nitrophenol concentrations; ● 50 mg dm^{-3}, ■ 100 mg dm^{-3}, and ▲500 mg dm^{-3}.

The curve-fitting plots of the intraparticle diffusion model of adsorption of 2-nitrophenol onto the copper modified Beta zeolite samples at 24°C, are demonstrated in Figures 4.12 (A & B). The plots were not linear over the whole time range. The values of k_{id} and C_i obtained from the plot at 24°C in Table 4.9 - 4.10 indicated that the intraparticle diffusion model is not applicable. Since the plots of q_t versus $t^{0.5}$ (Figures 4.12 (A & B)) do not pass through the origin and based on the poor coefficients (R^2 values) of the plots (Table 4.9 – 4.10) the intraparticle diffusion model was found not to be the sole rate determining step in the adsorption mechanism.

Table 4.9: Effect of initial 2-nitrophenol concentration on sorption data on 1.95%Cuβ(25) using the intra-particle diffusion model.

C_0 (mg dm^{-3})	(R^2)	K_{di} (mg/g h$^{0.5}$)	Ci
50	0.308	1.177	2.237
100	0.306	2.461	4.668
500	0.265	14.116	28.178

Table 4.10: Effect of initial 2-nitrophenol concentration on sorption data on 1.30%Cuβ(300) zeolite using the intra-particle diffusion model.

C_0 (mg dm^{-3})	(R^2)	K_{di} (mg/g h$^{0.5}$)	Ci
50	0.637	1.904	1.578
100	0.514	3.669	3.814
500	0.232	13.096	26.515

It may be seen in Figures 4.12 (A & B) that initially there is a rapid uptake of 2-nitrophenol over all applied concentration ranges by copper modified Beta zeolite samples within a $t^{0.5}$ value of 0.2 hr. This can be attributed to the instantaneous utilisation of the most readily available adsorbing sites on the surface of the copper modified Beta zeolite samples. Rapid uptake has also been reported previously as macropore diffusion, which occurred during the adsorption of orange-G and methyl violet dyes onto bagasse fly ash (Mall et al., 2006) however the initial rapid uptake of 2-nitrophenol is due to the availability of free adsorption surface sites on the copper modified Beta zeolite. The initial rapid uptake of 2-nitrophenol leads rapidly to an equilibrium phase where a low slope corresponded to a slower adsorption process during which period the intraparticle diffusion started to slow down due to the decrease in availability of adsorption sites demonstrated in Figures 4.12 (A & B). The reported deviation of the plots of q_t versus $t^{0.5}$ from the origin may be due to the difference in rate of mass transfer in the initial and final stages of adsorption (Mall et al., 2006). These findings correspond to the fitting of the pseudo-second-order kinetic model to the adsorption data as the adsorption rate was found to be controlled by the availability of outer adsorbent surface in addition to the adsorbate solution concentration.

These results on the mechanism and kinetics of 2-nitrophenol adsorption onto copper modified Beta zeolite samples correlate with the results reported in chapter 2 section 2.3.3 on the adsorption of 2-nitrophenol on the unmodified Beta zeolite (β(25), β(75), β(150), β(300)) with the introduction of copper into the Beta zeolite framework having no overall effect on the intraparticle diffusion of 2-nitrophenol with surface adsorption dominating. These findings suggest that the modification of the Beta zeolites (β(25), β(75), β(150), β(300)) with a catalytic component copper by ion exchange procedure outlined in chapter 3 section 3.2.1 does not alter the type of kinetics of the adsorption process.

Table 4.11 shows the pseudo-second-order rate constants k_2 for the β(25) and β(300) samples before and after modification. It is evident that the rate constants all decrease as the initial 2-nitrophenol concentration increases however when the initial 2-nitrophenol concentration is held constant the pseudo-second-order rate constant k_2 is found to decrease after modification with copper. This decrease in the pseudo-second-order rate constant after modification with copper maybe related to the change in the adsorption surface sites of the Beta zeolite.

Table 4.11: Effect of modification of the Beta zeolite with a catalytic component (copper) on the pseudo - second order rate constant k_2 (g mg^{-1}h^{-1}) at varying initial 2-nitrophenol concentrations (C_0, (mg dm^{-3})).

C_0 (mg dm^{-3})	k_2 (g mg^{-1}min^{-1})			
	β(25)	1.95%Cuβ(25)	β(300)	1.30%Cuβ(300)
50	5.600	1.842	0.151	0.0287
100	3.282	1.943	5.053	0.0117
500	0.138	0.942	0.018	0.0109

In chapter 2 section 2.3.1 the adsorption of 2-nitrophenol from aqueous solutions onto unmodified Beta zeolite (β(25), β(75), β(150) and β(300)) samples did not conform to the Freudlich adsorption model due to the homogeneous nature of the surface sites. In contrast to monolayer adsorption which is characteristic of the Langmuir model, the Freundlich isotherm does not predict any saturation of the adsorbent by the sorbate thus infinite surface coverage is predicted, indicating multilayer sorption of the surface. The modification of Beta zeolite (β(25), β(150) and β(300))) with copper has altered the surface sites of Beta zeolite from the uniform Langmuir type of adsorption isotherm model to a more heterogeneous adsorption surface which is a characteristic of a Freundlich adsorption isotherm. As the adsorption rate was found to be controlled by the availability of adsorbent surface sites and the adsorbate solution concentration, the change in the adsorption mechanism from monolayer to multilayer adsorption has resulted in a decrease in the pseudo-second-order rate constant k_2.

These results on the mechanism and kinetics of 2-nitrophenol adsorption onto copper modified Beta zeolites are also comparable with other studies previously published by Yousef et al., 2011 on the adsorption of phenol from aqueous solutions onto Jordanian zeolitic tuff. They reported the phenol adsorption process to follow a pseudo-second-order reaction model, while the rate limiting step was reported not to be intraparticle diffusion (Yousef et al., 2011). While Tsai et al., reported a similar finding on the adsorption of the organic compounds methylene blue and bisphenol A onto synthesized zeolites whereby the adsorption kinetics of the cationic dye onto the zeolite adsorbent was well described by pseudo-second-order reaction model as compared to the intra particle model (Tsai et al., 2009).

From literature it is known that external mass transport of sorbate is usually the rate-limiting step in systems which have poor mixing, low concentration of adsorbate, small particle size and high affinity of adsorbate for adsorbent. On the contrary, the intra-particle step controls the overall transfer for those systems that have high concentration of adsorbate, good mixing, large particle size of adsorbent and low affinity of adsorbate for adsorbent (Kumar and Kumaran 2005).

An adsorption reaction is said to be intra-particle diffusion controlled if the reaction sites are internally located in the porous adsorbents and the external resistance to diffusive transport process is much less than the internal resistance (Tsai et al., 2009) however in this study the adsorption sites were found to be on the external surface of the copper modified Beta zeolite. In order to investigate the contribution of film resistance to the kinetics of 2-nitrophenol adsorption, the Boyds film-diffussion model was employed (Boyd et al., 1947). This model has the assumption that the boundary layer surrounding the adsorbent particle is the main resistance to diffusion. According to this model, the plot of Bt against time should be linear and pass through the origin if the intra-particle diffusion controls the rate of mass transfer. If the plot is nonlinear or linear but does not pass through the origin, then it can be concluded that the adsorption rate is controlled by film-diffusion or chemical reaction. Due to the rapid attainment of equilibrium Boyds film diffusion model was found to have minimal influence on the overall adsorption process.

As the adsorption of 2-nitrophenol onto copper modified Beta zeolite did not follow the pseudo-first-order reaction model and it was not controlled by the intraparticle or the film diffusion models, suggests that the rate limiting step is the availability of adsorption sites on the copper modified Beta zeolite surface as predicted by the fitting of kinetic data to the pseudo-second-order kinetic model.

4.4. Conclusion

The introduction of extra-framework copper cations into the Beta zeolite samples enhanced the adsorption capacity of 2-nitrophenol over the applied concentration range. The adsorption of 2-nitrophenol was also found to increase with increasing copper loadings on all the Beta zeolite samples. In this study two adsorption isotherms namely the Langmuir and the Freundlich were applied to the equilibrium data of the adsorption of 2-nitrophenol onto copper modified Beta zeolite. In chapter 2 section 2.3.1 the Langmuir model which assumes the formation of a monolayer on a homogenous surface was reported to describe the equilibrium adsorption of 2-nitrophenol from aqueous solution by the unmodified Beta zeolites (β(25), β(75) and β(150).

In this study however after the introduction of extra-framework cations the Langmuir isotherm model provided a poor fit to the equilibrium adsorption data with low correlation coefficients and noticeable variations between experimental and theoretical 2-nitrophenol uptakes reported for copper modified β(25), β(150) and β(300) samples. However the Langmuir model was still found to be an appropriate fit for the adsorption data on β(75) after the introduction of extra-frame work cations.

The Freundlich isotherm was also applied to the equilibrium adsorption data. The Freundlich model yielded the better fit to the adsorption data based on the observed correlation coefficients for copper modified β(25), β(150) and β(300) samples. By contrast to the Langmuir, the Freundlich isotherm can be applied to non-ideal adsorption on heterogeneous surfaces. The suitability of the Freundlich model to the adsorption data after the introduction of extra-framework cations suggests that the presence of copper species on the Beta zeolite alters the surface adsorption sites of the Beta zeolite leading to heterogeneous surface sites. Therefore the presence of copper species was found to alter the adsorption isotherm profiles from a type I profile characteristic of monolayer adsorption to type V profile which is characteristic of multilayer adsorption isotherms for the β(25), β(150) and β(300) samples, while the change in shape of the adsorption isotherm for β(75) was not as pronounced in comparison to the other Beta zeolite samples.

The adsorption of 2-nitrophenol onto copper modified Beta zeolite at various initial 2-nitrophenol concentrations was studied as a function of contact time in order to determine the necessary equilibrium time. The kinetic plots showed that the adsorption attains equilibrium rapidly over the applied concentration range for all copper modified Beta zeolites. In this study, the kinetics of the adsorption data were further analysed using two different kinetic models, the pseudo-first-order and the pseudo-second-order models. Low R^2 values and notable variances between the experimental and the theoretical 2-nitrophenol uptakes levels revealed the poor fitting of the pseudo-first-order model to the kinetic data while higher correlation coefficients for the linear plots for the pseudo-second order model suggested that the adsorption of 2-nitrophenol from aqueous solution by copper modified Beta zeolite follows a pseudo-second order kinetics. The suitability of the pseudo-second-order model to the adsorption data suggests that the rate of adsorption of 2-nitrophenol from aqueous solutions was dependent on the availability of adsorption surface sites and on the adsorbate concentration in solution. The introduction of framework cations into the Beta zeolite structure did not seem to alter the overall adsorption rate with the pseudo-second-order kinetics model being reported to describe the adsorption rate of 2-nitrophenol in chapter 2 section 2.3 prior to modification of the parent Beta zeolite.

In order to investigate the mechanism of adsorption, the intraparticle diffusion model was applied to the adsorption of 2-nitrophenol onto copper modified Beta zeolite samples. Initially there is a rapid uptake of 2-nitrophenol over all applied concentration ranges by all copper modified Beta zeolite samples. This can be attributed to the instantaneous utilisation of the most readily available adsorbing sites on the surface of the copper modified Beta zeolite samples. After the initial rapid uptake of 2-nitrophenol the uptake rate decreases as demonstrated by the plateau of intraparticle diffusion plots. Since the plots of q_t versus $t^{0.5}$ do not pass through the origin and based on the poor coefficients of the plots the intraparticle diffusion model was found not to be the sole rate determining step in the adsorption of 2-nitrophenol by copper modified Beta zeolites. Similar results were obtained in chapter 2 section 2.3.3 in respect of the boundary layer thickness of the interface between adsorbate and adsorbent with similar values being reported for unmodified and copper modified Beta zeolites. These results on the mechanism and kinetics of 2-nitrophenol adsorption onto copper modified Beta zeolite samples correlate with the results reported in chapter 2 sections 2.3.1 and 2.3.3 on the adsorption of 2-nitrophenol on unmodified Beta zeolite (β(25), β(75), β(150), β(300)) samples, which suggest that the rate and mechanism of 2-nitrophenol was independent of the presence of extra-framework cations in the Beta zeolite.

The thermodynamic parameters that were investigated in order to determine the adsorption process were the changes in standard enthalpy (ΔH°), standard entropy (ΔS°) and free energy (ΔG°). The negative ΔH° values for 0.2%Cuβ(75), 2.0%Cuβ(150) and 1.30%Cuβ(300) samples demonstrate the mildly exothermic nature of the adsorption process. Based on the magnitude of the calculated ΔH° values the adsorption process was found to be physical in nature with weak interactions such as electrostatic interactions and Van der Waals forces giving rise to the adsorption of 2-nitrophenol on the outer surface of the copper modified Beta zeolite samples. The thermodynamic study showed that the adsorption of 2-nitrophenol onto the copper modified Beta zeolite samples was influenced by the presence of extra-framework copper cations as it increased the spontaneous nature of the overall adsorption process from what was previously reported in chapter 2 section 2.3.2.

The findings of this work suggest that the modification of Beta zeolite with the catalytic component has not negatively affected the 2-nitrophenol adsorption capacities of the Beta zeolites (β(25), β(75), β(150) and β(300) under the employed conditions but was found to enhance the overall adsorption process.

Step two of this work involves the study of the catalytic oxidation of the adsorbed pollutant (2-nitrophenol) on the Beta zeolite samples. The catalytic oxidation of adsorbed 2-nitrophenol is carried out in a temperature programmed oxidation rig. The composition of the gas stream leaving the reactor is monitored using a Mass Spectrometer (M.S.). This work will investigate the influence of copper on the oxidation of adsorbed 2-nitrophenol on the Beta zeolite samples. The overall aim would be to produce carbon dioxide, water and nitrogen whilst minimising the formation of carbon monoxide and nitrous oxide. Finally this study seeks to propose a potential breakdown pathway for 2-nitrophenol during the temperature programmed oxidation process by monitoring the composition of the exit stream leaving the reactor.

4.5. References

Almeida, C. A. P., Debacher, N. A., Downs, A. J., Cottet, L. and C. A. D. Mello (2009) ' Removal of methylene blue from coloured effluents by adsorption on montmorillonite clay', *Journal of Colloid and Interface Science*, **332**, 46-53.

Anirudhan, T. S. and M. Ramachandran (2006) 'Adsorptive removal of tannin from aqueous solutions by cationic surfactant-modified bentonite clay', *Journal of Colloid Interface Science*, **299**, 116-124.

Anirudhan, R., Rao, J. R., and B. U. Nair (2009) 'Application of chemically modified green macro alga as a biosorbent for phenol removal', *Journal of Environmental Management*, **90**, 1877-1883.

Boyd, G. E., Adamson, A. W. and L. S. Jr. Myers (1947) 'The exchange adsorption of ions from aqueous solutions by organic zeolites. II. Kinetics', *Journal of the American Chemical Society*, **69**, 2836-2848.

Bretag, J., Kammerer, D. J., Jensen, U. and R. Carle (2009b) 'Evaluation of the adsorption behaviour of flavonoids and phenolic acids onto a food grade resin using a D-optimal design', *European Food Research and Technology*, **228**, 985-999.

Brunauer, S., Demming, L .S., Demming, W. E. and E. Teller (1940) 'On a theory of the Van der Waals adsorption of gas', *Journal of American Chemical Society*, **62**, 172-1732.

Damjanovic, L., Rakic, V., Rac, V., Stosic, D., and A. Auroux (2010) 'The investigation of phenol removal from aqueous solutions by zeolites as solid adsorbents', *Journal of Hazardous Material*s, **184**, 477-484.

Freundlich, H. A. (1906) 'Uber die Adsorption in Losungen', *Journal of Physical Chemistry*, **57 A**, 385-470.

Gregorio, C. and P. M. Badot (2008) 'Application of chitosan, a nutral aminopolysaccharide, for dye removal from aqueous solutions by adsorption processes using batch studies: A review of recent literature', *Progress in Polymer Science*, **33**, 399-447.

Guibal, E., Milot, C. and J. M. Tobin (1998) 'Metal-anion sorption by chitosan beads: Equilibrium and kinetic studies', Industrial and Engineering Chemistry Research, **37**, 1454-1463.

Ho, Y. S., Mckay, G., Wase, D. A. J. and C. F. Forster (2000) 'Study of the Sorption of Diavalent Metal Ions onto Peat', *Adsorption Science and Technology*, **18**, 639-650.

Hong – Yu, W., Hui-Fei, H. and J. Jia-Qian (2011) 'The effect of metal cations on phenol adsorption by hexadecyl-trimethyl-ammonium bromide (hdtma) modified clinoptilolite (Ct.)', *Separation and Purification Technology*, **80**, 658-662.

Huang, J., Huang, K. and C. Yan (2009a) 'Application of an easily water compatible hypercrosslinked polymeric resin for efficient removal of catechol and resorcinol in aqueous solutions', *Journal of Hazardous Materials*, **167**, 69-74.

Ivanovic, S. M., Smiciklas, I. and S. Pejanovic (2013) 'Analysis and comparison of mass transfer phenomena related to Cu^{2+} sorption by hydroxyapatite and zeolite', *Chemical Engineering Journal*, **223**, 833-843.

Jaynes, W. F. and S. A. Boyd (1991)'Hydrophobicity of siloxane surfaces in smectities as revealed by aromatic hydrocarbon adsorption from water' *Clays and Clay Minerals*, **39**, 428-436.

Kumar, V. K. and A. Kumaram 2005 'Removal of methylene blue by mango seed kernel powder', *Biochemical Engineering Journal*, **27**, 83-93.

Kuleyin, A., (2007) 'Removal of phenol and 4-chlorophenol by surfactant modified natural zeolite', *Journal of Hazardous Materials,* **144**, 307-315.

Langmuir, I. (1918) 'The Adsorption of Gases on Plane Surfaces of Glass, Mica and Platinum', *Journal of American Chemistry Society*, **40,** 1361-1403.

Lenihan, S., Curtin, T. (2003) 'Copper Exchanged Beta Zeolites for Catalytic Oxidation of Ammonia' *Journal of Chemical Communication*, **11**, 1280-1281.

Li, A., Zhang, Q., Zhang, G., Chen, J., Fei, Z., and F. Liu (2002a) 'Adsorpion of phenolic compounds from aqueous solutions by water-compatible hypercrosslinked polymeric adsorbent', *Chemosphere*, **47**, 981-989.

Li, Z., Li, X., Xi, H. and B. Hua (2002b) 'Effects of ultrasound on adsorption equilibrium of phenol on polymeric adsorption resin', *Chemical Engineering Journal*, **86**, 375-379.

Lopez - Fonseca, R., Gutierrez - Otizr, I. J., Guiterrez - Ortiz, A. M., Gonzalez-Velasco, R. J. (2005) 'Catalytic oxidation of aliphatic chlorinated volatile organic compounds over Pt/H-BETA zeolite catalysts under dry and humid conditions', *Catalysis Today*, **107-108**, 200-207.

Mall, I. D., Srivastava, V. C. and N. K. Agarwal (2006) 'Removal of Orange – G and Methyl Violet dyes by adsorption onto bagasse fly ash-kinetic study and equilibrium isotherm analyses', *Dyes and Pigments*, **69**, 210-223.

Pan, B., Pan, B., Zhang, W., Zhang, Q., Zhang, Q., and S. Zheng (2008) 'Adsorptive removal of phenol from aqueous phase by using a porous acrylic ester polymer', *Journal of Hazardous Material*, **157**, 293-299.

Soto, M. L. Moure, A., Dominguez, H. and J. C. Parajo (2011) 'Recovery, concentration and purification off phenolic compounds by adsorption: A review, *Journal of Food Engineering*, **105**, 1-27.

Topallar, H. and Y. Bayrak (1999) 'Investigation of Adsorption Isotherms of Myristic, Palmitic and Stearic Acids on Rice Hull Ash', *Turkish Journal of Chemistry*, **23,** 193-198.

Tsai, W. T., Hsien, K. J. and H. C. Hsu (2009) 'Adsorption of organic compounds from aqueous solution onto the synthesized zeolite', *Journal of Hazardous Material*, **166**, 635-641.

Ugurlu, M., Gurses, A., Yalcin, M. and C. Dogar (2005) 'Removal of phenolic and Lignin compounds from bleached kraft mill effluents by fly ash and sepiolite', *Adsorption*, **11**, 87-97.

Webber, W. J. and J. C. Morris (1963) 'Kinetics of adsorption on carbon from solution', *Journal of Sanitary Engineering Division American Society of Civil Engineers*, **89**, 31-59.

Xiaohong, L., Baowei, Z., Kun, Z., and H. Xuekui (2011) ' Removal of nitrophenols by adsorption using β-cyclodextrin modified zeolites', *Chinese Journal of Chemical Engineering*, **19(6),** 938-943.

Yousef, R. I., El – Eswed, B. and A. H. Al – Muhtaseb (2011) 'Adsorption characteristics of natural zeolites as solid adsorbents for phenol removal from aqueous solutions: Kinetics, mechanism and thermodynamics studies', *Chemical Engineering Journal*, **171**, 1143-1149.

Yu, L. (2008) 'New insights into pseudo-second –order kinetic equation for adsorption', *Colloids and Surfaces A: Physicochemical and Engineering Aspects*, **320**, 257-278.

Zahir, R. and N. Najwa (2006) 'Characteristic of phenol and chlorinated phenols sorption onto surfactant modified bentonite' *Journal of Colloid and Interface Science*, **298**, 39-49.

Chapter 5

Catalytic Oxidation of 2-Nitrophenol

5.1. Introduction

Purification of wastewater polluted by nitrophenolic compounds is a very challenging task. The presence of the nitro group in the aromatic ring enhances the stability of these molecules to chemical and biological degradation. Furthermore, these compounds cannot be effectively treated by conventional water treatment technologies such as biological degradation, physical and physicochemical processes. Aerobic biodegradation is weakly efficient and takes place over a long treatment period, while anaerobic degradation leads to the formation of nitroso and hydroxylamine compounds which are known carcinogens (Oturan et al. 2011). Direct photochemistry is not efficient either. Ozone treatment is an attractive and increasingly important method for degradation of organic pollutants in aqueous solution, however refractory organic compounds are not usually oxidized totally and only minor levels of mineralization are achieved (Gharbani and Mehrizad, 2012). In contrast, advanced oxidation processes (AOPs), which involve the highly oxidizing hydroxyl radicals ($^{\cdot}OH$), such as: H_2O_2 photolysis, Fenton's reagent, Photo-Fentons and heterogeneous photocatalysis were shown to be able to degrade nitrophenols efficiently (Oturan et al. 2011). A work reported in literature by Liotta et al. successively oxidized phenol adsorbed onto a copper modified zeolite (CuY-5) via wet hydrogen peroxide (Liotta et al. 2009).

Other reports in literature citing catalytic oxidation as an effective method for the complete destruction of organic compounds (such as phenol and aniline) include works by Adam et al., Shukla et al. and O'Brien et al. (Adam et al., 2013, Shukla et al., 2010 and O'Brien et al., 2008). These works investigate the potential benefits of coupling an adsorption process with a catalytic oxidation step. The use of a high Si/Al ratio Beta zeolite for the dual function adsorbent / catalysts is justified in two aspects.

One is ease of safe operation of catalytic oxidation at high temperature, and another is the high adsorption capacity for 2-nitrophenol. Activated carbons, as discussed in chapter 1 section 1.5.2, are generally used in many adsorption processes because of their high adsorption capacity and good economy. However, their regeneration is very difficult because of their thermal and chemical instability causing significant safety problems.

The selection of an effective and economical catalytic component is as important as the selection of a good adsorbent material to embody the best dual functional adsorbent / catalytic media. Noble metal-based catalysts, such as supported platinum and palladium, are traditional catalysts for low temperature complete oxidation (Baek et al., 2004). However, these catalysts, although very active for oxidation, are too expensive and susceptible to poisoning by chlorine / chloride products (Agarwal and Spivey, 1992). Catalytic dry oxidation of organic pollutants adsorbed on regenerable catalyst–sorbents has been reported to be promising for treatment of toxic and/or biorefractory wastewater streams. Research work by Zhao et al. has investigated the use of activated carbon supported copper catalysts for the sorption and subsequent temperature programmed catalytic dry oxidation of phenol from solution (Zhao et al., 2004).

A catalytic combustion process, if properly designed, must lead to the complete destruction of the 2-nitrophenol compound, including the harmful by-products which can be produced by the incomplete destruction of the starting nitrophenol compound. The catalytic combustion is also interesting on account of the potential selectivity to harmless final products. The ideal catalytic combustion products of 2-nitrophenol would be water, carbon dioxide and nitrogen. Nitrogen gas is the preferred nitrogen product as opposed to nitrogen oxides. Nitrogen oxides are listed as criteria air pollutants because of their involvement in chemical reactions that can lead to the formation of acid rain, photochemical smog and to the destruction of ozone in the stratosphere. Their role in these chemical reactions in the environment can ultimately lead to human health effects such as bronchitis, emphysema, skin cancer and cataracts (Chang et al., 2013).

Taking these points into consideration, research in the catalytic oxidation of low concentrations of 2-nitrophenol with air must focus on identifying highly active catalysts and obtaining benign reaction products at moderate temperatures. As a result, reaction conditions resulting in the complete oxidation to H_2O, CO_2 and N_2 must be chosen. Since the discovery by Iwamoto et al. of the remarkable activity of Cu-ZMS-5 zeolite in the selective catalytic reduction (SCR) of NO by hydrocarbons (Iwamoto et al., 1993), a lot of investigations have been performed to describe the nature of copper sites active in this process (Sultana et al., 2011, Franch-Martí et al., 2012, Carniti et al., 2000, Corma et al., 1997 and Gopalakrishnan et al., 1993). The transition metal ions are introduced in the extra-framework position of the zeolite structure by a variety of methods such as ion exchange and impregnation (Zhang et al., 2011, De La Torre et al., 2012, Metkar et al., 2012, Liu et al., 2009 and Janas et al., 2009) as outlined in chapter 3 section 3.1 which discusses the modification of Beta zeolite with a catalytic component.

The findings of step one of this work suggest that in a controlled aqueous pH environment, unmodified Beta zeolites have significant potential as adsorbents in the removal of low concentrations of 2-nitrophenol. In step 1 Beta zeolite was also successfully modified with a catalytic component with the aim of enhancing and promoting its catalytic activity. The introduction of the catalytic component also resulted in an increased adsorption capacity for the lower silica-to-alumina ratio Beta zeolites and maintained its adsorption capacity for the higher silica-to-alumina ratio Beta zeolites.

Step two of this work involves the study of the catalytic oxidation of the adsorbed pollutant (2-nitrophenol) with the simultaneous regeneration of the adsorbent/catalysts. The overall aim would be to produce carbon dioxide, water and nitrogen whilst minimising the formation of carbon monoxide, nitrogen oxide, benzene and phenol.

5.2 Experimental

5.2.1 Sample Preparation and Testing

The Temperature Programmed Oxidation (TPO) rig illustrated in Figure 5.1, was used to test the oxidation characteristics of the different prepared adsorbents/catalysts. The set up consisted of a gas delivery system, a detector and a reactor. The gas flow rates were regulated by mass flow controllers. The feed stream of oxygen and helium entered a system of three way valves, allowing it either to flow through the reactor or to bypass it. The compositions of the gases leaving the reactor or the by-pass were measured using a Hewlett Packard HP5971A Mass Spectrometer (M.S.). The solid adsorbent/catalyst was supported between two pieces of loosely packed quartz wool in a reactor. The reactor itself was comprised of quartz glass with 8 mm internal diameter (i.e. a conventional plug flow reactor setup). A type K thermocouple was inserted directly into the catalyst bed. The temperature of the furnace (vertical Stanton Redcroft VB100) was controlled using a Eurotherm 818P controller and programmer.

All Beta zeolite samples, with adsorbed 2-nitrophenol from the adsorption studies, were tested in the catalytic rig illustrated in Figure 5.1. The 2-nitrophenol loaded Beta zeolite (100 mg) were individually placed in the quartz reactor. Before testing, the spent adsorbent sample was pre-treated for 60 minutes in a stream of a 3% oxygen-helium mixture at a flow rate of 50 ml/min at room temperature. The samples were then subjected to a temperature increase of 10°C/min up to 750°C. Products leaving the reactor were continuously monitored using the M.S. detector. These results were collected by specialised Chemstation software HP5970C (Microsoft Windows based) on a Hewlett Packard 486S/20 personal computer.

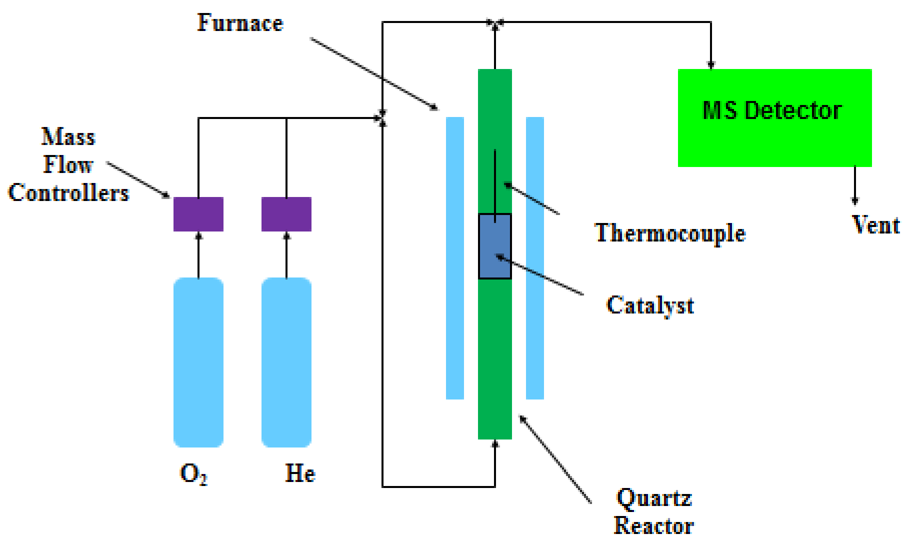

Figure 5.1: The temperature programmed oxidation (TPO) rig setup.

In the mass spectrometer, the sample gas molecules are ionised. The molecular ions formed are then separated according to their mass to charge (m/z) ratio in a high vacuum. Ionisation also causes molecules to fragment, resulting in the formation of a small family of charged particles rather than a single ion. The fragmentation pattern produced is different for every ion, thus each ion has a characteristic fingerprint. Problems may be encountered with gas mixtures where there is superimposition of fragment ion intensities at the same atomic mass unit (a.m.u.) (e.g. S^+ and O_2^+ at 32 a.m.u.).

2-nitrophenol was the model organic pollutant chosen for study in this work, as discusses in chapter 1 section 1.2. It is a nitrated phenol with a molecular formula of $C_6H_5NO_3$. The mass spectrum fragment pattern of 2-nitrophenol is presented in Figure 5.2 (NIST Chemistry WebBook (http://webbook.nist.gov/chemistry). The fragmentation pattern shows the range of ions and their relative intensities that are detected, which span a mass charge ratio (m/z) of 15 to 139 atomic mass units. Some of the principle peaks detected over this m/z range are $C_5H_6^+$, $C_5H_7^+$,$C_6H_7NO^+$ and $C_6H_5NO_3$.

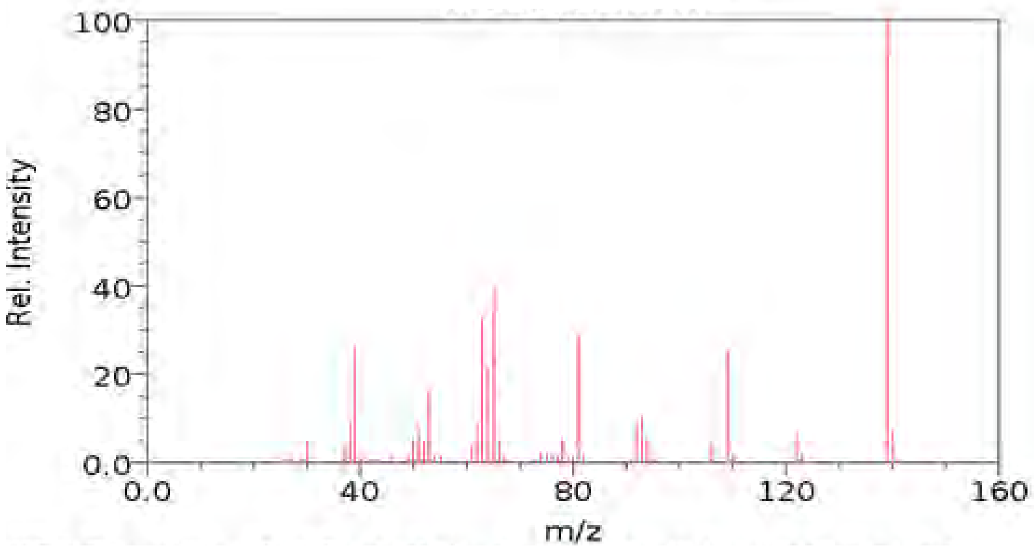

Figure 5.2: Mass Spectrum fragment pattern for 2-nitrophenol. (NIST Chemistry WebBook (http://webbook.nist.gov/chemistry)).

As this study seeks to evaluate the feasibility of catalytically oxidizing the adsorbed 2-nitrophenol to carbon dioxide, water and nitrogen, whilst minimizing the formation of nitrogen oxides, Figure 5.2 provided information regarding the ions to investigate as potential breakdown products during the temperature programme oxidation of adsorbed 2-nitrophenol on the Beta zeolite. The range of m/z analysed during the temperature programmed oxidation of adsorbed 2-nitrophenol was therefore from 16 to 139 atomic mass units, which are outlined in Table 5.1. The most common ions investigated during the temperature programmed oxidation of adsorbed 2-nitrophenol were the total oxidation product CO_2^+ and other minor species such as NO_2^+, NO^+, $C_6H_6^+$ and C_6H_5OH.

Table 5.1: Ions monitored during the temperature programed oxidation of adsorbed 2-nitrophenol.

Ion Monitored	A.M.U.	Most common ions detected
$C_6H_5NO_3$	139	$C_6H_5NO_3$
$C_6H_4\ NO_2^+$	122	$C_6H_4\ NO_2^+$
$C_6H_7NO^+$	109	$C_6H_7NO^+$
C_6H_5OH	94	C_6H_5OH
$C_6H_7N^+$	93	-
$C_6H_6^+$	78	$C_6H_6^+$
$C_5H_7^+$	66	-
$C_5H_6^+$	65	-
NO_2^+	46	NO_2^+
CO_2^+	44	CO_2^+
O_2^+	32	O_2^+
NO^+	30	NO^+
N_2^+/CO	28	N_2^+/CO
H_2O^+	18	H_2O^+
O_2^+	16	O_2^+

5.3 Results and Discussion

5.3.1 Catalytic oxidation of adsorbed 2-nitrophenol

During the adsorption step significant uptake levels of 2-nitrophenol was possible on the unmodified Beta zeolite with maximum uptake levels of 90 – 100 mg g^{-1} typically being achieved. This can be seen in chapter 2 section 2.3.1 and a summary of these results are presented here in Figure 5.3. In chapter 3 section 3.1 the Beta zeolite samples were modified with a catalytic component in an effort to enhance the catalytic oxidation of the adsorbed 2-nitrophenol, in the second stage of this adsorption/oxidation process. Table 5.2 lists the adsorbent catalysts that have been prepared for testing in this second step of the adsorption/oxidation process. The adsorbent catalysts listed were prepared using a one-step exchange procedure as outlined in chapter 3 section 3.2.1. The table includes the theoretical copper loadings, the actual copper loadings and the Si/Al ratio of the zeolite. Also included in the table are the amounts of 2-nitrophenol adsorbed by the adsorbent catalysts during the adsorption studies outlined in chapter 2 section 2.3.1 and chapter 4 section 4.3.1. The theoretical Cu loading refer to the amount of copper nitrate in the exchanging solution while the actual wt% copper loadings of the exchanged zeolites were determined by atomic absorption of the prepared solids as discussed in chapter 3 section 3.3.1.

Figure 5.3 illustrates the effect of increasing the Si/Al ratio and the introduction of extra-framework copper into the Beta zeolite on the adsorption of 2-nitrophenol from aqueous solution. It is evident that increasing the Si/Al ratio of the Beta zeolite enhances 2-nitrophenol adsorption levels. While the introduction of extra-framework cations into the lower SiO_2/Al_2O_3 ratio Beta zeolite, β(25), enhanced the adsorption uptake of 2-nitrophenol, with uptake levels increasing with increasing copper loadings. While the introduction of extra-framework copper does not enhance the adsorption uptake of 2-nitrophenol by the higher Si/Al ratio Beta zeolites, β(150) and β(300).

Table 5.2: Catalysts prepared using Beta zeolite of different Si/Al ratios.

Sample Name	Theoretical wt.% Cu loading	Actual wt. % Cu loading	Si/Al Ratio	2-Nitrophenol adsorbed mg g^{-1}
β(25)	-	-	25:1	40-50
1.20%Cuβ(25)	1.5	1.2	25:1	80-90
1.95%Cuβ(25)	2.0	1.95	25:1	90-100
Cuβ(150)	-	-	150:1	90-100
0.1 %Cuβ(150)	0.5	0.1	150:1	50-60
1.02%Cuβ(150)	1	1.02	150:1	70-80
2.00%Cuβ(150)	2	1.98	150:1	90-100
Cuβ(300)	-	-	300:1	70-80
1.30%Cu β(300)	2	1.30	300:1	70-80

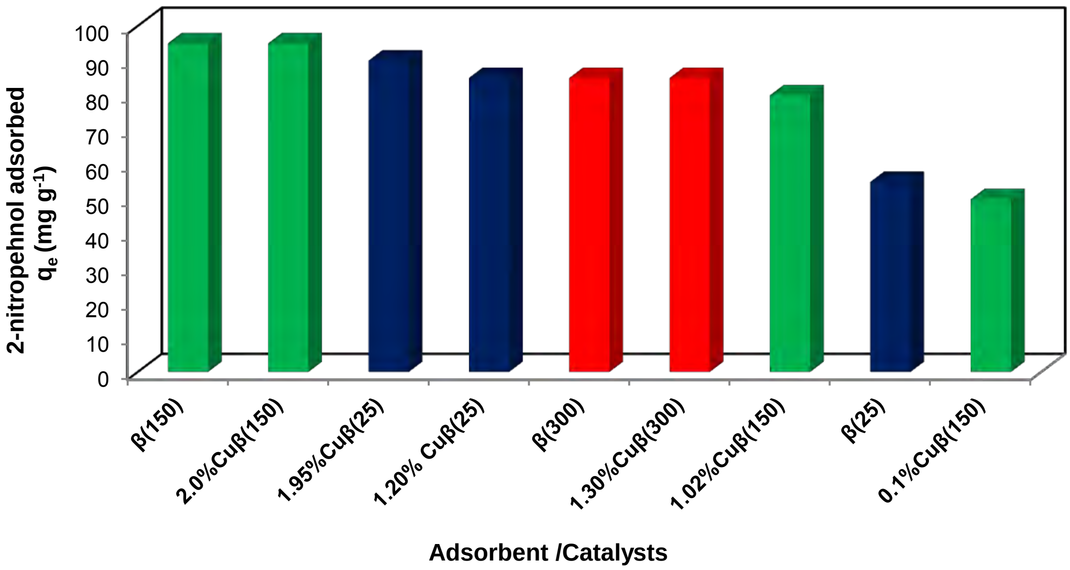

Figure 5.3: The influence of copper on the adsorption of 2-nitrophenol in mg g^{-1} on the indicated Beta zeolite samples.

This study seeks to evaluate the feasibility of catalytically oxidizing the adsorbed 2-nitrophenol to carbon dioxide, water and nitrogen whilst minimizing the formation of nitrogen oxides. The unmodified Beta zeolite samples (β(25), β(150) and β(300)) were used as comparators to assess the influence of copper loading on the catalytic oxidation of adsorbed 2-nitrophenol.

The catalytic oxidation performance of each of the catalysts listed in Table 5.2 was assessed by monitoring the composition of the exhaust gas stream from the reactor during the temperature programmed catalytic oxidation of adsorbed 2-nitrophenol, as described in section 5.2.1. Figure 5.4 shows a typical temperature programmed oxidation profile of adsorbed 2-nitrophenol (in this case 2.0%Cuβ(150)). The degradation of the adsorbed 2-nitrophenol on 2.0%Cuβ(150) is accompanied by a corresponding increase in carbon dioxide levels detected in the exhaust gas stream. The carbon dioxide begins to form at temperatures above 300°C and continues to rise sharply up to about 420°C. During this time there is a sharp decrease in the oxygen content of the exit stream, indicating that the 2-nitrophenol is being oxidized by O_2 to CO_2. In this particular sample, 2-nitrophenol was not detected in the exit stream which would indicate its oxidation. Water vapour is also detected in the exhaust gas stream during the catalytic oxidation process. While carbon dioxide and sometimes desorbed 2-nitrophenol were the main species detected in the exit stream during the temperature programmed oxidation of prepared samples, other minor species were also detected. These compounds included water, nitrogen/carbon monoxide, nitrogen oxide, nitrogen dioxide, phenol and benzene. For all samples, the exhaust gas stream was also further analysed for other potential organic and nitrogen breakdown products of 2-nitrophenol during the catalytic oxidation process such as those outlined in Table 5.1. These will be discussed within the following sections.

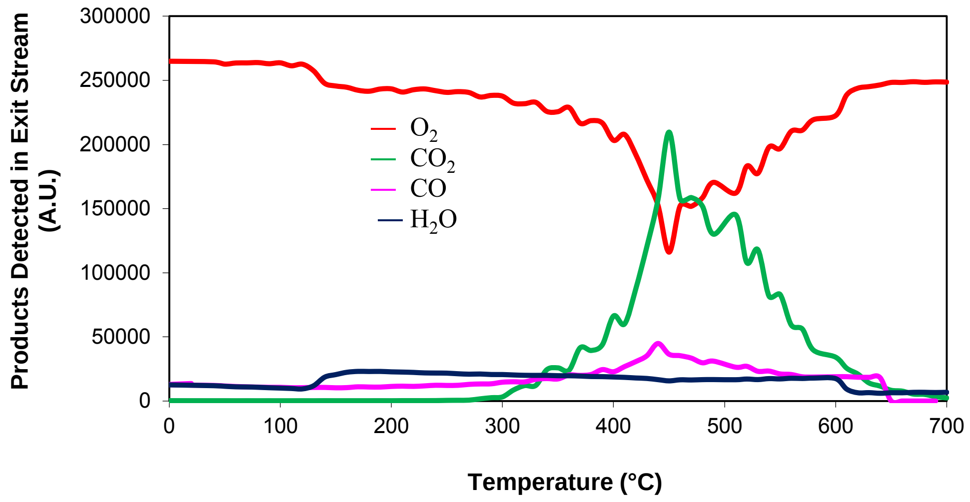

Figure 5.4: Products detected in the exit stream during the catalytic temperature programmed oxidation of adsorbed 2-nitrophenol on 2.0%Cuβ(150). (Conditions: 100 mg sample containing 90 – 100 mg g^{-1} 2-nitrophenol, 3% (v/v) O_2 / He at 50 ml min^{-1}, temperature ramp 10°C min^{-1}).

As reported in the adsorption step of this work significant uptake levels of 2-nitrophenol were achieved on the prepared catalysts listed in Table 5.2 . Figures 5.5 (A - C) illustrate the desorption profiles of 2-nitrophenol during the temperature programmed oxidation process over the prepared catalysts outlined in Table 5.2. In the absence of copper, i.e. the β(25), β(150) and β(300) samples, unreacted 2-nitrophenol was detected in the exhaust gas stream during the temperature programmed oxidation process, Figures 5.5 (A - C) respectively. The presence of 2-nitrophenol indicates the limited catalytic oxidation of adsorbed 2-nitrophenol over the unmodified zeolites. The presence of copper on the zeolite was found to enhanced the catalytic oxidation of adsorbed 2-nitrophenol, as 2-nitrophenol was not detected in the exit stream using the Cu modified samples. The only exception was 0.1%Cuβ(150), the sample containing the lowest copper loading, which exhibited relatively low quantities of 2-nitrophenol. It is evident that only a small percentage of extra-framework copper is required to enhance the Beta zeolites potential to catalytically oxidise the adsorbed 2-nitrophenol as highlighted by the decreases in 2-nitrophenol desorbed from the 0.1%Cuβ(150) in comparison to the β(150) sample. Increasing the copper content on the β zeolite further enhances the catalytic oxidation of adsorbed 2-nitrophenol. This can be observed in Figure 5.5 where increasing the percentage loading of copper on β(150) up to 1.02%Cuβ(150) results in the elimination of 2-nitrophenol detected in the exit stream.

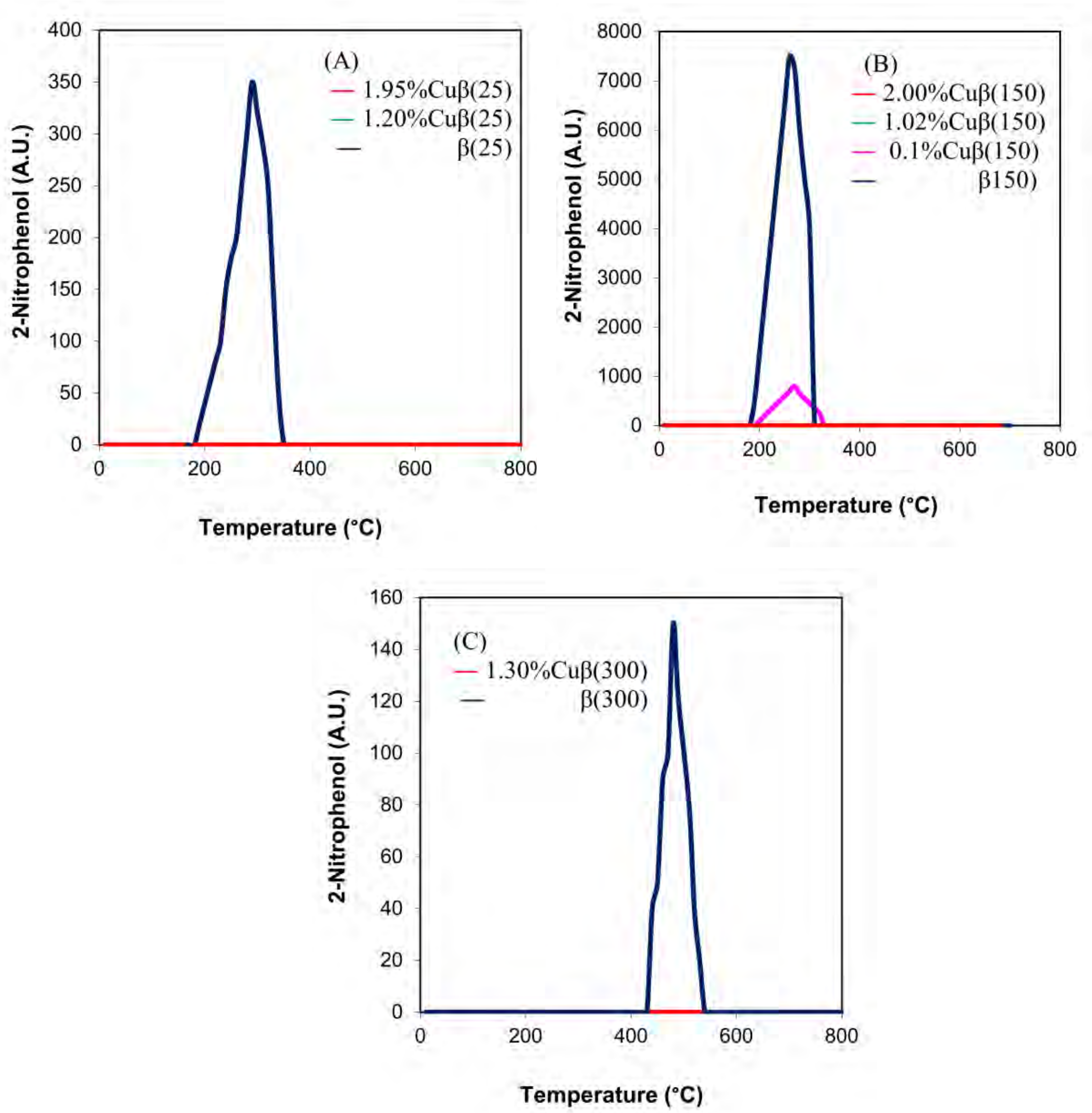

Figure 5.5: Desorption of 2-nitrophenol during TPO testing from (A) the β(25) samples containing 40 – 100 mg g^{-1} 2-nitrophenol, (B) β(150) samples containing 50 – 100 mg g^{-1} 2-nitrophenol and (C) β(300) samples containing 70 – 80 mg g^{-1} 2-nitrophenol. Conditions: 100 mg sample, 3% (v/v) O_2 in He at 50 ml min^{-1}, Temperature ramped 10°C min^{-1}).

During the temperature programmed oxidation of the various zeolite samples with adsorbed 2-nitrophenol, a variety of products were detected in the gas exit stream as highlighted in Table 5.1. However, the most significant product observed was the total oxidation product, CO_2.

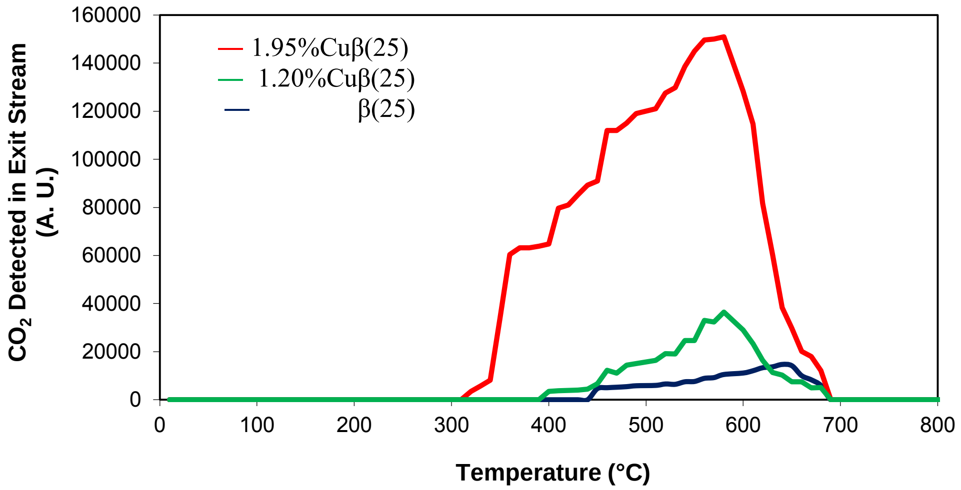

Figure 5.6: Formation and desorption of CO_2 from the indicated β(25) samples. (Conditions: 100 mg of sample containing 40 - 100 mg g $^{-1}$ 2-nitrophenol, 3% (v/v) O_2 / He gas flow rate 50 ml min $^{-1}$, temperature ramped at 10°C min^{-1}).

Figure 5.6 shows the evolution of CO_2 from the gas stream during the temperature programmed oxidation of adsorbed 2-nitrophenol on 1.95%Cuβ(25), 1.20%Cuβ(25) and β(25). In the absence of copper (β(25) sample), formation of carbon dioxide occurs at temperatures in excess of 450°C. The presence of copper on the Beta zeolite reduces the temperature of formation of CO_2 to 320°C and 400°C for the 1.95%Cuβ(25) and 1.20%Cuβ(25) samples, respectively. The presence of extra-framework copper not only reduces the temperature of formation of CO_2 but it also increases the total oxidation of the adsorbed 2-nitrophenol into CO_2 which is evident by the increase in evolution of CO_2 from 1.95%Cuβ(25) and 1.20%Cuβ(25).

It is clearly shown in Figure 5.6 that the total oxidation of adsorbed 2-nitrophenol into CO_2 is also enhanced by increasing the percentage of extra-framework copper on the Beta zeolite. For example, increasing the percentage copper on the β(25) up to 1.95%Cuβ(25) resulted in an increase in the extent of evolution of carbon dioxide during the temperature programmed oxidation of adsorbed 2-nitrophenol. Analysis of the areas under the curves of β(25), 1.20%Cuβ(25) and 1.95%Cuβ(25) in Figure 5.6 was performed in order to investigate the difference in evolution of carbon dioxide between the adsorbent/catalysts. Table 5.3 outlines the peak area counts of CO_2 and the peak area counts of 2-nitrophenol, in addition to the amount of 2-nitrophenol adsorbed on each of the Beta zeolite samples.

Table 5.3: Carbon dioxide and 2-nitrophenol detected in the exhaust gas stream during the temperature programmed oxidation of adsorbed 2-nitrophenol on each of the prepared adsorbent catalysts.

Sample Name	CO_2 Peak Area Arbitrary Units	$C_6H_5NO_3$ Peak Area A.U.	2-Nitrophenol adsorbed (mg g^{-1})
β(25)	2936400	27920	40 -50
1.20%Cuβ(25)	4818140	-	80-90
1.95%Cuβ(25)	31845520	-	90-100
Cuβ(150)	5280085	58500	90-100
0.1 %Cuβ(150)	5848435	3730	50-60
1.02%Cuβ(150)	11568885	-	70-80
2.0 %Cuβ(150)	25646990	-	90-100
Cuβ(300)	2384990	29590	70-80
1.3% Cuβ(300)	3176775	-	70-80

It is evident from Table 5.3 that there is an increase in the level of 2-nitrophenol adsorbed, during the adsorption step, with increasing Cu levels for the β(25) samples. It would be expected therefore that there should be an increase in the CO_2 peak area counts with increase in copper levels and from Table 5.3 this seems to be the case for the β(25) samples. Figure 5.7 is a plot of the CO_2 area counts versus the initial 2-

nitrophenol loadings. It is clear from this Figure the relationship is not a linear one. The difference in evolution in CO_2 between the adsorbent catalysts may therefore be related to differences in the catalytic oxidation potential of each of the Beta zeolite samples. For example, in the presence of copper, unreacted 2-nitrophenol was not observed from 1.95%Cuβ(25) and 1.20%Cuβ(25) during the temperature programmed oxidation of adsorbed 2-nitrophenol. This would indicate decomposition of the adsorbed 2-nitrophenol and would account for the increase in evolution of CO_2 from the copper modified Beta zeolites. While the variation in evolution of CO_2 between the adsorbent catalysts may also be related to the formation of minor incomplete oxidation products such as benzene, phenol or coke formation which would account for the lower than expected CO_2 level observed for 1.2%Cuβ(25).

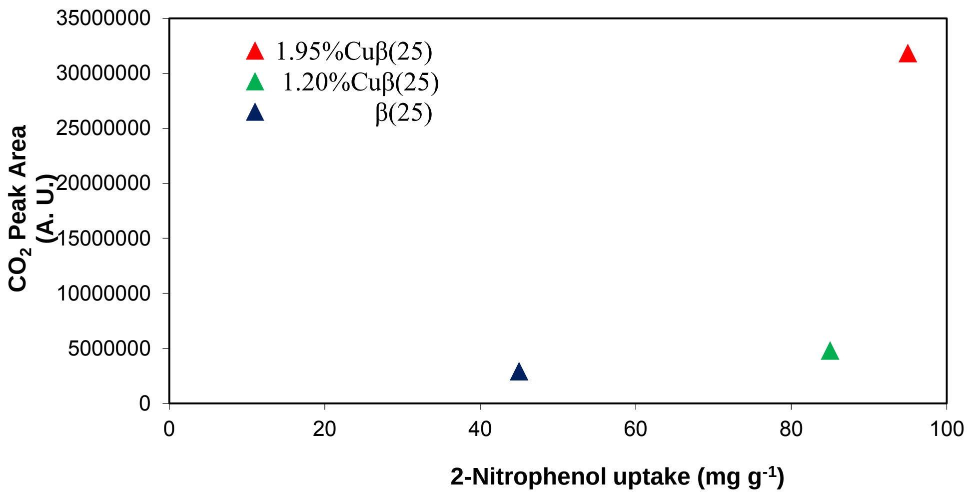

Figure 5.7: The relationship between CO_2 peak area versus initial 2-nitrophenol uptake (40 - 100 mg g^{-1}) for each of the indcated β(25) samples.

Figure 5.8 illustrates the carbon dioxide profiles from the temperature programmed oxidation of adsorbed 2-nitrophenol on 2.0%Cuβ(150), 1.02%Cuβ(150), 0.1%Cuβ(150) and β(150). In the absence of copper, formation of carbon dioxide occurs at temperatures above 500°C (β(150) sample), while similar to β(25), the presence of copper on the Beta zeolite significantly lowers the temperature required for the oxidation of adsorbed 2-nitrophenol into CO_2.

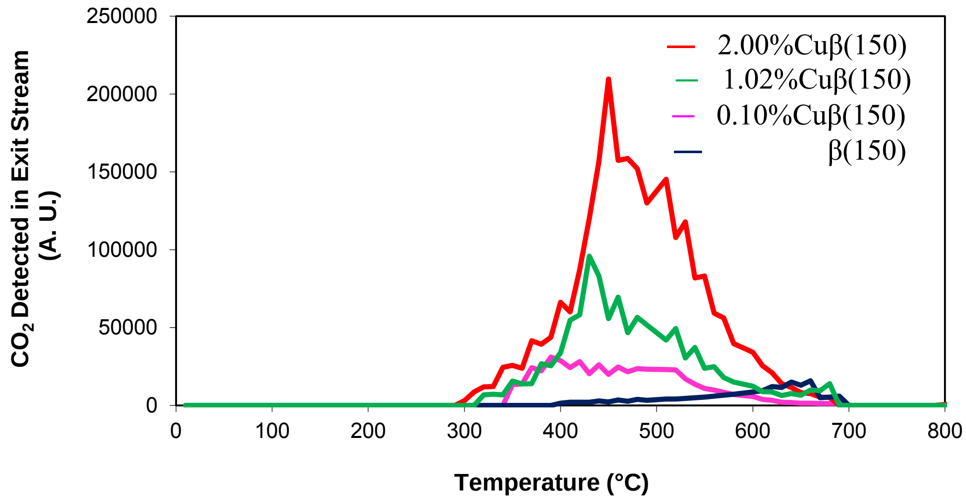

Figure 5.8: Formation and desorption of CO_2 from the indicated β(150) samples. (Conditions: 100 mg of sample containing 50 - 100 mg g^{-1} 2-nitrophenol, 3% (v/v) O_2 / He gas flow rate 50 ml min^{-1}, temperature ramped at 10°C min^{-1}).

Similar to the β(25) samples, the presence of copper on β(150) increases the total oxidation of adsorbed 2-nitrophenol into CO_2 and increasing the level of Cu results in increased production of CO_2. Analysis of the areas under the curves of β(150), 2.0%Cuβ(150), 1.02%Cuβ(150) and 0.1%Cuβ(150) in Figure 5.9 was performed in order to investigate the difference in carbon dioxide levels between the adsorbent/catalysts. Table 5.3 outlines the peak area counts of CO_2 and the amount of 2-nitrophenol adsorbed on each of the copper modified Beta zeolite samples. Figure 5.9 presents a plot of CO_2 peak area versus the initial 2-nitrophenol loadings. The unmodified β(150) showed one of the highest uptake levels of 2-nitrophenol from aqueous solution during the adsorption step with an adsorption level of 90-100 mg g^{-1}. However, during the temperature programme oxidation studies it reported the lowest detected levels in CO_2 and did not fit the relatively linear relationship that the copper modified samples displayed in Figure 5.9. This low level of CO_2 observed may be explained by the relatively high levels of unreacted 2-nitrophenol detected in the exit stream as shown in Figure 5.5 (B). This highlights, that in the absence of copper, the β(150) sample is limited in its ability to decompose the adsorbed 2-nitrophenol into CO_2. While the resultant plot is not completely linear for the copper modified samples and therefore the peak area counts of CO_2 cannot be completely accounted for by the initial 2-nitrophenol loadings only and similar to the β(25) samples. Other factors must be taken into consideration such as desorption of unreacted 2-nitrophenol (from the 0.1%Cuβ(150) only), the formation of other intermediate byproducts such as phenol and benzene, fragmentation / formation of CO, possible coke formation and also the catalytic activity of the Beta zeolite for the oxidation of adsorbed 2-nitrophenol.

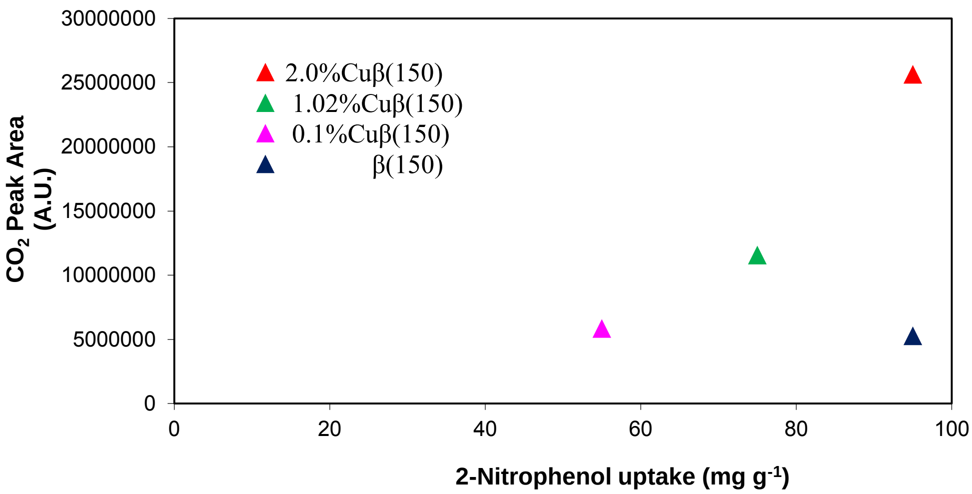

Figure 5.9: The relationship between CO_2 peak area versus initial 2-nitrophenol uptake (50 - 100 mg g^{-1}) for each of the indcated β(150) samples.

Figure 5.10 illustrates the carbon dioxide profile during the temperature programmed catalytic oxidation of adsorbed 2-nitrophenol on 1.30%Cuβ(300) and β(300). In the absence of copper, formation of CO_2 occurs at 400°C, while in the presence of copper the formation of CO_2 occurs at a lower temperature of 300°C. 2-Nitrophenol adsorption levels of 70-80 mg g^{-1} were achieved on both β(300) and 1.3%Cuβ(300) as shown in Table 5.3. In Figure 5.10 the presence of the copper (1.30%Cuβ(300)) resulted in increased amounts of carbon dioxide being produced as evidence by the significantly larger peak in contrast to the unmodified sample (β(300)). As both samples had similar amounts of 2-nitrophenol from the adsorption step, the difference in evolution in CO_2 between the two samples must be related to the difference in catalytic activity between the copper modified Beta zeolite and the unmodified Beta zeolite similar, to β(25) and β(150) samples. The presence of copper significantly enhances the total oxidation the adsorbed 2-nitrophenol and would account for the increase in CO_2 detected from the copper modified Beta zeolite 1.30%Cuβ(300). In addition, β(300) displayed limited catalytic performance as 2-nitrophenol was found to be desorbed from the sample during temperature programmed oxidation as displayed in figure 5.5 (C).

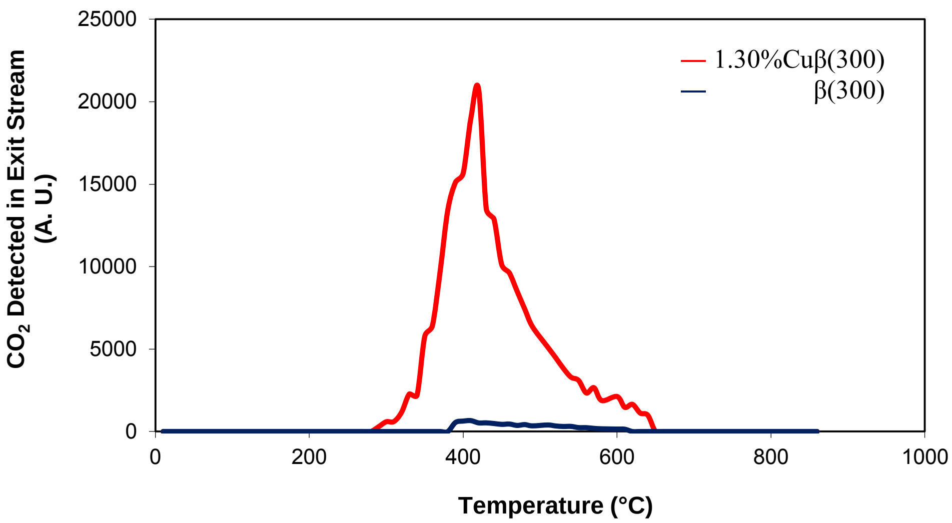

Figure 5.10: Formation and desorption of CO_2 from the indicated β(300) samples. (Conditions: 100mg of sample containing 70 – 80 mg g^{-1} 2-nitrophenol, 3% (v/v) O_2 / He gas flow rate 50 ml min^{-1}, temperature ramped at 10°C min^{-1}).

While carbon dioxide and desorbed 2-nitrophenol were the main species detected in the exit stream during the temperature programmed oxidation of prepared samples, other minor species were also detected. These include benzene and phenol. Figures 5.11 (A - C) illustrate the desorption profiles for phenol and benzene from β(25), 1.20%Cuβ(25) and 1.95%Cuβ(25), respectively during the temperature programmed oxidation of adsorbed 2-nitrophenol.

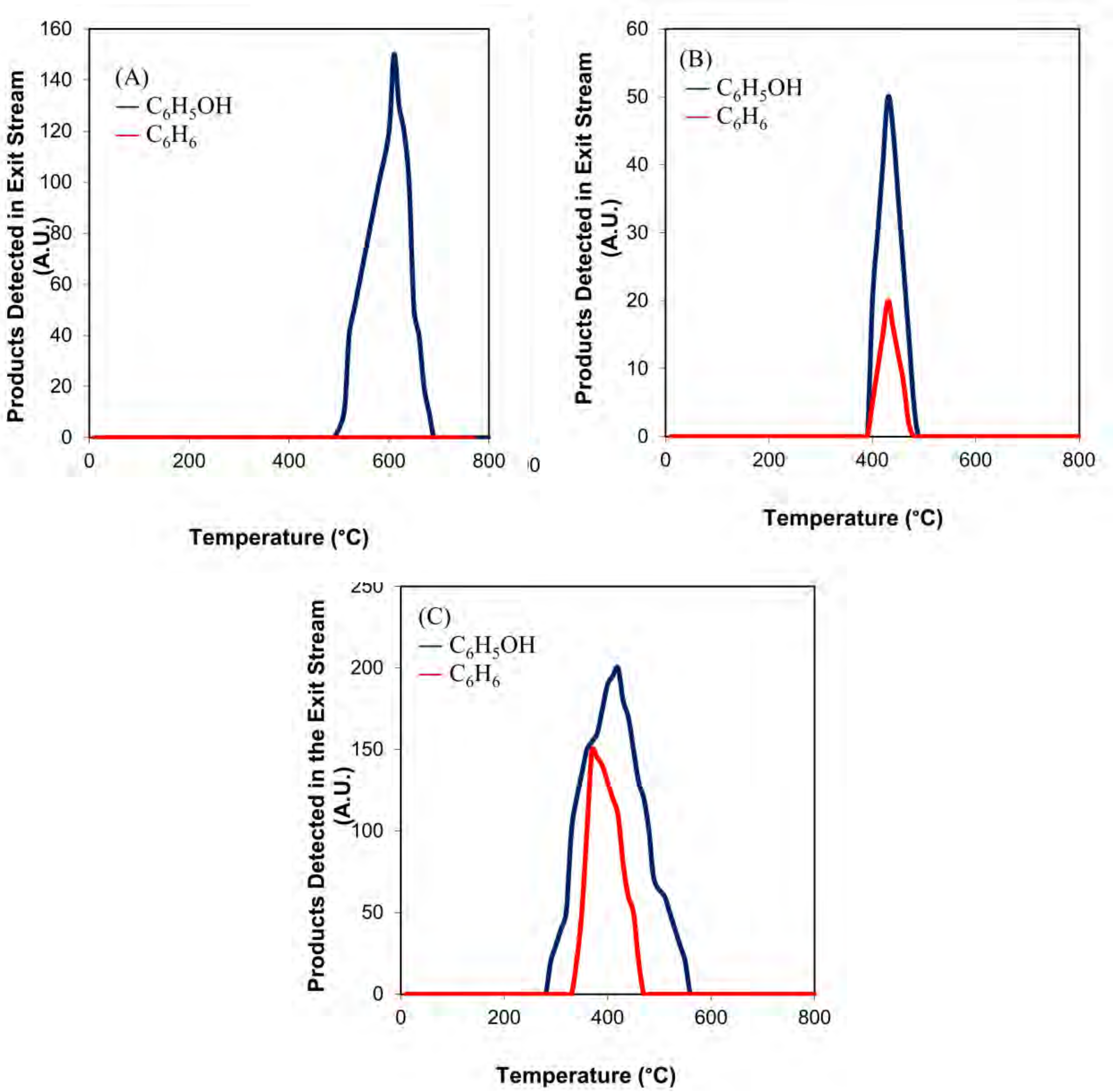

Figure 5.11: Benzene and phenol detected in the exit stream during TPO testing from (A) the β(25) sample containing 40 – 50 mg g^{-1} 2-nitrophenol, (B) 1.20%Cuβ(25) sample containing 80 – 90mg g^{-1} 2-nitrophenol and (C) 1.95%Cuβ(25) sample containing 90 – 100 mg g^{-1} 2-nitrophenol. (Conditions: 100 mg sample, 3% (v/v) O_2 in He at 50 ml min^{-1}, Temperature ramped 10°C min^{-1}).

In the absence of copper on β(25), a small amount of phenol is detected in the exhaust gas stream during the temperature programmed oxidation process as shown in Figure 5.11 (A). The presence of copper on the zeolite, 1.20%Cuβ(25) and 2.0%Cuβ(25), resulted in the desorption of both phenol and benzene during the temperature programmed oxidation of adsorbed 2-nitrophenol as shown in Figures 5.11 (B) and 5.11 (C), respectively. From Figure 5.5 (A) it is evident that complete decomposition of the adsorbed 2-nitrophenol is achieved by both the 1.95%Cu(25) and the 1.20%Cu(25), while some of the 2-nitrophenol decomposes into these minor products, phenol and benzene. It is also clear that the presence of extra-framework copper on the Beta zeolite reduces the temperature of formation of these organic compounds. In the absence of Cu, phenol is observed between 500 - 700°C, this reduces considerably in the presence of copper for example between 300 - 580°C from the 1.20%Cuβ(25).

Figures 5.12 (A – D) illustrates the desorption profile for phenol and benzene from β(150), 0.1%Cuβ(150) 1.02%Cuβ(150) and 2.00%Cuβ(150) during the temperature programmed oxidation of adsorbed 2-nitrophenol. The trends observed here were similar to those observed for the (25) Beta zeolites. In the absence of copper, a small amount of phenol was detected in the exhaust gas stream as shown in figure 5.12 (A). The presence of copper on the Beta zeolite, (i.e. for the 2.00%Cuβ(150), 1.02%Cuβ(150) and 0.01%Cuβ(150) sample), resulted in the formation of both phenol and benzene as shown in Figures 5.12 (B - D), respectively. From Figure 5.5 (B) it is evident that complete decomposition of the adsorbed 2-nitrophenol is achieved by both the 1.02%Cuβ(150) and the 2.00%Cuβ(150).

From Figures 5.12 (B - D) it is clear that following this decomposition of adsorbed 2-nitrophenol both phenol and benzene are formed. The presence of extra-framework copper on the Beta zeolite reduces the temperature of formation of these organic compounds. For example the peak temperature of phenol formation decreases from 420°C to 320°C for the β(25) and 1.20%Cuβ(25) sample, respectively.

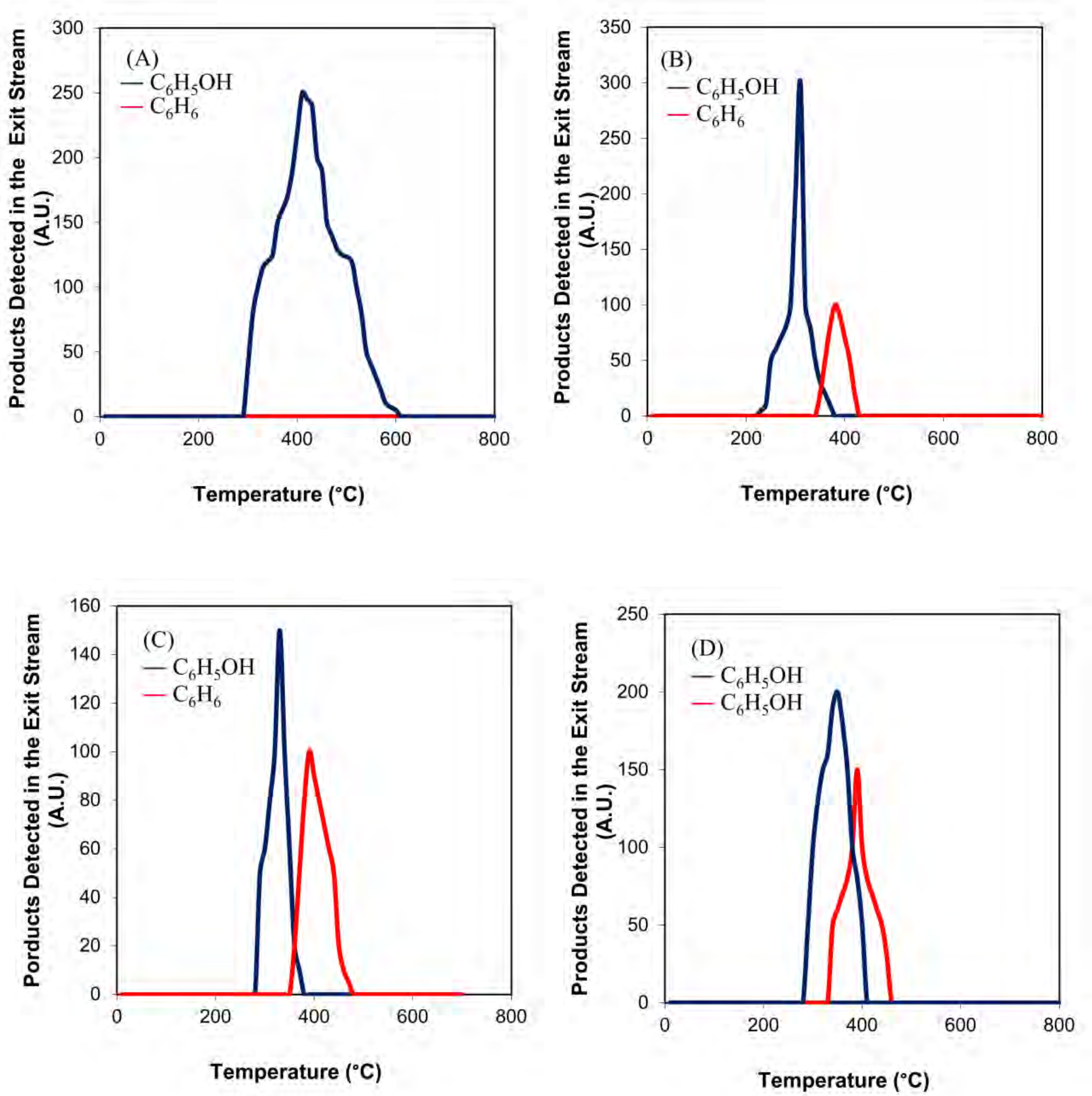

Figure 5.12: Benzene phenol detected in the exit stream during TPO testing from ((A) the β(150) sample containing 90 – 100 mg g^{-1} 2-nitrophenol, (B) 0.1%Cuβ(150) sample containing 50 – 60mg g^{-1} 2-nitrophenol, (C) 1.02%Cuβ(150) sample containing 70 – 80 mg g^{-1} 2-nitrophenol and (D) 2.0%Cuβ(150) sample containing 90 –100 mg g^{-1} 2-nitrophenol. (Conditions: 100 mg sample, 3% (v/v) O_2 in He at 50 ml min^{-1}, Temperature ramped 10°C min^{-1}).

Figures 5.13 (A & B) illustrate the desorption profile of phenol and benzene over β(300) and 1.30%Cuβ(300) during the temperature programmed oxidation of adsorbed 2-nitrophenol. In the absence of copper, phenol only is detected in the exhaust gas stream as shown in Figure 5.13 (A). Similar to the (25) and (150) Beta zeolites, there was no evidence of benzene.

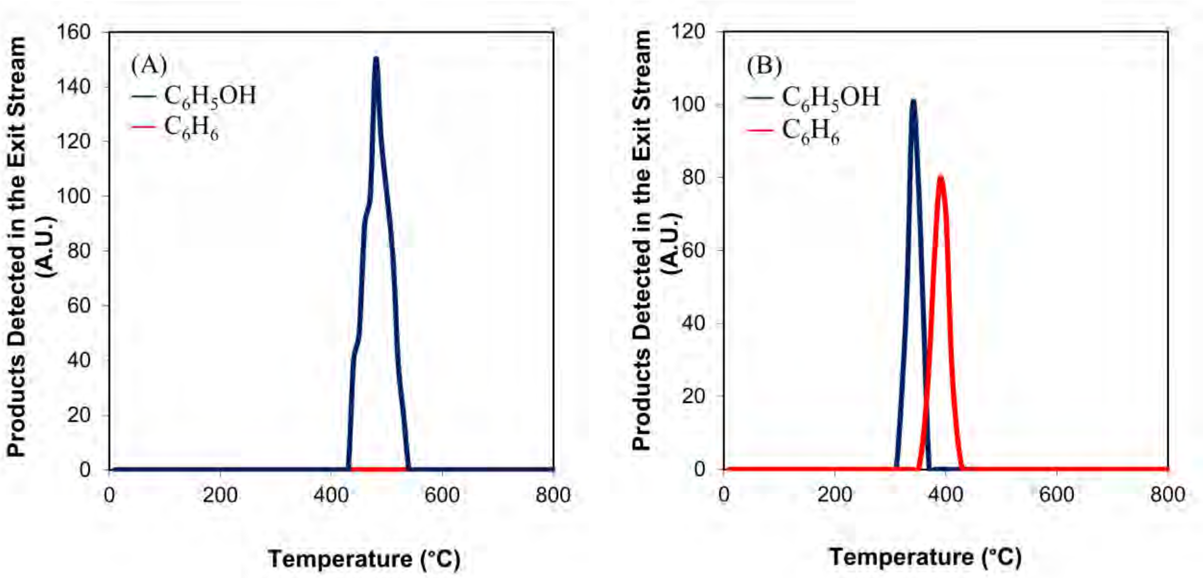

Figure 5.13: Benzene and phenol detected in the exit stream during TPO testing from (A) the β(300) sample containing 70 – 80 mg g^{-1} 2-nitrophenol and (B) 1.30%Cuβ(300) sample containing 70 – 80mg g^{-1} 2-nitrophenol. (Conditions: 100 mg sample, 3% (v/v) O_2 in He at 50 ml min^{-1}, Temperature ramped 10°C min^{-1}).

The presence of copper on the Beta zeolite, 1.30%Cuβ(300), resulted in the desorption of both phenol and benzene. The presence of extra-framework copper reduces the temperature of formation of these organic compounds. In the absence of copper, phenol is observed between 410 – 550°C. This reduces considerably, in the presence of copper, to 350 – 410°C.

Minor levels of nitrogen oxides (NO and NO_2) were also detected in the exit stream during the temperature programmed desorption of 2-nitrophenol. Figures 5.14 (A - C) displays the evolution of these nitrogen oxide compounds from the β(25), 1.20%Cuβ(25) and 1.95%Cuβ(25) samples, respectively.

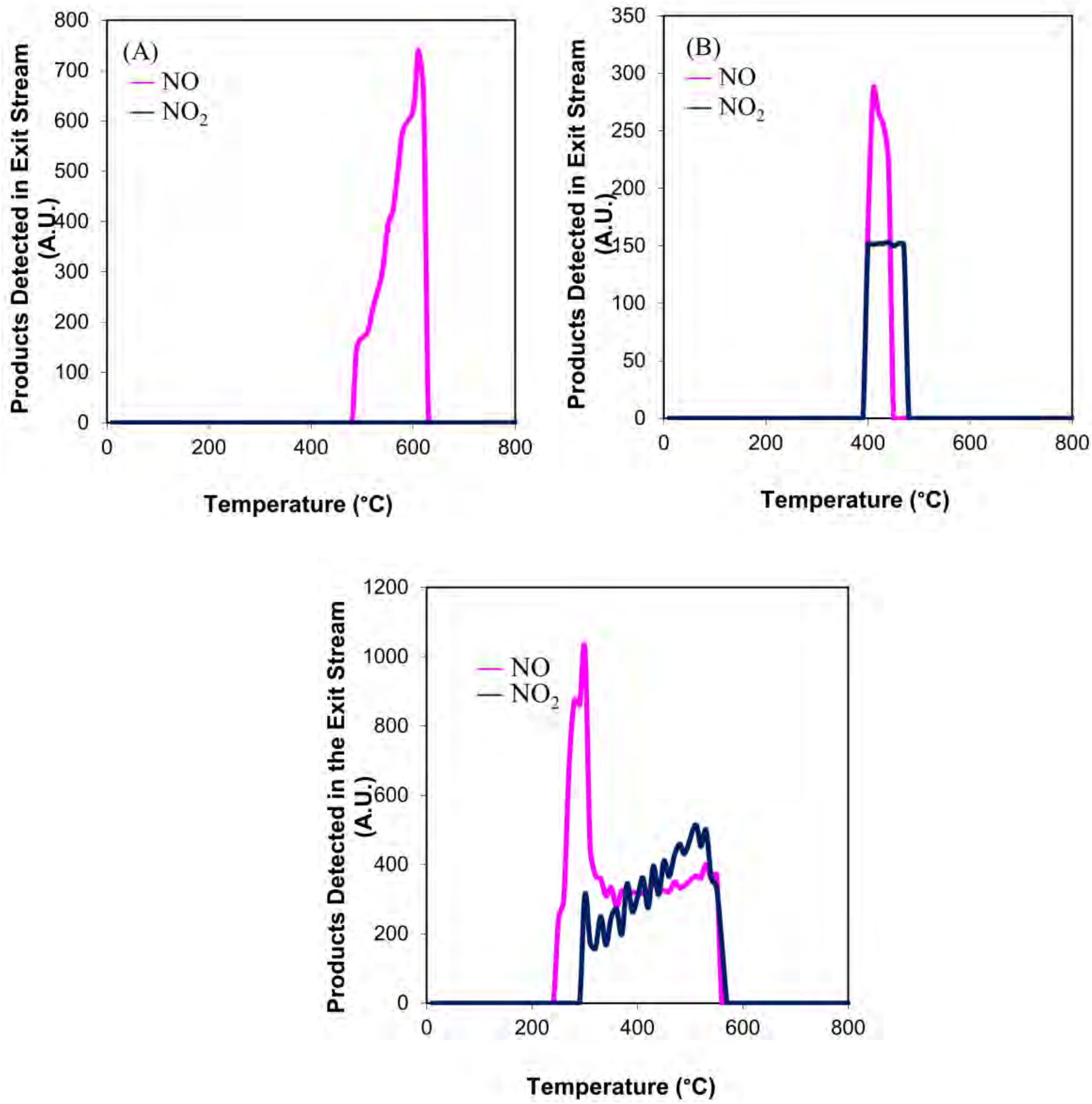

Figure 5.14: Nitrogen oxide and nitrogen dioxide detected in the exit stream during TPO testing from (A) the β(25) sample containing 40 – 50 mg g^{-1} 2-nitrophenol, (B) 1.20%Cuβ(25) sample containing 80 – 90mg g^{-1} 2-nitrophenol and (C) 1.95%Cuβ(25) sample containing 90 – 100 mg g^{-1} 2-nitrophenol. (Conditions: 100 mg sample, 3% (v/v) O_2 in He at 50 ml min^{-1}, Temperature ramped 10°C min^{-1}).

Figure 5.14 (A) illustrates the evolution of nitrogen oxides from the unmodified Beta zeolite β(25). NO_2 was not detected and NO was only observed at temperatures in excess of 600°C. Figures 5.14 (B & C) display the principle nitrogen oxides detected in the exhaust gas stream during the catalytic oxidation of adsorbed 2-nitrophenol from the 1.20%Cu(25) and 1.95%Cuβ(25) samples. Both NO and NO_2 are detected. Both species are detected at temperatures above 395°C from the 1.20%Cuβ(25) sample. Increasing the copper content on the Beta zeolite to 1.95% reduces the temperature at which both NO and NO_2 are detected (Figure 5.14 (C)). For this sample initially there is a relatively high level of NO above 200°C however as the temperature increases above 250°C there is a decrease in NO emitted and a corresponding increase in emission levels of NO_2. The temperature programmed oxidation profile of CO_2 illustrated in Figure 5.8 overlaps with the temperature programmed oxidation profile of nitrogen oxides. For example, CO_2 was detected between 320 – 680°C while NO and NO_2 were detected at temperature in excess of 200°C from the 1.95%Cuβ(25) sample. It is evident that the presence of copper on the Beta zeolite effectively lowers the temperature at which the nitrogen oxides are detected. This is illustrated by the shift to lower temperatures as shown in Figures 5.14 (A - C). It is also clear that the presence of extra-frame work copper promotes the formation of NO_2. NO_2 is not detected on the β(25).

Figures 5.15 (A - D) display the nitrogen oxides detected in the exhaust gas stream during the temperature programmed oxidation of adsorbed 2-nitrophenol from β(150), 0.1%Cuβ(150), 1.02%Cuβ(150) and 2.0%Cuβ(150), respectively. Similar to the β(25) sample, nitrogen monoxide is the only nitrogen oxide detected as illustrated in Figure 5.15 (A) for β(150).

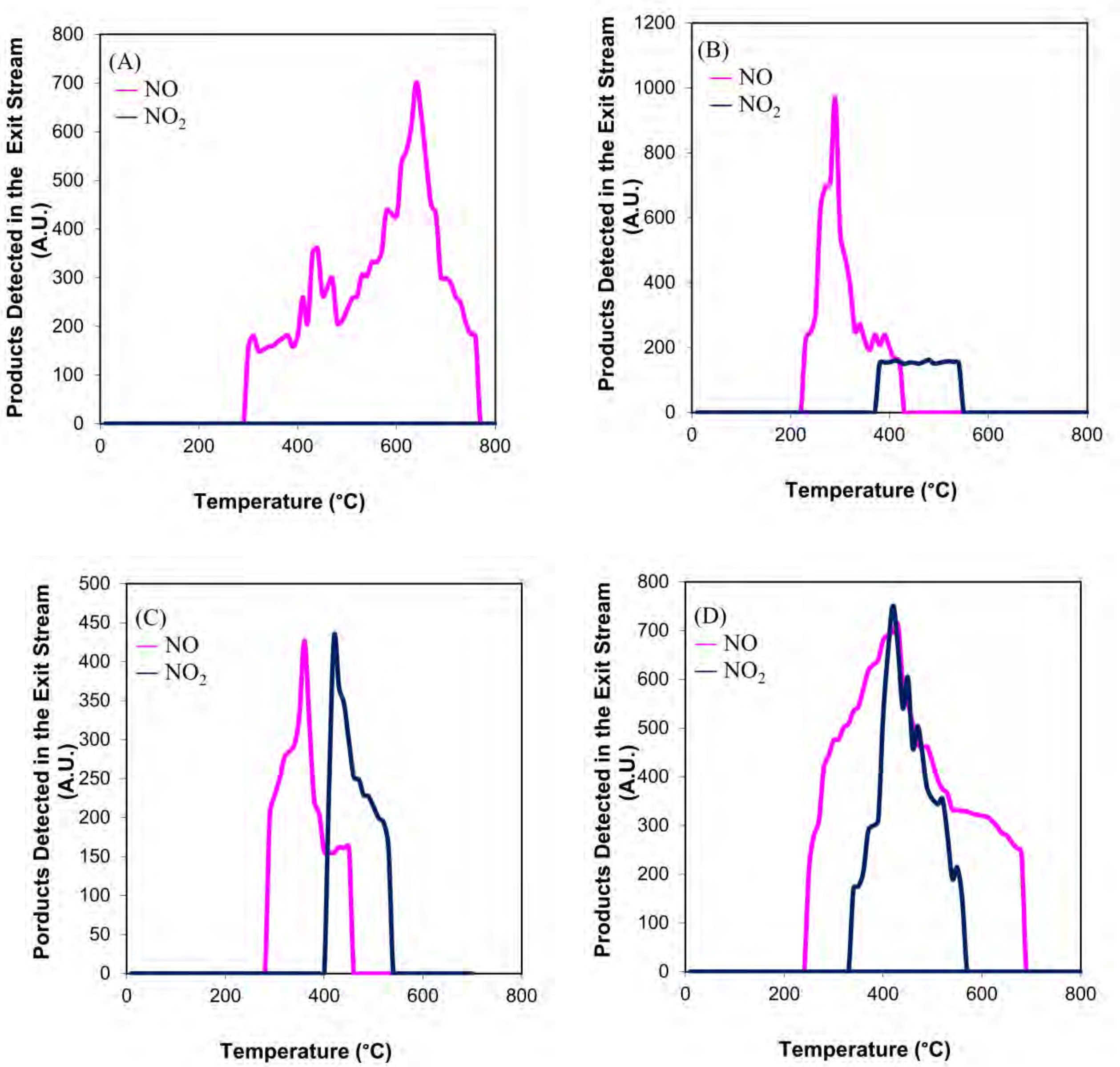

Figure 5.15: Nitrogen oxide and nitrogen dioxide detected in the exit stream during TPO testing from ((A) the β(150) sample containing 90 – 100 mg g^{-1} 2-nitrophenol, (B) 0.1%Cuβ(150) sample containing 50 – 60mg g^{-1} 2-nitrophenol, (C) 1.02%Cuβ(150) sample containing 70 – 80 mg g^{-1} 2-nitrophenol and (D) 2.0%Cuβ(150) sample containing 90 –100 mg g^{-1} 2-nitrophenol. (Conditions: 100 mg sample, 3% (v/v) O_2 in He at 50 ml min^{-1}, Temperature ramped 10°C min^{-1}).

Figure 5.16 (A & B) displays the nitrogen oxide compounds detected from the catalytic oxidation of 2-nitrophenol adsorbed on (300) and 1.30%Cuβ(300), respectively. In figure 5.16 (A), similar to both the β(25) and β(150) sample, only NO is detected from the β(300) sample at temperatures of 420°C. In Figure 5.16 (B), both NO and NO_2 are detected at temperatures between 300 – 420°C from the 1.30%Cuβ(300) sample. Compared to the β(300) sample the levels of NO are significantly less, and the oxides are detected at lower temperatures.

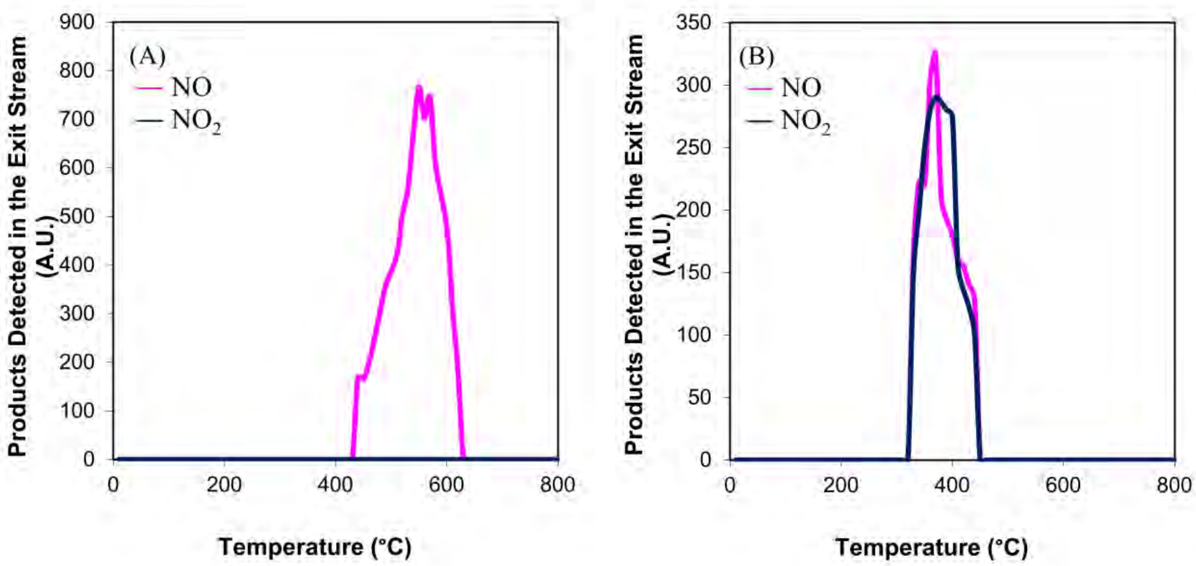

Figure 5.16: Nitrogen oxide and nitrogen dioxide detected in the exit stream during TPO testing from (A) the β(300) sample containing 70 – 80 mg g^{-1} 2-nitrophenol and (B) 1.30%Cuβ(300) sample containing 70 – 80 mg g^{-1} 2-nitrophenol. (Conditions: 100 mg sample, 3% (v/v) O_2 in He at 50 ml min^{-1}, Temperature ramped 10°C min^{-1}).

During the temperature programmed oxidation of adsorbed 2-nitrophenol, a product with an a.m.u. of 28 was also detected from all samples. This corresponds to that of nitrogen and / or carbon monoxide. Figure 5.17 (A - C) illustrate the CO/N_2 profiles observed following the TPO of adsorbed 2-nitrophenol from all the prepared samples. These profiles may correspond to that of CO, which maybe formed as an incomplete oxidation production during TPO or formed from the fragmentation of CO_2 in the mass spectrometer.

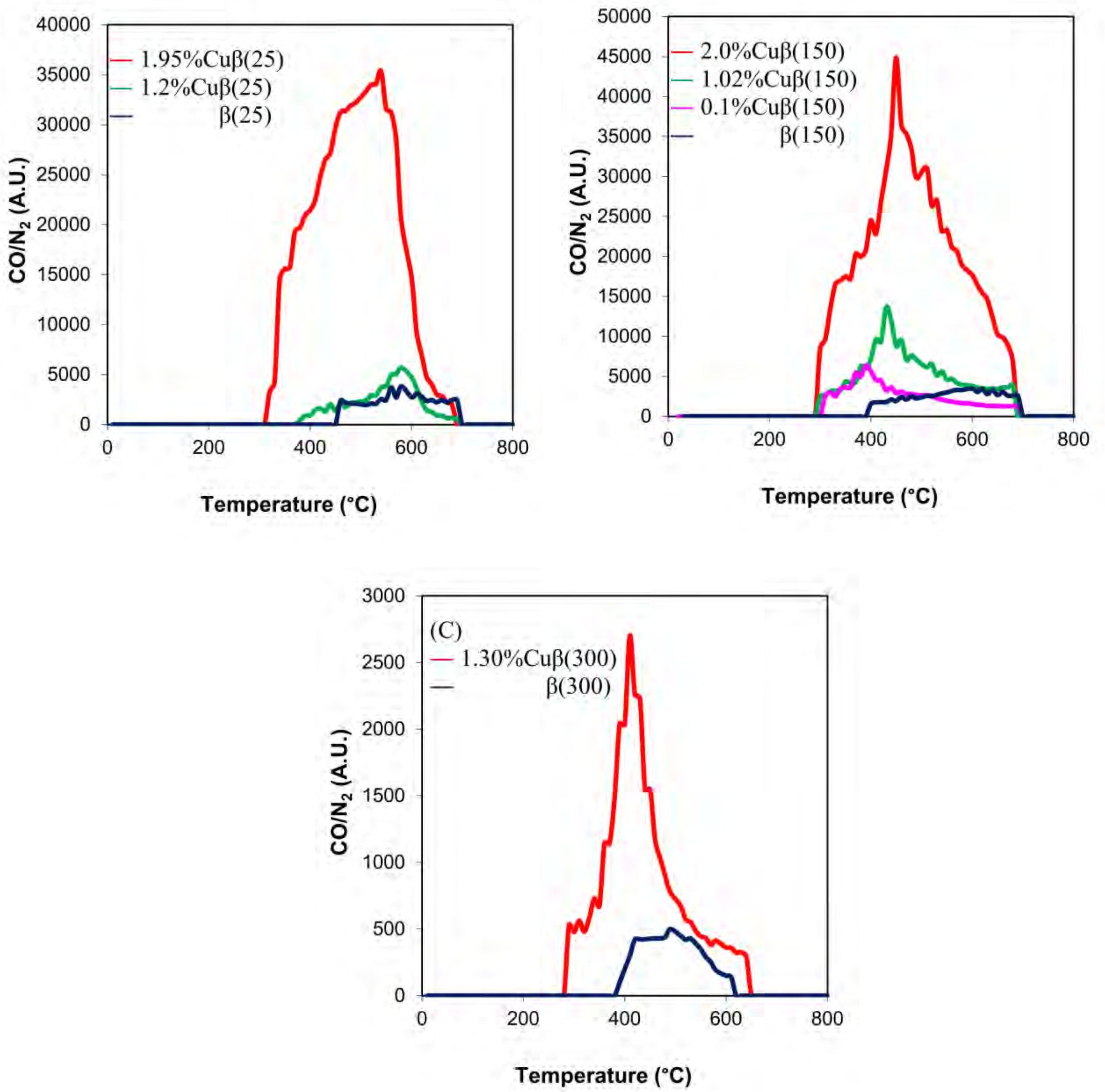

Figure 5.17: CO/N_2 detected in the exit stream during TPO testing from (A) the β(25) samples containing 40 – 100 mg g^{-1} 2-nitrophenol, (B) β(150) samples containing 50 – 100 mg g^{-1} 2-nitrophenol and (C) β(300) samples containing 70 – 80 mg g^{-1} 2-nitrophenol. (Conditions: 100 mg sample, 3% (v/v) O_2 in He at 50 ml min^{-1}, Temperature ramped 10°C min^{-1}).

Figure 5.18 shows a typical temperature programmed oxidation profile of adsorbed 2-nitrophenol (in this case 1.02%Cuβ(150)). The degradation of the adsorbed 2-nitrophenol on 1.02%Cuβ(150) is accompanied by an increase in carbon dioxide levels detected in the exhaust gas stream. The carbon dioxide begins to form at temperatures above 300°C and continues to rise sharply up to about 420°C. During this time there is a sharp decrease in the oxygen content of the exit stream, indicating that the 2-nitrophenol is being oxidized by O_2 to

CO_2. The CO_2 profile is very similar to the CO profile. The greatest reduction in the level of O_2 detected occurs at a temperature of 420°C which corresponds to the peak in the detection of both CO_2 (the complete oxidation product) and CO. There is clearly sufficient O_2 for the complete oxidation process, therefore the CO detected is a fragment formed from CO_2 in the mass spectrometer.

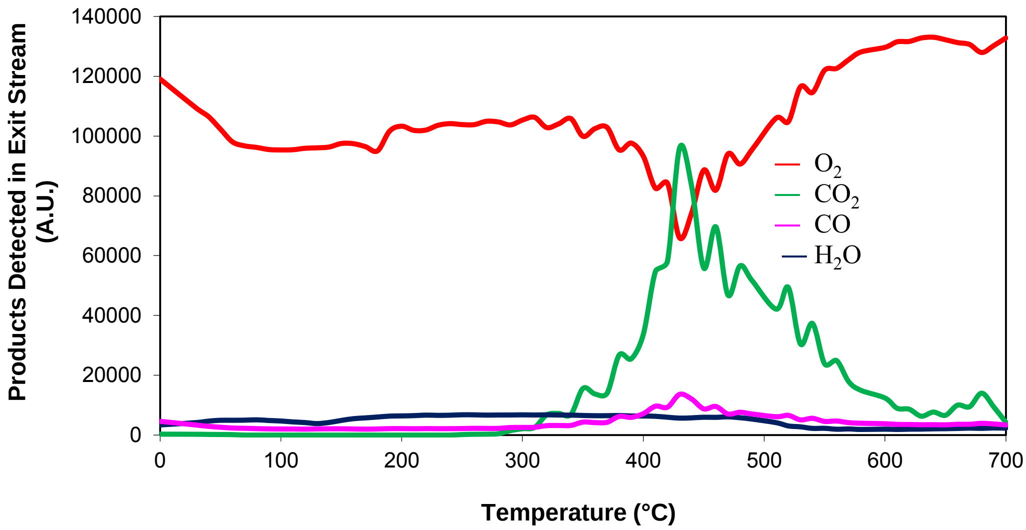

Figure 5.18: Products detected in the exit stream from the catalytic temperature programmed oxidation of adsorbed 2-nitrophenol on 1.02%Cuβ(150). (Conditions: 100 mg of sample containing 70 -80 mg g^{-1} 2-nitrophenol, 3% (v/v) O_2 / He gas flow rate 50ml min^{-1}, temperature ramped at 10°C min^{-1}).

It cannot be ruled out that the species observed at a.m.u. of 28 by the Beta zeolites is not nitrogen. Formation of nitrogen may occur by the oxidation of the nitrogen present in the 2-nitrophenol compound. For example, when nitrogen oxide species are formed during the temperature programmed oxidation of adsorbed 2-nitrophenol, they may be reduced in the presence of hydrocarbons such as benzene and phenol to N_2. For example, Figure 5.11 (C) and 5.14 (C) display the temperature profiles of benzene, phenol and nitrogen oxides, respectively, during the temperature programmed oxidation of adsorbed 2-nitrophenol on

1.95%Cuβ(25) sample. It is clearly shown in Figures 5.11 (C) and 5.14 (C) that as the levels of nitrogen oxides decrease so also do the levels of phenol and benzene this would indicate that as the nitrogen oxides are being reduced to N_2 in the presence of these hydrocarbons.

5.3.2 Potential breakdown pathway of 2-nitrophenol during the temperature programmed oxidation process.

This study seeks to evaluate the feasibility of catalytically oxidizing the adsorbed 2-nitrophenol into carbon dioxide, water and nitrogen, whilst minimizing the formation of nitrogen oxides. Given that the complete oxidation of 2-nitrophenol would result in the formation of CO_2, NO_2 and H_2O, these were therefore the most common ions detected during the temperature programmed oxidation of adsorbed 2-nitrophenol on all Beta zeolite samples. However minor incomplete oxidation product such as NO, C_6H_6 C_6H_5OH and N_2/CO were also detected.

In order to establish the potential breakdown pathways of the adsorbed 2-nitrophenol during the temperature programmed oxidation process it is necessary to investigate the temperatures at which each species were detected. Table 5.4 lists each of the species detected during the catalytic oxidation of adsorbed 2-nitrophenol from each of the prepared catalysts, along with the temperature range at which each species were detected. From Table 5.4 the first species detected in the exhaust gas stream is unreacted 2-nitrophenol which is simply desorbed at temperatures in excess of 190 °C from β(25), β(150), β(300) and 0.1%Cuβ(150) samples. No other species was detected during the desorption of 2-nitrophenol from the unmodified samples as shown in Table 5.4, indicating that it is a simple desorption process. As the temperature increases above 200°C it is evident that some of the 2-nitrophenol remains adsorbed onto the Beta zeolite as a variety of oxidation products are detected in the exhaust gas stream such as CO_2, NO, C_6H_5OH, CO/N_2, H_2O. While it is evident from Table 5.4 that the presence of copper results in a reduction in the desorption of 2-nitrophenol, it also reduces the temperatures at which the oxidation of the remaining adsorbed 2-nitrophenol commences at and it also increases the number of oxidation products detected in the exhaust gas stream during TPO testing.

Figure 5.4: Species detected from all Beta zeolite samples during the temperature programmed oxidation of adsorbed 2-nitrophenol with respect of temperature (°C).

Sample Name	$C_6H_5NO_3$	C_6H_5OH	C_6H_6	NO_2	NO	CO_2	CO/N_2
β(25)	190 -350	490 – 670	-	-	490 – 620	460 – 690	460 – 690
1.20%Cuβ(25)	-	400 – 470	400 – 470	400 – 470	400 - 440	380 - 690	380 – 690
1.95%Cuβ(25)	-	290 – 550	340 - 460	300- 560	250 – 550	320 – 690	320 – 690
Cuβ(150)	180 - 300	330 – 600	-	-	300 – 650	400 – 690	400 – 690
0.1%Cuβ(150)	190 -320	230 - 370	350 - 420	380 – 540	230 – 420	350 - 690	340 – 690
1.02%Cuβ(15)	-	290 - 370	360 – 470	410 – 530	290 - 450	310 – 680	310 – 680
2.0%Cuβ(150)	-	290 - 400	350 - 450	340 – 560	250 - 680	300 – 680	300 – 680
Cuβ(300)	200 - 320	440 - 530	-	-	440 - 620	390 – 610	390 – 610
1.3%Cuβ(300)	-	320 – 360	360 - 420	330 – 440	330 - 440	290 – 640	290 – 640

Figures 5.19 (A - C) illustrates the temperature programmed oxidation profiles of 2-nitrophenol, nitrogen oxide, phenol, benzene, and nitrogen dioxide detected from β(25), 1.20%Cuβ(25) and 1.95%Cuβ(25) respectively, during the TPO of adsorbed 2-nitrophenol. It is evident in Figure 5.19 (A) that unreacted 2-nitrophenol is simply being desorbed from the solid during TPO testing as no other products are simultaneously detected. Carbon dioxide is the first oxidation product to be detected at temperatures in excess of 460°C, while both nitrogen monoxide and phenol are detected at temperatures in excess of 440°C which indicate that the unmodified Beta zeolite has catalytic properties which are independent of the copper active sites. However in Figure 5.19 (B - C) it is evident that in the presence of copper, 2-nitrophenol is retained on the Beta zeolite above the temperatures at which it desorbed from the unmodified sample (i.e. temperatures in excess of 190°C). As the temperature increases it is evident from Table 5.4 that the adsorbed 2-nitrophenol is oxidized in the presence of copper with the detection of additional breakdown species such as NO_2 and C_6H_6.

Currently disagreements remain in the literature regarding the mechanism of NO oxidation over zeolites. Studies by Artioli et al., (2013) and Loiland and Lobo (2014) suggest that microporous void spaces provide catalytic sites that accelerate steady state NO conversion by means of transitional state confinement and stabilization. Other studies by Zhang et al., (2015) investigated the influence of Si/Al ratio on the NO to NO_2 conversion and reported that lower Si/Al ratios was not expected to have higher conversions and that the influence of Si/Al ratio is less significant than that of other factors such as pore volume and size which is in agreement with the results presented in Table 5.4 where the temperature ranges at which NO and NO_2 are detected at from the unmodified samples (β(25), β(150) and β(300)) appear to be independent on Si/Al ratio of the Beta zeolite. While Pereda-Ayo et al., (2014) investigated the role of different copper species on the activity of Cu/zeolite catalysts for SCR of NO_x. They reported on the presence of different Cu species such as CuO and Cu(II) which were exchanged on the tetrahedral and octahedral positions of the zeolite framework. They concluded that the CuO species were more abundant on higher copper loading catalysts such as ZSM5 catalysts while isolated Cu(II) ions are more abundant on lower copper content catalysts and Beta catalysts. They concluded that CuO catalyzes the oxidation of NO to NO_2 and this favours the reduction of NO_x at lower temperatures while isolated Cu(II) ions maintain high NO_x conversion at high temperatures They also reported that catalysts with low CuO content exhibited higher selectivity towards N_2 at increasing temperatures. Their finding support what was observed in this work regarding the temperatures at which NO and NO_2 and CO/N_2 were detected at as outlined in Table 5.4, with NO being detected at lower temperatures and NO_2 detected at higher temperatures. It is also evident from Table 5.4 that the temperature range at which CO_2 is detected at overlaps the temperature ranges of both NO and NO_2 which suggest the complete oxidation of adsorption 2-nitrophenol with minor amounts of NO and NO_2 being produced. This is further supported by the higher levels of CO_2 being detected (Figures 5.6, 5.8 & 5.10) in comparison to both NO and NO_2 (Figure 5.14 – 5.17).

In relation to the detection of both NO and NO_2 during TPO testing of adsorbed 2-nitrophenol from the copper modified samples (Figures 5.18 (A - C)) these previous studies and other influencing factors must be taken into consideration. As Cu modified zeolites have been reported to be highly effective in the oxidation of NO to NO_2 (Yokoyama and Misono (1994)), NO maybe oxidised in the presence of Cu to NO_2 and this would therefore account for the absence of NO_2 in Figure 5.18 (A). It is evident in Figures 5.18 (B - C) that NO is being oxidised to NO_2 in the presence of copper in the modified zeolites. In Figure 5.18 (C) NO is first detected at a temperature of 250°C with NO_2 being detected at a higher temperature of 300°C. This is possibly due to it being retained on the Cu Beta zeolite until being desorbed at these higher temperatures.

As nitrogen oxides are the first species detected during the TPO testing of the adsorbed 2-nitrophenol it suggests that the oxidation of the adsorbed 2-nitrophenol commences with the breakdown of the nitro group on the 2-nitrophenol molecule adsorbed on both the unmodified and the copper modified Beta zeolites. The decomposition of the 2-nitrophenol in this manner results in the formation of phenol as the nitrogen group is oxidised into NO and subsequently into NO_2 in the presence of copper. This is evident in Figure 5.18 (A - B) as NO is formed C_6H_5OH is also detected.

While the presence of copper results in a downward shift in temperatures at which each of these species are detected at (Figure 5.18 (B-C)) it also results in the formation of benzene. In Figure 5.18 (B) it appears that the decomposition of the adsorbed 2-nitrophenol commences with an attack on the nitro group with the detection of NO, NO_2, C_6H_5NO and C_6H_6 all at temperatures in excess of 400°C, with CO_2 being detected at 280°C. While in Figure 5.18 (C) these species are detected at slightly different temperatures to each other. In order to understand the possible reasons for (1) the detection of benzene and (2) the temperature difference between the detection of each species it is necessary to take two factors into consideration. Firstly that transition metal cations have been reported to improve the activity of zeolites for the oxidation of hydrocarbons by increasing the zeolite acidity (Antunes et al., 2001) and secondly copper displays strong interactions towards benzene molecules, which has been reported previously by Talber et al., 2013 to be a problem for benzene desorption from copper exchanged HZSM5. In the absence of copper only phenol is detected which is clearly shown in Figure 5.18 (A) which demonstrates that the zeolite has some capability for decomposition/oxidation of hydrocarbons. While in Figures 5.18 (B – C) greater levels of phenol are detected in comparison to benzene, with lower levels of benzene detected at slightly higher temperatures (Figure 5.18 (C) only). Therefore it is possible that benzene is produced at lower temperatures with phenol but is retained on the copper modified zeolites with subsequent desorption occurring at higher temperatures. Increasing temperatures not only results in the desorption of benzene but also promotes the complete oxidation of benzene into CO_2 which would account for the decrease in benzene emissions at temperatures in excess of 400°C. The fact that no other organic species were detected in the exit stream during TPO of adsorbed 2-nitrophenol on the copper modified Beta zeolite would further support the complete oxidation of benzene to CO_2, this is also supported by the larger levels of CO_2 observed during the TPO of adsorbed 2-nitrophenol.

It is evident in Figures 5.18 (A – C) that not all the phenol is converted into benzene as seen by the larger emission profile of phenol, which could be due to phenol being more stable at higher temperatures or due to NO/NO_2 molecules competing with phenol molecules for the Cu active sites.

As shown in Table 5.4 the temperature range at which CO_2 is detected overlaps with the temperatures ranges at which both phenol and benzene are detected during the temperature programmed oxidation of adsorbed 2-nitrophenol which would suggest that the total oxidation of the adsorbed 2-nitrophenol to CO_2 is favoured, for example the temperature at which CO_2 is detected ranges from 300 to 700°C, while the temperature range of phenol and benzene are 290 – 550 °C and 340 – 460°C respectively for the 1.95%Cuβ(25) sample (Figure 5.19 (C)).

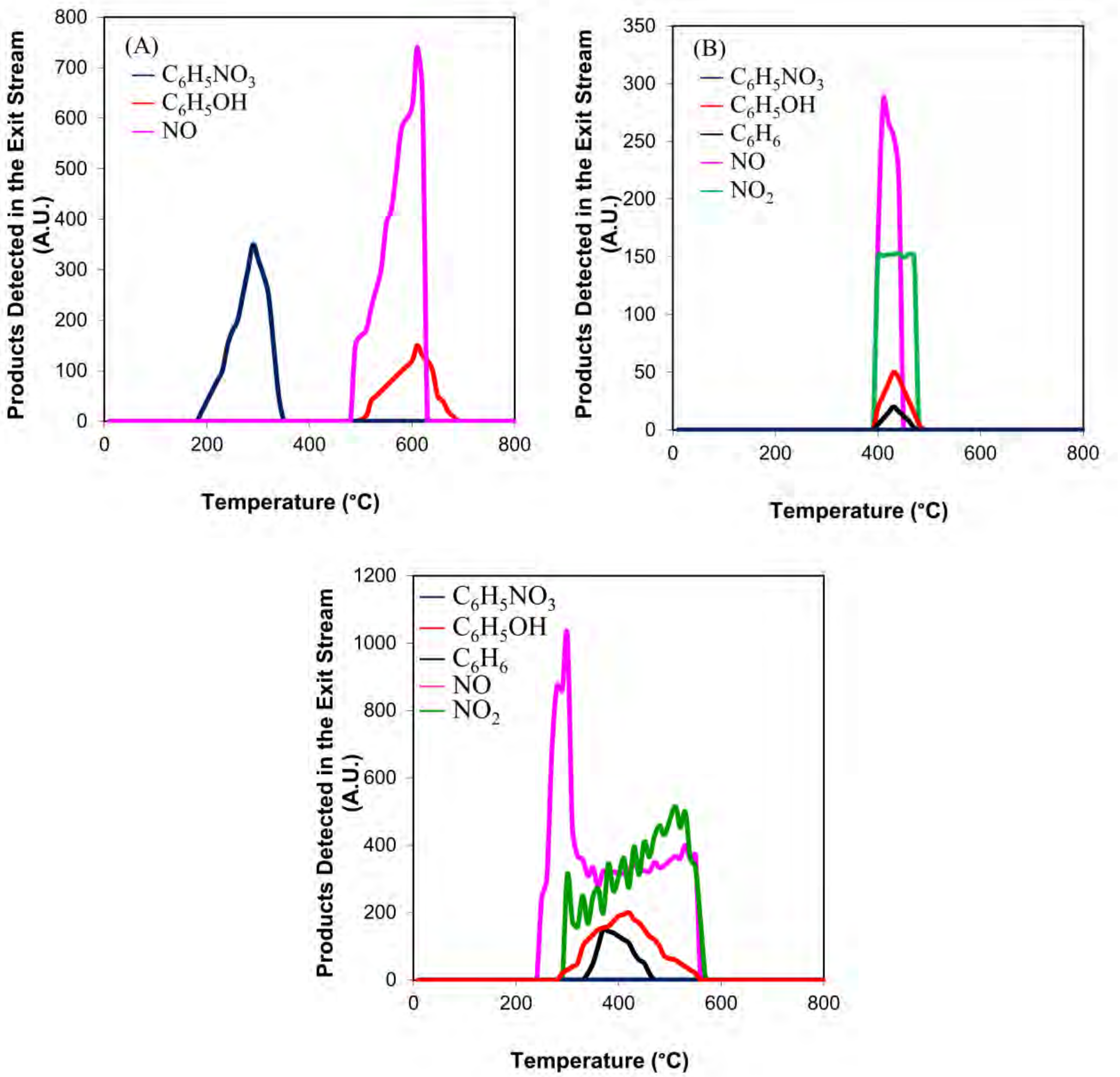

Figure 5.19: Products detected in the exit stream during TPO testing of (A) the β(25) sample containing 40 – 50 mg g^{-1} 2-nitrophenol, (B) 1.20%Cuβ(25) sample containing 80 – 90mg g^{-1} 2-nitrophenol and (C) 1.95%Cuβ(25) sample containing 90 – 100 mg g^{-1} 2-nitrophenol. (Conditions: 100 mg sample, 3% (v/v) O_2 in He at 50 ml min^{-1}, Temperature ramped 10°C min^{-1}).

Greater levels of CO_2 as illustrated in Figures 5.8, 5.10 and 5.12 in comparison to benzene and phenol, Figures 5.19 (A - C), are consistently observed during the oxidation process. This suggests that the copper modified Beta zeolite is capable of totally oxidising the adsorbed 2-nitrophenol to CO_2, while the decrease in the levels of phenol and benzene would also indicate their total oxidation to CO_2. However after the TPO testing of adsorbed 2-nitrophenol on all the beta zeolite samples a noticeable colour change of the sample from light green to a pale brown colour was observed. This indicated that during the temperature programmed oxidation of adsorbed 2-nitrophenol coke is formed. The presence of coke results in some of the carbon content of the adsorbed 2-nitrophenol being retained on the zeolites after TPO testing and therefore may account for variations in the levels of CO_2, phenol and benzene detected. This formation of carbonaceous compounds (coke) has been reported to be catalysed by the presence of Bronsted acid sites in the zeolite (Tabler et al., 2013).

The temperature programmed oxidation profiles of 2-nitrophenol, phenol, benzene and the nitrogen oxides detected from the exhaust gas stream during the temperature programmed oxidation of adsorbed 2-nitrophenol from the β(150), 0.1%Cuβ(150), 1.02%Cuβ(150) and the 2.0%Cuβ(150) are displayed in Figure 5.20 (A - D), respectively. Similar to β(25), 2-nitrophenol is desorbed from the β(150) sample at 190°C in the absence of any other species while as the temperature increases above 290°C NO and phenol are simultaneously detected as the remaining adsorbed 2-nitrophenol is partial oxidised by the Beta zeolite (Figure 5.20 (A)). In the presence of copper however the levels of 2-nitrophenol desorbed are greatly reduced with copper again displaying a strong interaction with the adsorbed 2-nitrophenol on the Beta zeolite. As temperatures increase above 200°C a variety of breakdown products such as nitrogen oxide, phenol, benzene and nitrogen dioxide are detected from the 0.1%Cuβ(150), 1.02%Cuβ(150) and 2.0%Cuβ(150) samples. Similar to the β(25) samples, the oxidation of the adsorbed 2-nitrophenol commences with the detection of NO, indicating that the decomposition of 2-nitrophenol on the β(150) samples is also initiated by the oxidation of the nitrogen containing group on the 2-nitrophenol molecule resulting in an increase in NO and phenol in the exit stream. Indeed both are detected at the same temperatures as indicated in Figures 5.20 (B - C) while in Figure 5.20 (D) NO is detected at a temperature of 250°C while phenol is detected at a higher temperature of 290°C. This would suggest that the phenol is adsorbed onto the copper modified Beta zeolite and therefore only being detected when desorbed at higher temperatures.

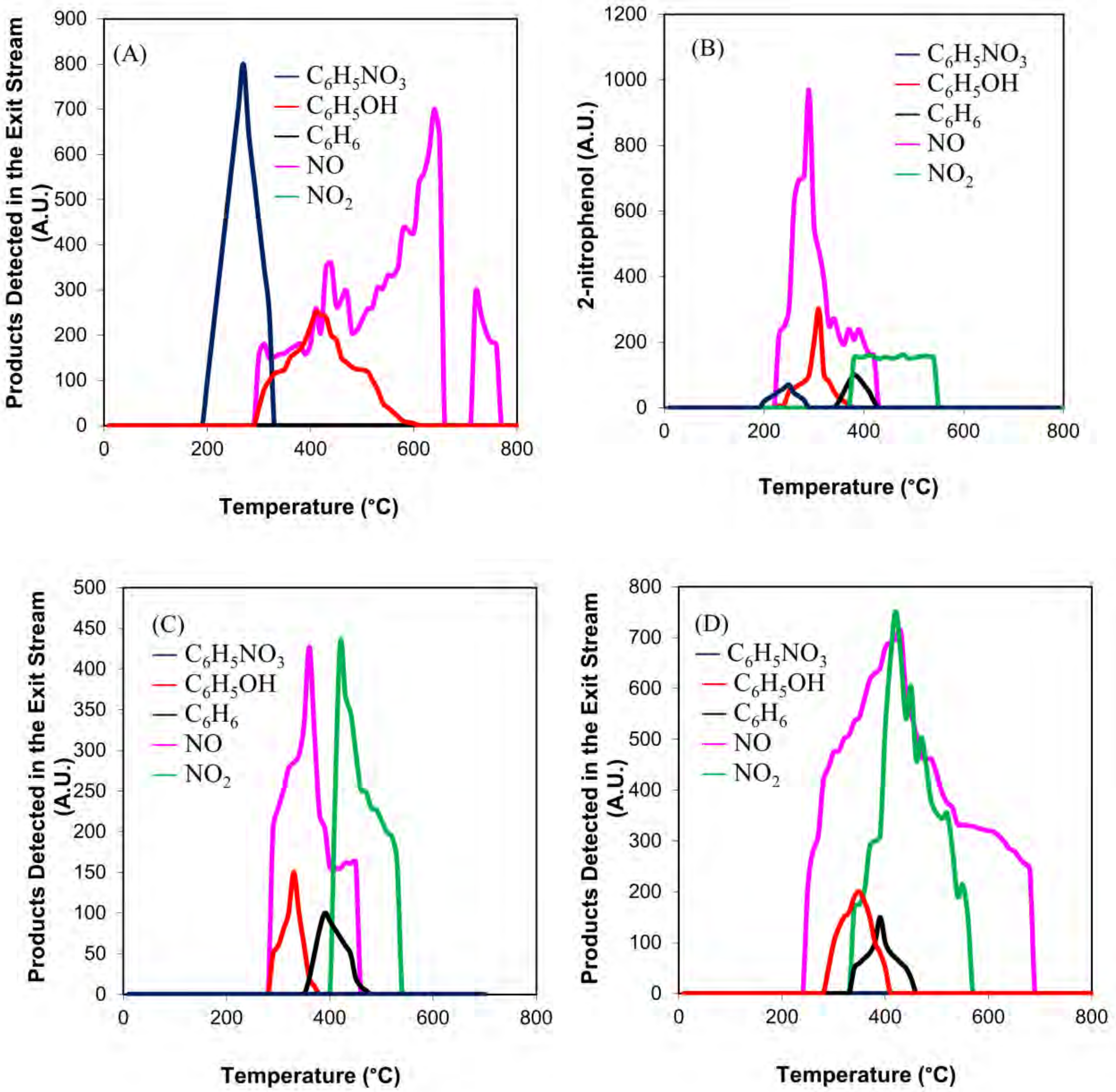

Figure 5.20: Products detected in the exit stream during TPO testing of (A) the β(150) sample containing 90 – 100 mg g^{-1} 2-nitrophenol, (B) 0.1%Cuβ(150) sample containing 50 – 60mg g^{-1} 2-nitrophenol, (C) 1.02%Cuβ(150) sample containing 70 – 80 mg g^{-1} 2-nitrophenol and (D) 2.0%Cuβ(150) sample containing 90 –100 mg g^{-1} 2-nitrophenol. (Conditions: 100 mg sample, 3% (v/v) O_2 in He at 50 ml min^{-1}, Temperature ramped 10°C min^{-1}).

The oxidation of NO to NO_2 commences at temperatures above 340°C in the presence of copper as shown in Figure 5.20 (B - D) which corresponds to the decrease in the detection levels of NO. While it is clearly shown in Figures 5.20 (B - D) that as the levels of phenol decreases there is a corresponding increase in the levels of benzene detected. This would suggest the decomposition of phenol in the presence of copper into benzene. The observed decrease in the benzene profiles in Figures 5.20 (B - D) is due to its complete oxidation to CO_2.While these organic molecules may play a role in the reduction of nitrogen oxides to N_2 which may be contributing to the detection of CO/N_2 over the temperature ranges outlined in Table 5.4. The temperatures at which these species are detected during TPO testing outlined in Table 5.4 would indicated that the decomposition of the adsorbed 2-nitrophenol on the unmodified and copper modified β(150) sample is initiated by the oxidation of the nitrogen group on the 2-nitrophenol molecule similar to the β(25) samples. This breakdown pathway is further supported by the detection of CO_2 at higher temperatures and over a larger temperature range to that of all the other species detected during TPO testing of adsorbed 2-nitrophenol on all the β(150) samples. This overlap in temperature range between the detection of CO_2 and all other species detected would suggest the complete oxidation of the remaining organic intermediates into CO_2.

Similar to β(25) and β(150) in the absence of copper, 2-nitrophenol is desorbed at temperature of 190°C while at a temperatures above 430°C the remaining adsorbed 2-nitrophenol undergoes partial oxidation producing NO and phenol from the β(300) sample. Once again, Figure 5.21 (B) illustrates the influence of copper on the oxidation process as an absence of 2-nitrophenol in the exhaust gas stream indicates its complete decomposition with the formation of NO, NO_2, phenol and benzene. Also the presence of copper greatly reduces the temperature at which these products are formed. For example, NO is detected at 440°C from the β(300) while at 330°C from the 1.30%Cuβ(300) samples. Similar to Figure 5.19 (A) and 5.20 (A) the detection of both NO and phenol at a temperature of 440°C would suggest that oxidation of the adsorbed 2-nitrophenol is initiated at the nitro group. In Figure 5.21 (B) NO, NO_2 and phenol are all detected at a similar temperature. NO and the NO_2

peaks seem to mirror each other which suggest that not all the NO is being oxidises into NO_2 which may be due to some of NO/NO_2 being adsorbed onto the copper sites on the Beta zeolite or due to saturation of copper active sites. While as the phenol peak decreases there is a corresponds increase in the detection of benzene similar to that observed for the β(25) and β(150) samples.

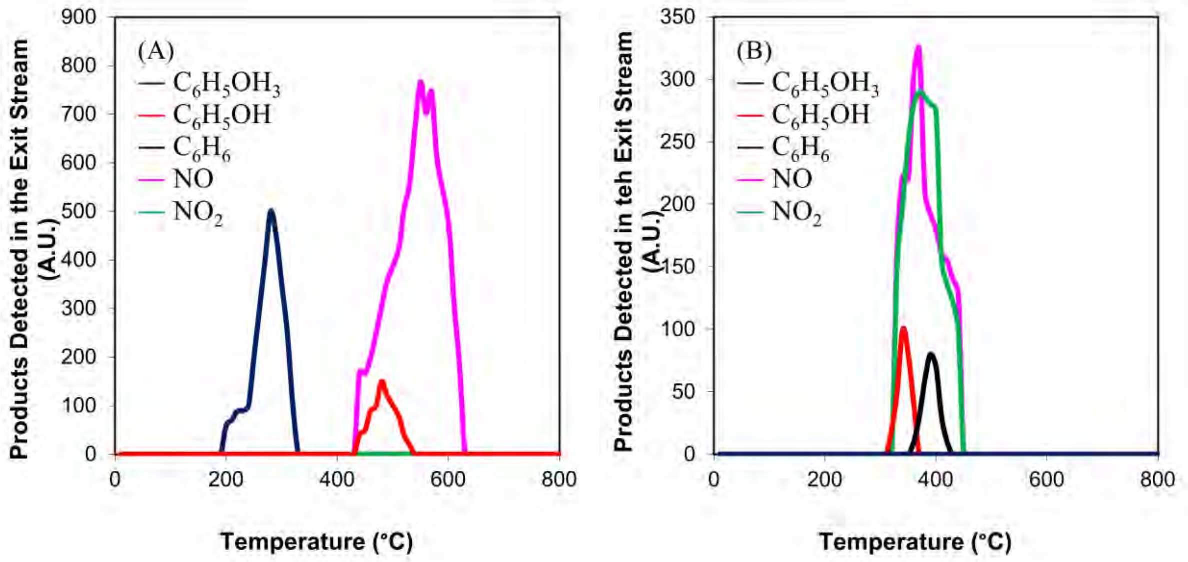

Figure 5.21: Benzene and phenol detected in the exit stream during TPO testing of (A) the β(300) sample containing 70 – 80 mg g^{-1} 2-nitrophenol and (B) 1.30%Cuβ(150) sample containing 70 – 80mg g^{-1} 2-nitrophenol. (Conditions: 100 mg sample, 3% (v/v) O_2 in He at 50 ml min^{-1}, Temperature ramped 10°C min^{-1}).

It is evident from this study that the temperature programmed oxidation of adsorbed 2-nitrophenol commences with the partial oxidation of the nitrogen group with a decrease in the levels of O_2 detected and an increase in the levels of CO_2. Given that the most significant product formed during the temperature programmed oxidation of adsorbed 2-nitrophenol is CO_2, these minor organic compounds produced are oxidised into the complete oxidation product CO_2. It is evident by the increase in levels of CO_2 observed that in the presence of copper the complete oxidation of the adsorbed 2-nitrophenol is enhanced, as benzene is completely oxidised to CO_2 and no other breakdown species are detected during the TPO testing. The formation of both phenol and benzene at such trace levels suggests that the copper modified beta zeolite is capable of oxidising 2-nitrophenol to CO_2 directly as evidenced by the greater levels of CO_2 observed. As shown in Table 5.4 the temperature range at which CO_2 is detected overlaps with the temperatures ranges at which both phenol and benzene are detected during the temperature programmed oxidation of adsorbed 2-nitrophenol which would suggest that as the decomposition of adsorbed 2-nitrophenol proceeds its total oxidation to CO_2 is favoured; for example the temperature emission profile of CO_2 ranges from 300 to 700°C, while the temperature ranges of phenol and benzene are 290 – 550 °C and 340 – 460°C respectively for the 1.95%Cuβ(25) sample. Greater emission profiles of CO_2 as illustrated in Figures 5.8, 5.10 and 5.12 in comparison to the emission profiles of benzene and phenol presented in Figures 5.19 to 5.21 also suggests that the adsorbed 2-nitrophenol is being completely oxidised into CO_2, while the decrease in emission profiles of phenol and benzene would indicate their total oxidation to CO_2.

The formation of CO_2 is also accompanied by an increase in the levels of CO detected as detailed in Table 5.4. This CO maybe formed due to the fragmentation of CO_2 during the mass spectrometry analysis or it may be an incomplete oxidation product formed during the incomplete oxidation of benzene. It has been reported previously by Tabler et al., 2013 that higher oxidation temperatures and higher copper loadings promote the oxidation of benzene to CO_2 whilst also increasing the CO formation by Cu/HZMS5 samples.

In chapters 2 and 4 of this work the adsorption of 2-nitrophenol from aqueous solution by unmodified Beta zeolites and copper modified Beta zeolites was found to be physical in nature, based on weak interactions such as Van der Waals forces. The adsorption process was found to be largely independent on the presence of copper with the silica-to-alumina ratio of the Beta zeolite having a greater influence on the adsorption levels of 2-nitrophenol. During the catalytic oxidation of adsorbed 2-nitrophenol it is apparent from Figures 5.19 (A), 5.20 (A) and 5.21 (A) that the silica-to-alumina ratio of the Beta zeolite does not affect the oxidation of the adsorbed 2-nitrophenol with 2-nitrophenol, nitrogen oxide and phenol being detected from β(25),β(150) and β(300) in similar temperature ranges.

In the absence of copper, the Beta zeolites display some activity in the catalytic oxidation of the adsorbed 2-nitrophenol possibly due to the presence of Bronsted acid sites. The Bronsted acid sites are essential for the formation of radical cations from unsaturated organic molecules and have been reported by Tabler et al., 2013 to be active in the cracking of benzene molecules in the oxidation of benzene to phenol. It is proposed that they play a role in the oxidation of the adsorbed 2-nitrophenol molecule. While it is evident that the presence of copper on the Beta zeolite greatly influences the overall oxidation process in relation to the temperature and the oxidation products detected. This suggests that the copper modified Beta zeolite possesses bifuntionality with the oxidation of the adsorbed 2-nitrophenol being carried out by both the Bronsted acid sites on the Beta zeolite and copper active sites such as Cu^{2+}. The main difference between these two catalysts (modified and unmodified Beta zeolites) is the increase in detection of oxidation products in the presence of copper. This observation leads to the conclusion that the copper active species enhance the oxidation of the adsorbed 2-nitrophenol.

.

5.4 References

Agarwal, S. K. and J. J. Spivey (1992) 'High – temperature SCR catalysts', *Applied Catalysis A: General*, **90**, 4.

Adam, F., Wong, J. –T. and Eng – Poh Ng (2013) 'Fast catalytic oxidation of phenol over iron modified zeolite L nanocrystals',*Chemical Engineering Journal*, **214**, 63-67.

Antunes, A. P., Ribeiro, M. F., Silva , J. M., Ribeiro, F. R., Magnoux, P. and M. Guisnet (2001) 'Catalytic oxidation of toluene over CuNaHY zeolites: Coke formation and removal' *Applied Catalysis B: Environmental*, **33**,149-164.

Artioli, N, Lobo, R. F. and E. Iglesia (2013) 'Catalysis by Confinement: Enthalpic Stabilization of NO Oxidation Transition States by Micropororous and Mesoporous Siliceous Materials' *Journal of Physical Chemistry, **117***, 20666-20674.

Baek, W. S., Kim, J. R. and S. K. Ihm (2004) ' Design of dual functional adsorbent / catalysts system for the control of VOC's by using metal loaded hydrophobic Y- zeolites', *Catalysis Today*, **93-95**, 575-581.

Carniti, P., Gervasini. A., Modica, V. H. and Nicoletta Ravasio (2000) 'Catalytic selective reduction of NO with ethylene over a series of copper catalysts on amorphous silicas', *Applied Catalysis B: Environmental*, **28**,175-185.

Chang, X., Guanzhong, L., Guo, Y., Wang, Y. and Y. Guo (2013) 'A high effective adsorbent of NO_x: Preparation, characterization and performance of Ca-beta zeolites', *Microporous and Mesoporous Materials*, **165**, 113-120.

Corma, A., Forne´s, V. and E. Palomares (1997) 'Selective catalytic reduction of NO*x* on Cu-beta zeolites', *Applied Catalysis B: Environmental*, **11**, 233-242.

De La Torre, U., Pereda – Ayo, B. and J. R. Gonzalez – Velasco (2012) ' Cu- zeolite NH_3-SCR catalysts for the NO_x removal in the combined NSR-SCR technology', *Chemical Engineering journal*, **207-208**, 10-17.

Despres, J., Koebel, M., Krocher, O., Elsener, M. and A. Wokaun (2003) 'Adsorption and desorption of NO and NO_2 on Cu-ZSM-5' *Microporous and Mesoporous Materials*, 58*,*175-183.

Franch-Martí, C., Jorda, J. L. C., Peral, I., Hernández-Fenollosa, J., Corma, A., Palomares, A.E., Rey, F. and G. Guilera (2012) ' TNU-9, a new zeolite for the selective catalytic reduction of NO: An in situ X-ray absorption spectroscopy study', *Journal of Catalysis*, **295**, 22-30.

Gharbani, P. and Mehrizad, A. (2012) 'Heterogeneous catalytic ozonation process for removal of 4-chloro-2-nitrophenol from aqueous solutions', *Journal of Saudi Chemical Society*, htt://dx.doi.org/10.1016/j.jscs.2012.07.013

Gopalakrishnan, R., Stafford, P. R., Davidson, J. E., Hecker, W. C. and C. H. Bartholomew (1993) 'Selective catalytic reduction of nitric oxide by propane in oxidizing atmosphere over copper-exchanged zeolites', *Applied Catalysis B: Environmental*, **2**, 165-182.

Iwamoto, M., Mizuni, N. and H. Yahiro (1993) 'Selective catalytic reduction of NO by hydrocarbon in oxidizing atmosphere', *Studies in Surface Science and Catalysis* **75**, 1285-1298.

Janas, J., Gurgul, J., Socha, P. R. and S. Dzwigaj (2009) 'Effect of Cu content on the catalytic activity of CuSiBEA zeolite in the SCR of NO by ethanol: Nature of the copper species', *Applied Catalysts B: Environmental*, **91**, 217-224.

Liotta, L. F., Gruttadauria, M., Carlo, D. G., Perrini, G. and V. Librando (2009) ' Heterogenous catalytic degradation of phenolic substrates: Catalysts activity', *Journal of Hazardous Materials*, **162**, 588-606.

Liu, P, Zhang, X., Yao, Y. and J. Wang (2009) 'Pt supported on β zeolite ion exchanged with Cr (III) for hydroisomerization of n-heptane', *Applied Catalysis A: General*, **371**, 142-147.

Loiland, J. A and R. F. Lobo (2014) 'Low temperature catalytic NO oxidation over microporous materials' *Journal of Catalysis*,. **311**, 412-423.

Metkar, S. P., Harold, P. M. and V. Balakotaiah (2012) 'Selective catalytic reduction of NO_x on combined Fe- and Cu- zeolite monolithic catalyst: sequential and dual layer configurations' *Applied Catalysis B: Environmental,* **111-112**, 76-80.

O' Brien, J., O'Dwyer. F. T. and T. Curtin (2008) 'A novel process for the removal of aniline from wastewaters' *Journal of Hazardous Materials*, **159**, 476-482.

Oturan, N., Hamza, M., Ammar, S., Abdelhedi, R. and A. M. Oturan (2011) 'Oxidation / mineralization of 2-nitrophenol in aqueous medium by electrochemical advanced oxidation processes using Pt / carbon-felt and BDD / carbon-felt cells'. *Journal of Electroanalytical Chemistry*, **661**, 66-71.

Shukla, P., Wang, S., Sing, K., Ang, H. M. and M. O. Tade (2010) 'Cobalt exchanged zeolites for heterogeneous catalytic oxidation of catalytic oxidation of phenol in the presence of peroxymonosulphate', *Applied Catalysis B: Environmental*, **99**, 163-169.

Sultana, A., Nanba, T., Sasaki, M., Haneda, M., Suzuki, K. and H. Hamada (2011) 'Selective catalytic reduction of NO_x with NH_3 over different copper exchanged zeolites in the presence of decane', *Catalysis Today*, **164**, 295-499.

Tabler, A., Häusser, A. and E. Roduner (2013) 'Aerobic one-step oxidation of benzene to phenol on copper exchanged HZSM5 zeolites: A mechanistic study', *Journal of Molecular Catalysis A: Chemical*, **379**, 139-145.

Yokoyama, C. and M. Misono (1994) 'Selective reduction of nitrogen monoxide by propene over cerium-doped zeolites' *Catalysis Today*, **22**, 59-7.

Zhao, J., Liu, Z. and D. Sun. (2004) 'TPO-TPD study of an activated carbon-support copper catalyst – sorbent used for catalytic dry oxidation of phenol', *Catalysis*, **227**, 296-303.

Zhang, Z., Atkinson, J. D., Jiang, B., Rood, M. J. and Z. Yan (2015) 'NO oxidation by microporous zeolites: Isolating the impact of pore structure to predict NO conversion' *Applied Catalysis B: Environmental*,**163**, 573-583.

Zhang, X., Shen, Q., He, C., Wang, Y., Cheng, J. and Z. Hao (2011) 'CoMOR zeolite catalysts prepared by buffered ion exchange for effective decomposition of nitrous oxide', *Journal of Hazardous Materials*, **192**, 1756-1765.

Chapter 6

Conclusion

6.1. Conclusion

The aim of this research work was to develop a solid regenerable catalytic adsorbent capable of oxidising 2-nitrophenol into CO_2, H_2O and N_2 while minimising the formation of nitrogen oxides. The main findings of this thesis are outlined in this following section.

During the initial adsorption study, the unmodified Beta zeolite with silica-to-alumina ratios of 25:1, 75:1, 150:1 and 300:1 achieved 2-nitrophenol adsorption levels of 40 - 50 mg g^{-1}, 80 - 90 mg g^{-1}, 80 - 90 mg g^{-1} and 80 - 90 mg g^{-1} respectively. Increasing the Si/Al ratio of the Beta zeolite was found to enhance the adsorption of 2-nitrophenol from aqueous solutions. The 2-nitrophenol adsorption isotherms were found to be of a Type I profile where the isotherm approaches a limiting value. Equilibrium adsorption data for β(25), β(75) and β(150) were represented by the Langmuir isotherm models while the adsorption data for β(300) was best described by Freundlich model. Fitting of the Langmuir adsorption isotherm to the experimental data suggests that the adsorption of 2-nitrophenol results in the formation of a monolayer on the Beta zeolite surface. The adsorption process was found to be largely independent of the pH of the adsorbate solution below pH 7 for all Beta zeolite samples irrespective of Si/Al ratio.

The kinetic data for the adsorption of 2-nitrophenol by β(25), β(75), β(150) and β(300) was found to be rapid with equilibrium being attained in 10 minutes and it was found to follow pseudo-second-order reaction kinetics which suggests that the rate of adsorption was dependent on the availability of adsorption surface sites and on the adsorbate concentration in solution. The thermodynamics of the adsorption process suggest that it is exothermic and physical in nature involving weak forces of attraction. The Gibbs free energy was found to be small and positive in magnitude indicating that the equilibrium position favours 2-nitrophenol in aqueous solution, however the $\Delta G°$ values became less positive with decreasing temperature which suggests that the adsorption will be more spontaneous at lower temperatures.

The next stage in this research work focused on the modification of the Beta zeolite to incorporate a catalytic component in order to enhance its adsorption capabilities and its potential catalytic oxidation activity. A series of copper-exchanged Beta zeolites were prepared using a one-step ion exchange procedure. During the modification process the effects of the SiO_2:Al_2O_3 ratio of the Beta zeolite, the exchange solution pH and ultimately the stability of the catalytically modified Beta zeolites were investigated.

The one step ion exchange procedure was carried out over the range of pH 3.0 – pH 10 by the addition of ammonium hydroxide to the exchange solution. Increasing the pH of the exchange solution resulted in an increase in the % Cu exchanged with neutral to alkaline pHs providing the optimum copper exchange conditions on all Beta zeolite samples prepared. It was found that acidic pHs could potentially cause dealumination of framework aluminium ions, resulting in destabilisation of the Beta zeolite which would lead to leaching of copper from the Beta zeolite samples. Increasing the Si/Al ratio of the Beta zeolite was found to influence the copper loading on the Beta zeolite as it resulted in a decrease in the cation exchange capacity of the Beta zeolite. XRD analysis of both β(25) and 1.95%Cuβ(25) revealed that the crystalline nature of the Beta zeolite was not modified after the incorporation of copper, while the presence of the CuO within the framework could not be ruled out especially among the samples that reported high or over 100% Cu exchange levels such as 1.30%Cuβ(300). The copper content of the prepared samples was found to be resistant to leaching in aqueous solution if the pH range was maintained between 5 - 11.

The next section of this work investigated the influence of extra-framework copper cations in the Beta zeolite samples on the adsorption of 2-nitrophenol from aqueous solution. It was found that the presence of copper enhanced the adsorption capacity of 2-nitrophenol over the applied concentration range for all Beta zeolite samples however the most significant of these was the lowest Si/Al ratio β(25). The adsorption of 2-nitrophenol was also found to increase with increasing copper loadings on all the Beta zeolite samples. The presence of copper within the Beta zeolite framework was found to alter the adsorption isotherm profiles from a Type I profile characteristic of monolayer adsorption to Type V profile which is characteristic of multilayer adsorption isotherms. The presence of copper within the Beta zeolite framework resulted in a change in the proposed adsorption model from the Langmuir to the Freundlich model for β(25), β(150) and β(300). This further suggests that the presence of copper promotes multilayer adsorption on the Beta zeolite surface. However the Langmuir model was still found to be an appropriate fit for the adsorption data on β(75) after the introduction of extra-framework cations. The suitability of the Freundlich model to the adsorption data after the introduction of extra-framework cations suggests that the presence of copper species on the Beta zeolite alters the surface adsorption sites of the Beta zeolite leading to more heterogeneous surface sites.

The introduction of framework cations into the Beta zeolite structure did not seem to alter the overall adsorption rate with the pseudo-second-order kinetics model being reported to describe the adsorption rate of 2-nitrophenol by the copper modified Beta zeolites. The thermodynamic study revealed that the adsorption of 2-nitrophenol onto the copper modified Beta zeolite samples was influenced by the presence of extra-framework copper cations as it increased the spontaneous nature of the overall adsorption process.

Step two of this work involves the study of the catalytic oxidation of the adsorbed pollutant (2-nitrophenol) on the Beta zeolite samples. This work investigated the influence of copper on the oxidation of adsorbed 2-nitrophenol on the Beta zeolite samples. During temperature programmed oxidation of adsorbed 2-nitrophenol, the main species detected from the exit stream were CO_2 (the total oxidation product) and (desorbed) 2-nitrophenol. The presence of copper in the Beta zeolite framework was found to enhance the catalytic oxidation of the adsorbed 2-nitrophenol, as in the absence of copper, 2-nitrophenol was detected in the exit stream during TPO testing which demonstrates the limited oxidation potential of the parent zeolites over the Cu modified Beta zeolites.

The presence of copper on the Beta zeolite was found to enhance the oxidation process by increasing the total oxidation of the adsorbed 2-nitrophenol to CO_2 as evidenced by the increase in evolution of CO_2 from the copper modified samples, while it also reduced the temperature of formation of CO_2. The total oxidation of adsorbed 2-nitrophenol to CO_2 is further enhanced by increasing the percentage of extra-framework copper on the Beta zeolite. While carbon dioxide and 2-nitrophenol were the main species detected in the exit steam during the temperature programmed oxidation of the prepared samples, other minor products were also detected such as phenol, benzene, nitrogen oxide, nitrogen dioxide and carbon monoxide/nitrogen. In the absence of copper, phenol and nitrogen oxide are detected in the exit stream which suggested that the unmodified Beta zeolites has some catalytic potential. In the presence of copper the complete decomposition of the adsorbed 2-nitrophenol is achieved, while some of the 2-nitrophenol decomposes into phenol, benzene, nitrogen monoxide and nitrogen dioxide. The presence of copper significantly reduces the temperature of formation of these species and also promotes the oxidation of NO to NO_2.

As nitrogen oxides are the first species detected during the TPO testing of the adsorbed 2-nitrophenol, it suggests that the oxidation of the adsorbed 2-nitrophenol commences with the breakdown of the nitro group on the 2-nitrophenol molecule adsorbed on both the unmodified and the copper modified Beta zeolites. The decomposition of the 2-nitrophenol in this manner results in the formation of phenol as the nitro group is oxidised into NO and subsequently into NO_2 in the presence of copper. The temperature range at which CO_2 is detected overlaps with the temperatures ranges at which phenol, benzene, nitrogen oxide and nitrogen dioxide are detected during the temperature programmed oxidation of adsorbed 2-nitrophenol which would suggest that the total oxidation of the adsorbed 2-nitrophenol to CO_2 is favoured. Also greater levels of CO_2 in comparison to these breakdown products are consistently observed during the oxidation process. This suggests that the copper modified Beta zeolite is capable of totally oxidising the adsorbed 2-nitrophenol into CO_2, while the decrease in the levels of phenol and benzene would also indicate their total oxidation to CO_2.

It is evident from the research work in this thesis that copper modified Beta zeolite has potential as dual adsorbent catalysts for the removal of 2-nitrophenol from wastewater with subsequent catalytic oxidation into CO_2, H_2O, N_2. It is envisaged that future studies in this area are likely to focus on the reuse of the solid adsorbent/catalyst, allowing multiple adsorption and catalytic oxidation cycles to be carried out without compromising the adsorption capacity or the catalytic oxidation performance of the adsorbent/catalysts. Further research is needed to investigate the ability of adsorbent/catalyst to cope with mixed organic waste streams in relation to the adsorption and kinetic mechanisms and the potential catalytic oxidation breakdown pathways involved.

.

Conferences

Enright D., Smart D., Curtin T. and O'Dwyer T.F., 2008, 9th European Meeting on Environmental Chemistry, Girona, Spain, 3-6 Dec, (Poster Presentation)

Smart D., Enright D., Curtin T. and O'Dwyer T.F., 2008, Development of a Novel Process for the Removal of Selected Organic Compounds from Waste Streams Strive EPA Conference, Dublin, 3-6 Nov, (Oral Presentation)

Smart D., Enright D., Curtin T., O'Dwyer T.F.*, 2008, Development of a Novel Process for the Removal of Selected Organic Compounds from Waste Streams, Environ 08, 1-3 Feb, Dundalk IT, Ireland. (Oral presentation)